STUDY OF ACOUSTIC AND VOLUMETRIC PROPERTIES OF AQUEOUS POLYHYDROXY ACIDS AND GLYCOLS MIXTURES AT DIFFERENT TEMPERATURES USING ULTRASONIC TECHNIQUE

Thesis Submitted for the Award of the Degree of

DOCTOR OF PHILOSOPHY

in

Physics

By

Kanika Bhakri

Registration Number: 42000056

Supervised By

Dr. Kailash Chandra Juglan (11468)

Professor, Department of Physics

LPU, Phagwara

LOVELY PROFESSIONAL UNIVERSITY, PUNJAB

2026

DECLARATION

I, hereby declared that the presented work in the thesis entitled "Study of Acoustic and Volumetric properties of aqueous Polyhydroxy acids and glycols mixtures at different temperatures using Ultrasonic Technique" in fulfilment of degree of **Doctor of Philosophy (Ph. D.)** is outcome of research work conducted by me under the supervision of Dr. Kailash Chandra Juglan, working as Professor, in the Department of Physics of Lovely Professional University, Phagwara, Punjab. In keeping with general practice of reporting scientific observations, due acknowledgements have been made whenever work described here has been based on findings of another investigator. This work has not been submitted in part or full to any other University or Institute for the award of any degree.

(Signature of Scholar)

Name of the scholar: Kanika Bhakri

Registration No.: 42000056

Department/school: School of Chemical Engineering and Physical Sciences

Lovely Professional University,

Punjab, India

CERTIFICATE

This is to certify that the work reported in the Ph.D. thesis entitled "Study of Acoustic and Volumetric properties of aqueous Polyhydroxy acids and glycols mixtures at different temperatures using Ultrasonic Technique" submitted in fulfillment of the requirement for the award of degree of **Doctor of Philosophy (Ph.D.)** in the Department of Physics, is a research work carried out by Kanika Bhakri, 42000056, is bonafide record of her original work carried out under my supervision and that no part of thesis has been submitted for any other degree, diploma or equivalent course.

(Signature of Supervisor)

Name of supervisor: Dr. Kailash Chandra Juglan

Designation: Professor

Department/school: School of Chemical Engineering and Physical Sciences

University: Lovely Professional University, Phagwara, Punjab

ABSTRACT

Ultrasonic investigations of liquid mixtures have become a powerful tool to understand molecular interactions, thermo-acoustic properties, and physico-chemical behavior of solutions. Such studies help in elucidating the role of molecular bonding, solute–solvent interactions, and structural changes in complex systems. They have wide applications in engineering, pharmaceuticals, food, leather, textiles, chemicals, and solvent solutions because ultrasonic techniques are non-destructive and provide reliable thermodynamic data. The present research focuses on ternary liquid mixtures of polyhydroxy acids (PHAs: gluconolactone, lactobionic acid, and galactose) with various glycols (ethylene glycol, diethylene glycol, triethylene glycol, PEGs, propylene glycol, and hexylene glycol). Using precise measurements of density and ultrasonic velocity with Anton Paar DSA 5000M at constant pressure (0.1 MPa) and varying temperatures (288.15–318.15K), a range of volumetric and acoustic parameters were derived to understand the solute–solvent and solute–solute interactions.

For different ternary and binary systems, density and sound velocity were measured at various concentrations and temperatures. From these measurements, several derived thermodynamic and acoustic properties were calculated. These included apparent and partial molar volumes (V_ϕ ,V_ϕ^0), molar volume of transfer ΔV_ϕ^0, apparent and partial molar isentropic compressions, ($K_{\phi,s}$ and $K_{\phi,s}^0$) transfer compressions $\Delta K_{\phi,s}^0$, and apparent molar expansibilities, E_ϕ^0 along with their temperature derivatives $\left(\partial E_\phi^0 \partial T\right)_P$. Interaction coefficients (V_{AB}, V_{ABB}, K_{AB} and K_{ABB}) were determined using McMillan–Mayer theory. Some other important thermo-acoustic parameters such as acoustic impedance (Z), Rao's constant (R), Vander Waal's constant (b), adiabatic compressibility (β), intermolecular free length (L_f), and Wada's constant (W) were also evaluated. Collectively, these parameters provide insights into molecular interactions, solute–solvent synergy, and the structure-making or structure-breaking tendencies of the studied mixtures.

In the case of gluconolactone with glycols (EG, DEG, TEG), strong solute–solvent interactions were observed, influenced by gluconolactone concentration. Volumetric and acoustic parameters confirmed the structure-making tendency of glycols in aqueous gluconolactone solutions. For lactobionic acid with PEG-200 and PEG-400, the systems

exhibited concentration- and temperature-dependent interactions. Transfer properties and interaction coefficients confirmed that hydrophilic interactions and hydrogen bonding were dominant forces in these mixtures. Similarly, galactose with PEG (400/600) revealed the presence of solute–cosolute interactions, and analysis of derived parameters indicated that hydrophilic interactions and hydrogen bonding contributed significantly to the molecular behavior of these mixtures.

Further studies on polyhydroxy acids with higher PEGs (PEG-4000) demonstrated strong solvent–solute synergy, where hydrophilic interactions prevailed over hydrophobic ones. Application of Hepler's criterion distinguished between structure-making and structure-breaking effects. Parameters such as expansibility and transfer volumes indicated co-sphere overlap and tight molecular associations. In binary aqueous solutions of galactose with propylene glycol and hexylene glycol, strong solute–solvent interactions were confirmed, and the dominant role of hydrophilic effects was observed. Differences in molecular size and polarity between glycols accounted for variations in interaction strengths. Likewise, lactobionic acid with propylene glycol and hexylene glycol showed significant differences in the strength and nature of interactions across systems, with a progressive shift in molecular behavior observed from PG to HG.

This comprehensive ultrasonic study demonstrates that PHAs and glycols interact predominantly through hydrophilic forces and hydrogen bonding, with solute–solvent interactions playing a more critical role than solute–solute interactions. The variation of temperature and concentration strongly influences the magnitude and direction of these interactions. The analysis highlights that structure-making and structure-breaking tendencies of solutes can be predicted from transfer properties and expansibility derivatives. Hydrophilic interactions dominate across systems, though differences in glycol chain length and molecular structure alter the strength of interactions. The derived parameters also provide reliable input for theoretical modeling and have implications for industrial, pharmaceutical, and biochemical applications, especially in processes where solution behavior under varying conditions is crucial. Ultimately, ultrasonic and volumetric analyses serve as powerful diagnostic tools for probing molecular interactions, offering both fundamental understanding and practical applications in multidisciplinary fields.

ACKNOWLEDGEMENT

I am profoundly thankful to **Almighty God** for His unparalleled mercy, wisdom, and strength that have sustained me throughout the entirety of my Ph.D. journey. In both moments of difficulty and success, His divine favor and unwavering encouragement have been the cornerstone of my ability to persevere. Without His heavenly support, the completion of this academic endeavor would have been unattainable. His continuous guidance, boundless patience, and steadfast strength have been invaluable assets, guiding me along this path with grace and purpose. For His endless blessings and support, I remain eternally grateful. My deepest gratitude goes to my esteemed supervisor, **Dr. Kailash Chandra Juglan**, Professor of the Department of Physics at Lovely Professional University, Phagwara. His unwavering support, insightful guidance, and profound expertise have been the cornerstone of my research journey. Dr. Juglan's dedication to academic excellence and his commitment to fostering a nurturing research environment have significantly shaped the trajectory of my thesis. His ability to challenge me intellectually while providing the necessary support has not only enhanced my research capabilities but also instilled in me a deep sense of confidence and perseverance. I would also like to extend my heartfelt appreciation to my seniors **Dr. Nabaparna Chakraborty and Dr. Parminder Kaur** for their invaluable support and guidance throughout my research. Their extensive knowledge and expertise in the field have provided me with critical insights that have greatly enriched my work. Dr. Chakraborty's analytical approach and keen eye for detail have been particularly beneficial in refining my experimental designs. I express my profound gratitude to **Dr. Mukesh Kumar,** Professor of the Department of Physics at Lovely Professional University, Phagwara for his invaluable suggestions and constructive feedback throughout the course of my research. His insightful observations and thoughtful guidance during each ETP have significantly enhanced the quality and depth of this thesis. The clarity and perspective he brought to various aspects of the work were instrumental in shaping its final form.

Beyond my immediate supervisors, I have been fortunate to receive guidance from Late **Dr. Harsh Manchnada**, Professor of the Department of chemistry at Dr. B.R. Ambedkar National Institute of Technology (Jalandhar) who have contributed to my

academic growth. His wisdom, diverse perspectives, and generous sharing of knowledge have broadened my understanding of the subject matter and enhanced the quality of my research. I also owe thanks to the laboratory candidates at the **National Institute of Technology (Jalandhar)** and **Guru Nanak Dev University (Amritsar)** for their collaborative efforts and technical assistance throughout my research. Their expertise in laboratory procedures, data collection, and experimental setups has been indispensable in the successful execution of my experiments.

My sincere thanks go to my friends, **Manisha Lamba, Harsimaran Kaur, and Ashpinder Kaur Gill** for their unwavering support, valuable advice, and constant motivation throughout my academic journey. Their friendship and collaborative spirit have been a source of comfort and encouragement, especially during the most challenging phases of my research. Above all, I express my heartfelt appreciation to my family, whose unwavering support and encouragement have been the bedrock of my academic achievements. I am profoundly grateful to my husband, **Mr. Ankur Khanna** and mother-in-law, **Ms. Rajni Khanna** for their constant belief in me, their boundless patience, and their steadfast support throughout the duration of my research. Their understanding and willingness to accommodate the demands of my academic pursuits have provided me with the emotional strength and stability needed to navigate the challenges and stresses inherent in thesis writing. The sacrifices they have made and the grace with which they have stood by my side are truly immeasurable, and I dedicate this accomplishment to their unwavering love and support.

In conclusion, the successful completion of this thesis is the result of the collective efforts, support, and guidance of numerous individuals and institutions. From the exemplary mentorship provided by my supervisors and advisors to the collaborative efforts with laboratory teams and the unwavering support of my peers and family, each contributor has played a vital role in this academic achievement.

This journey has not only been an academic pursuit but also a testament to the power of collaboration, support, and dedication. I am profoundly grateful to everyone who has been a part of this journey, and I dedicate this accomplishment to all who have contributed to my growth and success.

Kanika Bhakri

TABLE OF CONTENTS

LIST OF TABLES

LIST OF FIGURES

Nomenclature

v	Ultrasonic speed
ρ	Density of material
K	Kelvin (Temperature in absolute)
ρ_0	Density of solvent
Z	Acoustic impedance
β	Adiabatic compressibility
W	Wada's constant
R	Rao's constant
L_f	Intermolecular free length
K_T	Temperature dependent Jacobson's constant
b	Vander Waal's Constant
M_{eff}	Solution's effective molecular weight
M	Solute's molar mass
m_A	Solute's molality
T	Temperature
V_ϕ	Apparent molar volume
S_V^*	Experimental Slope for volume
V_ϕ^0	Partial molar volume
ΔV_ϕ^0	Partial molar volume of transfer
$K_{\phi,S}$	Apparent molar isentropic compression
k_S	Isentropic compressibility
T_m	Temperature range midpoint
p	Pressure
MPa	Mega Pascal
$k_{S,0}$	Isentropic compressibility of solvent
$K_{\phi,S}^0$	Partial molar isentropic compression
S_K^*	Experimental Slope for isentropic compression
a, b, c	Empirical Constants
E_ϕ^0	Partial molar expansibility
$\Delta K_{\phi,S}^0$	Partial molar isentropic compression of transfer
m_B	Molal concentration of cosolute
V_{AB}	Pair interaction coefficient for volume
K_{AB}	Pair interaction coefficient for isentropic compression

V_{ABB}	Triplet interaction coefficient for volume
K_{ABB}	Triplet interaction coefficient for isentropic compression
PHAs	Polyhydroxy acids
EG	Ethylene Glycol
DEG	Diethylene Glycol
TEG	Triethylene Glycol
PG	Propylene Glycol
HG	Hexylene Glycol
PEG-200	Polyethylene Glycol-200
PEG-400	Polyethylene Glycol-400
PEG-4000	Polyethylene Glycol-4000
GLA	Gluconolactone
LBA	Lactobionic acid
GAL	Galactose
Sol.	Solutions

CHAPTER 1

INTRODUCTION

1.1 Ultrasonics

Acoustics is an area of science that deals with the production, transmission, and utilization of inaudible sound waves. Ultrasonics is included in this branch. In general, it is concerned with sound waves that have a frequency that is more than 20,000 Hz, which is the maximum audible frequency that a human being is capable of hearing. Moreover, it addresses their application in scientific research. These are the mechanical, longitudinal, and elastic vibrations that, to travel across a physical medium, need to be transmitted via that medium [1]. For directing experiments and carrying out measurements, the Ultrasonic Testing takes advantage of high-frequency vibrations. There are a variety of applications for ultrasonic examination, including dimensional measurements, the detection of flaws, the characterization of materials, and more. Ultrasonic inspection is a Non-Destructive Technique (NDT) that is extremely adaptable and useful. The ultrasonic testing is sensitive to irregularities on both the surface and the subsurface that are present. The determination and estimation of the size and shape of molecules can be done with a high degree of precision. Since it does not disrupt the structure, the NDT is utilized for testing purposes. To explore qualities without inflicting any damage, this method employs a wide variety of scientific and business studies throughout the process. Low coherence interferometry, radiography, magnetic particle, and eddy current testing are some of the non-destructive tests that are included in the non-destructive testing (NDT) suite.

1.2 Ultrasonic Testing

Based on the collection and measurement of either the waves that are emitted (pulse-echo) or the received waves (through-transmission), the ultrasonic testing is carried out. Both techniques have their utility in a variety of areas; however, pulse-echo systems prove to be more beneficial than transmission systems since they only require accessibility from one side of the object being studied and reveal more information about concrete than transmission systems do. By using pulse-echo, it is possible to identify substantial vacancies in the back walls. The ultrasonic technique is a non-destructive method that uses high-frequency ultrasonic waves to evaluate the internal structure of test material. The frequencies that are often employed for this approach vary from 500 kilohertz to 20 megahertz [MHz]. The waves of high frequency sound are very

directed up until the point where they encounter a boundary with another medium; at that point, they reflect back to their original source. As a result of the development of standing waves, a great deal can be deduced from the reflected wave. For instance, ultrasonic thickness measurement of metallic pipelines and aircraft bodies can be derived from this phenomenon. For the purpose of identifying defects in massive metal objects or materials, this technique is utilized. This technique is utilized in a wide variety of domains, including but not limited to industries, investigations, metal working, aviation, medical, and a bunch of other fields.

1.2.1 Characteristics of Ultrasound Testing

- Operate in a highly automated and portable manner.
- Extremely reactive
- A higher level of penetration power that leads to a more accurate assessment of flaws in the tested material.
- Compared to other harmless techniques, it has more accuracy when evaluating part width and interior material faults.
- The use of various acoustical qualities to ascertain the size, shape, and composition of materials, as well as to study the structure and composition of alloys.
- Because the outcomes are immediate, decisions may be made instantly.

1.3 Ultrasonic Investigations

Ultrasonic investigations of liquid mixtures and pure solutions are an effective tool for understanding intermolecular interactions, structural arrangements, and molecular processes [2]. They provide detailed insights into association–dissociation phenomena in binary and ternary systems, where deviations from linear acoustical behavior with concentration confirm the presence of specific molecular interactions [3,4,8–10].

The physicochemical behavior of liquids under varying temperature, pressure, and concentration is critical in both fundamental research and industrial applications. Ultrasonic methods are especially valuable as they are non-destructive, allowing evaluation of molecular packing, internal structure, and strength [5–7,11–15]. These studies have been widely applied in physics, chemistry, and engineering to elucidate solute–solvent effects, dipole–dipole and ion–dipole interactions, and deviations from ideal solution behavior [6,7,18,19,32–36].

Beyond fundamental understanding, ultrasonics have broad industrial and technological applications, including catalysis, cleaning, blending, and non-destructive testing [16,17,25–29]. Acoustic and volumetric properties derived from experimental measurements (e.g., densimetry) provide accurate calculation of thermodynamic parameters, enabling detailed interpretation of solute–solvent interactions and molecular environments [20–24,30,31].

Recent research highlights the role of ultrasonic studies in diverse fields, such as food, pharmaceutical, chemical, agricultural, and petroleum industries, where binary and ternary liquid mixtures are extensively used [24–28,37–41]. For instance, ultrasonic methods have proven useful in enhanced oil recovery and in characterizing ternary mixtures at different temperatures. Despite substantial progress, there remains significant scope for further investigation into acoustical and transport properties of complex liquid systems relevant to manufacturing and processing technologies [42–45].

1.4 Density and sound velocity analyzer

Designed by Anton Paar, the density and speed analyzer (Model 5000 M) analyzes both ρ and v simultaneously and accurately in a single setup and under identical conditions. Only with this device can the density and velocity of sound be measured simultaneously. This groundbreaking digital density meter achieves its unprecedented level of repeatability—down to the seventh digit—by utilizing the proprietary Pulsed Excitation Method in conjunction with U-tube technology. Featuring state-of-the-art sound velocity measurement technology and the world's most accurate density measurement, DSA 5000 M is a reflection of absolute perfection in every respect. For effective quality control of a wide range of chemicals, the DSA 5000 M is the tool of choice due to its high sample throughput (up to 30 samples per hour) and short measuring durations (up to 4 minutes). Researchers can save time by measuring two parameters simultaneously. The reliability, precision, and efficiency of DSA 5000 M are relied upon by research and development teams across numerous sectors. By automatically detecting filling issues like bubbles or particles in both measuring cells, the Filling Check feature ensures the quality of the measured results. The filled U-tube can be seen in high-definition live photographs by using the U-View camera. Along with the measurement findings, the photos are saved and printed. It keeps the temperature constant, measures the density, and calculates the velocity by applying the following

principles:

1.4.1 Density

The freshly prepared mixture is inserted into a borosilicate glass tube (of U shape), which is then triggered to oscillate at a frequency that is proportional to the sample's density. Once the oscillation has stabilized, the stimulation is turned off, allowing it to die away naturally. The pulsed excitation method is patented and uses a continuous sequence of stimulation and fade-out. This pattern can be used to evaluate the sample's viscosity, find air bubbles or particles, adjust for the effects of viscosity, and get very accurate density readings.

1.4.2 Temperature regulation

Both measurement cells are precisely temperature-regulated using Peltier technology to ensure that the physical conditions are identical for both sets of findings.

1.4.3 Sound velocity

Pulses of ultrasonic sound are sent through the material by means of a piezoelectric actuator. The journey distance is known as well since the sample is placed in a known-length compartment. In order to determine how long it takes for ultrasonic waves to move through samples, a second piezoelectric device is used to detect the sound pulse. After then, the relationship between distance (m) and time (s) is all that's needed to determine the sound velocity (m/s).

1.4.4 Some important features of Density and speed analyzer:

- The highest possible repeatability and reproducibility.
- Extra measurement of the sample's viscosity.
- Thermo Balance eliminates temperature-dependent measurement errors.
- High-end touchscreen display simplifies operation.
- Automatic calibration and verification using recognized standards.
- Constant monitoring of conditions to rule out the possibility of outside influences affecting outcomes.
- Filling Check accurately detects gas bubbles or particles in samples. [14, 23, 32-35]

1.5 Polyhydroxy acids (PHAs)

Polyhydroxy acids (PHAs) are a type of organic carboxylic acid. A PHA molecule has an aliphatic or alicyclic chain with carbon atoms linked to two or more hydroxyl groups. A carboxyl group is added to PHA to make it acidic, as the hydroxyl groups already present are neutral. In-terrestrial metabolites or tissue-level carbohydrate metabolic intermediates, such glucose, can produce PHAs [14]. Three PHAs have the potential to regulate the skin barrier function. For people with sensitive skin conditions like rosacea or atopy, PHAs are a better option than AHAs because they are less prone to irritate the skin when administered. Polyhydroxy acids (PHAs) are the next logical step after AHAs. They provide the same rejuvenating and skin-smoothing benefits as AHAs without the risk of burning or stinging. Because of their larger molecular structure, PHAs are able to permeate the skin more slowly than AHAs, causing less adverse effects. In addition to their protective effects, most PHAs exhibit antioxidant properties. Because of their humectant properties and the exfoliating actions of AHAs, PHAs are excellent moisturizers because they increase the stratum corneum barrier's capacity to retain moisture. The outcome is a skin-friendly formula that works wonders on all kinds of skin, including the most delicate ones. By reducing the enzyme activity of matrix metalloproteinase, PHA helps prevent more UV damage and is also used as an antioxidant chelating agent. [46–51] When it comes to skin care, polyhydroxy acids (PHAs) are superior to more conventional alpha hydroxyacids (AHAs). Just like alpha hydroxy acids (AHAs), poly hydroxy acids (PHAs) have anti-aging, skin-softening, and exfoliating properties [52-54]. Most PHAs have antioxidant capabilities, and are hydrating agents and moisturising as well [55,56]. Unlike traditional AHAs, which can elicit unpleasant sensations in the skin, PHAs have no such side effects [53- 55]. Corrective cosmetics that contain PHAs can help cover up skin discolorations on sensitive skin, such post-laser purpura or hemonagema, which can be seen in Sturge-Weber Syndrome. Another benefit of PHAs is that they strengthen the stratum corneum barrier, which makes the skin more resistant to chemicals.[47] For the best results in treating skin problems, PHAs are often applied in conjunction with other superficial treatment procedures. [57,58]

Chemical exfoliants termed polyhydroxy acids (PHAs) are frequently referred to as "relatives" of AHAs since they are second-generation alpha hydroxy acids (AHAs). These acids are fundamental to the synthesis or utilization of numerous common compounds used in a wide range of medical and cosmetic applications, as well as in chemical synthesis, drug

delivery systems, tissue engineering, biopolymers, and bioplastics. In recent times, polyhydroxy acids have gained significant interest as a possible eco-friendly substitute for petrochemical polymers in packaging. Compounds like gluconolactone, galactose and lactobionic acid are all part of the PHA class.

1.5.1 Gluconolactone

Gluconolactone is an acid that belongs to the PHA family; it is a white, odourless crystalline powder. What makes them unique and sets them apart from other AHAs and BHAs is the number of hydroxyl groups they contain. The acronym GDL stands for "glucono-delta-lactone," another name for the compound. Gluconolactone is a crystalline powder that is white in colour and has no discernible odour. It is an acid that is classified as a polyhydroxy acid (PHA). Gluconolactone is one oxidized derivative of glucose lactone. In place of the tetrahydropyrate ring, the molecule has one hydroxymethyl group, three hydroxyl groups, and one ketone group. Natural foods that include GLA, a food additive with the European number E575, include honey, tofu, cheese, wine, bread, and fruit juices, among many others. [59] There are many applications for this naturally occurring cyclic ester of D-gluconic acid in the food and cosmetic industries. As an acidifier and sequestrant, it is useful in food items. Furthermore, it enhances both the texture and flavor [60]. It also acts as a humectant, or skin-hydrating agent, due to the hydroxyl groups it contains. Gluconolactone is clearly gentler than other acids because it hydrates and exfoliates at the same time [61]. As an acidifier, sequestrant, curing, pickling, or raising agent, gluconolactone is a naturally occurring food component [62]. Aside from its antioxidant benefits, it hydrates the skin, improves its tone and texture, and eliminates the dead skin cells that make your face look dull and lifeless [63]. In addition to reducing inflammatory lesions, gluconolactone influences the keratinization process. Plus, it's safer than benzoyl peroxide [64].

The effects of Gluconolactone (GLA) on sebum production, pH, and the depth of Trans Epidermal Water Loss (TEWL) were investigated by JarzČbek-Perz S et al. [65]. There was a marked decrease in skin pH and TEWL when GLA was administered. Furthermore, numerous studies have shown that it has the ability to improve skin texture and reduce wrinkles, making it a promising anti-aging treatment [66]. Antileishmanial activities and anticancer characteristics of gluconolactone produced gold(I) complexes are two examples

of its possible broader applications that have lately attracted the attention of researchers [67].

1.5.2 Galactose

Galactose, also known as D-Galactose, is the PHA that we have utilized throughout our work. Galactose was named "lactose" after its discovery in 1856 by Louis Pasteur, who separated it from other sugars in milk. A name derived from the Greek word "galakt," meaning "milk," was applied to it until very later. Most sugars found in nature and galactose have the D-configuration. Despite having a different arrangement of hydroxyl groups at the carbon-4 position than glucose, galactose fulfils several structural and functional functions in living organisms [68]. There are several foods and the body itself that contain D-galactose, a kind of PHA. Plums, cherries, figs, celery, butter, milk, cheese, yogurt, honey, and reducing sugars are some of its foodstuffs. One example of a legume that contains galactose is dried peas and beans [69]. Beyond its vast importance in human physiology, galactose has recently been discovered to be useful in treating several diseases, particularly those that impact brain function [70,71]. Oral galactose supplementation was linked with significant alterations in clinical presentation; supplemental galactose enhanced glycosylation in fibroblasts of phosphoglucomutase 1 deficient individuals [72]. For both in vitro and in vivo artificial senescence induction studies, D-galactose has been utilized [73]. This has been done in the context of anti-aging pharmaceutical interventions. As a sugar, galactose is normally converted into energy by the liver. Despite its prevalence in food, galactose also finds several applications in skin care products. Many studies have investigated the effects of galactose on the skin and its effectiveness because of its many antioxidant and prebiotic properties. This chemical has great potential as an ingredient in skincare products that nourish and exfoliate due to its unique features. Regular use of galactose, which has chemical exfoliant characteristics, helps keep skin from looking dull, dry, and even acne-prone by removing the buildup of dead skin cells. [74]

1.5.3 Lactobionic acid

Lactobionic acid, a member of the PHA family, is derived from a combination of Galactose, an inert sugar, and gluconic acid, a naturally occurring substance in the skin and able to hold a significant quantity of water, with many hydroxy groups. The formal name of lactobionic

acid (LBA) is 4-O-β-Dgalactopyranosylo-D-gluconic acid, an aldonic acid. It has a molecular weight of 358.296 $g \cdot mol^{-1}$, and it is a weak acid which tastes sweet [75,76]. LBA has received a lot of attention from the chemical and pharmaceutical industries. While the chemical industries are seeking for new strategies to improve bio-production and more effective techniques to purify this substance, it is regarded as a viable therapeutic excipient in the pharmaceutical industry [77]. In order to create biodegradable detergents, lactobionic acid (LBA) is used due to its surface-active qualities. Making anticorrosive chemicals and covers for ships and oil platforms is an intriguing application [78]. It has a variety of possible uses in pharmacology, cosmetics, and medicine. It is useful as an ingredient in fluid formulations that aid in the stabilization of organs for transplantation due to its antioxidant qualities and capacity to chelate metals [79]. It plays a critical role in treating skin conditions like rosacea, dandruff, and different kinds of acne and lesions on skin. It is an ingredient in products used after prolonged sun exposure, as well as after peeling or laser treatment. The hydrating and exfoliating qualities of LBA are helpful in the cosmetics business, additionally, it can aid in strengthening the protective barrier of epidermis. Lactobionic acid stimulates phytoblasts, assisting in the synthesis of collagen fibrils [80].

1.6 Glycols

Glycols are viscous, colorless, and odorless alcohols containing two hydroxyl groups. They exhibit broad **industrial and biotechnological applications** in pharmaceuticals, cosmetics, beverages, and biotechnology [81–85]. Extensive research has focused on their **thermo-physical properties in aqueous systems** due to their roles as conditioning agents, solvents, lubricants, and hygroscopic materials [86–94]. Glycols are also used in the production of plastics, fibers, plasticizers, and as coupling agents that enhance solubility of aromatic compounds in water [95–97]. Their viscosity and hydration behavior are highly dependent on temperature, with increased viscosity at lower temperatures reducing molecular mobility [98].

Ethylene glycol (EG) is a widely used coolant, antifreeze, and raw material in polyester production, inks, dyes, and vaccines [99]. **Diethylene glycol (DEG)**, a hygroscopic liquid, finds applications in cosmetics, automotive, agriculture, and paints, mainly due to its humectant properties [99,100]. **Triethylene glycol (TEG)** is non-flammable and valued for

its antibacterial properties, enabling use in disinfectants, lubricants, plastics, and construction industries [99].

Polyethylene glycols (PEGs) are polyether compounds with extensive applications across pharmaceutical, chemical, food, textile, and cosmetic industries [101]. Their ability to form hydrogen bonds and conjugate with biomolecules makes them essential in detergents, surfactants, antifreeze, emulsifiers, and clinical formulations. PEGs of molecular weights 200–4000 are most commonly employed. **Propylene glycol (PG)** is a humectant with strong hydrogen bonding and good solvent properties, extensively used in pharmaceuticals, cosmetics, food products, and unsaturated polyester resins [102–104]. Finally, **hexylene glycol (HG)**, soluble in diverse organic solvents, is applied in pesticides, coatings, textiles, printing, paints, and medical formulations, serving as both solvent and transport medium [105–107].

In the present study, the molecular interactions of glycols with polyhydroxy acids in aqueous medium are investigated. These systems are chosen because glycols, with their multiple hydroxyl and ether groups, readily engage in hydrogen bonding and dipole–dipole interactions, with polyhydroxyacids (gluconolactone, lactobionic acid and galactose) in aqueous medium. Understanding the strength and nature of these interactions is essential to elucidate solute–solute and solute–solvent behavior, which governs the physicochemical properties of the mixtures. Such insights are important not only for fundamental knowledge of hydrogen-bonding networks in multicomponent systems but also for practical applications in food, pharmaceutical, and chemical industries where glycols and Polyhydroxyacids are widely utilized.

1.7 Thermodynamic Study

The thermodynamic and acoustic behavior of liquid mixtures has attracted considerable attention due to its importance in understanding the nature of molecular interactions and structural organization in multicomponent systems. In recent years, many researchers have extensively explored these properties using ultrasonic techniques to evaluate parameters such as excess molar volume, adiabatic compressibility, and intermolecular free length, which serve as sensitive indicators of solute–solvent and solute–solute interactions. Temperature-dependent acoustic and volumetric data further help to reveal the strength and type of these interactions, providing insight into molecular association, hydrogen bonding,

and structural effects in solution. Several recent investigations on aqueous and non-aqueous glycol systems and related compounds have emphasized the usefulness of such studies in interpreting physicochemical behavior and designing industrial and biochemical processes. [108-112] The present work aims to extend this understanding by studying the acoustic and volumetric properties of aqueous mixtures of polyhydroxy acids and glycols at different temperatures using ultrasonic techniques to elucidate the molecular interactions and structural changes occurring in these systems.

References

[1] P. K. Singh and S.C. Bhatt, Appl. Phy. Res. 2, 35-45 (2010).

[2] A.A. Mistry, V.D. Bhandakkar and O.P. Chimankar, Adv. Appl. Sci. Res. 4, 54-59 (2013).

[3] A.B. Dikko, A.D. Ahmed and N.Z. Oriolowo, Int. J. Appl. Res. 1, 75-77 (2015).

[4] A.B. Dikko and E. Eke, Int. J. Multidiscip. Res. Dev. 2, 412-413 (2015).

[5] A. K. Gupta, K. Kumar and Birendra Kumar Karn, J. Ind. Counc. Chem. 26, 77-81 (2009).

[6] B. Hemaltha, P. V. Rani and N. S. Kumar, Int. J. Rec. Adv. Eng. Technol. 6, 795-803 (2013).

[7] A. O. Deshmukh and P.B. Raghuwanshi, Sci. Revs. Chem. Commun. 4, 91-100 (2014).

[8] A. K. Dash and R. Paikaray, Int. J. Adv. Eng. Technol. 66, 89-104 (2014).

[9] A. K. Dash and R. Paikaray, Res. J. Phy. Sci. 1, 12-20 (2013).

[10] A. Kumar Dash and R. Paikaray, Der Chemica Sinica 5, 81-88 (2014).

[11] R. A. Durst and J. K. Taylor, J. Res. Natll. Bur. Stand. 68, 625-630 (1964).

[12] D.H. Dagade, S.P. Shinde, K.R. Madkar and S.S. Barge, J. Chem. Thermodyn. 79, 192 204 (2014).

[13] S. Ernst and B. Jewowska-Trzeblalowska, J. Phys. Chem. 79, 2113 2116 (1975).

[14] Ashima, K. C. Juglan and H. Kumar, J. Chem. Thermodynamics 140, 105916 (2020).

[15] X. Jiang, C. Zhu, and Y. Ma, J. Chem. Eng. Data, 58, 2970-2978 (2013).

[16] T. Kalimulla, S. Babu, D. Das, M. Gowrisankar, K.G. Rao. J Pharm Sci Res, 11(7):2645–55 (2019).

[17] R. Novelline. Squire's Fundamentals of Radiology. 5th ed. Harvard University Press; pp. 34–35 (1997).

[18] T.M. Letcher, G.G. Redhi, Fluid Phase Equilib, 198(2), 257-266 (2002)

[19] J.D. Pandey, N.K. Soni, R. Dey, R. Verma, Fluid phase equilibria. Jan 15;215(1):17-22 (2004).

[20] G.G. Hammes, P.B. Roberts, J Chem Phys. *52*(10), 5496-5497 (1970).

[21] K. Kaur, K.C. Juglan, J Chem Pharm. 8, 49–53 (2016).

[22] H. Kumar, I. Behal, J Chem Thermodynamics. 102, 48-62 (2016).

[23] N. Chakraborty, K.C. Juglan, H. Kumar, Brazil J Chem Eng. 1-16 (2021).

[24] P.K. Banipal, S. Arti, T.S. Banipal, J Chem Eng Data. 60(4), 1023-1047, (2015).

[25] M.P. Longinotti, H.R. Corti, J Solution Chem. *33*, 1029-1040 (2004).

[26] M.F. Mazzobre, M.P. Longinotti, H.R. Corti, M.P. Buera, Cryobiology. *43*(3), 199-210 (2001).

[27] R.N. Goldberg RN, Y.B. Tewari, J.C. Ahluwalia, J Biol Chem. 264(17), 9901-9904 (1989).

[28] P. Bordat, F. Affouard, M. Descamps, K.L. Ngai. Phys Rev Lett. *93*(10), 105502 (2004).

[29] P. Vasantharani, L. Balu, R.E. Pavai, S. Shailajha, Global J. Mol. Sci. 4, 42-48 (2009).

[30] S. Srilalitha, M.C.S. Subha, K.C. Rao, J. Pure Appl. Ultrason. 18, 59-73 (1996).

[31] J.D. Pandey, N.K. Soni, R. Dey and R. Verma, Fluid Ph. Equilib. (2004).

[32] N. Chakraborty, K.C. Juglan and H. Kumar, J. Am. Chem. Soc. 5, 32357-32365 (2020).

[33] P.H. Von Hippel and T. Schleich, Acc. Chem. Res. 2, 257–265 (1969).

[34] D.B. Northrop and F.B. Simpson, Bioorg. Med. Chem. 5, 641–644 (1997).

[35] H. Kumar, C. Chadha, A. Verma and M. Singla, J. Mol. Liq. 242, 560–570 (2017).

[36] S. Fang and D.H. Ren, J. Chem. Eng. Data. 58, 845–850 (2013).

[37] K. Kumari and S. Maken, J. Mol. Liq. 325, 115170 (2021).

[38] M. Dzida, E. Zorebski, M. Zorebski, M. Zarska, M.G. Rybczynska, M. Chorazewski, J. Jacquemin and I. Cibulka, Chem. Rev. 117, 3883–3929 (2017).

[39] H. Hamidi, A.S. Haddad, R. Rafati, E.W. Otumudia, E. Mohammadian, A. Azdarpour, W.G. Pilcher, P.W. Fuehrmann, L.R. Sosa, N. Cota, D.C. Garcia, R.M. Ibrahim, M. Damiev and E. Tanujaya, Ultrasonics. 110, 106288 (2021).

[40] Y. Jin, H. Heo, A. Krokhin, E. Walker, T.Y. Choi and A. Neogi, Ultrasonics. 104, 105931 (2020).

[41] L.C.S. Nobre, A.F. Cristino, A.F.S. Santos, C.A. Castro and I.M.S. Lampreia, J. Chem. Therm. 18, 106226 (2020).

[42] P.S.S. Ibrahim, S.C. Vinayagam, J.S. Murugan and J.E. Jeyakumar, J. Mol. Liq. 304, 112752 (2020).

[43] F.E. Alaoui, E.A. Montero, J.P. Bazile, F. Aguilar and C. Boned, J. Chem. Thermodyn. 43, 1768−1774 (2011).

[44] M. Rani, S. Agarwal, P. Lahot and S. Maken, J. Ind. Eng. Chem. 19, 1715−1721 (2013).

[45] R. Devi, S. Gahlyan, M. Rani and S. Maken, J. Mol. Liq. 275, 364−377 (2019).

[46] B.A. Green, R.J. Yu, E.J. Van Scott, Clin Dermatol. 27(5):495-501 (2009).

[47] E. Berardesca, F. Distante, G.P. Vignoli, C. Oresajo, B. Green, Br J Dermatol. 137(6):934-938 (1997).

[48] A. Kornhauser, S.G. Coelho, V.J. Hearing, Clin Cosmet Investig Dermatol. 24(3):135-142 (2010).

[49] P.E. Grimes, B.A. Green, R.H. Wildnauer, B.L. Edison, Cutis. 73(2 Suppl):3-13 (2004).

[50] A. Kornhauser, Clin Cosmet Investig Dermatol, 135 (2010).

[51] M. Audina, World J. Pharm. Res. 10, 137-141 (2021).

[52] B. Green, C. Tseng, R. Wildnauer, J. Herndon, R. Rizer, Amer Acad of Derm Poster Exhibit. Mar 19 (1999).

[53] W.F. Bergfeld, B.K. Remzi, B. Green, P. Patel, R. Ravas, Amer Acad of Derm Poster Exhibit. Feb 27 (1998).

[54] E.F. Bernstein, B.A. Green, B. Edison, R.H. Wildnauer, *Skin & Aging Supplement* Sep. (2001).

[55] E.J. Van Scott, R.J. Yu, Cosmet Dermatol 9(6), 54-62 (1996).

[56] R.J. Yu, E.J. Van Scott, Cosmet Dermatol Supplement1 -6 (1994).

[57] M.A. Petratos, Cutis. Aug 1;66(2), 107-11 (2000).

[58] L. Kakita, MD. Correspondence on file. Item#13039: Neo Strata Company, Inc., Princeton, NJ.

[59] X. Qin, B. Liu, F. Gao, Y. Hu, Z. Chen, J. Xu, & X. Zhang. *Frontiers in Physiology* (2022).

[60] F. Martin, N. Cayot, A. Marin, L. Journaux, P. Cayot, P. Gervais, R. Cachon, J. dairy sci. 92 5898-5906 (2009).

[61] J. Levin, R. Miller, J Clin Aesthet Dermatol. 4(8):31 (2011).

[62] F. Martin, N. Cayot, A. Marin, L. Journaux, P. Cayot, P. Gervais, R. Cachon, J Dairy Sci. *92*(12), pp.5898-5906 (2009).

[63] A. Kornhauser, S.G. Coelho, V.J. Hearing, Clin Cosmet Investig Dermatol. Nov 24:135-42 (2010).

[64] M.J. Hunt, R.S. Barnetson, Australas J Dermatol. *33*(3), 131-134 (1992).

[65] S. Jarząbek-Perz, P. Mucha, H. Rotsztejn. Skin Res Technol. *27*(5), 925-930 (2021).

[66] R.J. Yu, E.J.V. Scott, U.S. Patent Number: 5, 677, 340 (1997).

[67] A.V. Espinosa, D.D.S. Costa, L.G. Tunes, R.L.D.R.M. Monte-Neto, M.V. Grazul De

Almeida, H. Silva, Chem. Biol. Drug Des. (2021).

[68] A.I. Coelho, G.T. Berry, M.E. Rubio-Gozalbo, Curr Opin Clin Nutr Metab Care, 18(4), 422–427 (2015).

[69] P.B. Acosta, K.C. Gross, Eur J Pediatr, 154, 87–92 (1995).

[70] M. Roser, D. Josic, M. Kontou, K. Mosetter, P. Maurer, W. Reutter, J Neural Transm 116, 131–139 (2009).

[71] M. Salkovic-Petrisic, J. Osmanovic-Barilar, A. Knezovic, S. Hoyer, K. Mosetter, W. Reutter, Neuropharmacology, 77, 68–80 (2014).

[72] L. Tegtmeyer, S. Rust, M. van Scherpenzeel, B.G. Ng, M.E. Losfeld, S. Timal, T. Marquardt, N Engl J Med, 370, 533–542 (2014).

[73] K.F. Azman, R. Zakaria, Biogerontology, 20, 763–782 (2019).

[74] Procoal. (n.d.). What does galactose do in skin care and what are its benefits? Procoal London. https://procoal.co.uk/blogs/beauty/what-does-galactose-do-in-skin-care-and-what-are-its-benefits#:~:text=Here%20are%20the%20main%20benefits%20of%20galactose%3B%20Galactose,some%20suffering%20from%20frequent%20breakouts%20and%20other%20blemishes

[75] K. Goderska, Appl Microbiol Biotechnol, 103 (9), 3737–3751 (2019).

[76] J.C.B. Ribeiro, D. Granato, M.L. Masson, I. Andriot, A.C. Mosca, C. Salles, E. Guichard, Food Chem. 207, 101–106 (2016).

[77] S. Alonso, M. Rendueles, M. Díaz, Biotechnol Adv. 31 (8), 1275–1291 (2013).

[78] T.L.M. Alves, H.C. Ferraz, J.C. Pinto, J.B. Severo, J Ind Microbiol Biotechnol, 38, 1575–11158 (2011).

[79] B. Beden, H. Druliolle, K.B. Kokoh, J. Electroanal Chem. 385, 77–83 (1995).

[80] M. Warowna, B. Kręcisz, A. Sobolewska-Samorek, A. Hordyjewska, T, Kosmetologia Estetyczna, 6, 651–666 (2018).

[81] A.V. Sarode and A.C. Kumbharkhane, J. Mol Liq., 164, 226-232 (2011).

[82] M.C. Brundrett, B. Kendrick and A.C. Peterson, Biotech. Histochem., 66, 111-116 (1991).

[83] V.K. Syal, A. Chauhan, S. Chauhan, Pure Appl. Ultrason., 27, 61-69 (2005).

[84] D.B. Barr, J.R.G. Weerasekera and J. Wamsley, J. Anal. Toxicol., 31, 295-303 (2007).

[85] H.C. Fuller, Ind. Eng. Chem., 16, 624-626 (1924).

[86] C.M. Kinart, M. Klimczak and A. Cwiklinska, J. Mol. Liq., 135, 192-195 (2007).

[87] H.C. Ku and C.H. Tu, J. Chem. Eng. Data, 45, 391-394 (2000).

[88] X.X. Li, Y.X. Liu and X.H. Wei, J. Chem. Eng. Data, 49, 1043-1045 (2004).

[89] C.M. Kinart and M. Klimczak, J. Mol. Liq., 148, 132-139 (2009). 17

[90] X. Esteve, A. Conesa, A. Coronas, J. Chem. Eng. Data, 48, 392-397 (2003).

[91] A. Pal, H. Kumar and R. Maan, J. Solution Chem., 42, 1988-2011 (2013).

[92] G.P. Dubey and K. Kumar, J. Chem. Eng. Data, 55, 1700-1703 (2010).

[93] K. Kaur, I. Behal and K.C. Juglan, J. Chem. Thermodyn., 125, 93-106 (2018).

[94] T. Sun and A.S. Teja, J. Chem. Eng. Data, 48, 198–202 (2003).

[95] G. I. Egorov, D. M. Makarov, and A. M. Kolker, Russ. J. Gen. Chem. 80, 1267-1275 (2010).

[96] C. M. Kinart, M. Klimczak, W. J. Kinart, J. Mol. Liq. 145, 8 13 (2009).

[97] K. Kiyosawa, BBA. 1064, 251-255. (1991).

[98] R. Sharma, R. C. Thakur, H. Kumar, Physics and chemistry of liquids, 57, 1-12 (2018).

[99] K. Bhakri, N. Chakraborty, K.C. Juglan, H. Kumar, R. Sharma, J Therm Anal Calorim., 148(14), 7185-205 (2023).

[100] P. Kaur, K. C. Juglan, H. Kumar, M. Singla, Braz. J. Chem. Eng. 40, 1213–1226 (2023).

[101] K. Bhakri, M. Lamba, K.C. Juglan, N. Chakraborty, J. Mol. Liq., 15; 406, 125117 (2024).

[102] R. Rodriguez-Melendez and J. Zempleni, J. Nutr. Biochem.14, 680-690 (2003).

[103] J. Zempleni and D. M. Mock, J. Nutr. Biochem. 10, 128-138 (1999).

[104] A. Thakur, J.C. Juglan, H. Kumar and K. Kaur, J. Mol. Liq. 288, 111014 (2019).

[105] E. Zorebski, M. Dzida, M. Cempa, J. Chem. Eng. Data. 53, 1950–1955 (2008).

[106] J. Zhang, P. Zhang, K. Ma, F. Han, G. Chen, X. Wei, Sci. China Ser. B: Chem. 51, 420−426 (2008).

[107] K. Anand, D. Pal, R. Hilgenfeld, Acta Crystallogr. Sect. D. 58, 1722–1728 (2002).

[108] R. Neerup, P.L. Fosbol J. Solution Chem. **54**, 1595 (2025).

[109] N. Dhanorkar and A.B. Dhote, The Bioscan **20**(SI-2), 128 (2025).

[110] M. Leonard and B.H. Milosavljevic, Phys. Chem. Chem. Phys. (2025).

[111] A. Rezaei and A. Jouyban, Liquids **5**(1), 5 (2025).

CHAPTER 2

REVIEW OF LITERATURE

This chapter provides an overview of the existing research relevant to the present study. It begins by summarizing the fundamental concepts of molecular interactions, hydrogen bonding, and hydration effects in organic acids and glycols. The review then highlights key findings from previous ultrasonic, volumetric, and acoustic investigations on similar systems, with particular attention to their applications in food and pharmaceutical formulations. Gaps and limitations in the available literature are identified, thereby establishing the need and justification for the current work.

Hammes and Lewis (1966) [1] had tested the sound velocity and absorption in polyethylene glycol solutions. The Zimm theory is used to analyse viscosity in polymer solutions across several frequencies, concentrations and temperatures demonstrating that viscous relaxation is not present.

Hammes and Schimme (1967) [2] determined the ultrasonic attenuation of polyethylene glycol solutions over the molecular weight range in the presence and absence of a synthetic polymer. The relaxation time is not dependent on the concentration across the entire spectrum of molecular weights, although it does increase with molecular weight.

Kessler *et al.* (1970) [3] had investigated the ultrasonic absorption spectra of polyethylene glycol in aqueous solution. Across a wide frequency range, several relaxation mechanisms have been identified. The presence of bulk viscosity was explored since the observed ultrasonic absorption was not considered by shear visco-elasticity.

Morenas and Douheret (1978) [4] By examining the excess and partial molar characteristics of a few glycol and water mixes, the thermodynamic behaviour of the mixtures was investigated. At different temperatures, the density of pure glycols and binary mixes was determined using a Y-shaped pycnometer in a thermostat water bath. Densities of pure liquids and liquid mixtures were utilised to determine ‘partial molar volume’ and ‘excess molar volume’. The variations from optimum mixing volumes

were found to be negative. Excess values for monoethylene glycol-water combinations were also shown to be temperature dependent.

Bohne *et al.* (1984) [5] described the thermo-physical characteristics of binary ethylene glycol and water mixes, including thermal conductivity, density, and viscosity. To test thermal conductivity, density, and viscosity, a concentric cylinder device, a digital density metre, and an Ubbelohde viscometer were utilised. Using observed experimental data, Prandtl-numbers were computed.

Bagchi *et al.* (1986) [6] evaluated the density, absolute viscosities, and ultrasonic velocity of ISRO polyol solutions employed by the Indian Space Research Organization. It's been tested in a variety of solvents. The solvation number is observed to be greater in strongly hydrogen-bonded liquids.

Juni and Nakano (1987) [7] have investigated the use of polyhydroxyacids in drug administration, including lactic acid and glycolic acid homo- and copolymers, poly-beta-hydroxybutyric acid and polycaprolactone. They also investigated the polymers' physicochemical characteristics such as biodegradability and biocompatibility, as well as in vitro and in vivo evaluations of various dosage forms made using the polymers.

Hout *et al.* (1988) [8] studied the thermodynamics of ethylene glycol with water at temperatures of 5, 25, and 450 degrees Celsius. The micro calorimeter and flow densimeter were used to calculate acoustical characteristics such as isobaric heat capacity and densities. The computed density data was used to estimate the excess and apparent characteristics, as well as the partial molar properties. The hydroxyl group has a negative influence, resulting in negative excess values; on the other hand, the methylene group has a positive impact, resulting in positive contribution. Exothermic mixing of water-ethylene glycol had considerably overcome by interactions involving the hydroxyl group of ethylene glycol, according to the quantity of excess enthalpies.

Rao *et al.* (1990) [9] investigated the acoustic properties of polyvinyl pyrrolidone mixes with N, N-dimethyl formamide solutions. The density measurements were done with a pycnometer. The Ostwald's viscometer was used to measure viscosity. The presence of solvent-solute interaction was demonstrated by studies of refractive index, viscosity, and ultrasonic velocity on PVP-DMF solutions.

Lee *et al.* (1990) [10] observed excess molar quantities for ternary as well as binary

combinations of methanol, ethylene glycol and water. At various temperatures, the densities of four systems (ethylene glycol (EG) + methanol), (water + ethylene glycol (EG)), (water + methanol), and (water + ethyleneglycol (EG) + methanol) were determined using Anton Paar DMA.

Douheret *et al.* (1991) [11] tested densities, isobaric heat capacities, and ultrasonic velocities for binary EG/water mixtures at variety of temperatures. Using ρ and v data, the 'isentropic compressibility' and 'the additional molar volume' were computed. The results were also used to calculate isobaric and isentropic expansivities.

Hunt *et al.* (1992) [12] have done a trial to evaluate the effectiveness and skin acceptance of the alpha hydroxy acid gluconolactone 14 percent in solution (NuvodermTM lotion) in the care of mild to milder acne were analyzed, and it was contrasted to 5 percent benzoyl peroxide lotion. It was discovered that 14 percent gluconolactone lotion is successful as a topical acne treatment. Gluconolactone is as effective in minimizing the amount of inflamed and complete lesions as benzoyl peroxide, however it is somewhat less effective at lowering the amount of non-inflamed lesions.

Rajulu and Sab (1995) [13] examined the sound velocity and density of polyethylene glycol and a combination of water at a temperature of 30°C. The variation of the various parameters such as the van der Waals constant (b), Rao number (R), `molar compressibility(β), specific acoustic impedance and adiabatic compressibility (βad) have been analyzed with respect to mole ratio.

Magazu *et al.* (1997) [14] used ultrasonic methods to determine ρ and v of α-α-trehalose in aqueous solutions. The findings revealed that these aqueous solutions lacked an appropriate mixing procedure. The excess of compressibility's behaviour as a function of concentration was attributed to the fact that at high levels of concentrations, the α-α-trehalose molecules form intramolecular hydrogen bonds.

Ali *et al.* (1999) [15] measured the viscosities, densities, and sound velocity of pure '1-octanol, ethanol, acetonitrile, N, N-dimethylformamide, & 1-hexanol' The association molecule's éxcess-adiabatic compressibility, volume, (Lf)intermolecular fee length, acoustic impedance, and viscosity at constant temperature, have all been determined.

Henni *et al.* (1999) [16] measured the viscosity and density of triethylene glycol monomethyl ether experimentally. They used Helper's technique of research, which further indicates that adding water had no influence on the structure of triethylene glycol monomethyl ether. For Grunberg-Nissan, positive values were calculated.

Baluja and Oza (2001) [17] are two individuals who have collaborated on a project. For methanol, anisole + dimethyl foramide, and anisole + chloroform, determined Gibb's free energy, specific impedance, excess molar volume, isentropic compressibility, molar sound velocity, excess viscosity (η_E), and various basic parameters.

Orge *et al.* (2001) [18] calculated values from experiments of sound velocity (v), density(ρ) and refractive index of methanol/acetone with propylene glycol, ethylene glycol, 3-methyl, 1-butanol, 1, 3-propanediol, 2-methyl, 1 propanol comprising mole fraction with respect to atmospheric pressure and temperature. From the experimentally calculated speed of sound and density, several excess parameters after mixing were determined.

Sastry and Patel (2003) [19] computed the relative permittivities, densities, viscosities, and ultrasonic velocity of alkyl acetates + glycols at different temperatures. To match all of these deviation functions, a Ṛedlich-Kister equation is utilised. The values of sound velocity in these mixes are determined using collision factor theory.

Yan *et al.* (2004) [20] had examined the impact of temperature on the volumetric properties of certain amino acids in an aq. calcium chloride solution. At temperatures of 278.15, 288.15.298.15, and 308.15K, the viscosity and density of certain amino acids in a calcium chloride solution were calculated. The apparent molar characteristics of amino acids and their viscosity β coefficients were determined. At diverse temperatures, hydration number and standard partial molar volume have been determined. The activation free energy was calculated using theory of transition state. Viscosity data was used to investigate the influence of amino acid structure.

Schmelzer *et al.* (2004) [21] had determined sound velocity and density for mixes of water and polyethylene glycols. Using Laplace's equation, a new acoustical characteristic, namely adiabatic compressibility, was derived from the experimental data.

Bernstein *et al.* (2004) [22] had shown that PHA gluconolactone defends against Ultraviolet radiation elastin enhancer activation, and Gluconolactone provided up to 50% UV protection in our in vitro system while having little effect on sunburn cells in human skin.

Syal *et al.* (2005) [23] studied and evaluated the viscosity, sound velocity, and density of PEG solutions in water and with Acetonitrile at constant temperature. The density, velocity, and viscosity measurements collected from the experiment were utilised to determine the various acoustical characteristics.

Zwirbla *et al.* (2005) [24] computed the sound densities and velocities for mixes of water+ EG+ PEG 200, 400, and the adiabatic compressibilities using Laplace's equation.

Kumar and Rao (2007) [25] examined and evaluated the and v, viscosity, ρ of a combination of methanol and ethanol with aqueous propylene glycol. Excess adiabatic compressibility, excess viscosity, excess free volume, viscous relaxation time, excess free length, and excess molar volume were among the thermodynamical and acoustical characteristics discovered. Rao's sound velocity relation, Jacobson's equation, and impedance relation were all tested using the experimental data.

Ayranci and Sahin (2008) [26] had determined density and velocity of polyethylene glycol and ethylene glycols. Numerous parameters were evaluated and represented graphically.

Green, Edison and Sigler (2008) [27] undertook a research project to evaluate the effectiveness of topical lactobionic acid (LA) 8% to minimize visible signs of ageing skin on the face and to assess histologic and dermal thickness changes on the arm during 12 weeks of controlled usage, and it was discovered that Lactobionic acid benefits all layers of the skin, including the stratum corneum, epidermis, and dermis. Furthermore, it is non-irritating, non-stinging, and hydrating. It's also a powerful antioxidant.

Palani and Geetha (2009) [28] measured the density, viscosity, and ultrasonic velocity of water + PG, glycol + dimethylformamide, water + PG, glycol+ tetrahydrofuran, water+ propylene glycol 1,4-dioxane and water+ PG, glycol + dimethylsulphoxide as a function of composition and temperature. Several

thermodynamic characteristics were calculated using experimental data.

Green *et al.* (2009) [29] have shown that class of Hydroxyacid compounds have unrivalled skin advantages and cosmeceutical market use in both cosmetic and therapeutic formulations. These are antiaging formulations, moisturisers, and peels, as well as therapy treatments to improve hyperpigmentation. Additionally, they have antioxidant/chelation, barrier-strengthening properties. Bionic acids counteract the ageing process by inhibiting matrix metalloproteinase enzymes in the skin.

Shanmuga *et al.* (2010) [30] investigated density, the viscosity, and ultrasonic velocity of solutions containing Methylmethacrylate+2- Ethoxy ethanol, Methylmethacrylate +2- Methoxy ethanol, and Methylmethacrylate+2 Butoxy ethanol. Experimental data is used to determine adiabatic compression, internal pressure, Gibbs free energy values, and free volume.

Nithiyanantham and Palaniappan (2010) [31] had calculated the viscosity, density, and ultrasonic velocity of the ternary system of galactose with α-amylase in aqueous medium at 303 K. Several acoustic properties were also calculated to analyse the molecular interactions of the mixture. He had confirmed the existence of weak interactions by the observed excess values.

Kornhauser *et al.* (2010) [32] had investigated hydroxy acids'(Has) diverse important uses, categorization, processes and photoactivity. They have also proved that HAs been used in cosmetic formulations as well as various dermatological uses, including the treatment of acne, photoaging, rosacea, ichthyosis, psoriasis, and pigmentation disorders.

Kostov *et al.* (2010) [33] had done investigation in which Lactobionic acid (LA) was compared to glycolic acid in terms of efficacy and irritation potential in gel and emulsion carriers and had proved that LA-containing samples generated improved skin performance, notably in terms of skin irritation and skin barrier damage. LA and GA have showed improved efficacy when used in vehicles based on a novel APG emulsifier, highlighting the relevance of the vehicle in the effects of topical actives.

Thirumarran and Rajeshwari (2011) [34] had determined the sound velocity, density and viscosity of aromatic hydrocarbon and chlorobenzene mixes with DMSO (dimethylsulphoxide). The experimental data was used to determine the

acoustic parameters.

Palani et al. (2011) [35] measured the ultrasonic velocity, viscosity, and density of arginine in three different aqueous disaccharide solutions: maltose, galactose, and lactose (0.3m) at 298.15K. Using experimental values, various acoustic and thermodynamic parameters were estimated for all ternary systems, and the outcomes were discussed in the context of ion-solvent intumescence.

Nithiyanantham and Palaniappan (2012) [36] measured the basic parameters such as density, viscosity and ultrasonic velocity of binary monosaccharide systems containing glucose, galactose, and fructose in environment at 298.15 K. They evaluated the molar sound compressibility, adiabatic compressibility, internal pressure, free length, relative association, free volume, acoustical impedance, and molar sound velocity. The results were explained using molecular interactions among the constituents of the combination.

Godhani *et al.* (2012) [37] investigated viscosity, ultrasonic velocity, and density of chloroform, N-N dimethyl formide and solutions of 2-((4-acetyl-5-(2-hydroxyphenyl)-5-methyl-4,5-dihydro-1,3,4-oxadiazol-2-yl) methylthio)-3-o-tolyquinazolin-4(3H)-1 (PD1-C) in CF and DMF are determined at different temperature and atmospheric pressure. Using these experimental results, several thermodynamic parameters were calculated.

Pathak *et al.* (2012) [38] used epoxy resin solutions to evaluate the viscosity, density, and ultrasonic speed of different solvents, including THF, chloroform, and 1,4-dioxane, at constant temperature. Several thermodynamic parameters were calculated.

Kornhauser *et al.* (2012) [39] looked at the impact of various skin compounds containing hydroxyacids and similar things, as well as their use in cosmetic products on sun-exposed skin. Stress was paid to the protection of these compositions, especially the long-term consequences of their use on skin mostly exposed to sun. They also demonstrated that, contrary to popular belief, the effects of medicated hydroxyacids are not restricted to their keratolytic characteristics.

Alonso *et al.* (2013) [40] had looked at current developments and research in lactobionic acid (LA) bio-production, either by microbial or enzymatic techniques, and had highlighted key bioprocessing factors for better bio-production. There were

also comprehensive overviews of existing microbial cell producers and lactobionic acid downstream production technologies. The relevance of LA as a significant base in the growth of novel medications, nanoparticles, biological materials, and polymer systems were also investigated, with a focus on the polyhydroxy acid's prospects and current applications.

Kaur and Juglan (2013) [41] utilised a gravity bottle, an ultrasonic interferometer, and a viscometer to determine the density, ultrasonic speed, and viscosity of mixture of liquid acetic acid and polyvinyl acetate at a frequency of 2MHz and a constant temperature of 295K. The experimental figures were used to determine numerous thermodynamic and acoustic parameters. The variations in the parameters suggest that the mixture contains a binding interaction. As the concentration grows, so does the velocity.

Pal and Kundu (2013) [42] investigated the attenuation constant (α) and velocity (v) of ultrasonic waves travelling through aqueous sodium chloride solution at room temperature at frequencies of 1MHz and 2MHz (250 C). The velocity (v) and attenuation constant (α) rise as the concentration increases, implying that the ions and water molecules in the solution have a stronger bond.

Das *et al.* (2013) [43] examined sodium nitroprusside sound velocity and density in solutions including ethylene glycol, CH_3OH, n-propanol, DMSO, and solvents at a constant temperature. The parameters and constants for the experiment were derived from the data.

Pal *et al.* (2013) [44] used DSA and investigated the, viscosity, ρ and v of a binary mixture of 1,4-dioxane, 1-propanol, 2-propanol, 1-butanol, and 2-butanol under atmospheric pressure at various temperatures and concentrations. The experimental results are required to evaluate the excess molar concentration, KES, and excess molar volume. Different parameters and their infinite dilution limits were computed based on the experimental density data.

Pal *et al.* (2013) [45] used a DSA to measure ultrasonic speeds and densities in liquid mixtures comprising dimethyl ether, dipropylene glycol, methyl acetate, n-butyl acetate, and ethyl acetate at various temperatures and pressures.

Bhavani *et al.* (2013) [46] used Rao's specific velocity connection, Van Dael mixing

relation, Nomoto's relation, impedance relation, and Jungie's theory to estimate ultrasonic velocities. The theoretical values were compared to the empirical facts.

Dhonge *et al.* (2013) [47] At different temperatures and molalities, researchers looked at the sound speed, refractive index, density and viscosity of thiamine hydrochloride and pyridoxine hydrochloride aqueous solutions. The experimental values were used to calculate number of thermodynamic parameters.

Dixit *et al.* (2014) [48] used ultrasonic method at a constant temperature of 289K to evaluate the viscosity, density, and velocity of liquid mixes of water, n-butanol, and acetic acid ($C_4H_9OH + H_2O + CH_3COOH$) at various concentrations. Vander Waal constant, β, relaxation time, adiabatic impedance, free intermolecular length ultrasound attenuation, volume present, effective molecular weight, Wada constant, molar volume, free energy, Rao constant, Gibb's enthalpy, and internal pressure were all calculated using the obtained values.

Kumari *et al.* (2014) [49] used an ultrasonic interferometer to evaluate the viscosity, density, and ultrasonic velocity of a tyrosine derivative made using non-aqueous dimethyl sulpho oxide (DMSO) at a constant temperature of 290K. These essential parameters were used to compute the results. The nonlinear fluctuations were calculated using these values, indicating that the solute and solvent molecules have just a weak contact.

Kumar *et al.* (2014) [50] used a combination of acoustic and volumetric measures to study the interactions of L-valine and L-alanine, amino acids glycine, at various temperatures and pressures in binary sodium dihydrogen phosphate solutions.

Kaur and Juglan (2015) [51] used an ultrasonic interfering device, a 30 ml bottle of viscosimeter, and an Oswald viscometer at 2MHz at constant temperature of 295K to measure the viscosity, ultrasonic velocity, and density of a liquid combination of chloroform and methanol. The experimental results were then utilised to calculate mole mass, free intermolecular length, adiabatic compression, acoustic impedance, relaxation time, molecular weight volume, constant Wada, ultrasonic attenuation, intrinsic pressure constant, free energy, and Gibb's enthalpy.

Wananjea *et al.* (2015) [52] investigated ultrasonic velocity and other acoustic characteristics for aqueous polypropylene glycols at room temperature, including free

length, adiabatic compressibility, acoustic impedance, and viscous relaxation time. In terms of concentration and structural dynamics, ultrasonic velocity, free length, acoustic impedance, relaxation time, and adiabatic compressibility have all been computed and analyzed for the given system. With the increased concentration of water PPG-425 in the region, the variation in acoustic characteristics was discovered to be more complicated.

Kaur and Juglan (2016) [53] used an ultrasonic interferometer to calculate the viscosity, ρ and v of binary liquid mixes of ethyl acetate and hexane at a constant temperature of 292K and a frequency of 2MHz. The experimental results are then utilised to calculate acoustic impedance, adiabatic compressibility, ultrasonic attenuation, viscosity, internal pressure, free volume, free intermolecular length, Gibb's free energy and enthalpy, among other acoustic characteristics.

Kumar *et al.* (2016) [54] examined the ultrasonic speed, v, and densities (ρ) of aqueous solutions containing mono methyl ether, ethylene glycol, in sodium dodecyl sulphate solutions at different temperatures. From density data, many characteristics are computed, including transfer volume, partial molar stretch ability, limiting visible molar and V_{ϕ}. The molar volume values of all alkoxyalkanols drops when sodium dodecyl sulphate concentration rises, but these values rise as sodium dodecyl sulphate concentration rises.

Sarkar *et al.* (2016) [55] investigated pyridoxine hydrochloride density and viscosity in 'aqueous tetrabutylammonium hydrogen sulphate (TBAHS)' at various concentrations and temperatures. Various thermodynamical and acoustical characteristics were computed using these experimental results.

Marczyk *et al.* (2016) [56] compared the lipid layer of the epidermis in Acne Vulgaris patients after their treatment with 50% Lactobionic Acid, Corundum Microdermabrasion, and a combined effect of both. The treatments led to a substantial decrease in sebaceous secretion, as indicated by the data. The most substantial diminution was observed in patients who were administered lactobionic acid (LA), which is structurally like alpha-hydroxy acids and possesses exfoliating properties.

Kaur *et al.* (2017) [57] investigated the velocity and density of EG, DEG, TEG in sorbitol (aqueous) of various molalities at various temperatures. Different

thermodynamic and acoustic parameters were computed from the experimental values.

Kaur *et al.* (2018) [58] studied PEG 400 and PEG 4000 in sorbitol at 0.1 MPa and various temperatures for determining sound speed and density, along with apparent and partial molar properties. The calculated value of speed and ρ of the mixture is further used to compute several other thermodynamic parameters.

Chakraborty *et al.* (2018) [59] used DSA 5000M to measure the velocity and density of glycols with biologically dynamic D-panthenol as a temperature dependent using a combination of acoustic & volumetric matter at (T=293.15, 298.15, 303.15, 308.15), and different thermodynamic characteristics were determined using the obtained data of densities and velocities. The theoretical values (ion-hydrophilic and hydrophilic-hydrophilic interaction) were discovered, and the interaction extent increased as the amount of D-panthenol and the molar mass of the glycols is increased.

Kaur *et al.* (2018) [60] examined the velocity and density of (EG), (DEG), and (TEG) in glycerol at (0.00, 0.01, 0.03, 0.05) molalities at variety of temperatures and a constant pressure (0.01 MPa). Several thermodynamic and Acoustic characteristics were computed from the experimental data.

Kaur *et al.* (2018) [61] investigated the v and density, along with the apparent and partial molar characteristics of PEG 400 and 4000 in glycerol at various temperatures. Different acoustic and thermodynamic parameters were also measured from investigational data.

Sharma *et al.* (2018) [62] studied the viscosity, velocity, and density of L-ascorbic acid in the presence of D-lactose and D-fructose at various temperatures.

Kaur *et al.* (2018) [63] investigated the density and velocity of aniline in the presence of (EG), (DEG), and (TEG) at different temperatures. Different acoustical and thermodynamical parameters were determined from the experimental values to analyze the molecular interactions between them.

Lomesh *et al.* (2018) [64] investigated the conductance, sound's speed, and densities of DSS in water and water-soluble sorbitol at various molalities of 0.002, 0.004, 0.006 $mol.kg^{-1}$ solutions at different temperatures and atmospheric pressures. Different acoustic and thermodynamic properties were computed by using experimental collected data.

Olivieri *et al.* (2018) [65] investigated the properties of lactobionic acid (LA) as a potential component of artificial tears using in vitro and in vivo experimental model systems. The results of their research indicate that LA, whether it contains HA, favours WH in vitro and in vivo. The WH test indicated that the combination of 4 percent LA and 0.15 percent HA in the rabbit cornea resulted in a reduced increase in MMP-9 and TGF-b levels in corneal tissue and tears. Lastly, the development of cultured bacterial isolates was slowed by the addition of 4% LA.

Rani *et al.* (2019) [66] examined the viscometry along with volumetric characteristics of L-arginine and L-serine in thiamine hydrochloride mediums at various temperatures. Different acoustic and thermodynamic variables were computed from the experimental values.

Vuksanovic *et al.* (2019) [67] evaluated the density, viscosity, and refractive index of polypropylene glycol mixed with toluene, o-xylene, m-xylene, and p-xylene at various temperatures and pressures. Excess molar volumes were estimated from the experimental data, and variations in refractive index and viscosity were determined. To investigate non-ideal behavior of the analyzed mixes, excess Gibbs free energy was calculated and fitted using a Redlich-Kister polynomial.

Mirheydari *et al.* (2019) [68] investigated the sound speed, density, and viscosity of diethylene glycol monoethyl ether caritol, water ethanol, and N, N-dimethylformamide at various temperatures and constant pressures of 0.0868 MPa. The various thermodynamic and partial parameters were all computed to analyze the interactions between them.

Cardoso *et al.* (2019) [69] discussed existing LBA manufacturing techniques, patents connected to the acid, broad usage and rules, research findings, future scenarios, and an explanation of the food industry's challenges in integrating the acid into their products are all included.

Kantikosum et al. (2019) [70] examined the impact of cosmeceutical products containing glycolic acid (GA) and salicylic acid (SA) on mild to moderate acne vulgaris. Lactic acid, licochalcone, and gluconolactone were also evaluated as supportive treatments alongside adapalene. The results showed that while combining these cosmeceuticals with adapalene did not enhance therapeutic effectiveness

compared to adapalene alone, it did help reduce side effects. Importantly, the study reported no adverse effects when cosmeceuticals were used with standard acne treatment.

Thakur *et al.* (2019) [71] explored ρ and v of PG and HG in (MePB–MeOH) were at temperatures varying($293.15K$ to $308.15K$) and at a constant pressure of 0.1 MPa to assess the nature of the connection between EG, PG, and HG. The calculated ρ and v were utilized to find different apparent properties in the binary solvent.

Jain and Juglan (2020) [72] used an effective ultrasonication technique to employ NMP as a base liquid for the suspension of GO nanoparticles. The created nanosuspension was tested for stability using DLS. This nanosuspension was utilised to investigate a variety of thermoacoustic variables. The velocity of the samples was determined by the interferometer, the density of the GO-NMP nanosuspension was assessed by the pycnometer, and the viscosity of the nanosuspension was determined by the rotating viscometer. All of these experiments were conducted at temperatures of 298 to 313 K were used.

Abbot and Sharma (2020) [73] observed quercetin binary solution sound speed at varied concentrations and temperatures. Density data determines compressibility, standard enthalpy, apparent molar volume, entropy change, and Gibb's energy. There was hydrophobic contact in the combination.

Chakraborty et al. (2020) [74] evaluated thermo-acoustic parameters such as isentropic compression, apparent and partial molar volume estimated by v values, and density at variant temperatures (293.15-308.15) K. In a solution of nicotinic acid with hexylene glycol and propylene glycol, their research led them to the conclusion that the ternary mixture exhibits robust interaction.

One study by **Sharma et al. (2020) [75]** investigated and examined streptomycin sulphate and aqueous cosolute solutions at various temperatures and compositions to find their apparent molar volumes, isentropic compressibility, and relative viscosities. The Falkenhagen coefficient and transfer parameter were calculated using the viscosity data. In addition to measuring the absorption spectra with a UV-visible spectrophotometer, the research calculated streptomycin sulphate's solvation behaviour.

In **2020, Palaniappan et al. [76]** studied the thermo-acoustical characteristics from the experimental investigation are used to examine the real nature of molecular interaction. These parameters include molar volume, β, L_f, free volume, inner stress, their additional values. Here, we incorporate the critical standard values of each component. To accurately estimate the azeotropic formation and determine its mole fraction, it is helpful to consider the existence of the cautioned interaction.

Brinzei et al. (2020) [77] offered updated information on the ρ and viscosity of L-serine and L-valine in solutions of sodium chloride. The qualities were evaluated throughout a range of salt concentrations and temperature points. The criteria of solute-solvent interactions and structural effects were used to identify and assess the derived characteristics and activation parameters. A discussion of the mixture's amino acids' structure-making and -breaking capabilities followed the data' interpretation using the co-sphere overlap model.

Chakraborty et al. (2021) [78] deals with the analysis of the molecular interactions among the glycol's molecules in biotin at constant experimental pressure 0.1 MPa and temperature range (288.15 K to 318.15 K). The v and ρ for the liquid mixtures is measured and numerous thermodynamic and acoustic parameters are determined using these obtained data.

Richu et al. **(2021) [79]** tested Thiamine hydrochloride and L-ascorbic acid in binary aqueous 1-ethyl-3-methylimidazolium hydrogen sulphate media to determine their characteristics. Using six different temperatures and the ambient pressure, physical and thermophysical characteristics were estimated.

Amirchand et al. (2021) [80] studied the molecules of saccharide at two different temperatures in a solution of water and calcium salts. Evaluated volumetric properties and interactions affecting taste behaviour. They discovered that hydrophobic interactions were the most common. An existence of hydrophobic-ionic connections was demonstrated by 1H NMR.

Patnaik et al. (2022) [81] investigated the combinations of PEG 200/400 and D-panthenol in liquid form for their densities and ultrasonic velocities at varying concentrations and temperatures. Quantifying the ternary mixture's intermolecular processes and determining its thermodynamic and acoustic properties were both aided

by the examination of experimental data.

Masilo et al. (2022) [82] measured thermophysical properties such as ρ, v, refractive index, and surface tension at temperatures (293.15 to 333.15) K and pressures of 0.1 MPa to examine the molecular interactions of binary mixtures of acetophenone with carboxylic acids like acetic and propionic acid. To gain insight into the chemical interactions present in the binary mixes, the thermodynamic characteristics were computed.

Pantanaik et al. (2022) [83] investigated ionic liquids based on imidazolium in water and citrate salts under varying pressure and temperature conditions. Compressibility and apparent molar volume were determined using spectroscopic, acoustic, and volumetric data. To study the interactions between solutes and solvents, we also assessed transfer properties. The results showed that most molecular interactions were hydrogen bonds and that ionic liquid was able to structure solutions.

Bandral et al. (2022) [84] In this experiment, glycine and glycylglycine were tested in varying concentrations in water-based betaine hydrochloride for their density, ultrasonic velocity, and viscosity. A multitude of rheological, viscosity, molar, and transfer characteristics, as well as other volumetric and compressibility metrics, were computed. The ability of each solute to shatter structures was also tested.

Sharma et al. (2022) [85] investigated the interactions between D-maltose and D-lactose in the presence of trisodium citrate in water at temperatures (293.15 to 313.15) K and pressures of 0.1 MPa. Molar volume and compressibility were among the several parameters computed from density and sound speed observations. The findings indicate that the ternary systems involve distinct intermolecular interactions, whereas Hepler's constant verifies that the solute is capable of breaking structural bonds.

Devi et al. (2022) [86] examined solute-solvent interactions together with volumetric, acoustic, and viscometrical properties. They employed experimental density to assess volumetric factors and utilized the speed of sound to determine compressibility metrics. They additionally computed pair and triplet coefficients, along with viscosity data. The researchers examined the role of the solute as either a structure creator or breaker by employing Hepler's constant and the initial temperature derivative of the B-coefficient.

Singh et al. (2023) [87] investigated the efficacy of several aqueous ethanol combinations as solvents for aspirin with low water solubility. Experimental measurements of solution densities at different temperatures were performed. Supplementary parameters demonstrated robust interactions between solute and solvent in the solutions. Favourable values for multiple metrics indicated strong interactions and structural improvement due to aspirin. Hepler's constant further corroborated the structural effects of aspirin. The research validated interactions among ionic, polar, and nonpolar constituents in the solutions.

Kaur et al. (2023) [88] looks at the interactions between PG and HG in hexachlorophene at various temperatures, pressures up to 0.1 MPa. Thermodynamic properties are computed in addition to the mixes' densities and sound velocities. Based on the apparent molar parameters, the results show that the solute and solvent in the ternary mixture have substantial interactions.

Amirchand et al. (2023) [89] reported the thermodynamic study of L-ascorbic acid (AA) in L-histidine (L-His) solutions which uncovered robust hydrophilic-ionic interactions, we can learn more about ascorbic acid's solvation pattern in food from these interactions.

Kaur et al. (2023) [90] measured the ρ and v of EG, DEG, TEG at different temperatures and pressures as they interacted with a chloroxylenol-methanol combination. It was from these values that the V_ϕ, V_ϕ° compressibility was computed. They also calculated empirical constants and partial molar expansibility.

Castro et al. (2023) [91] investigated the density, sound speed, thermal conductivity, and viscosity of $[C_{12}mim]$ $[(CF_3SO_2)_2N]$ within temperature (293.15 to 343.15) K and with a pressure of 0.1 MPa. The results showed that both the ionanofluid with graphene and $[C_{12}mim]$ $[(CF_3SO_2)_2N]$ were Newtonian fluids, which helped stabilize the nanoparticle dispersed in the nanofluid.

Nikode et al. (2023) [92] studied glycol-based binary mixtures using ultrasonic and physicochemical parameters. They observed a decrease in ultrasonic velocity with temperature due to weakened hydrogen bonding, validating the use of acoustic methods for characterizing molecular interactions in polar mixtures.

Verma et al. (2024) [93] investigated, the molecular interactions of propanol and n-butylamine mixtures. Excess isentropic compressibility, excess molar volume, v deviation was all examined. The secondary qualities such as apparent, partial, excess partial properties were all inferred. Chemical engineers and those working to optimize industrial processes can benefit from these results, which provide light on the thermodynamic and acoustic aspects of amine-alcohol combinations.

Godhani et al. (2024) [94] measured ultrasonic velocities, densities, and viscosities in a binary liquid mixture containing pyrimidine-substituted azetidinone at different temperatures. The properties of the mixture, including density, dynamic viscosity, and sound velocity, were also studied, using molecular interactions to explain the findings.

Lamba et al. (2024) [95] estimates the V_ϕ and K_ϕ of EG, DEG, TEG in trisodium EDTA mixture using measured experiments and Fourier transform infrared spectroscopy. It also investigates the interactions among three glycol's and EDTA in the mixture.

Sharma et al. (2024) [96] measured the densities, v in L-phenylalanine and glycyl-L-phenylalanine with 1-decyl-3-methylimidazolium bromide. The experiment revealed a range of acoustic and physicochemical properties, including apparent and partial molar properties, compression and transfer properties.

Das et al. (2024) [97] reviewed molecular interactions research using an ultrasonic/ultrasonic technique. They used an ultrasonic interferometer to measure ultrasonic wave velocity, liquid density, and viscosity, analysing acoustic and thermodynamic properties, providing a detailed explanation of measured parameters.

Ansari et al. (2024) [98] analyzed polar liquid mixtures through ultrasonic and thermophysical techniques, finding notable associative and dissociative molecular interactions. The results highlighted ultrasonic velocity as a sensitive tool for probing solute–solvent behavior in multicomponent systems.

Nidhi and Nain (2024) [99] studied binary mixtures of *N,N-dimethylacetamide* with polyethylene glycols between 293.15–323.15 K using ultrasonic and volumetric methods. They observed strong dipole–dipole and hydrogen bonding interactions that varied with temperature, showing that glycols act as structure-making components in polar solvents due to their hydroxyl functionality.

S.Bhathley (2024) [100] performed acoustic and spectroscopic analysis of glycol-based liquid mixtures to understand molecular interactions. The study reported that variations in glycol chain length and polarity significantly affect ultrasonic parameters, confirming hydrogen bonding and molecular association as key contributors to the acoustic behavior of such mixtures.

Gill et al. (2025) [101] studied the ρ, c in mixture, including sodium benzoate, water, lactic acid/malic acid. The study revealed various volumetric and acoustical properties, including V_ϕ, apparent specific volume, V_ϕ°, transfer properties, and thermal expansion coefficient. This research offers insights into molecular interactions and structural behaviour.

Das et al. (2025) [102] investigated the molecular interactions between polyethylene glycol (PEG) and ethanol at different concentrations using ultrasonic techniques. They evaluated key acoustic parameters and found that higher PEG concentrations increase molecular interactions, leading to increased acoustic impedance and decreased adiabatic compressibility. As temperature rises, these interactions weaken, resulting in reduced acoustic impedance and altered thermodynamic properties. The molecular interaction was examined using an ultrasonic method.

Panda et al. (2025) [103] examined density, viscosity, and ultrasonic velocity to calculate thermoacoustical parameters. Ultrasonic methods have been used to study polymer molecular interactions as a function of temperature, concentration, and frequency. The viscosity (η), density (d), and ultrasonic speed (U) of polymer dextran and aqueous 6(M) urea were tested at 5 K intervals from 303 K to 323 K.

Gill (2025) et al. [104] examined the ultrasonic and thermodynamic behavior of glycolic acid and lactobionic acid in aqueous sodium benzoate systems. They measured density and sound velocity over a range of concentrations and temperatures to calculate volumetric and acoustic parameters. To interpret solute–solvent interactions, they employed interaction coefficients along with the co-sphere overlap theory. Nevertheless, their work remained limited, as it did not address the influence of charge distribution in complex acids.

Choudhary (2025) et al. [105] investigated Density, sound velocity, and FTIR analyses which revealed strong solute–solvent interactions in sodium salicylate +

$KCl/NaHCO_3$ mixtures, with $NaHCO_3$ showing a greater structure-making effect. Temperature rise weakens interactions, while pair/triplet coefficients confirmed complex structural changes relevant to pharmaceutical and industrial applications.

A.A. Firdaus (2025) [106] explored ultrasonic and volumetric properties of glycols mixed with aqueous potassium sorbate. Deviations in excess parameters indicated strong hydrogen bonding between glycol hydroxyl groups and carboxylate ions of the preservative, with interaction strength depending on both glycol chain length and temperature.

The following summary table **Table-2.1** includes some of the recent references which summarize the system studied, technique used, major findings and research gap/significance.

Table 2.1 Summary table of recent Literature References

Ref. No.	System Studied	Technique Used	Major Findings	Research Gap / Significance
[94]	Aqueous glycol + acid systems	Ultrasonic and thermodynamic study	Reported strong associative interactions governed by hydrogen bonding	Limited concentration range; requires expansion to multi-component systems
[95]	Ionic and polar liquid mixtures	Density and sound velocity	Observed structure-breaking effects at higher temperatures	Molecular dynamics validation needed
[96]	Polyhydroxy acid + water systems	Ultrasonic velocity, viscosity, and density	Confirmed molecular association due to H-bonding	Did not include temperature-dependent modeling
[97]	Glycol-based binary mixtures	Acoustic and volumetric measurements	Explained temperature influence on excess parameters	Constrained to limited thermodynamic models

Ref. No.	System Studied	Technique Used	Major Findings	Research Gap / Significance
[98]	Aqueous acid + glycol systems	Density, viscosity, ultrasonic velocity	Identified non-ideal behavior and strong solute–solvent interactions	Lack of comparison with theoretical predictions
[99]	Polar organic solvents	Microwave-assisted and thermodynamic analysis	Demonstrated interaction energy variation with composition	Study restricted to limited solvent types
[100]	Aqueous polyhydroxy compound mixtures	Ultrasonic and calorimetric analysis	Showed consistent variation of adiabatic compressibility with temperature	Data interpretation could be extended to multicomponent systems
[101]	Aqueous glycolic acid + polyol systems	Acoustic and volumetric study	Reported strong specific interactions; temperature-dependence evident	More detailed analysis of intermolecular free length required
[89]	Aqueous glycol + acid solutions	Ultrasonic velocity and density	Found structure-making tendency of solutes in water-rich region	Study lacks molecular interaction modeling
[90]	Binary and ternary glycolic acid systems	Thermodynamic and acoustic methods	Observed temperature-dependent variation in excess properties	Future work suggested on temperature and compositional effects

Although numerous studies have been conducted, considerable ambiguities and debates remain regarding hydration phenomena, solute–solvent interactions, and compressibility, particularly in ternary liquid systems containing glycols and polyhydroxyacids. Much of this uncertainty stems from the dynamic and cooperative behavior of hydration shells, where water molecules continuously exchange between bulk and bound states, making it challenging to accurately define hydration numbers or the precise shell structure. Moreover, while hydration plays a pivotal role in explaining

solute–solvent behavior, the molecular basis of reduced compressibility around solutes is still not completely understood. Some researchers attribute this effect to restricted water dynamics, whereas others point to ion-specific electrostriction or co-sphere overlap phenomena. Within this framework, measurements of density and ultrasonic velocity provide a highly sensitive and reliable means of exploring solute–solvent as well as solute–solute interactions. Despite valuable findings, comprehensive insights into temperature-dependent excess properties and molecular interactions in multicomponent aqueous polyhydroxy acid systems remain scarce. Therefore, the present work aims to bridge this gap by systematically exploring the thermodynamic and acoustic properties of such systems over an extended range of compositions and temperatures.

Research Gap

While glycols are widely utilized in diverse industrial sectors such as pharmaceuticals, food, and cosmetics, and polyhydroxy acids (PHAs) are increasingly recognized for their applications in skincare and therapeutic formulations, their combined behavior in aqueous environments has not been adequately studied. Previous research has largely concentrated on the interaction of glycols with alcohols, amino acids, or other functional molecules, providing valuable insights into solvation dynamics and hydrogen bonding. However, systematic investigations on glycol–PHA mixtures, especially in ternary aqueous systems, are scarce. The lack of studies addressing how variations in temperature, pressure, and composition influence their physicochemical properties—such as density, sound velocity, compressibility, and molecular association—creates a significant knowledge gap. Understanding these parameters is essential, as they directly govern molecular interactions, stability, and compatibility in complex formulations. Without such insights, the development of optimized products in formulation science, particularly in pharmaceuticals and personal care, remains limited. Thus, a comprehensive study of glycol–PHA systems is crucial for advancing both theoretical understanding and practical applications.

References

[1] G.G Hammes and T.B. Lewis, J. Phys. Chem. 70, 1610-1614 (1966).

[2] G.G. Hammes and P.R. Schimme, J. Am. Chem. Soc. 89, (1967).

[3] L.W. Kessler et al., J. Phys. Chem. 74, 4096-4102 (1970).

[4] M. Morenas and G. Douheret, Thermochim. Acta 25, 217–224 (1978).

[5] D. Bohne, S. Fischer and E. Obermeier, Ber. Bunsenges. Phys. Chem. 88, 739-742 (1984).

[6] S. Bagchi, S.K. Nema and R.P. Singh, Eur. Polym. J. 22, 851-857 (1986).

[7] K. Juni and M. Nakano, Crit. Rev. Ther. Drug Carrier Syst. 3, 209-232 (1987).

[8] J.Y. Huot, E. Battistel, R. Lumry, G. Villeneuve, J.F. Lavallee, A. Anusiem and C. Jolicoeur, J. Solution Chem. 17, 601-636 (1988).

[9] K.C. Rao, S.V. Naidu and A.V. Rajulu, Eur. Polym. J. 26, 657-659 (1990).

[10] H. Lee, W.H. Hong and H. Kim, J. Chem. Eng. Data 35, 371-374 (1990).

[11] G. Douheret, A. Pal, H. Hoiland, O. Anowi and M.I. Davis, J. Chem. Thermodyn. 23, 569-580 (1991).

[12] M.J. Hunt and R.S. Barnetson, Australas. J. Dermatol. 33, 131-134 (1992).

[13] A.V. Rajulu and P.M. Sab, Bull. Mater. Sci. 18, 247-253 (1995).

[14] S. Magazu, P. Migliardo, A.M. Musolino and M.T. Sciortino, J. Phys. Chem. B 101, 2348-2351 (1997).

[15] A. Ali, S. Hyder and A.K. Nain, J. Mol. Liq. 79, 89-99 (1999).

[16] A. Henni, P. Tontiwachwuthikul, A. Chakma and A.E. Mather, J. Chem. Eng. Data 44, 101-107 (1999).

[17] S. Baluja and S. Oza, Fluid Phase Equilib. 178, 233-238 (2001).

[18] B. Orge, B.E. de Cominges, G. Marino, M. Iglesias and J. Tojo, Phys. Chem. Liq. 39, 99-116 (2001).

[19] N.V. Sastry and M.C. Patel, J. Chem. Eng. Data 48, 1019-1027 (2003).

[20] Z. Yan, J. Wang, W. Kong and J. Lu, Fluid Phase Equilib. 215, 143-150 (2004).

[21] C.E.H. Schmelzer et al., J. Mol. Struct. 699, 47-51 (2004).

[22] E.F. Bernstein et al., Dermatol. Surg. 30, 189–196 (2004).

[23] V.K. Syal, A. Chauhan and S. Chauhan, J. Pure Appl. Ultrason. 27, 61-69 (2005).

[24] W. Zwirbla et al., J. Mol. Struct. 743, 49-52 (2005).

[25] D.S. Kumar and D.K. Rao, Indian J. Pure Appl. Phys. 45, 210-220 (2007).

[26] E. Ayranci and M. Sahin, J. Chem. Thermodyn. 40, 1200–1207 (2008).

[27] B.A. Green, B.L. Edison and M.L. Sigler, Cosmet. Dermatol. 21, 76-82 (2008).

[28] R. Palani and A. Geetha, Phys. Chem. Liq. 47, 542–552 (2009).

[29] B.A. Green, R.J. Yu and E.J.V. Scott, Clin. Dermatol. 27, 495–501 (2009).

[30] P. Shanmuga, S. Nithya, G. Velraj and A.N. Kanappan, Int. J. Adv. Sci. Technol. 18, (2010).

[31] S. Nithiyanantham and L. Palaniappan, Asian J. Chem. 22, 5413-5418 (2010).

[32] A. Kornhauser, S.G. Coelho and V.J. Hearing, Clin. Cosmet. Investig. Dermatol. 3, 135–142 (2010).

[33] M.T. Kostov et al., J. Cosmet. Dermatol. 9, 3–10 (2010).

[34] S. Thirumarran and M. Rajeshwari, Arch. Phys. Res. 2, 149-156 (2011).

[35] R. Palani, G. Srinivasan and B. Geeta Lakshmi, Int. J. ChemTech Res. 3, 284-289 (2011).

[36] S. Nithiyanantham and L. Palaniappan, Arab. J. Chem. 5, 25–30 (2012).

[37] D.R. Godhani, P.B. Dobriya, A.M. Sanghani and J.P. Mehta, Arab. J. Chem., (2012).

[38] U.G. Pathak, J.V. Patel and P.H. Parsania, J. Solution Chem. 41, 755–765 (2012).

[39] A. Kornhauser, S.G. Coelho and V.J. Hearing, Dermatol. Res. Pract. *2012*(1), 710893 (2012).

[40] S. Alonso, M. Rendueles and M. Díaz, Biotechnol. Adv. JBA-06680, 17 pages (2013).

[41] B. Kaur and K.C. Juglan, J. Polym. Eng. 33, 851 (2013).

[42] B. Pal and S. Kundu, J. Chem. *arXiv preprint arXiv:1206.2779* (2013).

[43] M. Das, S. Das, and A.K. Pattanaik, J. Chem. 2013, 942430 (2013).

[44] A. Pal, H. Kumar, B. Kumar and R. Gaba, J. Mol. Liq. 187, 278 (2013).

[45] A. Pal, H. Kumar, R. Maan and H.K. Sharma, J. Solut. Chem. 42, 1988 (2013).

[46] M.D. Bhavani et al., Int. Lett. Chem. Phys. Astron. 10, 1 (2013).

[47] S.S. Dhondge, D.W. Deshmukh, L.J. Paliwal, J. Chem. Eng. Data 58, 149 (2013).

[48] A. Dixit, K.C. Juglan and A. Sharma, J. Chem. Pharm. Res. 6, 93 (2014).

[49] S. Kumari, K.C. Juglan and A. Sharma, J. Chem. Pharm. Res. 6, 782 (2014).

[50] H. Kumar, M. Singla and R. Jindal, Monatsh. Chem. 145, 1063 (2014).

[51] K. Kaur and K.C. Juglan, Der Pharma Chem. 7, 160 (2015).

[52] K.H. Wananjea, K.B. Kabarab, A.C. Kumbharkhane and A.V. Sarodeb, Bionano Front. 8, 381 (2015).

[53] K. Kaur and K.C. Juglan, J. Chem. Pharm. Res. 8, 49 (2016).

[54] H. Kumar, K. Kaur, S. Arti and M. Singla, J. Mol. Liq. 221, 526 (2016).

[55] A. Sarkar, B.K. Pandit, B. Sinha, J. Chem. Thermodyn. 103, 36 (2016).

[56] B. Marczyk, P. Mucha, H. Rotsztejn and E. Budzisz, J. Cosmet. Dermatol. Sci. Appl. 6, 156 (2016).

[57] K. Kaur, K.C. Juglan, H. Kumar, J. Chem. Eng. Data 62, 3769 (2017).

[58] K. Kaur, I. Behal, K.C. Juglan, H. Kumar, J. Mol. Liq. 268, 700 (2018).

[59] N. Chakraborty, H. Kumar, K. Kaur, K.C. Juglan, J. Chem. Thermodyn. 126, 137 (2018).

[60] K. Kaur, I. Behal, K.C. Juglan, H. Kumar, J. Chem. Thermodyn. 125, 93 (2018).

[61] K. Kaur, K. C. Juglan, H. Kumar, J. Chem. Thermodyn. 127, 8 (2018).

[62] R. Sharma, R. C. Thakur, H. Kumar, Phys. Chem. Liq. 57, 1 (2018).

[63] K. Kaur, K. C. Juglan, H. Kumar, J. Chem. Eng. Data 63, 3237 (2018).

[64] S. K. Lomesh, M. Bala, D. Kumar, I. Kumar, J. Chem. Thermodyn. (2018).

[65] M. Olivieri, M. Cristaldi, S. Pezzino, G. Lupo, C. D. Anfuso, C. Gagliano, C. Genovese, D. Rusciano, Cornea 0, 1 (2018).

[66] R. Rani, A. Kumar, T. Sharma, T. Sharma, R. K. Bamezai, J. Chem. Thermodyn. 135, 260 (2019).

[67] J. Vuksanovic, D. Soldatovic, I. Radovic, Z. Višak, M. Kijevcanin, J. Chem. Thermodyn. 131, 393 (2019).

[68] S. N. Mirheydari, Md. B. Jalali, B. Golmohamadi, H. Shekaari, F. Martinez, A. Jouyban, J. Chem. Eng. Data 64, 1425 (2019).

[69] T. Cardoso, C. Marques, J. L. A. Dagostin, M. L. Masson, J. Food Sci. 84, 1672 (2019).

[70] K. Kantikosum, Y. Chongpison, N. Chottawornsak, P. Asawanonda, Clin. Cosmet. Investig. Dermatol. 12, 151 (2019).

[71] A. Thakur, K. C. Juglan, H. Kumar, K. Kaur, J. Mol. Liq. 288, 111014 (2019).

[72] A. Jain, K. C. Juglan, Int. J. Mech. Prod. Eng. Res. Dev. 10, 8555 (2020).

[73] V. Abbot, P. Sharma, Chem. Phys. 538, 110921 (2020).

[74] N. Chakraborty, K. C. Juglan, H. Kumar, ACS Omega 5, 32357 (2020).

[75] S. K. Sharma, A. Thakur, D. Kumar, V. Nathan, J. Mol. Liq. 297, 111941 (2020).

[76] L. Palaniappan, S. Nithiyanantham, J. Mol. Liq. 312, 113423 (2020).

[77] M. Brinzei, O. Ciocirlan, J. Chem. Thermodyn. 154, 106335 (2021).

[78] N. Chakraborty, K. C. Juglan, H. Kumar, J. Mol. Liq. 337, 116605 (2021).

[79] Richu, A. Kumar, J. Chem. Eng. Data 66, 3859 (2021).

[80] K. D. Amirchand, S. Kaur, T. S. Banipal, V. Singh, J. Mol. Liq. 334, 116077 (2021).

[81] P. Patnaik, N. Chakraborty, P. Kaur, K. C. Juglan, H. Kumar, Adv. Funct. Smart Mater. 403, 424 (2022).

[82] K. Masilo, I. Bahadur, J. Chem. Thermodyn. 166, 106667 (2022).

[83] S. S. Pattanaik, B. Nanda, S. R. Panda, B. Dalai, B. B. Nanda, J. Mol. Liq. 351, 118644 (2022).

[84] A. Bandral, A. Kumar, J. Mol. Liq. 348, 118081 (2022).

[85] P. Sharma, S. Sharma, M. Sharma, Chem. Thermodyn. Therm. Anal. 6, 100051 (2022).

[86] S. Devi, U. Syal, C. Sharma, M. Kumar, N. Sawhney, A. K. Sharma, M. Sharma, J. Mol. Liq. 354, 118842 (2022).

[87] S. Singh, K. Dhal, M. Talukdar, Mater. Today: Proc. (2023).

[88] P. Kaur, N. Chakraborty, K. C. Juglan, H. Kumar, M. Singla, S. Afr. J. Chem. Eng. (2023).

[89] K. D. Amirchand, T. S. Banipal, Y. L. Yang, V. Singh, J. Mol. Liq. 370, 120839 (2023).

[90] P. Kaur, K. C. Juglan, H. Kumar, M. Singla, Braz. J. Chem. Eng. 1, 14 (2023).

[91] C. A. N. Castro, A. Lamas, X. Paredes, A. F. Santos, I. M. S. Lampreia, F. J. V. Santos, M. J. V. Lourenco, T. A. Graber, J. Chem. Eng. Data (2023).

[92] N.B. Nikode, U.P. Manik and P.L. Mishra, Int. J. Phys. Appl. 5, 44 (2023).

[93] S. Verma, M. Rani, H. Song, S. Maken, Phys. Chem. Liq. 1, 15 (2024).

[94] D. R. Godhani, U. P. Mehta, A. H. Saiyad, J. Solut. Chem. (2024).

[95] M. Lamba, N. Chakraborty, K. C. Juglan, M. Singla, Chem. Thermodyn. Therm. Anal. 13, 100129 (2024).

[96] R. Sharma, I. Bahadur, M. Gautam, M. M. S. Abdullah, S. Singh, K. Tumba, Ionics 30, 1653 (2024).

[97] N. Das, M. K. Praharaj, S. Panda, J. Mol. Liq. 403, 124841 (2024).

[98] S.N.A. Ansari, U.P. Manik and P.L. Mishra, World J. Adv. Res. Rev. 21, 1602 (2024).

[99] N. Nidhi and A.K. Nain, Discover Chemistry 1, 7 (2024).

[100] S. Bhathley, N. Chakraborty, and K.C. Juglan, Chemical Thermodynamics and Thermal Analysis 16, 100147 (2024).

[101] A. K. Gill, N. Chakraborty, K. C. Juglan, Chem. Phys. Impact 100843 (2025).

[102] N. Das, S. Panda, and M.K. Praharaj Chem. Thermodyn. Therm.100169 (2025).

[103] S. Panda Curr. Microw. Chem. (2025)

[104] A.K. Gill, N. Chakraborty, K.C. Juglan, Int. J. Thermophys. 46, 46 (2025).

[105] M.H. Choudhary, N. Chakraborty, K. C. Juglan, R. Kamboj, A. H. Syed, Chemical Physics 598,112804 (2025).

[106] A. A. Firdaus, N. Chakraborty and K.C. Juglan, International Journal of Thermophysics 46, 1-44 (2025).

CHAPTER 3

OBJECTIVES AND EXPERIMENTAL PROCEDURES

3.1 Objectives of the research

Polyhydroxy acids (organic acids) and glycols (alcohols) are well known for their capacity to form hydrogen bonds and display pronounced hydration effects, properties that make them highly useful in enhancing taste, stability, and bioavailability. Examining the molecular interactions in such systems not only deepens our understanding of their physicochemical properties but also carries important practical significance. For example, insights derived from volumetric and acoustic studies can aid in designing more stable and efficient preservative systems, extend shelf life, improve sensory qualities in food products, and support the formulation of excipients in pharmaceuticals. In addition, the thermodynamic data obtained enriches predictive models in solution chemistry, offering benefits for both applied and fundamental research. The present study investigates how these systems respond to temperature changes, employing ultrasonic methods to measure density and sound velocity. Since this specific mixture has not been previously examined, the work contributes novel findings to the field of ultrasonic analysis. To do this analysis, we have finalized the following **objectives of the research work:**

I. To determine the ultrasonic velocity and density of mixture of glycols and aqueous polyhydroxy acids (PHAs) at different temperatures and concentrations.

II. To study different thermodynamic and acoustic parameters of the liquid mixture of polyhydroxy acids and glycols by calculating different properties from the experimental data.

III. To investigate and analyse different forms of intermolecular interactions between the aqueous solutions of the above liquid mixtures at varied compositions and temperatures.

3.2 Experimental procedure

The ultrasonic velocity and density of a tertiary liquid combination was studied using the DSA instrument by Anton Paar, Model 5000 M. The mixture will include glycols of varying concentrations throughout a range of molalities, as well as aqueous solutions of water-soluble polyhydroxy acid.

3.2.1 Chemicals

Three types of Polyhydroxy acids (PHAs)—gluconolactone, galactose, and lactobionic acid—as well as some glycols, including EG, DEG, TEG, PG, HG, and PEGs of different molecular masses (PEG-200/400/4000), were employed in the study as chemicals in both binary and ternary solution form. Each of these compounds has a molecular mass of 178.14, 180.156, 358.296, 62.07, 106.12, 150.18, 76.09, 118.17, 200, 400 and 4000 g/mol respectively. The various chemicals which have been utilized in my research are tabulated in **Table 3.1** along with their chemical formula, 2D and 3D structures. The **Table 3.2** shows the specifications of the compounds used in the research along with their details like their CAS no., molecular mass, source, appearance, purification method and their mass fraction purity as provided by the supplier.

Table 3.1 Detailed list of chemicals used.

CHEMICAL NAME	CHEMICAL FORMULA	2D STRUCTURE	3D STRUCTURE
POLYHYDROXY ACIDS			
Gluconolactone	$C_6H_{10}O_6$	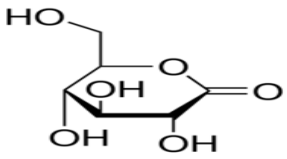	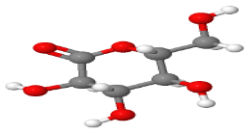
Galactose	$C_6H_{12}O_6$	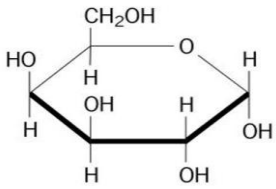	

Lactobionic acid	**$C_{12}H_{22}O_{12}$**	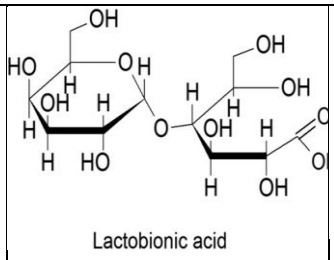 Lactobionic acid	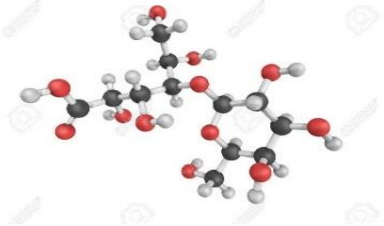
GLYCOLS			
Triethylene Glycol	**$C_2H_6O_2$**		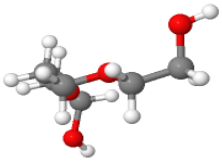
Ethylene glycol	**$C_4H_{10}O_3$**	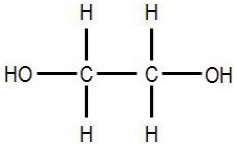	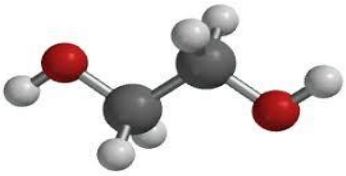
Diethylene Glycol	**$C_6H_{14}O_4$**	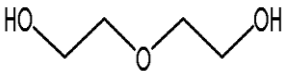	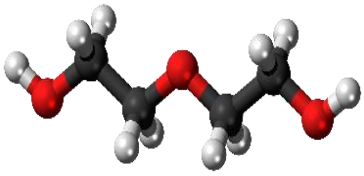
Propylene glycol	**$C_3H_8O_2$**	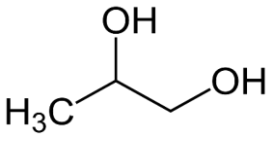	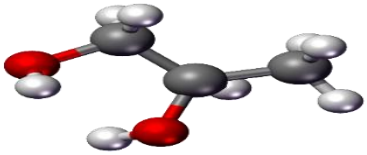
Hexylene glycol	**$C_6H_{14}O_2$**	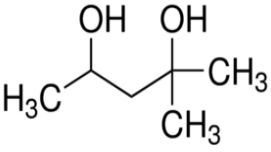	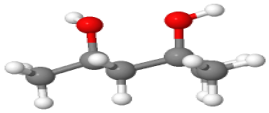

Polyethylene glycol 200	**$HO(C_2H_4O)_nH$**	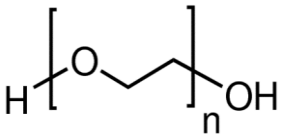	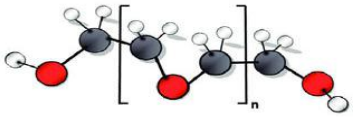
Polyethylene glycol 400	**$HO(C_2H_4O)_nH$**	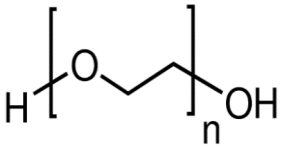	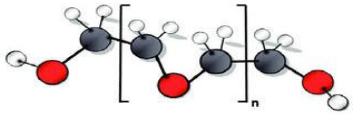
Polyethylene glycol 600	**$HO(C_2H_4O)_nH$**	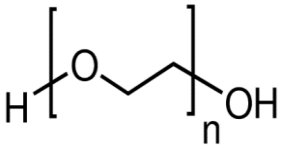	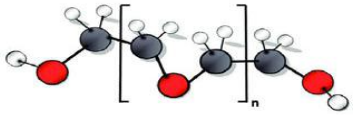
Polyethylene glycol 4000	**$HO(C_2H_4O)_nH$**	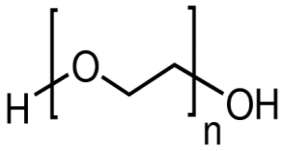	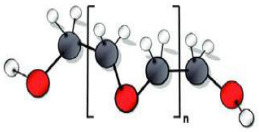

Table 3.2 Specifications of the Chemicals used

S.No.	Compound Name	Chemical Abstracts Service Registry Number	Molecular mass (in g.mol^{-1})	Chemical bought from	Procedure for purification	Purity of mass fraction (as per supplier)	Appearance
1.	Gluconolactone (GLA)	90-80-2	178.14	Sigma-Aldrich Chem. Private Ltd, India	Dried out in a vacuum	≥ 0.99	White crystalline powder
2.	Lactobionic Acid (LBA)	96-82-2	358.30			≥ 0.98	White crystalline powder
3.	Ethylene Glycol (EG)	107-21-1	62.07	Central Drug House (P) Ltd.		≥0.99	Colorless (viscous) liquid
4.	Diethylene Glycol (DEG)	111-46- 6	106.12	S.D. Fine Chemical Limited. India		≥0.98	Colorless (viscous) liquid
5.	Triethylene Glycol (TEG)	112-27-6	150.18	Qualigens Fine Chemicals		≥0.98	Colorless (viscous) liquid
6.	Galactose (GAL)	59-23-4	180.156	Loba Chemie Pvt. Ltd. India		≥0.99	White Amorphous powder
7.	Propylene Glycol (PG)	57-55-6	76.09			≥0.99	Colorless (slightly viscous) liquid

8.	Hexylene Glycol (HG)	107-41-5	118.17		Dried out in a vacuum	≥0.99	Colorless (viscous) liquid
9.	PEG-200	25322-68-3	200			≥0.99	Colorless (viscous) liquid
10.	PEG-400	25322-68-3	400			≥0.99	Colorless (viscous) liquid
11.	PEG-600	25322-68-3	400			≥0.99	Colorless (viscous) liquid
12.	PEG-4000	25322-68-3	4000			≥0.99	White waxy or flaky solid

3.2.2 Preparations

We have used the different chemicals listed in **Table 3.2.** For each experiment, we utilized freshly made, triple-distilled, degassed water that had a specific conductance of 10^{-6} Scm^{-1}. After being vacuum dried, the compounds are further purified by storing them in desiccators over P_2O_5 for a duration of two days. A highly precised weighing balance: 'Sartorius CPA 225D' was utilized to precisely measure all the liquid samples, which were then placed in borosilicate glass vials with tightly fitting lids to prevent any interference or water intrusion, as seen in **Figure 3.1**. The balance had an accuracy of ±0.00001g. To account for the effects of time on the measurements, freshly made samples were measured on the same day using a syringe. We have made a number of samples for different concentrations and molalities. The different problems done during the research are shown in **Table 3.3**.

Figure 3.1 Weighing Balance (Sartorius CPA 225D) and samples in glass vials

Table 3.3 Number of Problems done during the research.

Section -I	
Problem-1	
"Thermodynamic behaviour and physicochemical characteristics of EG, DEG, TEG in aqueous gluconolactone solutions"	
Solvent	**Solute**
Gluconolactone + water +	EG
	DEG
	TEG
Problem-2	
"Understanding of lactobionic acid in aqueous-glycol mixtures at different temperatures: Ultrasonic investigation"	
Solvent	**Solute**
Lactobionic Acid + Water +	Polyethylene glycol-200/
	Polyethylene glycol-400
Section -II	
Problem-3	
"An Investigation to Display Galactose's Physico-Chemical Behaviour with PEGs: A Thermo-Acoustical Study"	
Solvent	**Solute**
Galactose + Water +	Polyethylene glycol-400/
	Polyethylene glycol-600
Problem-4	
"An Investigation of The Effects of Glycols on The Thermodynamic and Acoustic Parameters of Polyhydroxy Acid at Different Temperatures"	
Solvent	**Solute**
Lactobionic acid + water	Polyethylene glycol-200/
	Polyethylene glycol-400
Section-III	

<table>
<tr><th colspan="2">Problem-5</th></tr>
<tr><td colspan="2">“Exploration of the Molecular Interactions between Polyhydroxy acid: Gluconolactone and Glycols: ‘A Thermoacoustic Method”</td></tr>
<tr><td>Solvent</td><td>Solute</td></tr>
<tr><td rowspan="2">Gluconolactone + Water +</td><td>Polyethylene glycol-400/</td></tr>
<tr><td>Polyethylene glycol-4000</td></tr>
<tr><th colspan="2">Problem-6</th></tr>
<tr><td colspan="2">“Exegesis of molecular interactions of mixes comprising Polyethylene glycol-4000 and Polyhydroxy acids (PHAs)”</td></tr>
<tr><td>Solvent</td><td>Solute</td></tr>
<tr><td>Gluconolactone +water +</td><td rowspan="3">Polyethylene glycol-4000</td></tr>
<tr><td>Galactose + water +</td></tr>
<tr><td>Lactobionic acid + water +</td></tr>
<tr><th colspan="2">Section-IV</th></tr>
<tr><th colspan="2">Problem-7</th></tr>
<tr><td colspan="2">“Ultrasonic Investigation of Molecular Interactions in Glycols & Polyhydroxyacids Aqueous Solutions”</td></tr>
<tr><td>Solvent</td><td>Solute</td></tr>
<tr><td rowspan="2">Galactose + Water +</td><td>Propylene glycol</td></tr>
<tr><td>Hexylene glycol</td></tr>
<tr><th colspan="2">Problem-8</th></tr>
<tr><td colspan="2">Volumetric and acoustical studies of glycols with water-soluble lactobionic acid solutions at different temperatures</td></tr>
<tr><td>Solvent</td><td>Solute</td></tr>
<tr><td rowspan="2">Lactobionic acid + water +</td><td>Propylene glycol</td></tr>
<tr><td>Hexylene glycol</td></tr>
</table>

3.2.3 Measurements

Densities (ρ) and velocities (c) in the ternary mixes were assessed by means of DSA at four diverse temperatures, at fixed frequency- 3 MHz, and consistent pressure- 0.1 MPa. A syringe is used to introduce the sample into the apparatus. The apparatus has a temperature controller that keeps the sample temperature within ±0.001 K and operates with remarkable precision. With temperature increments of 10 K, the temperature range (in K) observed at experimental pressure was 288.15 K to 318.15 K. As advised by the manufacturer, the DSA 5000 M was first calibrated and then used. Once this calibration is complete, the sample attributes may be measured with certainty. To create solutions of various molalities, a weighing instrument by Sartorius, Model- CPA 225D with a uncertainty of ±0.00001g was employed. The given purities provide a typical relative uncertainty in molality of $u_r(m) = 0.01$. An uncertainty of ±1.0 $mol.kg^{-1}$, ±0.15 $kg.m^{-3}$, and ±1.0 $m.s^{-1}$ was noted for the observed molality of the mixes, ρ, and v, respectively. Based on the data collected, we were able to infer the behavior of the mixes and the interactions between the components across the specified temperature range. Specific parameters are computed using the data gathered, and the acoustical parameters are acquired by experimental measurements. [1-6]

Various combinations of the glycols and PHAs as stated in **Table 3.3** have been made and then they were taken into study to check their behaviour on mixing with each other. The **Table 3.4** shows comprehensive flow chart summarizing all experiments and their corresponding objectives has been included to provide a clear and systematic overview of the entire research methodology. **Figure 3.2** shows the figure abstract of the whole methodology.

Table 3.4 Comprehensive Flow Chart of Experimental Work & Objectives

1. Sample Preparation:
- Selection of glycols & PHAs
- Prepare ternary mixtures
- Analytical balance (±0.00001 g)
- Prepare solutions of various molalities
Objective: Accurate mixture preparation for molecular interaction studies.
2. Calibration of Instruments:
- Anton Paar DSA 5000 M calibrated
Objective: Ensure accurate density (ρ) & velocity (c) measurements.
3. Experimental Measurements:
- Frequency: 3 MHz | Pressure: 0.1 MPa
- Temperature: 288.15–318.15 K (±0.001 K)
- Density uncertainty: ±0.15 $kg \cdot m^{-3}$
- Velocity uncertainty: ±1.0 $m \cdot s^{-1}$
Objective: Record precise thermophysical data across temperatures.
4. Data Processing:
- Compute acoustical and thermodynamic parameters.
Objective: Understand molecular interactions & structure.
5. Interpretation & Analysis:
- Study temperature effects & mixing behavior
- Identify interaction trends
Objective: Conclude structural and thermodynamic behavior of mixtures.

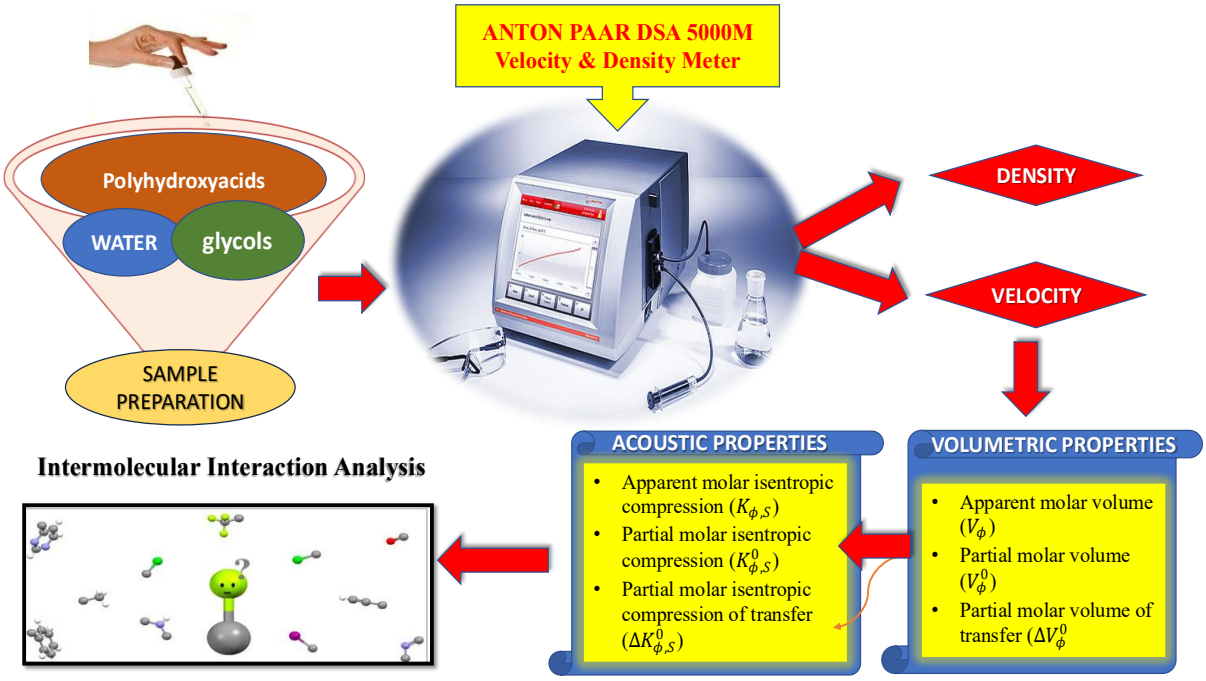

Figure 3.2 Methodology of the research.

3.3 Instrumentation

3.3.1 Anton Paar DSA 5000M

The highly accurate density and velocity analyser, DSA 5000 M by 'Anton Paar' was employed to ascertain the ρ and v of aqueous mixture of PHAs (Gluconolactone, galactose, and lactobionic acid) and their combinations with glycols, including (EG), (DEG), (TEG), (PEG-200), (PEG-400), (PEG-600), (PEG 4000), (PG), and (HG). Initially, 2-3 ml of the samples contained in the vials are individually introduced into the borosilicate U-tube of the density-velocity analyser using a syringe, as seen on the screen of densimeter in **Figure 3.3**. The **Figure 3.3 (left)** displays the instrument's measurement screen, showing the recorded density, sound velocity, and temperature of the sample during analysis and **figure 3.3 (right)** shows the sample loading setup of the Anton Paar DSA 5000 M, where the liquid sample is injected into the instrument using a syringe connected to the inlet tube.

Figure 3.3 DSA 5000 M Density and Velocity Meter from Anton Paar

The gadget records density and velocity and stores them in its memory. The operation and principles of the "Anton Paar DSA 5000 M" are explicitly detailed in Chapter 1, Section 1.4 (Density and Sound Velocity Analyzer). This equipment has cells for measuring density and pulse-echo speed of sound, with an inbuilt Pt 100 thermometer as seen in **Figure 3.4**, which concurrently estimate two physically independent variables: density and sound speed from a single sample.

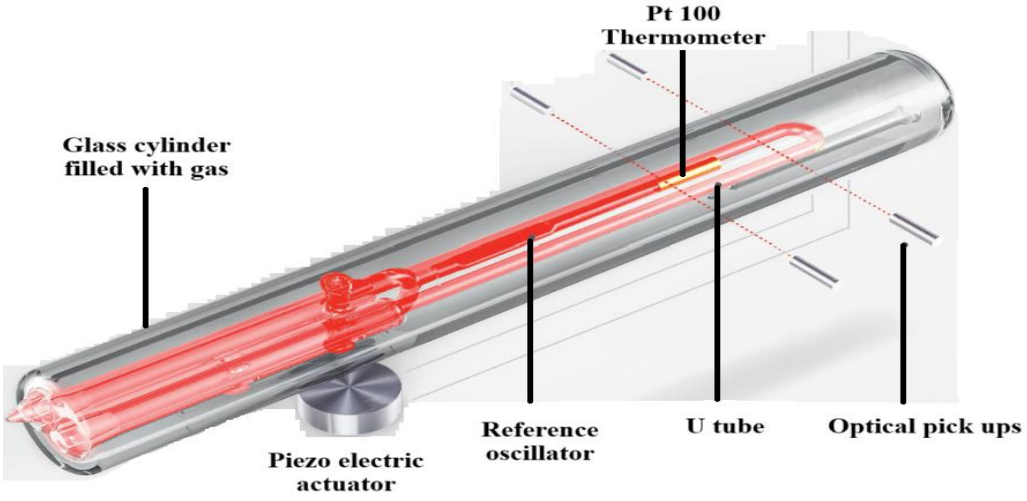

Figure 3.4 Inside view of U-tube

The temperature is controlled by an integrated thermostat within both measuring cells, which are made of stainless steel. A temperature control accuracy of 0.001 K is achieved by combining two Peltier components with integrated (Pt 100) platinum thermometers. This device employs the oscillating U-tube principle. The calibration, insertion, and cleaning procedure consist of five steps, as illustrated in **Figure 3.5**. Following each use, the measuring cells were cleaned with water and ethanol. A built-in pump was employed to remove excess liquid after the sample was extracted from the tube, followed by the measurement. The gadget was fine-tuned using varying temperatures of degassed air and double-distilled water before each set of measurements. Previous results corroborated the water's sound densities and velocities. The device is capable of detecting changes in pressure from 0 to 0.3 MPa, sound velocities from 1000 to 2000 ms^{-1}, and densities from 0 to 3 $g \cdot cm^{-3}$.

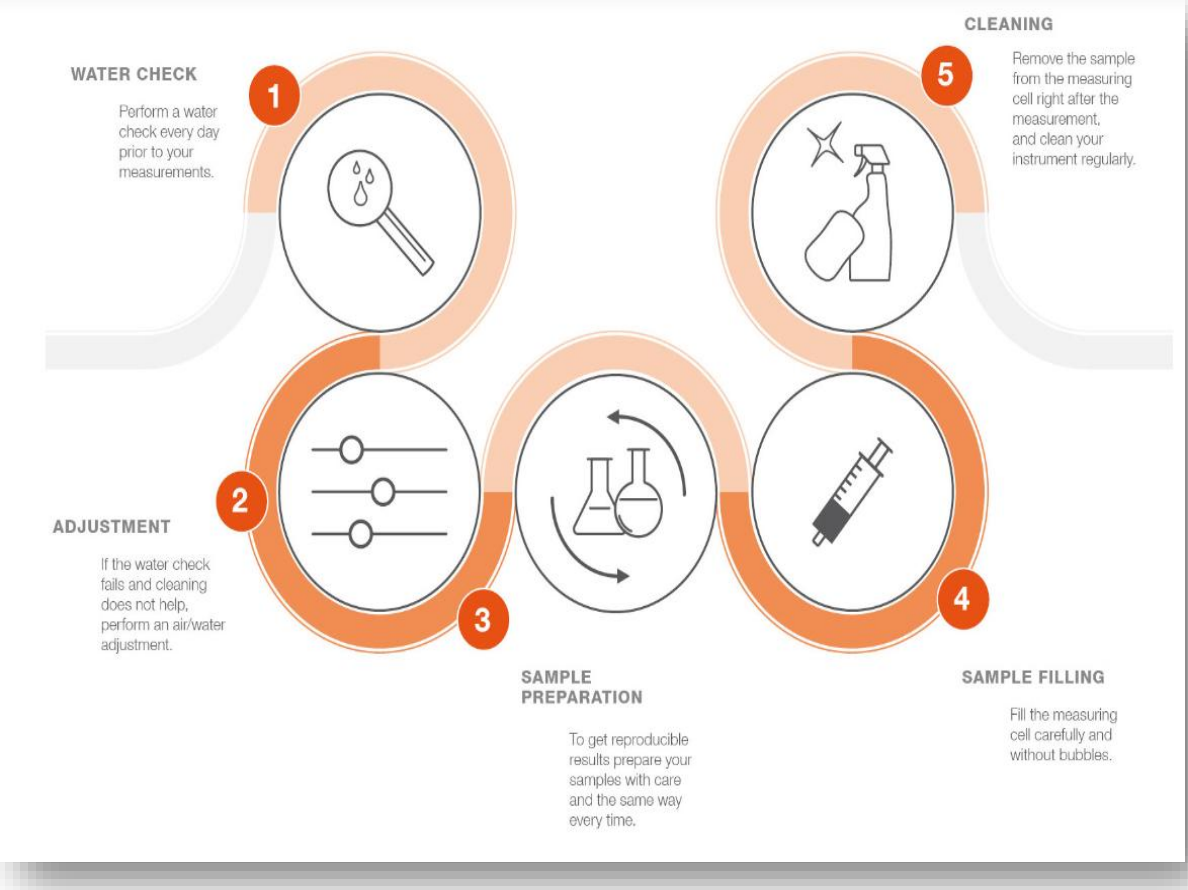

Figure 3.5 Five main aspects for accurate density and velocity measurement

3.4 Various Ultrasonic Parameters

3.4.1 Acoustic impedance (Z)

A medium's impedance, is the resistance it offers to an ultrasonic wave's propagation through it, and is equal to the product of its density (ρ) and its ultrasonic velocity (v). Sound travels through a wide variety of materials under the sound pressure. Put another way: Consider the challenge of propelling a ball through a dense mud versus a shallow puddle. It is more difficult for the ball (sound wave) to traverse the dense soil due to its increased resistance (higher acoustic impedance). The acoustic impedance is lower in the shallow puddle. In essence, it stands for the opposition to the transmission of sound waves. It is represented by Z. Numerically it is expressed as:

$$Z = \rho \times v \tag{1}$$

3.4.2 Adiabatic compressibility (β)

The compressibility of adiabatic phenomena is represented by symbol; β. As we are using the term adiabatic so, in the absence of both internal and external heat flows, it is defined as the ratio of volume loss to pressure increase. Changes in compressibility in a liquid media may be calculated using the following thermodynamic relation:

$$\beta = \frac{1}{V}\frac{dV}{dP} \tag{2}$$

Thermodynamics provides the basis for the link between these modifications and the material's compressibility. The following relation may also be used to compute it using (ρ)and (v).

$$\beta = \frac{1}{v^2\rho} \tag{3}$$

Adiabatic compressibility (β) reflects the ease with which a solution can be compressed under an applied pressure. Low compressibility indicates a tightly packed, strongly interacting system where molecules have limited freedom for rearrangement. This typically arises when hydrogen bonding or strong solute–solvent associations reduce the free space within the liquid matrix. High compressibility, in contrast, signifies a loosely packed arrangement where weaker interactions or disrupted molecular networks create greater flexibility and allow the medium to deform more easily.

3.4.3 Wada's constant (W)

We can use the adiabatic compressibility to find out a new parameter called Wada's constant. One relationship that Wada proposed involves the mixture's density, effective

molecular mass (M), and adiabatic compressibility. The equation for the relationship is

$$W = \left(\frac{M}{\rho}\right)\beta^{1/7} \quad (4)$$

Where W is the temperature-independent Wada's constant β corresponds to adiabatic compressibility. ρ stands for the mixture's density.

3.4.4 Intermolecular free length (L_f)

A measure of the rate at which a sound wave may travel from one surface to another. This measure measures how strongly the molecules in a binary mixture interact with one another. A change in free length indicates a change in the intensity of the intermolecular attraction. The ultrasonic velocity must decrease and the interaction free length must increase due to the concentration-dependent connection between the two. The formula for intermolecular free length (L_f) was proposed by Jacobson in 1952 and is expressed as

$$L_f = K_T(\beta)^{1/2} \quad (5)$$

Here K_T represents the Jacobsons constant. Rather of being a constant, the value of Jacobson's constant changes when the temperature changes. A direct relationship exists between temperature and Jacobson's constant. Its value is affected by variations in the liquid's temperature. If you want to know Jacobson's constant, we have used the calculation

$$K_T = (93.875 + 0.375\,T) \times 10^{-8} \quad (6)$$

where T is the temperature in Kelvin. An alternative way to express the intermolecular free length in terms of density and sound velocity is as follows:

$$L_f = K_T/(v \times \sqrt{\rho}) \quad (7)$$

Intermolecular free length L_f, derived from compressibility, provides complementary insight into the average spacing between molecules. A decrease in L^f signifies closer molecular proximity, often due to strong solute–solvent interactions, enhanced structuring, or the formation of associated species. An increase in L^f indicates expanded molecular separation, commonly caused by the weakening of hydrogen bonds, temperature-induced disruption of structured clusters, or the presence of bulky solute species that enlarge intermolecular gaps.

3.4.5 Rao's constant (R)

When trying to deduce how liquids behave and interact with one another, it is a valuable parameter. It is a derived parameter that may be determined by combining the density and effective molar mass of a material. It is Equal to the cube root of the sound velocity per unit volume of solution. Independent of the temperature, R is known as Rao's Constant. The following equation represents the relationship between the speed of sound (v), the mixture's effective molecular weight (Meff), and its density (ρ):

$$R = \sqrt[3]{v}\left(\frac{M_{eff}}{\rho}\right) \quad (8)$$

3.4.6 Vander Waal's Constant (b)

The co-volume, or Vander Waals' constant (b), fluctuated in a manner that was analogous to the variation of the available volume.

$$b = \left(\frac{M}{\rho}\right)[1 - \left(\frac{RT}{Mv^2}\right)\{\sqrt{(1 + Mv^2/3RT)} - 1\}] \quad (9)$$

Where, ρ=density, v=ultrasonic velocity, M=Molecular weight, R =8.3143 $JK^{-1}mol^{-1}$, is the gas constant and T is temperature in Kelvin.

3.5 Volume and Isentropic compressibility- Apparent and Partial Molar Characteristics

3.5.1 Apparent molar volume, V_ϕ

The "apparent molar volume" is the volume of the solution minus the volume of the pure solvent per mole of the solute. The property of the solution changes when the entire chemical is added; hence, it is the characteristic of the solution and is assessed by the formula shown below:

$$V_\phi = M/\rho - (\rho - \rho_0)/m_A\rho\rho_0 \quad (10)$$

3.5.2 Partial molar volume, V_ϕ^0

It is described as the difference in solution's volume owing to the addition of the solute in the entire quantity of the solution, while the total concentration of the solution remains constant under constant pressure, temperature, and number of molecules. It is also known as the volume difference per mole of the component that has been added to the solution. Partial molar volumes are among the most significant thermodynamic measures for determining the relative contributions of various components to the total quality of a solution. To find V_ϕ^0, experimental slope (S_V^*), and typical errors, the V_ϕ is

fitted using the method of least squares.

$$V_\phi = V_\phi^0 + S_V^* m_A \tag{11}$$

Here m_A is the molality of the solute.

3.5.3 Transfer of Partial molar Volume, ΔV_ϕ^0

Interactions between the solvent-solute in the mixture are investigated both quantitatively and qualitatively using partial molar volume of transfer, ignoring interactions generated by the solute molecules interacting with one another. It's a measure of how much the solute's partial molar volume varies when the solvent is changed or when the solvent environment changes, such when going from a pure solvent to a mixed one. It's a thermodynamic parameter. We use the following to calculate it,

$$\Delta V_\phi^0 = V_{\phi\,(\text{in aqueous PHA})}^0 - V_{\phi\,(\text{in water})}^0 \tag{12}$$

3.5.4 Partial molar volume dependent on Temperature

The dependence of a solute's V_ϕ^0 on temperature elucidates the variation of the solute's molar volume as a function of T. This parameter controls the temperature-dependent changes in solute-solvent interactions; thus, it influences the solution's compressibility, solvation dynamics, and structural organization.

$$V_\phi^0 = a + b\left(T - T_{ref}\right) + c\left(T - T_{ref}\right)^2 \tag{13}$$

T_m= Reference Temperature:$298.15K$ and a, b, c are empirical coefficients.

3.5.5 Apparent molar isentropic compression, $K_{\phi,S}$

It is a thermodynamic quantity, characterizes the compressibility of a solute in a solution under adiabatic (isentropic) conditions. It signifies about the interactions between the solvent and the solute, The term "isentropic" describes a process in which the entropy remains constant, meaning that no heat exchange takes place. It is found by the given relation:

$$K_{\phi,S} = (Mk_S/\rho) - \left\{\left(k_{S,0}\rho - k_{S,0}\rho_0\right)/m_A\rho\rho_0\right\} \tag{14}$$

Here, k_S is the compressibility in isentropic process and is found by means of the following Eq. (15)

$$k_S = \frac{1}{\rho v^2} \tag{15}$$

3.5.6 Partial molar isentropic compression, $K_{\phi,S}^{0}$

The modification in $k_{\phi,s}$ with the concentration is given by the following equation:

$$K_{\phi,s} = K_{\phi,S}^{0} + S_k^* m_A \tag{16}$$

Where, $K_{\phi,S}^{0}$, m_A and S_K^* are the limiting or the partial molar isentropic compression, solute's molality in water-based solutions and the solute's experimental slope and the interactions within the solute.

3.5.7 Transfer of Partial molar isentropic compression, $\Delta K_{\phi,S}^{0}$

The $\Delta K_{\phi,S}^{0}$ of glycol and water-based solution of chemical sample are computed by the following eq.:

$$\Delta K_{\phi,S}^{0} = K_{\phi,S}^{0}{}_{(\text{in aqueous chemical sample})} - K_{\phi,S}^{0}{}_{(\text{in water})} \tag{17}$$

3.5.8 Pair and triplet interaction coefficients

The $\Delta V_{\phi}^{0}$and ΔK_{ϕ}^{0} are produced by the stated relation:

$$\Delta V_{\phi}^{0}(\text{water to aqueous PHA solution}) = 2V_{AB} m_B + 3V_{ABB} {m_B}^2 \tag{18}$$

$$\Delta K_{\phi}^{0}(\text{water to aqueous PHA solution}) = 2K_{AB} m_B + 3K_{ABB} {m_B}^2 \tag{19}$$

Where A=Glycols, B= either PHA, m_B=molality of aqueous PHA solutions, V_{AB} and K_{AB}, V_{ABB} and K_{ABB} are Pairwise and triplet interaction for volume & isentropic compression respectively.

References

[1] H. Kumar, M. Singla and R. Jindal, Monatsh. Chem. 145, 1063 (2014).

[2] K. Kaur, I. Behal, K.C. Juglan, H. Kumar, J. Chem. Thermodyn. 125, 93 (2018).

[3] M. Lamba, N. Chakraborty, K. C. Juglan, M. Singla, Chem. Thermodyn. Therm. Anal. 13, 100129 (2024).

[4] A. K. Gill, N. Chakraborty, K. C. Juglan, Chem. Phys. Impact 100843 (2025).

[5] A.K. Gill, N. Chakraborty, K.C. Juglan, Int. J. Thermophys. 46, 46 (2025).

[6] A. A. Firdaus, N. Chakraborty and K.C. Juglan, International Journal of Thermophysics 46, 1-44 (2025).

CHAPTER 4

RESULTS AND DISCUSSION

Section I

Problem 1

"Thermodynamic behaviour and physicochemical characteristics of EG, DEG, TEG in aqueous gluconolactone solutions"

This problem offers a blend of volumetric and acoustic approaches to examine the interlinkage between homologous series of glycol molecules (EG, DEG and TEG) in water based gluconolactone mixtures. As a function of gluconolactone concentration (0.01, 0.02 and 0.03) $mol.kg^{-1}$, the ρ and v of taken ternary mixes of (H_2O + GLA + EG/DEG/TEG) were calculated at 288.15, 298.15, 308.15 and 318.15 K by means of DSA 5000 M.

Density and velocity measurements

The experimentally determined densities values for (gluconolactone + water) and (gluconolactone + water + glycols) are listed in **Table-4.1** for concentrations of (0.01, 0.02, and 0.03) $mol.kg^{-1}$ and temperature variations. The densities for (Glycols + water) are gotten straight from our earlier publication having reference number [1], and shown as subscript 'b' in the **Table-4.1**. The standard uncertainties for ρ, v, T and molality is same as provided in Chapter 3. Here the data clearly show that the density levels increase with gluconolactone concentration and glycol molality but decrease with temperature. The mass of the solution has grown, which is the primary cause of this surge. Increased density values suggest that interactions between solute and solvent are also increasing [2]. The density of a substance decreases as temperature increases. The rise in temperature weakens the structured hydrogen-bond network within the system, making these bonds less stable and resulting in a more loosely packed molecular arrangement. Consequently, the overall density decreases. Whereas, the sound speed increase as a function of gluconolactone concentration from (0.01 to 0.02 to 0.03) $mol \cdot kg^{-1}$ and temperature. This behaviour is caused by the 3-dimensional systems of hydrogen bonds that make up water's structure [3,4]. This upsurge in the sound speed for the mixture of glycols and gluconolactone is because of generation of intramolecular and hydrogen bonding within molecules of solvent and solute, which shows that

molecules in solutions are combining at a faster pace [5]. **Table 4.1** also makes it clear that the intensification in sound speed data with glycol molality is due to the H-bond being insoluble in the presence of the gluconolactone molecule. Moreover, fresh H_2 bonds are formed between the molecules of glycol and GLA [6].

Apparent molar properties

A measure designated to isolate each component's contribution to the combination's non-ideality is known as an apparent molar property of a solution component of a mixture or solution. When a component is fully incorporated into the solution, it displays the alteration in the relevant solution features (for instance, volume) per additional mole of the substance. If it is anticipated that the other solution components' characteristics will not change throughout the addition, it is defined as evident thus it appears to depict the component's molar characteristic in solution. We have calculated two apparent molar properties which are Apparent molar volume (V_ϕ) and Apparent molar isentropic compresion ($K_{\phi,S}$) by means of experimentally found data of ρ and v.

First Parameter: - V_ϕ

The property of the solution changes when the entire chemical is added, hence apparent molar volume is the characteristic of the solution. It is evaluated using the formulation shown below:

$$V_\phi = M/\rho - (\rho - \rho_0)/m_A\,\rho\rho_0 \qquad (4.1)$$

Table 4.2 represents the calculated V_ϕ at several temperatures. Also, **Figure 4.1** represents variation of V_ϕ of glycols at concentrations of Gluconolactone, against molality at all T. This is obvious from the **Table-4.2** that the value of V_ϕ is between $(53.44\ and\ 130.57) \times 10^6/(m^3.mol^{-1})$. According to the values listed in **Table 4.2**, the V_ϕ of all glycols rises with both temperature and gluconolactone concentration. The observations show that for all gluconolactone concentrations, the apparent molar volume's magnitude increases with temperature, leading to a larger attraction for the gluconolactone solvent and enhancing stronger solute-solvent interactions [7]. The electrostriction interactions that predominate in the mixture are described by the positive values of V_ϕ [8]. These positive values of V_ϕ also reflect the incidence of higher solute-solvent interactions, which in response rise from EG to TEG, as illustrated in

Figure 4.2 for all working temperatures. The **Figure 4.2** represents the molecular interactions of ethylene glycol (EG), diethylene glycol (DEG), and triethylene glycol (TEG) with gluconolactone in aqueous medium. Thus, the strength of molecular interactions with gluconolactone increases in the order: EG < DEG < TEG, owing to the progressive increase in hydroxyl/ether groups and chain length of glycols, which enhance hydrogen bonding and solute–solvent association.

The observed trends emphasize that solute–solvent interactions are strongly influenced by the intrinsic ionic characteristics, especially charge density and the ability to form hydrogen bonds. In the presence of water, the glycols exhibit interactions such as the inter and intramolecular H-link, dipole-induced dipole interactions, hydrophobic effect, interactions amongst two dipoles, and hydrophobic hydration. The V_{ϕ}values provide considerable information about the type of interactions between them [9-14].

Table 4.1

Measured ρ and v in the ternary mixture of gluconolactone with EG, DEG, TEG under a steady experimental pressure of 0.1 MPa and varied temperatures and concentrations.

$^{a}m_A/$	$\rho \times 10^{-3}/(kg \cdot m^{-3})$				$v/(m.s^{-1})$			
$(mol.kg^{-1})$	$288.15K$	$298.15K$	$308.15K$	$318.15K$	$288.15K$	$298.15K$	$308.15K$	$318.15K$
				0.01 ($mol.kg^{-1}$) Gluconolactone + EG				
0.00000	0.99988	0.99769	0.99468	0.99104[b]	1470.96	1499.97	1523.39	1540.94[b]
0.11890	1.00090	0.99868	0.99562	0.99196	1474.69	1503.21	1526.49	1544.89
0.18456	1.00144	0.99920	0.99612	0.99244	1476.56	1504.95	1528.05	1546.89
0.32119	1.00253	1.00025	0.99712	0.99339	1480.25	1508.61	1530.98	1550.89
0.40333	1.00316	1.00086	0.99769	0.99394	1482.97	1510.81	1532.86	1553.49
0.51406	1.00397	1.00164	0.99843	0.99466	1485.58	1513.39	1535.31	1556.45
				0.02 ($mol.kg^{-1}$) Gluconolactone + EG				
0.00000	1.00052	0.99836	0.99532	0.99172	1474.89	1503.75	1526.67	1545.02
0.10757	1.00144	0.99924	0.99616	0.99254	1478.16	1506.82	1529.74	1548.96
0.19838	1.00217	0.99996	0.99684	0.99319	1480.86	1509.13	1531.8	1551.83
0.29598	1.00294	1.00069	0.99754	0.99386	1483.43	1511.58	1533.97	1554.74
0.39446	1.00368	1.00140	0.99822	0.99450	1486.91	1514.11	1536.14	1557.78
0.49049	1.00437	1.00207	0.99885	0.99510	1489.13	1516.45	1538.44	1560.49
				0.03 ($mol.kg^{-1}$) Gluconolactone + EG				
0.00000	1.00133	0.99914	0.99600	0.99231	1477.78	1506.98	1530.36	1547.64
0.11576	1.00230	1.00008	0.99689	0.99316	1481.56	1510.39	1533.74	1551.76
0.16025	1.00266	1.00042	0.99722	0.99347	1483.00	1511.49	1534.86	1553.25

0.30876	1.00380	1.00151	0.99825	0.99445	1487.07	1515.28	1538.27	1557.78
0.38222	1.00433	1.00202	0.99873	0.99490	1489.53	1517.18	1539.87	1559.88
0.46596	1.00491	1.00256	0.99924	0.99539	1491.57	1519.42	1541.73	1562.51
			0.01 ($mol.kg^{-1}$) Gluconolactone + DEG					
0.00000	0.99988	0.99769	0.99468	0.99104	1470.96	1499.97	1523.39	1540.94
0.10159	1.00134	0.99912	0.99609	0.99245	1476.48	1504.89	1527.98	1546.47
0.20038	1.00269	1.00044	0.99740	0.99375	1482.12	1509.7	1532.28	1551.75
0.29800	1.00395	1.00167	0.99862	0.99497	1487.77	1514.27	1536.38	1556.8
0.39722	1.00518	1.00287	0.99980	0.99614	1492.54	1518.94	1540.49	1562.09
0.49234	1.00631	1.00397	1.00089	0.99722	1497.99	1523.04	1545.93	1567.11
			0.02 ($mol.kg^{-1}$) Gluconolactone + DEG					
0.00000	1.00052	0.99836	0.99532	0.99172	1474.89	1503.75	1526.67	1545.02
0.11587	1.00216	0.99997	0.99691	0.99331	1481.34	1508.99	1531.89	1551.15
0.20206	1.00332	1.00111	0.99804	0.99443	1486.33	1513.34	1535.93	1555.64
0.29956	1.00457	1.00234	0.99925	0.99564	1491.77	1518.1	1540.26	1560.78
0.38959	1.00567	1.00343	1.00033	0.99671	1496.03	1521.97	1544.21	1565.45
0.51207	1.00710	1.00483	1.00171	0.99808	1502.39	1527.65	1551.02	1572.09
			0.03 ($mol.kg^{-1}$) Gluconolactone + DEG					
0.00000	1.00133	0.99914	0.99600	0.99231	1477.78	1506.98	1530.36	1547.64
0.11437	1.00294	1.00072	0.99756	0.99387	1484.16	1512.31	1535.69	1553.95
0.20127	1.00410	1.00186	0.99869	0.99499	1489.06	1516.65	1539.89	1558.63
0.29627	1.00531	1.00306	0.99987	0.99616	1494.55	1521.1	1544.3	1563.7
0.39003	1.00645	1.00418	1.00099	0.99727	1499.03	1525.56	1548.46	1568.36

0.50681	1.00780	1.00550	1.00230	0.99858	1504.99	1530.92	1554.54	1574.34
			0.01 ($mol.kg^{-1}$) Gluconolactone + TEG					
0.00000	0.99988	0.99769	0.99468	0.99104	1470.96	1499.97	1523.39	1470.96
0.15183	1.00316	1.00092	0.99786	0.99420	1483.74	1511.52	1532.38	1483.74
0.20023	1.00416	1.00190	0.99883	0.99516	1488.09	1514.88	1535.55	1488.09
0.29620	1.00610	1.00379	1.00070	0.99701	1496.46	1521.86	1541.6	1496.46
0.39010	1.00792	1.00558	1.00246	0.99875	1502.54	1528.78	1547.39	1502.54
0.50148	1.01000	1.00762	1.00448	1.00076	1513.03	1536.13	1555.61	1513.03
			0.02 ($mol.kg^{-1}$) Gluconolactone + TEG					
0.00000	1.00052	0.99836	0.99532	0.99172	1474.89	1503.75	1526.67	1545.02
0.10066	1.00270	1.00050	0.99743	0.99382	1483.56	1511.4	1533.21	1553.52
0.20271	1.00482	1.00259	0.99950	0.99587	1492.41	1518.92	1539.41	1561.31
0.30009	1.00677	1.00451	1.00139	0.99774	1500.81	1525.66	1544.98	1569.9
0.39683	1.00865	1.00635	1.00320	0.99953	1507.08	1532.25	1551.34	1576.02
0.50141	1.01059	1.00827	1.00508	1.00140	1516.94	1539.61	1559.13	1584.87
			0.03 ($mol.kg^{-1}$) Gluconolactone + TEG					
0.00000	1.00133	0.99914	0.99600	0.99231	1477.78	1506.98	1530.36	1547.64
0.10576	1.00361	1.00138	0.99821	0.99451	1487.56	1514.58	1536.37	1556.32
0.20015	1.00556	1.00330	1.00011	0.99639	1495.61	1521.74	1542.56	1563.34
0.30379	1.00762	1.00533	1.00212	0.99837	1504.47	1528.75	1549.36	1572.29
0.39768	1.00942	1.00710	1.00386	1.00011	1510.41	1535.2	1555.64	1578.34
0.51064	1.01151	1.00916	1.00589	1.00211	1520.59	1543.17	1563.36	1587.73

Table 4.2

Calculated V_ϕ, and $K_{\phi,S}$, of the ternary system of gluconolactone with EG, DEG and TEG at several temperatures and concentrations.

$^a m_A/$ $(mol.kg^{-1})$	$V_\phi \times 10^6/(m^3.mol^{-1})$				$K_{\varphi,S} \times 10^6/(m^3.mol^{-1}.GPa^{-1})$			
	$288.15K$	$298.15K$	$308.15K$	$318.15K$	$288.15K$	$298.15K$	$308.15K$	$318.15K$
				0.01 ($mol.kg^{-1}$) Gluconolactone + EG				
0.11890	53.44	53.81	54.29	54.74	-45.88	-44.12	-42.77	-41.80
0.18456	53.54	53.90	54.39	54.86	-46.04	-44.27	-42.92	-41.94
0.32119	53.70	54.06	54.57	55.05	-46.20	-44.42	-43.06	-42.08
0.40333	53.78	54.15	54.67	55.16	-46.26	-44.48	-43.11	-42.13
0.51406	53.91	54.29	54.80	55.26	-46.32	-44.54	-43.17	-42.19
				0.02 ($mol.kg^{-1}$) Gluconolactone + EG				
0.10757	53.50	53.88	54.39	54.86	-45.59	-43.85	-42.54	-41.53
0.19838	53.65	54.01	54.53	55.01	-45.82	-44.07	-42.75	-41.74
0.29598	53.76	54.15	54.65	55.14	-45.93	-44.18	-42.86	-41.84
0.39446	53.88	54.27	54.77	55.27	-46.00	-44.25	-42.92	-41.90
0.49049	53.99	54.39	54.89	55.40	-46.06	-44.30	-42.97	-41.95
				0.03 ($mol.kg^{-1}$) Gluconolactone + EG				
0.11576	53.60	53.97	54.49	55.02	-45.44	-43.70	-42.37	-41.42
0.16025	53.68	54.06	54.59	55.13	-45.57	-43.82	-42.48	-41.54
0.30876	53.90	54.30	54.85	55.41	-45.76	-44.00	-42.66	-41.71
0.38222	54.00	54.43	54.97	55.53	-45.81	-44.05	-42.70	-41.75

0.46596	54.13	54.58	55.12	55.68	-45.86	-44.09	-42.75	-41.79
0.01 ($mol.kg^{-1}$) Gluconolactone + DEG								
0.10159	91.66	92.11	92.49	92.85	-45.83	-44.07	-42.73	-41.76
0.20038	91.87	92.34	92.71	93.08	-46.12	-44.35	-42.99	-42.02
0.29800	92.09	92.56	92.95	93.31	-46.25	-44.48	-43.12	-42.14
0.39722	92.30	92.78	93.16	93.52	-46.35	-44.57	-43.21	-42.23
0.49234	92.48	92.98	93.36	93.72	-46.42	-44.64	-43.27	-42.29
0.02 ($mol.kg^{-1}$) Gluconolactone + DEG								
0.11587	91.84	92.21	92.60	92.95	-45.65	-43.92	-42.60	-41.60
0.20206	92.00	92.39	92.78	93.13	-45.88	-44.13	-42.81	-41.80
0.29956	92.20	92.59	92.98	93.33	-46.01	-44.26	-42.93	-41.92
0.38959	92.38	92.78	93.17	93.52	-46.09	-44.34	-43.01	-42.00
0.51207	92.63	93.01	93.41	93.77	-46.19	-44.43	-43.10	-42.08
0.03 ($mol.kg^{-1}$) Gluconolactone + DEG								
0.11437	91.87	92.23	92.60	92.98	-45.47	-43.72	-42.39	-41.45
0.20127	92.04	92.41	92.79	93.17	-45.70	-43.94	-42.60	-41.66
0.29627	92.24	92.61	93.00	93.37	-45.82	-44.06	-42.72	-41.77
0.39003	92.42	92.80	93.19	93.56	-45.91	-44.15	-42.81	-41.85
0.50681	92.65	93.04	93.43	93.79	-46.00	-44.23	-42.89	-41.93
0.01 ($mol.kg^{-1}$) Gluconolactone + TEG								
0.15183	128.19	128.77	129.36	129.93	-46.07	-44.30	-42.95	-41.97
0.20023	128.28	128.87	129.47	130.05	-46.19	-44.42	-43.06	-42.08
0.29620	128.42	129.04	129.64	130.24	-46.35	-44.57	-43.21	-42.23

0.39010	128.57	129.18	129.79	130.39	-46.48	-44.69	-43.32	-42.34
0.50148	128.72	129.35	129.94	130.52	-46.60	-44.81	-43.43	-42.45
0.02 ($mol.kg^{-1}$) Gluconolactone + TEG								
0.10066	128.25	128.79	129.39	129.96	-45.62	-43.88	-42.57	-41.56
0.20271	128.38	128.93	129.52	130.11	-45.95	-44.20	-42.88	-41.86
0.30009	128.49	129.07	129.66	130.25	-46.11	-44.35	-43.03	-42.01
0.39683	128.61	129.19	129.81	130.40	-46.23	-44.47	-43.14	-42.12
0.50141	128.75	129.32	129.95	130.53	-46.35	-44.58	-43.24	-42.22
0.03 ($mol.kg^{-1}$) Gluconolactone + TEG								
0.10576	128.27	128.80	129.40	129.97	-45.47	-43.72	-42.39	-41.45
0.20015	128.40	128.94	129.54	130.12	-45.76	-44.00	-42.66	-41.72
0.30379	128.53	129.09	129.68	130.28	-45.94	-44.17	-42.82	-41.87
0.39768	128.65	129.23	129.83	130.41	-46.05	-44.28	-42.93	-41.98
0.51064	128.79	129.35	129.97	130.57	-46.17	-44.39	-43.04	-42.09

I (a)

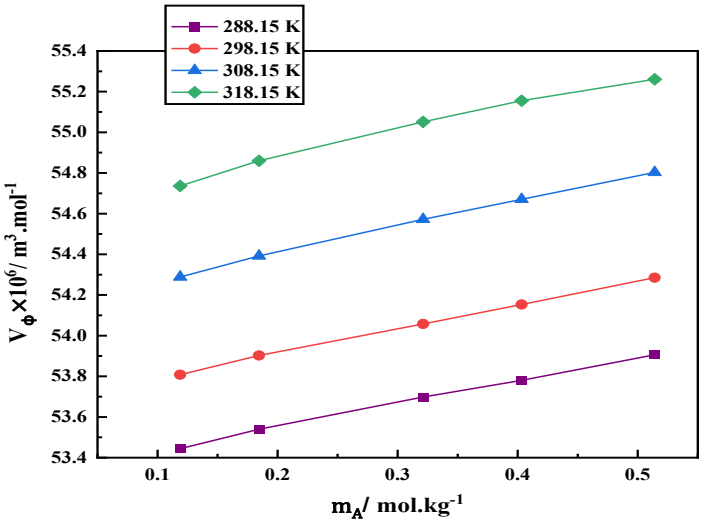
288.15 K
298.15 K
308.15 K
318.15 K
55.4
55.2
55.0
54.8
54.6
54.4
54.2
54.0
53.8
53.6
53.4
0.1
0.2
0.3
0.4
0.5
$V_\phi \times 10^6$/ m^3.mol^{-1}
m_A/ mol.kg^{-1}

I (b)

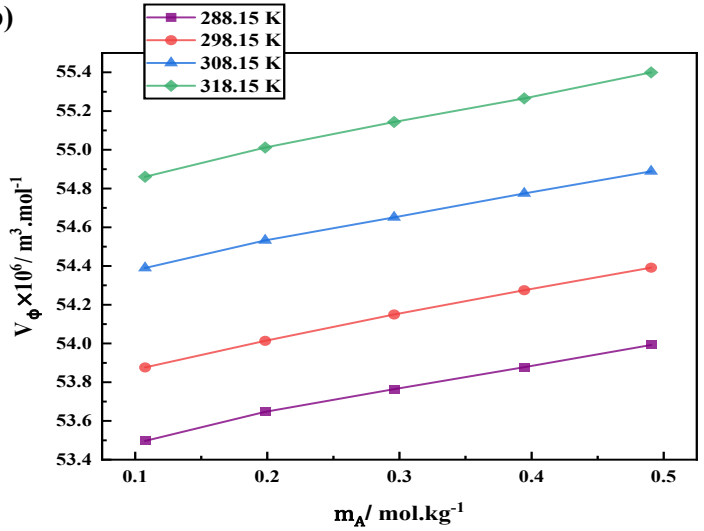
288.15 K
298.15 K
308.15 K
318.15 K
55.4
55.2
55.0
54.8
54.6
54.4
54.2
54.0
53.8
53.6
53.4
0.1
0.2
0.3
0.4
0.5
$V_\phi \times 10^6$/ m^3.mol^{-1}
m_A/ mol.kg^{-1}

I (c)

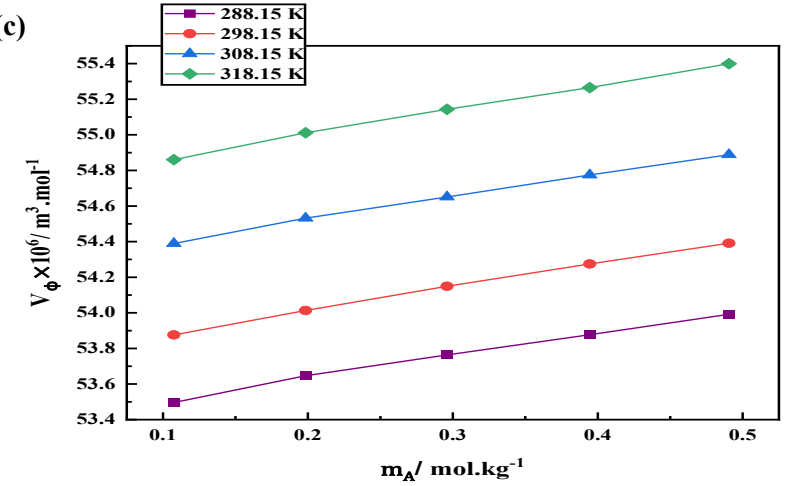
288.15 K
298.15 K
308.15 K
318.15 K
55.4
55.2
55.0
54.8
54.6
54.4
54.2
54.0
53.8
53.6
53.4
0.1
0.2
0.3
0.4
0.5
$V_\phi \times 10^6$/ m^3.mol^{-1}
m_A/ mol.kg^{-1}

II (a)

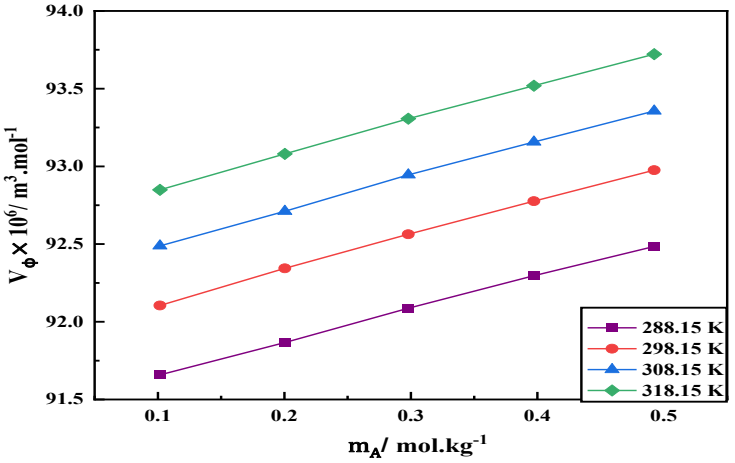
94.0
93.5
93.0
92.5
92.0
91.5
0.1
0.2
0.3
0.4
0.5
$V_\phi \times 10^6 / m^3.mol^{-1}$
m_A/ mol.kg^{-1}
288.15 K
298.15 K
308.15 K
318.15 K

II (b)

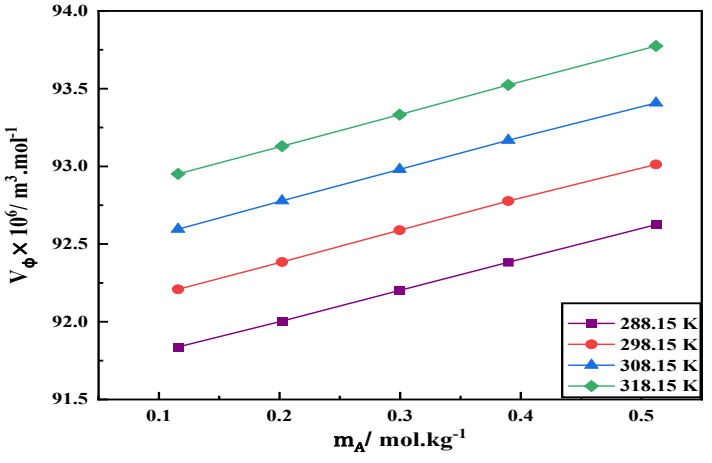
94.0
93.5
93.0
92.5
92.0
91.5
0.1
0.2
0.3
0.4
0.5
$V_\phi \times 10^6 / m^3.mol^{-1}$
m_A/ mol.kg^{-1}
288.15 K
298.15 K
308.15 K
318.15 K

II (c)

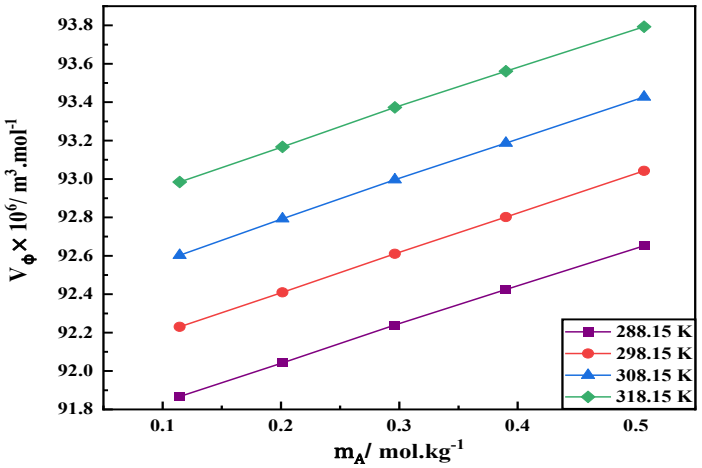
93.8
93.6
93.4
93.2
93.0
92.8
92.6
92.4
92.2
92.0
91.8
0.1
0.2
0.3
0.4
0.5
$V_\phi \times 10^6 / m^3.mol^{-1}$
m_A/ mol.kg^{-1}
288.15 K
298.15 K
308.15 K
318.15 K

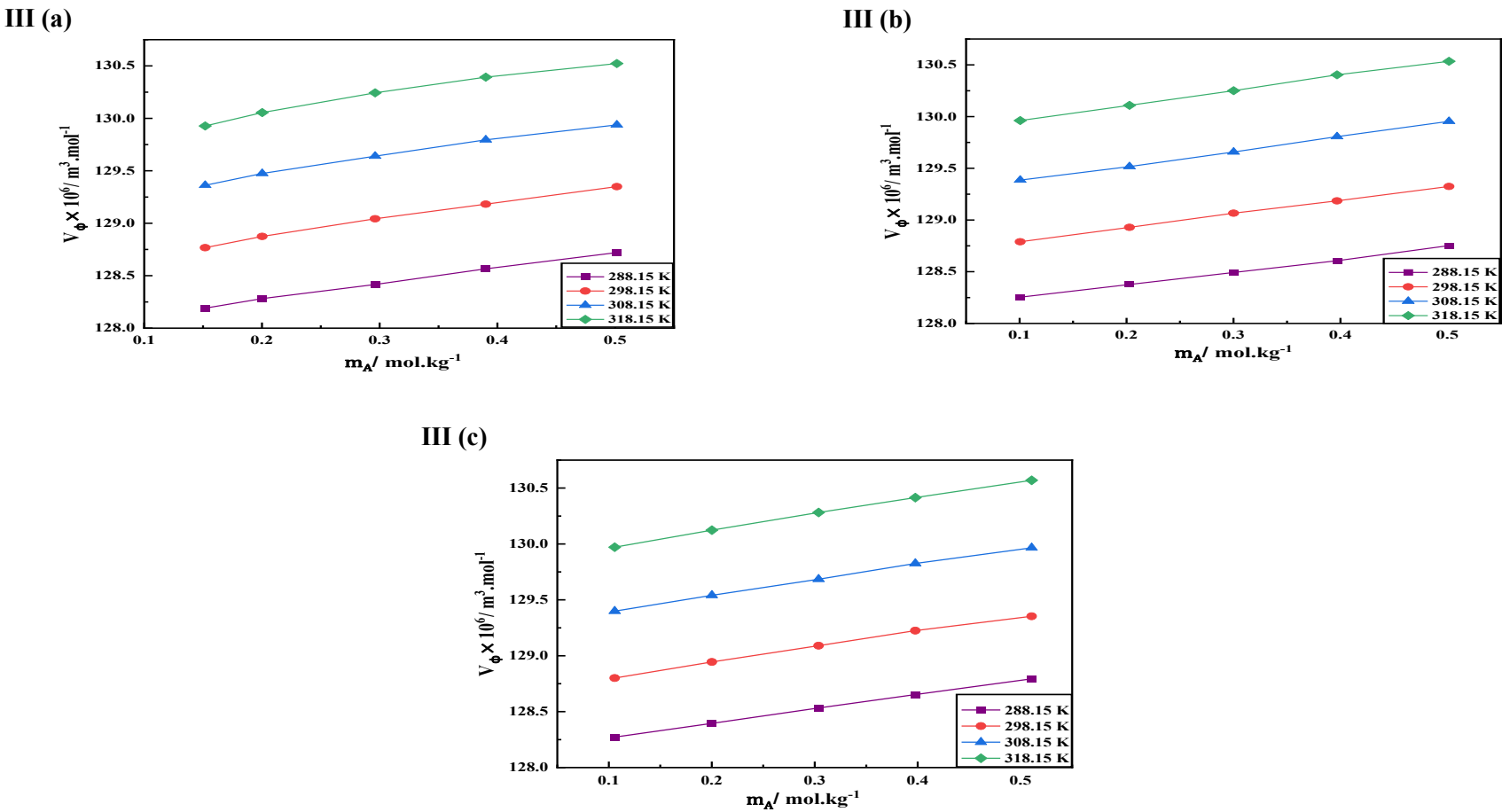

Figure 4.1: Variation of V_ϕ, of EG (I), DEG (II) and TEG (III) in (a) 0.01 Gluconolactone, (b) 0.02 Gluconolactone, (c) 0.03 Gluconolactone in mol.kg^{-1} aqueous solution against m_A at diverse temperatures [Purple (square), 288.15 K; red (circle), 298.15 K; blue (triangle), 308.15 K; green (diamond), 318.15 K]

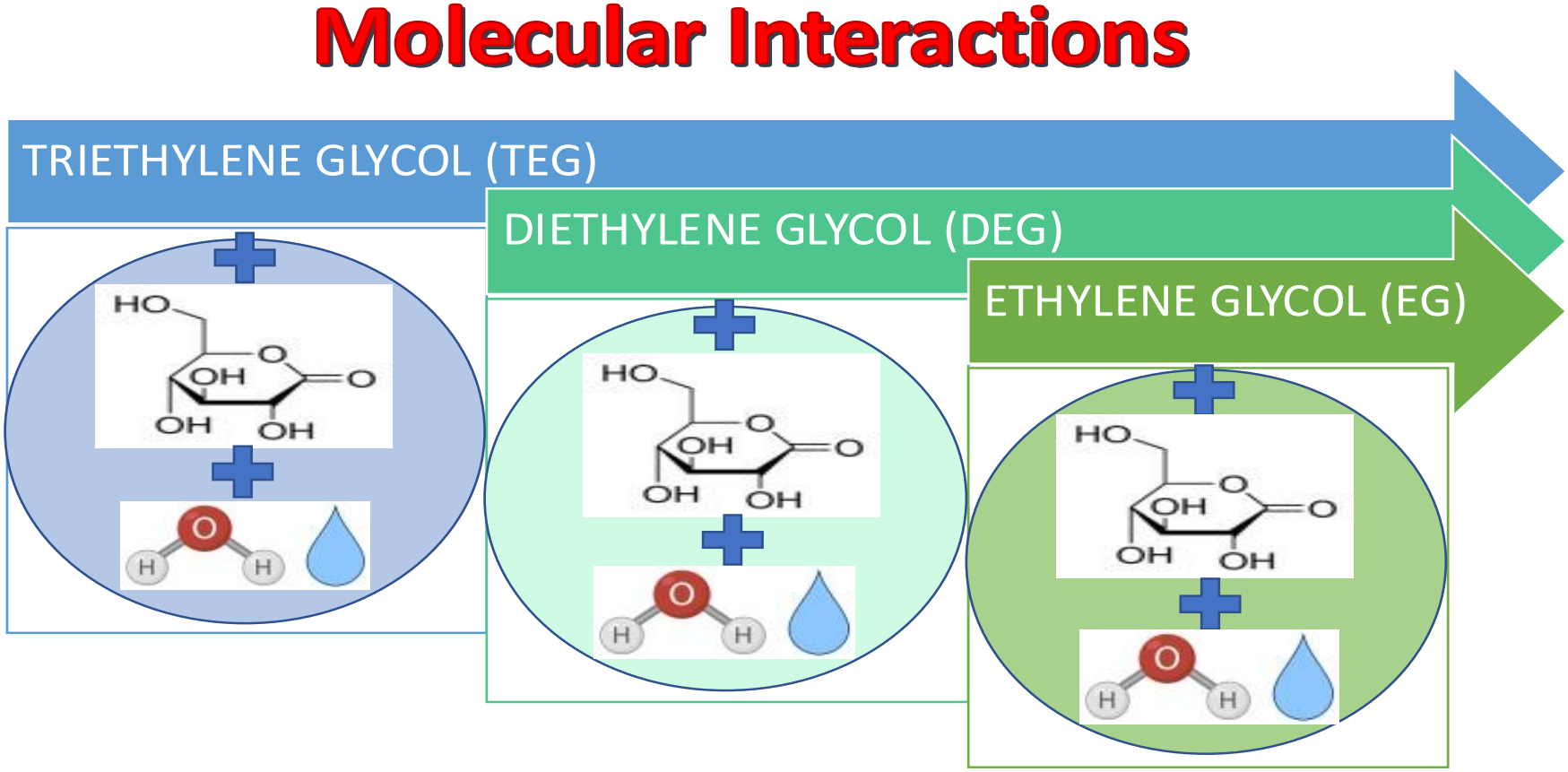

Figure 4.2 Variation of intermolecular interactions with increase in molecular mass of Glycols.

Second Parameter: $K_{\phi,S}$

The value of isentropic compressibility (k_s), which is found by the following equation (**4.2**) called as Laplace-Newton's formula [15], by plugging in the experimentally found values of ultrasonic velocity, v, and solutions' density, ρ, is utilized to estimate the ($K_{\phi,S}$) of a solute in an aqueous solution of a chemical sample by using the following equation (4.3);

$$k_s = 1/c^2\rho \tag{4.2}$$

$$K_{\phi,S} = (Mk_S/\rho) - \{(k_{S,0}\rho - k_{S,0}\rho_0)/m_A\rho\rho_0\} \tag{4.3}$$

In these formulae, M, ρ_0, ρ, m_A, $k_{S,0}$ and k_s, have their usual meanings. **Table 4.2** lists the $K_{\phi,S}$ at various gluconolactone concentrations (0.01, 0.02, and 0.03) $mol \cdot kg^{-1}$ and for different glycols. The $K_{\phi,S}$ for water + EG/DEG/TEG are obtained straight from the published study [1]. The **Table 4.2** shows the each negative $K_{\phi,S}$ values and it generally upsurges with temperature and m_B of GLA, but reduces with glycols molality, as seen in **Figure 4.3** The H_2O molecules around the glycols' ionized groups are less squeezable than those around the bulk, causing an accumulation of water molecules over the solute [16–18]. Glycols construct microscopic structures that reduce compressibility by creating intermolecular hydrogen bonds with gluconolactone particles. The interactions (dipole-dipole) within water molecules nearby and the hydroxyl groups of glycols promote strong solute-solvent interactions [19-21].

I (a)

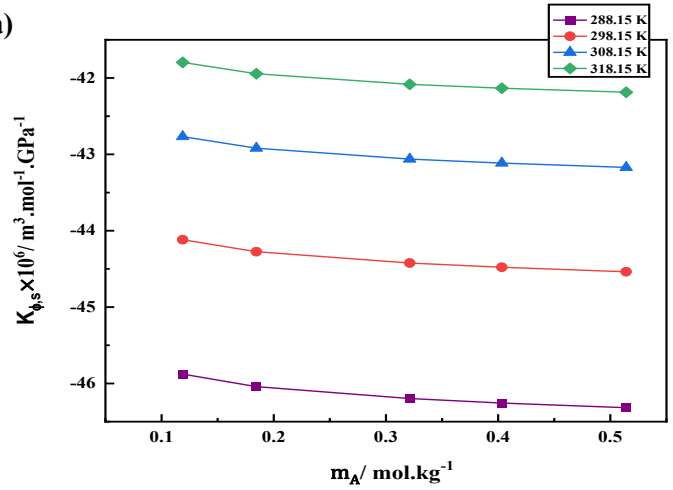
288.15 K
298.15 K
308.15 K
318.15 K
-42
-43
-44
-45
-46
0.1
0.2
0.3
0.4
0.5
$K_{\phi,s}\times10^{6}$/ $m^3.mol^{-1}.GPa^{-1}$
m_A/ $mol.kg^{-1}$

I (b)

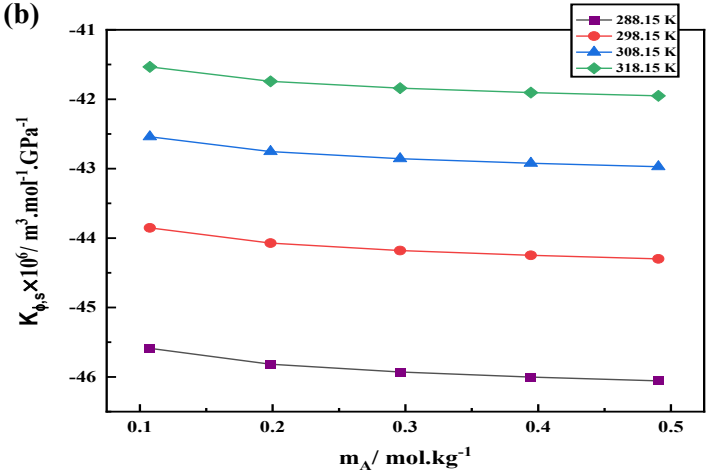
288.15 K
298.15 K
308.15 K
318.15 K
-41
-42
-43
-44
-45
-46
0.1
0.2
0.3
0.4
0.5
$K_{\phi,s}\times10^{6}$/ $m^3.mol^{-1}.GPa^{-1}$
m_A/ $mol.kg^{-1}$

I (c)

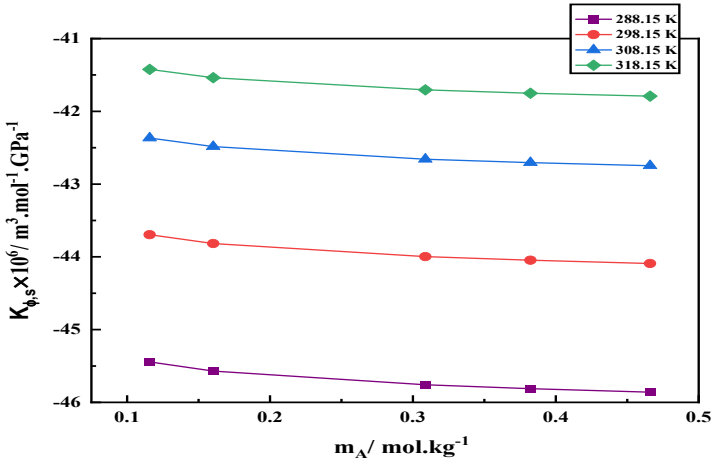
288.15 K
298.15 K
308.15 K
318.15 K
-41
-42
-43
-44
-45
-46
0.1
0.2
0.3
0.4
0.5
$K_{\phi,s}\times10^{6}$/ $m^3.mol^{-1}.GPa^{-1}$
m_A/ $mol.kg^{-1}$

II (a)

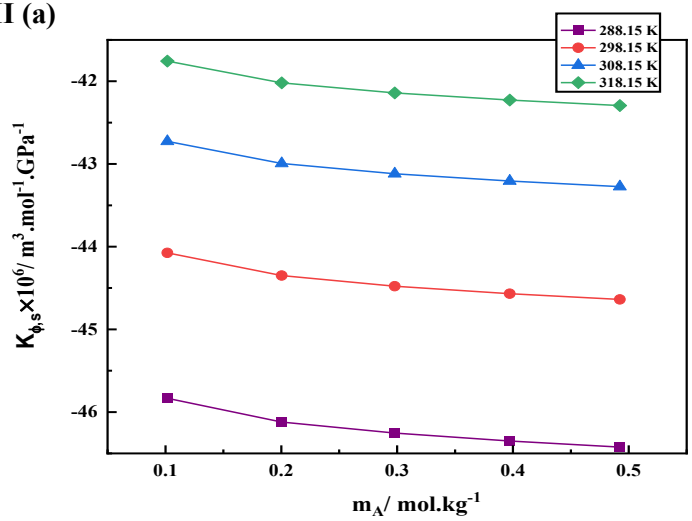
288.15 K
298.15 K
308.15 K
318.15 K
-42
-43
-44
-45
-46
0.1
0.2
0.3
0.4
0.5
$K_{\phi,s} \times 10^6$/ m^3.mol^{-1}.GPa^{-1}
m_A/ mol.kg^{-1}

II (b)

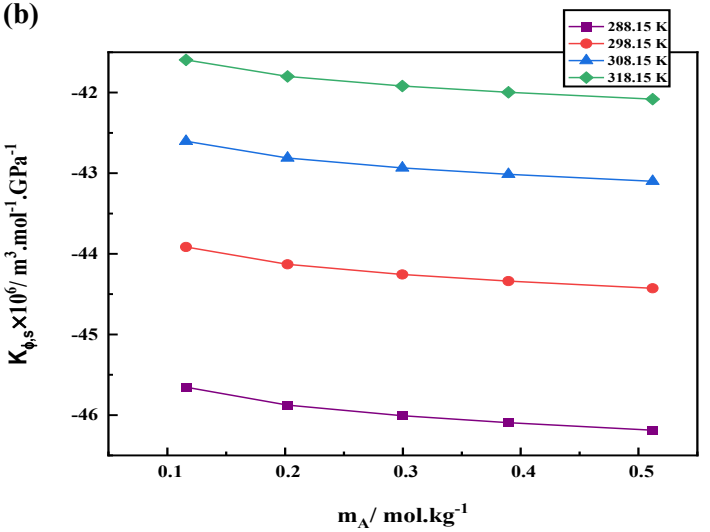
288.15 K
298.15 K
308.15 K
318.15 K
-42
-43
-44
-45
-46
0.1
0.2
0.3
0.4
0.5
$K_{\phi,s} \times 10^6$/ m^3.mol^{-1}.GPa^{-1}
m_A/ mol.kg^{-1}

II (c)

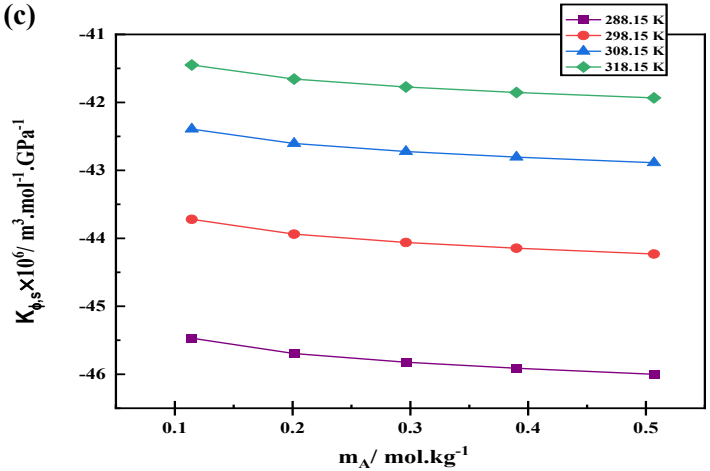
288.15 K
298.15 K
308.15 K
318.15 K
-41
-42
-43
-44
-45
-46
0.1
0.2
0.3
0.4
0.5
$K_{\phi,s} \times 10^6$/ m^3.mol^{-1}.GPa^{-1}
m_A/ mol.kg^{-1}

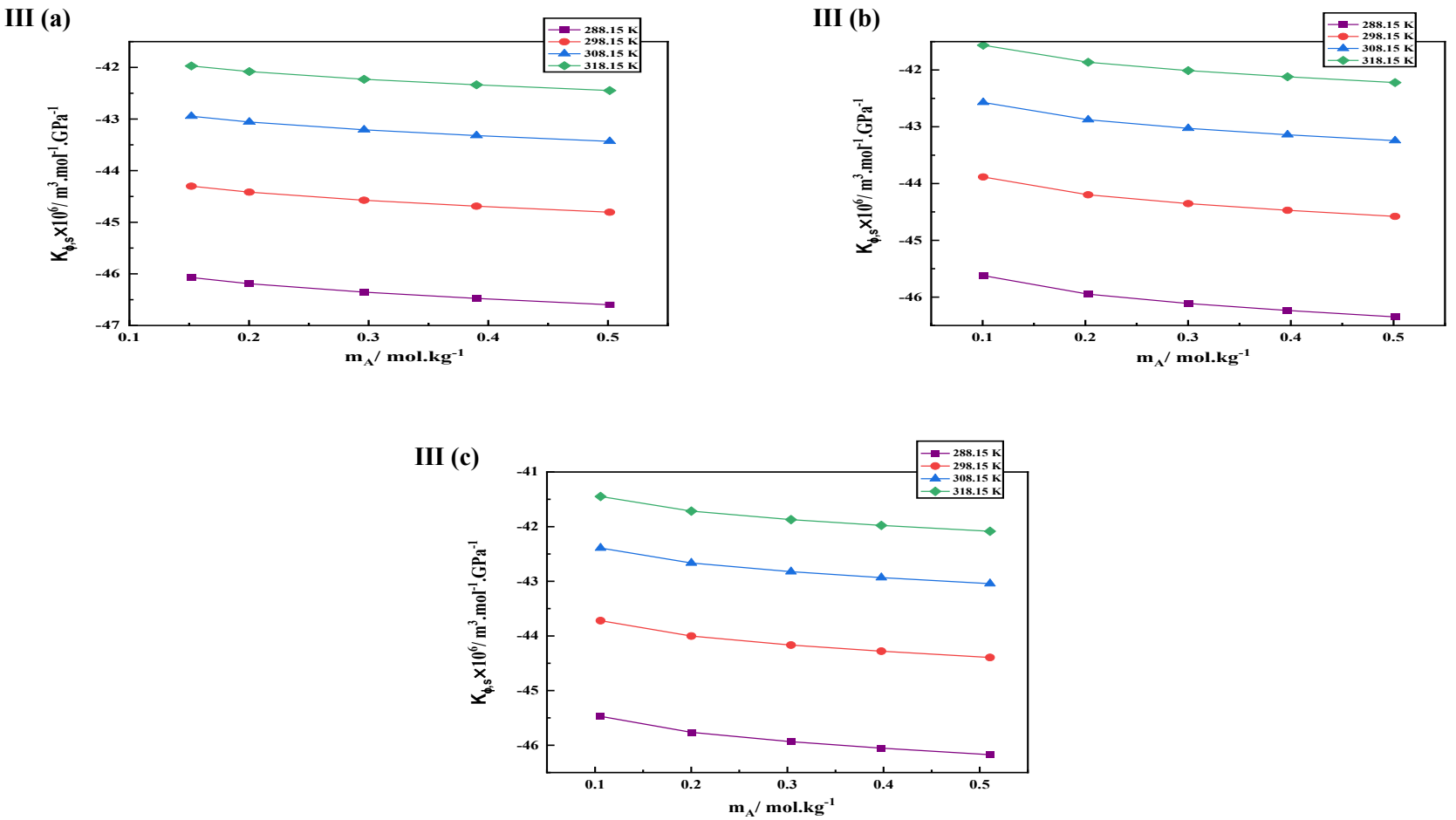

Figure 4.3: Variation of $K_{\phi,S}$, of EG (I), DEG (II) and TEG (III) in (a) 0.01 Gluconolactone, (b) 0.02 Gluconolactone, (c) 0.03 Gluconolactone aqueous solution against m_A at same temperatures [Purple (square), 288.15 K; red (circle), 298.15 K; blue (triangle), 308.15 K; green (diamond), 318.15 K]

Partial molar properties

These represent those thermodynamic variables which demonstrate how extensively variables fluctuate with variations in molar content when temperature and pressure are maintained constant [22-24]. The thermodynamics of multicomponent mixtures, particularly liquid ones, can be studied using partial molar characteristics, and they can also be used to develop new chemical and biological procedures [25–30]. We have calculated two properties; one is V_ϕ^0 and other is to study the sample's thermodynamics.

Partial molar volumes

The partial molar volume is described as the difference in the solution volume owing to the addition of the solute in the entire quantity of the solution while the total concentration of the solution remains constant under constant pressure, temperature, and number of molecules. It is also known as the volume difference per mole of the component that has been added to the solution. The subsequent formula is utilised to govern the partial molar volumes, V_ϕ^0 of liquid mixes comprising gluconolactone and glycol:

$$V_\phi = m_A S_V^* + V_\phi^0 \tag{4.4}$$

The apparent molar volume (V_ϕ) is fitted with the technique of least square to determine the (V_ϕ^0), (S_V^*), and standard errors. The m_A represents the molality of the solute in equation (4.4). The standard errors and all the values for (V_ϕ^0), (S_V^*) of the triple system of GLA sol. with EG, DEG and TEG at several concentrations and temperatures are tabulated in **Table 4.3**. The uncertainties, u of $\left(V_\phi^\circ\right) = \pm 0.01 \times 10^6/(m^3.mol^{-1}.GPa^{-1})$ and $(S_V^*) = \pm 0.03 \times 10^6/(m^3.kg.mol^{-2})$. V_ϕ^0 and associated standard errors for (H_2O and EG/DEG/TEG) are taken straight from the literature [1]. Within a system, the molecules of solutes are encased in solvents and are infinitesimally distant from one another, therefore interactions among the solute and solvent are minimal at infinite dilution. For example, ion-solvent, solute-solvent, ion-ion interactions that take place in both water based and non-water-based solutions, V_ϕ^0 is a vital means for describing these interactions [31,32]. Every positive value in the V_ϕ^0 range climb as the gluconolactone concentration and temperature increase, as understood in the **Table 4.3** and visibly shown in **Figure 4.4.** That pattern points to the occurrence of potent interactions (solute-solvent) in the sample, which intensify with T and gluconolactone m_B. As the T rises, Vo varies due to number of factors like creation of hydrogen bond, and removal of solvation particles from the solvation layer of glycol in

the sol. [33,34]. The **Table 4.3** shows that because of the molecular interaction, apparent molar volume also rises as depicted in **Figure 4.2** when the glycol's molecular mass rises from EG to TEG. In the presence of water, the glycols (EG, DEG, and TEG) exhibit interactions such as the dipole-induced dipole interactions, inter-intramolecular hydrogen link, dipole-dipole interactions, hydrophobic hydration, and hydrophobic effect [35-36]. On the other hand, it is discovered that the S_V^* values in the **Table 4.3** respond positively to individual temperature and gluconolactone content. As V_Φ^0 values are considerably higher than the S_V^* values so this depicts that interaction between solute and solvent is dominant over the interactions between solute and solute of sample [37-38].

Table 4.3

Calculated V_{ϕ}^{0} of the ternary mixture of gluconolactone with EG, DEG, TEG at same temperatures and m_B at pressure = 0.1 MPa and their experimental slopes, S_V^*.

[a]m_B/ $mol.kg^-$	$V_{\phi}^{0} \times 10^6/(m^3.mol^{-1})$				$S_V^* \times 10^6/(m^3.kg.mol^{-2})$			
	$288.15K$	$298.15K$	$308.15K$	$318.15K$	$288.15K$	$298.15K$	$308.15K$	$318.15K$
				EG				
0	53.27(±0.01)	53.66(±0.00)	54.08(±0.00)	54.51(±0.02)	0.92(±0.03)	1.06(±0.01)	1.28(±0.02)	1.25(±0.06)
0.01	53.32(±0.01)	53.67(±0.01)	54.15(±0.01)	54.60(±0.03)	1.15(±0.03)	1.19(±0.02)	1.29(±0.03)	1.33(±0.08)
0.02	53.38(±0.02)	53.74(±0.01)	54.26(±0.01)	54.72(±0.01)	1.27(±0.05)	1.34(±0.03)	1.29(±0.04)	1.38(±0.04)
0.03	53.43(±0.01)	53.78(±0.01)	54.30(±0.01)	54.83(±0.02)	1.51(±0.03)	1.71(±0.02)	1.77(±0.03)	1.85(±0.05)
				DEG				
0	91.38(±0.03)	91.81(±0.11)	92.06(±0.01)	92.32(±0.00)	1.64(±0.11)	1.89(±0.34)	1.94(±0.04)	2.00(±0.02)
0.01	91.44(±0.01)	91.89(±0.01)	92.27(±0.01)	92.63(±0.01)	2.13(±0.03)	2.22(±0.04)	2.23(±0.03)	2.23(±0.03)
0.02	91.61(±0.00)	91.98(±0.01)	92.36(±0.01)	92.71(±0.00)	1.99(±0.01)	2.04(±0.02)	2.05(±0.02)	2.08(±0.01)
0.03	91.64(±0.00)	91.99(±0.00)	92.37(±0.01)	92.75(±0.01)	2.00(±0.01)	2.07(±0.01)	2.10(±0.02)	2.06(±0.02)
				TEG				
0.00	127.99(±0.01)	128.55(±0.01)	129.11(±0.02)	129.58(±0.00)	1.38(±0.04)	1.48(±0.03)	1.61(±0.06)	1.52(±0.01)
0.01	127.97(±0.01)	128.54(±0.02)	129.14(±0.03)	129.71(±0.04)	1.50(±0.03)	1.64(±0.06)	1.64(±0.09)	1.69(±0.13)
0.02	128.13(±0.01)	128.66(±0.01)	129.23(±0.01)	129.82(±0.01)	1.23(±0.02)	1.33(±0.02)	1.43(±0.03)	1.45(±0.03)
0.03	128.14(±0.00)	128.67(±0.01)	129.26(±0.01)	129.82(±0.01)	1.29(±0.01)	1.37(±0.04)	1.41(±0.03)	1.48(±0.03)

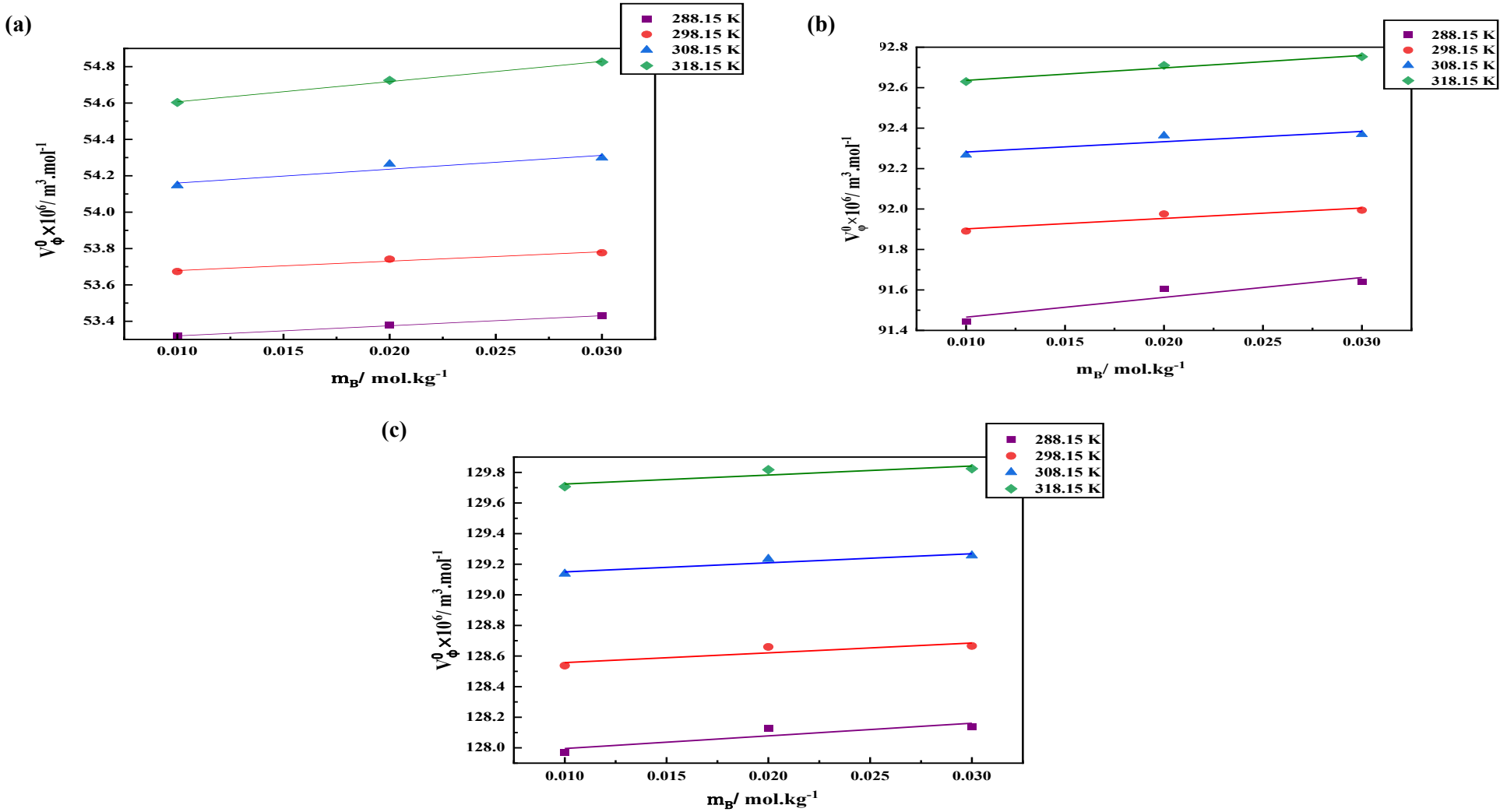

Figure 4.4: Variation of V_φ^0, of EG, DEG and TEG in (a), (b) and (c) respectively in m_B of gluconolactone at several T values [Purple (square), 288.15 K; red (circle), 298.15 K; blue (triangle), 308.15 K; green (diamond), 318.15 K]

Partial molar isentropic compressibility

The resulting equation describes how $K_{\phi,s}$ changes with molar concentration.

$$K_{\phi,s} = K^0_{\phi,S} + S^*_k m_A \quad (4.5)$$

Where, $K^0_{\phi,S}$, m_A and S^*_K are the limiting isentropic compression, the solute's molality in aqueous chemical solutions and experimentally determined slope of solute interactions respectively. The experimental slope (S^*_K) and the partial isentropic compression ($K^0_{\phi,S}$) are computed which are shown in **Table 4.4.** m_B stands for concentration of GLA and all the other variables have their usual uncertainties as mention in Chapter 3, and for $\left(K^{\circ}_{\phi,S}\right) = \pm 0.01 \times 10^6/(m^3.mol^{-1}.GPa^{-1})$ and for $(S^*_K) = \pm 0.24 \times 10^6/(kg.m^3.mol^{-2}.GPa^{-1})$. The values of $K^0_{\phi,S}$, S^*_K, and their standard errors are derived straight from the previous work for (water + EG/DEG/TEG) [1]. Two main factors contribute to partial molar isentropic compressibility ($K^0_{\phi,S}$): (i) the solvent intrinsic compressibility, which is a positive factor because it increases the compressibility of the solution or liquid mixture [39]; and (ii) the solute intrinsic compressibility, which is a negative factor due to interactions between the solute, solvent particles that produce it. This electrostriction phenomenon is also called as the penetration process that causes the sol. to become less squeezable. Because the negative effect outweighs the positive effect, all values of ($K^0_{\phi,S}$) are negative. The **Table 4.4** shows that the ($K^0_{\phi,S}$) values fall as the temperature and gluconolactone concentration increase, and **Figure 4.5** visually illustrates this. This indicates that the combinations amongst solvent and solute is directly proportional to gluconolactone concentration.

. The (solute-solute) associations in the system are essentially inconsequential since the S^*_K values in **Table 4.4** are so small in relation to the $K^0_{\phi,S}$ values, demonstrating the prominence of solute and solvent interactions in the sample mixes [11,40].

Table 4.4

Calculated K_{ϕ}^{0}, and S_{K}^{*}, of the ternary mixture of gluconolactone with EG, DEG, TEG at same temperatures ranges and m_B at pressure = 0.1 MPa.

[a]m_B/ $mol.kg^{-1}$	$K_{\phi,S}^{0} \times 10^{6}(m^{3}.mol^{-1}.GPa^{-1})$				$S_{K}^{*} \times 10^{6}(kg.m^{3}.mol^{-2}.GPa^{-1})$			
	288.15K	298.15K	308.15K	318.15K	288.15K	298.15K	308.15K	318.15K
				EG				
0.00	−46.03(±0.08)	−44.23(±0.07)	−42.89(±0.07)	−42.01(±0.07)	−1.24(±0.24)	−1.18(±0.23)	−1.13(±0.23)	−1.13(±0.23)
0.01	−45.81(±0.06)	−44.05(±0.05)	−42.70(±0.05)	−41.73(±0.05)	−1.07(±0.17)	−1.02(±0.16)	−0.98(±0.16)	−0.95(±0.15)
0.02	−45.53(±0.07)	−43.80(±0.07)	−42.49(±0.07)	−41.49(±0.07)	−1.16(±0.21)	−1.11(±0.21)	−1.06(±0.20)	−1.03(±0.20)
0.03	−45.36(±0.05)	−43.61(±0.05)	−42.29(±0.05)	−41.35(±0.05)	−1.16(±0.16)	−1.10(±0.15)	−1.06(±0.15)	−1.03(±0.15)
				DEG				
0.00	−46.03(±0.08)	−44.25(±0.07)	−42.90(±0.07)	−41.95(±0.07)	−1.47(±0.24)	−1.40(±0.23)	−1.36(±0.23)	−1.34(±0.23)
0.01	−45.77(±0.08)	−44.01(±0.08)	−42.67(±0.07)	−41.70(±0.07)	−1.44(±0.24)	−1.38(±0.23)	−1.34(±0.23)	−1.31(±0.22)
0.02	−45.57(±0.07)	−43.84(±0.06)	−42.53(±0.06)	−41.52(±0.06)	−1.29(±0.20)	−1.24(±0.19)	−1.20(±0.19)	−1.18(±0.18)
0.03	−45.39(±0.07)	−43.64(±0.06)	−42.32(±0.06)	−41.38(±0.06)	−1.30(±0.20)	−1.24(±0.19)	−1.21(±0.19)	−1.18(±0.19)
				TEG				
0.00	−46.03(±0.08)	−44.25(±0.08)	−42.90(±0.08)	−41.96(±0.08)	−1.81(±0.26)	−1.73(±0.25)	−1.68(±0.25)	−1.64(±0.24)
0.01	−45.88(±0.04)	−44.12(±0.04)	−42.77(±0.04)	−41.80(±0.04)	−1.48(±0.12)	−1.41(±0.12)	−1.37(±0.11)	−1.34(±0.11)
0.02	−45.53(±0.08)	−43.80(±0.08)	−42.49(±0.08)	−41.48(±0.08)	−1.75(±0.25)	−1.67(±0.24)	−1.62(±0.23)	−1.58(±0.23)
0.03	−45.37(±0.08)	−43.63(±0.07)	−42.30(±0.07)	−41.36(±0.07)	−1.68(±0.22)	−1.60(±0.22)	−1.55(±0.21)	−1.52(±0.21)

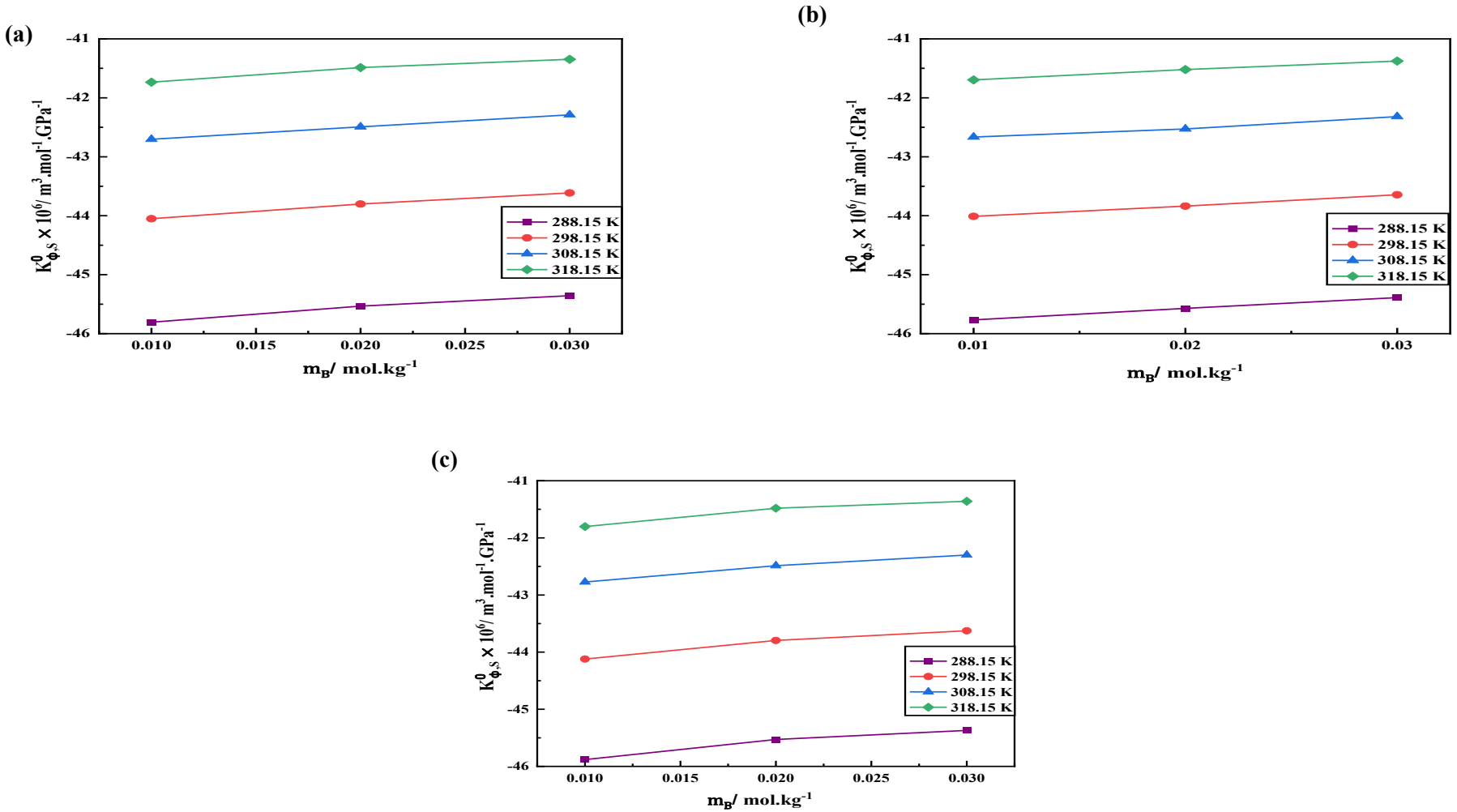

Figure 4.5: Change in $K^0_{\varphi,S}$, for EG, DEG and TEG in gluconolactone sol. with concentration at numerous T range shown in (a), (b) and (c) respectively, [Purple (square), $288.15K$; red (circle), $298.15K$; blue (triangle), $308.15K$; green (diamond), $318.15K$]

Transfer properties:

Partial molar volume of transfer

The following expression determines the glycols' V_ϕ^0 that are transferred from H_2O to water based GLA, and the results are shown in **Table 4.5**.

$$\Delta V_\phi^0 = V_{\phi\,(\text{in aqueous gluconolactone})}^0 - V_{\phi\,(\text{in water})}^0 \qquad (4.6)$$

With ΔV_ϕ^0, solvent and solute interactions within the mix are studied qualitatively as well as quantitatively without considering interactions caused by solute-solute molecules. As it is clearly visible from the **Table 4.5**, apart from 0.01 $mol.kg^{-1}$ water based GLA at T=$288.15K$ and $298.15K$ TEG at, the discovered positive values of ΔV_Φ^0, are intensifying with the upsurge in gluconolactone's m_B, as well as growing with glycol's molar mass. This suggests that because both gluconolactone and glycols contain polar groups, they have strong ion-ion interactions. Due to their interactions in the solution, the solute's capability to produce structures is improved. Therefore, as per the co-spheres overlap hypothesis and the positive ΔV_Φ^0 values, the structure composition comes from structural effects between the two co-spheres and solvophobic solvation [41,42]. The interactions between hydrophilic molecules and hydrophilic ions are related to the positive values, as per co-sphere overlap. Model in the current investigation (gluconolactone + water + glycols) demonstrates the existence of interactions between hydrophilic molecules and ions [40, 43–44].

Table 4.5

At constant pressure = 0.1 MPa, found values of ΔV_{Φ}^{0} of the ternary mixture of gluconolactone with EG, DEG, TEG and $\Delta K_{\Phi,S}^{0}$ at same temperatures and m_B

$^{a}m_B/$	$\Delta V_{\Phi}^{0} \times 10^{6}(m^3.mol^{-1})$				$\Delta K_{\Phi,S}^{0} \times 10^{6}(m^3.mol^{-1}.GPa^{-1})$			
$mol.kg^{-1}$	$288.15K$	$298.15K$	$308.15K$	$318.15K$	$288.15K$	$298.15K$	$308.15K$	$318.15K$
				EG				
0.01	0.05	0.01	0.07	0.09	0.22	0.18	0.19	0.28
0.02	0.11	0.08	0.18	0.21	0.50	0.43	0.40	0.52
0.03	0.16	0.12	0.22	0.32	0.67	0.62	0.60	0.66
				DEG				
0.01	0.06	0.08	0.21	0.31	0.26	0.24	0.23	0.25
0.02	0.23	0.17	0.30	0.39	0.46	0.41	0.37	0.43
0.03	0.26	0.18	0.31	0.43	0.64	0.61	0.58	0.57
				TEG				
0.01	−0.02	−0.01	0.03	0.13	0.15	0.13	0.13	0.16
0.02	0.14	0.11	0.12	0.24	0.50	0.45	0.41	0.48
0.03	0.15	0.12	0.15	0.24	0.66	0.62	0.60	0.60

The transfer property of $K^0_{\phi,S}$: $\Delta K^0_{\phi,S}$:

The understated expression (4.7) is used to compute the $\Delta K^0_{\phi,S}$ for glycol from water to aqueous gluconolactone.

$$\Delta K^0_{\phi,S} = K^0_{\phi,S}{}_{(\text{in aqueous gluconolactone})} - K^0_{\phi,S}{}_{(\text{in water})} \qquad (4.7)$$

Table 4.5 comprises the positive values of $\Delta K^0_{\phi,S}$. The positive $\Delta K^0_{\phi,S}$ values in the **Table 4.5** make it clear that the solute can form structures, and they also highlight the predominance of zwitterionic centre contacts of glycol and gluconolactone. The ternary system's solute-solvent interactions expand in size in tandem with its structural-making potential, as shown in the, which also shows that when gluconolactone concentration rises, the $\Delta K^0_{\phi,S}$values climb [7].

V^0_ϕ dependent on Temperature

The subsequent expression explains how (V^0_ϕ), varies with T at finite dilution:

$$V^0_\phi = a + b(T - T_{ref}) + c(T - T_{ref})^2 \qquad (4.8)$$

Here in equation (4.8), a, b and c are the empirical coefficients and T and T_{ref} denotes temperature and reference temperature i.e., taken to be $298.15K$. To acquire deviations termed as ARD (σ) that are derived using these empirical parameters, the calculated and experimental values of V^0_ϕ are employed. The following equation (4.9) is used to obtain these deviations (ARD).

$$\sigma = \left(\frac{1}{n}\right)\sum\left[\text{abs}\left(\left(Y_{\text{Exptl.}} - Y_{\text{calc.}}\right)/Y_{\text{Exptl.}}\right)\right] \qquad (4.9)$$

Where $Y = V^0_\phi$, so the equation becomes,

$$\sigma = \left(\frac{1}{n}\right)\sum\left[\text{abs}\left(\frac{V^0_{\phi\,\text{Exptl.}} - V^0_{\phi\,\text{calc.}}}{V^0_{\phi\,\text{Exptl.}}}\right)\right] \qquad (4.10)$$

We have used equation (4.10) to determine the deviations. Values of the deviation are quite smaller and the present work R^2 show that the equation is perfectly suited [41]. The values of empirical parameters a, b, c, $ARD\ (\sigma)$ and R^2 are all shown in '**Table 4.6'**. It shows c is negative at concentrations 0.01 and 0.02 $mol.kg^{-1}$ of gluconolactone and DEG, whereas it is positive for rest of the values for EG and TEG. These constants are used to derive the theoretic values of V^0_ϕ and compare them to the experimental results [45]. The main goal to determine V^0_ϕ is to obtain partial molar expansibility E^0_ϕ, which is produced by Eq. (**4.8**) w.r.t. temperature. Using the following formulae, the partial molar expansibilities values are obtained (4.11):

$$E_{\phi}^{0} = \left(\frac{\partial V_{\phi}^{0}}{\partial T}\right)_{P} = b + 2c(T - T_{ref}) \quad (4.11)$$

The partial molar expansibility is thought to be a crucial characteristic [45,46]. As given in **Table 4.7**, all E_{ϕ}^{0} are positive, showing that the compact volume as a outcome of the interaction of the glycols in the aqueous gluconolactone solution [47]. The following basic thermodynamic equation (4.12) provided by Hepler describes the solute's capacity to generate and disrupt structures in a mixed solvent system [48].

$$\left(\frac{\partial E_{\phi}^{0}}{\partial T}\right)_{P} = \left(\frac{\partial^{2} V_{\phi}^{0}}{\partial T^{2}}\right)_{P} = 2c \quad (4.12)$$

The capability of the solvent media to construct & demolish structures is indicated by the polarity of $\partial E_{\phi}^{0}/\partial T$ values. As long as the values of $\partial E_{\phi}^{0}/\partial T$ are positive, the solute can form structures, while structure disruption is shown by negative values of $\partial E_{\phi}^{0}/\partial T$ [49]. In the current investigation $\partial E_{\phi}^{0}/\partial T$ are showing all positive values except for concentrations 0.01 and 0.02 $mol.kg^{-1}$ of gluconolactone and DEG as evident from **Table 4.7**, hence majority of $\partial E_{\phi}^{0}/\partial T$ values are positive so it indicates structure making ability. It can be shown that as temperature and concentration rise, there is no discernible pattern for E_{ϕ}^{0} values.

Table 4.6

At pressure = 0.1 MPa, values of empirical parameters, a, b, c in equation (4.8), of the ternary mixture of gluconolactone with EG, DEG, TEG at same temperatures and m_B.

[a]m_B/ $mol.kg^{-1}$	$a \times 10^6/(m^3.mol^{-1})$	$b \times 10^6/(m^3.mol^{-1}K^{-1})$	$c \times 10^6$ $/(m^3.mol^{-1}K^{-2})$	R^2	ARD
		EG			
0.01	53.6937	0.0407	0.0003	0.9999	0.000248
0.02	53.7745	0.0432	0.0002	0.9999	0.000407
0.03	53.8022	0.0426	0.0004	0.9999	0.000316
		DEG			
0.01	91.8824	0.0414	-0.0002	0.9999	0.000061
0.02	91.9839	0.0376	-0.0001	0.9999	0.000060
0.03	91.9958	0.0364	0.0001	0.9999	0.000012
		TEG			
0.01	128.5472	0.0580	0.0000	0.9999	0.000050
0.02	128.6641	0.0553	0.0001	0.9999	0.000025
0.03	128.6783	0.0555	0.0001	0.9999	0.000066

Table 4.7

At pressure = 0.1 MPa, partial molar expansibilities, E_{Φ}^{0}, for the ternary mixture of gluconolactone with EG, DEG, TEG at same temperatures and m_B.

$^{a}m_B/$ $mol.kg^{-1}$	$E_{\Phi}^{0} \times 10^{6}/(m^{3}.mol^{-1}K^{-1})$				$\left(\frac{\partial E_{\Phi}^{0}}{\partial T}\right)_{P}$ / $(m^{3}.mol^{-1}K^{-2})$
	$288.15K$	$298.15K$	$308.15K$	$318.15K$	
			EG		
0.01	0.0356	0.0407	0.0458	0.0509	0.00051
0.02	0.0384	0.0432	0.0481	0.0529	0.00049
0.03	0.0336	0.0426	0.0516	0.0606	0.00090
			DEG		
0.01	0.0456	0.0414	0.0372	0.0331	-0.00042
0.02	0.0387	0.0376	0.0364	0.0353	-0.00011
0.03	0.0348	0.0364	0.0379	0.0394	0.00015
			TEG		
0.01	0.0578	0.0580	0.0581	0.0583	0.00002
0.02	0.0528	0.0553	0.0577	0.0602	0.00025
0.03	0.0535	0.0555	0.0575	0.0595	0.00020

Coefficients of Interaction

The (ΔV_ϕ^0 and ΔK_ϕ^0) are produced by the stated relation.

$$\Delta V_\phi^0(\text{water to aqueous gluconolactone solution}) = 2V_{AB}m_B + 3V_{ABB}{m_B}^2 \quad (4.13)$$

$$\Delta K_\phi^0(\text{water to aqueous gluconolactone solution}) = 2K_{AB}m_B + 3K_{ABB}{m_B}^2 \quad (4.14)$$

Here in above equation, A symbolizes glycols and B symbolizes gluconolactone. Interaction coefficients are shown in **Table 4.8** as V_{AB}; V_{ABB} and K_{AB}; K_{ABB}. As per the model of McMillian and Mayer [50], the V_ϕ^0 and K_ϕ^0 are fitted to these values to obtain the values, (ΔV_ϕ^0; ΔK_ϕ^0). This theory examines how interactions between molecules in pairs and triplets might separate effects in a liquid mixture. The similar theory had been further addressed by Franks *et al.* [51] and Friedman and Krishnan [52]. V_{AB} are all positive and V_{ABB} is all negative across all the temperatures for DEG whereas it is positive for EG and TEG except at temperature 308.15K and 318.15 K respectively. However, K_{AB} is positive across the board at all temperatures and glycols m_a. In the case of K_{ABB}, DEG show all the negative data however, EG and TEG have mixed results—both positive and negative. In combinations of glycol, gluconolactone and water, pairwise interactions are anticipated to outweigh due to the overall positive values of V_{AB} and K_{AB} [53].

Table 4.8

At constant pressure = 0.1 MPa, (V_{AB}, K_{AB}, V_{ABB} and K_{ABB}) for the ternary mixture of gluconolactone with EG, DEG, TEG at same temperatures and m_B.

T/(K)	$V_{AB} \times 10^6$ $/(m^3.mol^{-2}.kg)$	$V_{ABB} \times 10^6$ $/(m^3.mol^{-3}.kg^2)$	$K_{AB} \times 10^6$ $/(m^3.mol^{-3}.kg\ GPa^{-1})$	$K_{ABB} \times 10^6$ $/(m^3.mol^{-3}.kg^2\ GPa^{-1})$
		EG		
288.15	2.51	3.72	12.78	-31.59
298.15	1.04	21.69	9.84	12.27
308.15	4.68	-20.53	9.31	16.32
318.15	4.93	8.08	16.05	-109.71
		DEG		
288.15	5.20	-14.71	13.79	-69.81
298.15	5.33	-48.93	11.93	-42.24
308.15	12.70	-168.36	10.84	-28.75
318.15	17.44	-230.88	13.69	-92.72
		TEG		
288.15	0.98	38.86	10.22	24.94
298.15	0.95	26.56	8.47	49.84
308.15	2.47	2.05	7.51	60.44
318.15	8.47	-96.06	10.94	-13.55

Conclusion

A systematic study was carried out on the thermodynamic and ultrasonic properties of (gluconolactone + water + TEG/DEG/EG) mixtures at various temperatures, under constant pressure, and across the full m_B range of gluconolactone (0.01, 0.02, and 0.03 $mol.kg^{-1}$). High-precision measurements of solution ρ and v were obtained using DSA. From the experimental data, molar properties such as apparent, partial, and transfer properties were calculated, along with interaction parameters like pairwise and triplet coefficients. These analyses were aimed at understanding solute–solvent interactions within the mixtures. The apparent and partial molar properties indicated strong solvent-solute interactions, which were observed to intensify from EG to TEG because of growing molecular weight. The glycols exhibited various interactions with each other and with water, including dipole–dipole, effect of hydration of hydrophobes, and dipole-induced dipole interactions. Positive values of E_ϕ^0 suggested that the solute contributes to structural formation within the liquid mixtures. Furthermore, the pair and triplet interaction coefficients indicated that pairwise interactions are predominant in the (gluconolactone + water + glycol) systems.

Problem 2

"Understanding of lactobionic acid in aqueous-glycol mixtures at different temperatures: Ultrasonic investigation"

This investigation focused on the study of liquid mixtures that contain (PEGs) such as PEG-200/400, and lactobionic acid aqueous solutions. The study aimed to examine the ρ and v of these systems with varying T and m_B of lactobionic acid in aqueous medium.

Volumetric Properties:

Apparent Molar Volume

The densities (ρ) that were measured experimentally in lactobionic acid solutions at varied concentrations. The density measurements are obtained in a liquid combination (water + LBA + PEG 200/PEG 400) at pressure 0.01 MPa, (0.00, 0.01, 0.02, and 0.03) mol·kg^{-1} concentrations, and temperatures 288.15, 298.15, 308.15, and 318.15 K. **Table 4.9** includes an index of these experimental density values. The experimental results for density meet the stated density criteria at various temperatures. A comparison between experimental density values for aqueous PEG 200/400 solutions at various temperatures and literature values [76] has been provided in the graph in **Figure 4.6**. It is evident from **Figure 4.6** that the experimental values correlate with the values stated in the literature. These calculations were utilized to determine the *(V_ϕ)* by the formula given in equation **4.1. Table 4.9** provides information on the V_ϕ and ρ of the mixture. The data of density for (water + polyethylene glycols) are taken from our prior study [54] denoted as subscript b in the table. The ρ, T, p and have the same uncertainty as in problem-1 and of V_ϕ is found to be $u(V_\phi) = \pm(0.05 - 0.07) \times 10^6/(m^3.mol^{-1})$, also m_A denotes the molality of glycols in LBA. The statistics in **Table 4.9** clearly show that when the temperature goes up, density values fall and all V_ϕ values are positive, indicating a high particle association in the system. This tendency is more pronounced when the glycols molecular mass rises from PEG 200 to 400, which indicates an increase in the order of components interactions and is demonstrated by **Figure 4.7**. The V_ϕ values show an increase in accordance with the intensification in temperature and upsurge in PEGs molality at a certain concentration of lactobionic acid, as shown graphically in **Figure 4.8**. The significant linear connection amongst the values of V_ϕ and temperature, in

addition to the molality of polyethylene glycol explains the basis of molecules interacting in the composition. In the occurrence of water, dipole-dipole, hydrophobic hydration, the hydrophobic effect, dipole-induced dipole interactions & intermolecular hydrogen bonding are all established. Because hydrogen bonds in water molecules increase packing efficiency, and solute particles that have low V_ϕ values are highly hydrated.

High V_ϕ values, on the other hand, signify the presence of significant solute-co-solute interactions [12-14, 55-57, 36].

Table 4.9

Measured ρ and v in the ternary mixture of Lactobionic acid with PEG-200 and PEG-400 at various m_B and temperatures at the 0.1 MPa pressure.

Molality $^{a}m_A$ / $(mol.kg^{-1})$	$\rho \times 10^{-3}$ / $kg.m^{-3}$				$V_\phi \times 10^{6}$/ $(m^3.mol^{-1})$			
	288.15K	298.15K	308.15K	318.15K	288.15K	298.15K	308.15K	318.15K
				0.00 (mol. kg^{-1}) Lactobionic Acid + PEG-200				
0.00000	0.99926 [b]	0.99705 [b]	0.99404 [b]	0.99036 [b]				
0.10009	1.00221 [b]	1.00001 [b]	0.99701 [b]	0.99335 [b]	170.10 [b]	170.33 [b]	170.61 [b]	170.96 [b]
0.20044	1.00504 [b]	1.00284 [b]	0.99986 [b]	0.99621 [b]	170.28 [b]	170.52 [b]	170.83 [b]	171.18 [b]
0.30136	1.00777 [b]	1.00558 [b]	1.00260 [b]	0.99897 [b]	170.42 [b]	170.66 [b]	170.97 [b]	171.32 [b]
0.40026	1.01032 [b]	1.00815 [b]	1.00519 [b]	1.00157 [b]	170.58 [b]	170.79 [b]	171.10 [b]	171.44 [b]
0.49999	1.01280 [b]	1.01062 [b]	1.00767 [b]	1.00408 [b]	170.71 [b]	170.95 [b]	171.26 [b]	171.59 [b]
				0.01 (mol. kg^{-1}) Lactobionic Acid + PEG-200				
0.00000	1.00054	0.99819	0.99517	0.99144	170.30	170.56	170.90	171.30
0.10043	1.00347	1.00112	0.99811	0.99439	170.42	170.70	171.04	171.51
0.20062	1.00627	1.00392	1.00092	0.99720	170.55	170.83	171.20	171.67
0.29985	1.00892	1.00658	1.00358	0.99987	170.70	170.96	171.34	171.84
0.39982	1.01148	1.00915	1.00616	1.00244	170.83	171.09	171.48	171.99
0.50120	1.01397	1.01166	1.00865	1.00494	170.30	170.56	170.90	171.30
				0.02 (mol. kg^{-1}) Lactobionic Acid + PEG-200				
0.00000	1.00178	0.99949	0.99653	0.99267	170.44	171.00	171.57	172.14

0.10025	1.00467	1.00236	0.99938	0.99552	170.63	171.17	171.78	172.38
0.20017	1.00742	1.00508	1.00209	0.99822	170.81	171.36	171.99	172.60
0.29993	1.01004	1.00768	1.00466	1.00079	170.95	171.50	172.18	172.80
0.39956	1.01255	1.01017	1.00712	1.00324	171.12	171.66	172.34	172.95
0.49999	1.01496	1.01257	1.00950	1.00561	170.44	171.00	171.57	172.14
0.03 ($\mathbf{mol.kg^{-1}}$) Lactobionic Acid + PEG-200								
0.00000	1.00296	1.00086	0.99780	0.99395	170.61	171.28	171.88	172.48
0.10035	1.00582	1.00368	1.00060	0.99675	170.93	171.63	172.27	172.87
0.20053	1.00851	1.00634	1.00324	0.99938	171.25	171.98	172.59	173.21
0.29972	1.01103	1.00881	1.00570	1.00183	171.55	172.26	172.91	173.51
0.39985	1.01344	1.01119	1.00805	1.00419	171.82	172.57	173.22	173.81
0.50007	1.01574	1.01343	1.01027	1.00641	170.61	171.28	171.88	172.48
0.00 ($\mathbf{mol.kg^{-1}}$) Lactobionic Acid + PEG-400								
0.00000	0.99926 [b]	0.99705 [b]	0.99404 [b]	0.99036 [b]				
0.10015	1.00577 [b]	1.00349 [b]	1.00044 [b]	0.99673 [b]	333.00 [b]	334.28 [b]	335.56 [b]	336.82 [b]
0.20004	1.01179 [b]	1.00945 [b]	1.00636 [b]	1.00264 [b]	333.35 [b]	334.65 [b]	335.90 [b]	337.09 [b]
0.29995	1.01739 [b]	1.01499 [b]	1.01188 [b]	1.00813 [b]	333.69 [b]	334.99 [b]	336.18 [b]	337.42 [b]
0.40100	1.02267 [b]	1.02019 [b]	1.01705 [b]	1.01330 [b]	334.01 [b]	335.34 [b]	336.53 [b]	337.74 [b]
0.50006	1.02747 [b]	1.02496 [b]	1.02180 [b]	1.01804 [b]	334.35 [b]	335.64 [b]	336.82 [b]	338.00 [b]
0.01 ($\mathbf{mol.kg^{-1}}$) Lactobionic Acid + PEG-400								
0.00000	1.00054	0.99819	0.99517	0.99144				
0.09989	1.00699	1.00459	1.00152	0.99777	333.22	334.31	335.60	336.87
0.20029	1.01299	1.01054	1.00744	1.00367	333.56	334.67	335.95	337.21

0.29999	1.01854	1.01604	1.01290	1.00910	333.87	335.02	336.28	337.56
0.39959	1.02367	1.02113	1.01794	1.01413	334.25	335.41	336.69	337.95
0.50046	1.02852	1.02592	1.02271	1.01886	334.59	335.79	337.05	338.36
0.02 ($\mathbf{mol.kg^{-1}}$) Lactobionic Acid + PEG-400								
0.00000	1.00178	0.99949	0.99653	0.99267				
0.09998	1.00819	1.00585	1.00285	0.99897	333.31	334.38	335.63	336.89
0.20018	1.01414	1.01174	1.00870	1.00482	333.66	334.81	336.07	337.26
0.29984	1.01964	1.01718	1.01410	1.01020	333.98	335.19	336.44	337.67
0.40025	1.02479	1.02228	1.01917	1.01526	334.34	335.56	336.79	338.00
0.50040	1.02955	1.02703	1.02386	1.01992	334.73	335.86	337.14	338.41
0.03 ($\mathbf{mol.kg^{-1}}$) Lactobionic Acid + PEG-400								
0.00000	1.00296	1.00086	0.99780	0.99395				
0.10011	1.00933	1.00719	1.00408	1.00022	333.37	334.40	335.70	336.91
0.19995	1.01523	1.01302	1.00988	1.00600	333.72	334.83	336.10	337.34
0.29987	1.02070	1.01843	1.01526	1.01135	334.09	335.25	336.51	337.76
0.40004	1.02579	1.02347	1.02027	1.01635	334.46	335.64	336.87	338.14
0.49968	1.03049	1.02811	1.02491	1.02093	334.84	336.05	337.23	338.58

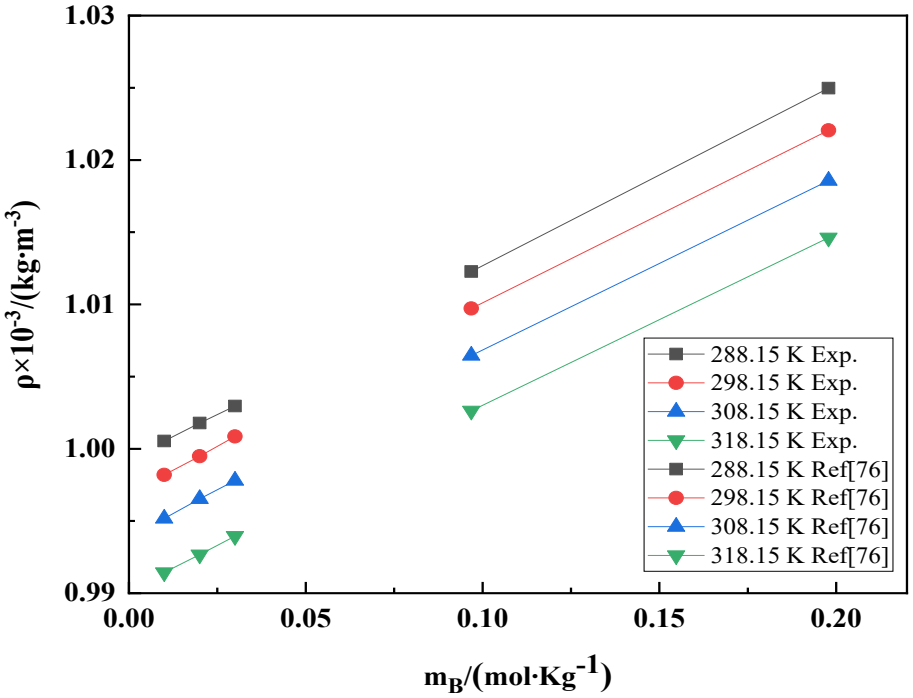

Figure 4.6 Variation in experimental and literature values [76] of density (ρ) for LBA+ Water at different concentrations.

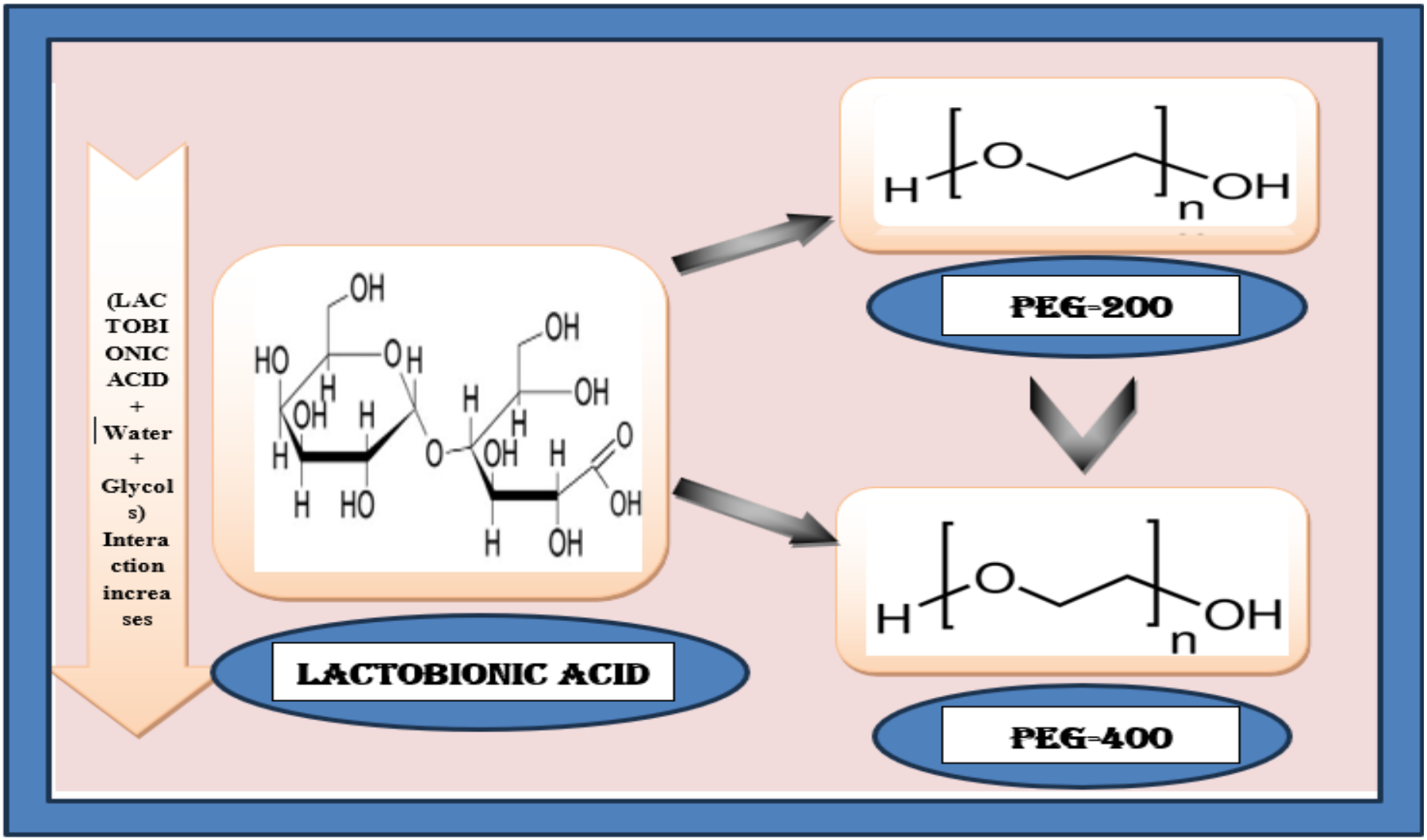

Figure 4.7 Interactions of Lactobionic acid with PEG 200 and PEG 400.

I.(a)

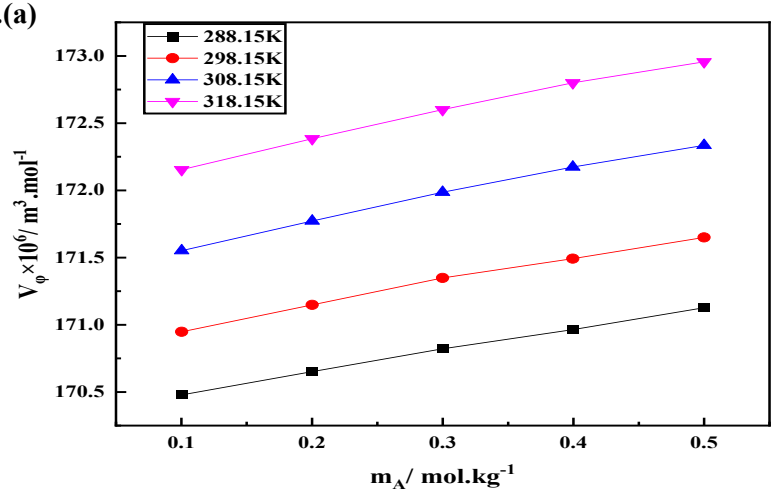
288.15K
298.15K
308.15K
318.15K
173.0
172.5
172.0
171.5
171.0
170.5
0.1
0.2
0.3
0.4
0.5
$V_\varphi \times 10^6$/ m^3.mol^{-1}
m_A/ mol.kg^{-1}

I.(b)

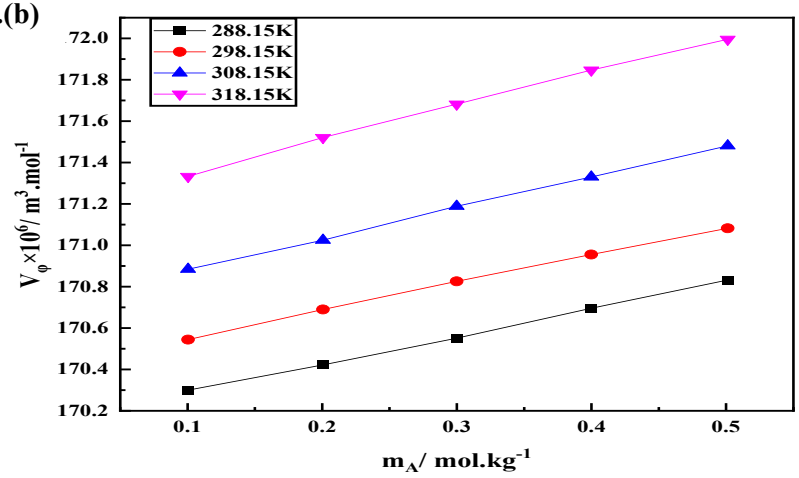
288.15K
298.15K
308.15K
318.15K
172.0
171.8
171.6
171.4
171.2
171.0
170.8
170.6
170.4
170.2
0.1
0.2
0.3
0.4
0.5
$V_\varphi \times 10^6$/ m^3.mol^{-1}
m_A/ mol.kg^{-1}

I.(c)

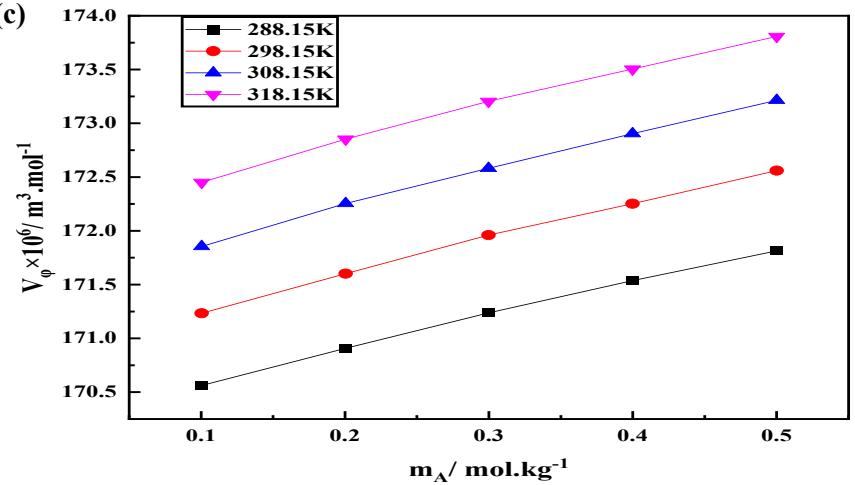
288.15K
298.15K
308.15K
318.15K
174.0
173.5
173.0
172.5
172.0
171.5
171.0
170.5
0.1
0.2
0.3
0.4
0.5
$V_\varphi \times 10^6$/ m^3.mol^{-1}
m_A/ mol.kg^{-1}

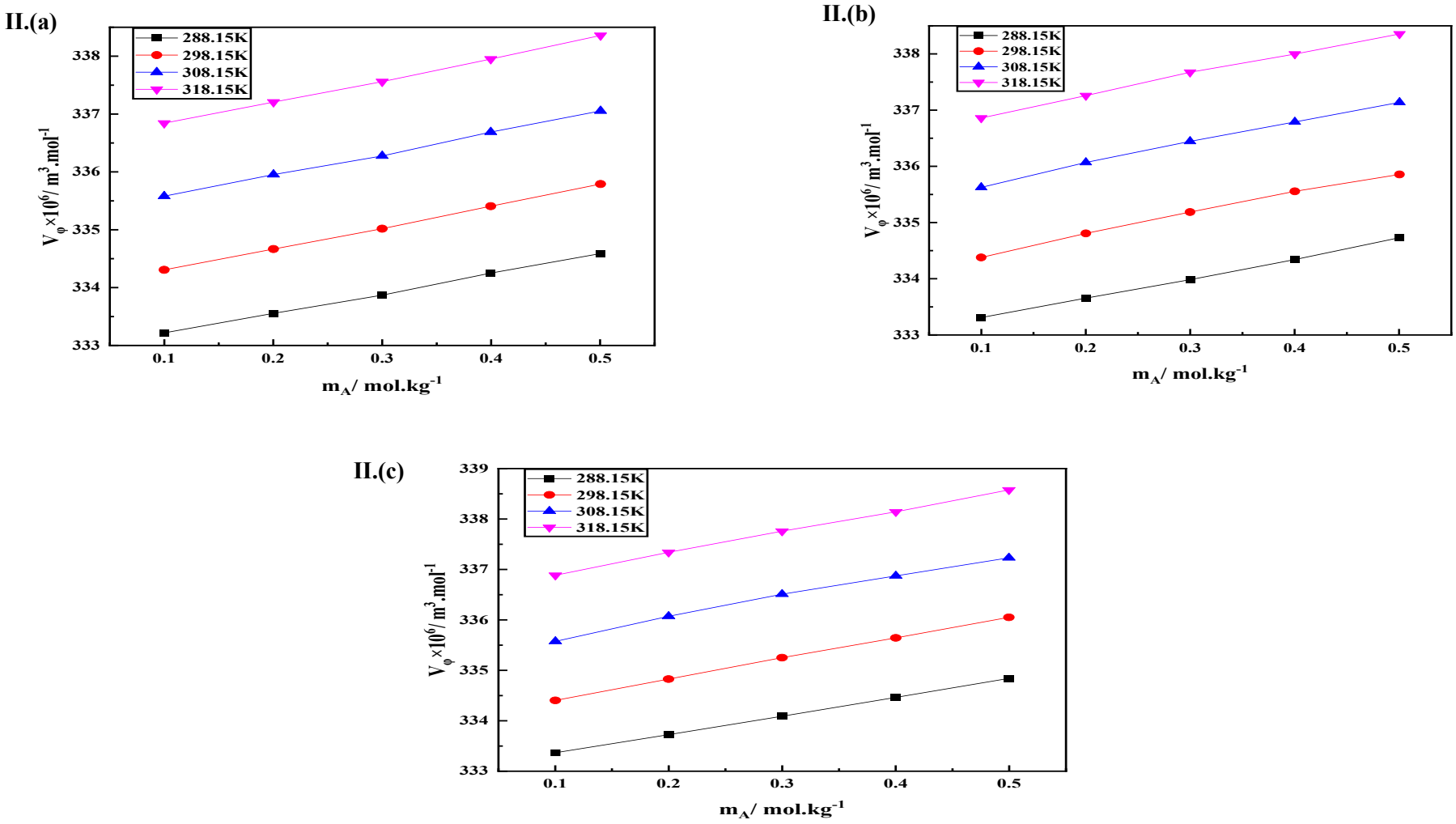

Figure 4.8 Change of V_ϕ, of PEG-200 (I) and PEG-400 (II), versus m_A, for 0.01, 0.02, 0.03 LBA at various temperatures in (a), (b) and (c) respectively [black, $288.15K$; red, $298.15K$; blue, $308.15K$ K; green, $318.15K$].

Partial Molar Volume

The V_ϕ^0 of the sample containing lactobionic acid and poly (ethylene glycol) are calculated by means of equation **4.4**. **Table 4.10** lists the experimental (V_ϕ^0) values as well as (S_V^*) also with their standard errors with uncertainty u (V_ϕ^0)= $\pm 0.01\times10^6/(m^3.mol^{-1})$ and u(S_V^*)=$\pm 0.03\times10^6/(m^3.kg.mol^{-2})$ and $^a m_B$ symbolizes concentration of water based LBA. For (water + PEG-200/400), the values of V_ϕ^0 and associated errors were taken straight from the literature [54] written as subscript b in the table. The (V_ϕ^0) provide further useful information about the combinations within particles of a solute and a solvent. In this case, V_ϕ^0 are positive and are graphically shown in **Figure 4.9.** They rise with rising temperatures, lactobionic acid concentration, and poly (ethylene glycols) molecular mass. [58-59]. These positive values of V_ϕ^0 indicate the presence of hydrophobic bonds and a potent hydrogen bond among the OH groups of PEGs and the water particles because the solvation molecules of the solute are freed from its solvation layer and enter the mixture. Furthermore, the way in which they change with temperature provides clues about several processes, such as the production of hydrogen bonds, etc. The current study's S_V^* values had positive signs at all temperatures and for all solution compositions, indicating pairwise interactions

The S_V^* numbers in this study were positive at all T and for all solution types, which shows that the ions that make up the solute molecules, with charged functional groups were interacting with each other pairwise. However, the solute-solute association was suppressed by smaller values of S_V^* compared to V_ϕ^0 values, by the solvent solute association [1, 28].

Table 4.10

Calculated V_ϕ^0 and slopes, S_V^* of the ternary mixture of lactobionic acid with PEG-200/400 at various m_B and temperatures at the fixed 0.1 MPa pressure.

$^a m_B$	$V_\phi^0 \times 10^6$ / $(m^3.mol^{-1})$				$S_V^* \times 10^6$ / $(m^3.kg.mol^{-2})$			
$(mol.kg^{-1})$	$288.15K$	$298.15K$	$308.15K$	$318.15K$	$288.15K$	$298.15K$	$308.15K$	$318.15K$
Poly(ethylene glycol)-200								
0.00	169.96(±0.01)[b]	170.20(±0.01)[b]	170.48(±0.03)[b]	170.85(±0.03) [b]	1.52 (±0.05) [b]	1.51 (±0.04)[b]	1.57 (±0.09)[b]	1.50 (±0.09)[b]
0.01	170.16(±0.01)	170.44(±0.00)	170.75(±0.01)	171.15(±0.02)	1.34 (±0.02)	1.30 (±0.01)	1.46 (±0.02)	1.71 (±0.06)
0.02	170.28(±0.02)	170.84(±0.02)	171.39(±0.02)	171.96(±0.03)	1.69 (±0.05)	1.66 (±0.05)	1.93 (±0.06)	2.04 (±0.09)
0.03	170.32(±0.02)	170.98(±0.03)	171.58(±0.03)	172.18(±0.04)	3.05 (±0.06)	3.21 (±0.08)	3.32 (±0.08)	3.31 (±0.11)
Poly(ethylene glycol)-400								
0.00	332.68 (±0.01)[b]	333.96 (±0.02)[b]	335.25 (±0.01) [b]	336.51 (±0.02) [b]	3.34 (± 0.03) [b]	3.41 (± 0.06) [b]	3.14 (± 0.05)[b]	3.00 (± 0.07)[b]
0.01	332.87 (±0.02)	333.93 (±0.01)	335.22 (±0.03)	336.47 (±0.03)	3.44 (±0.06)	3.71 (±0.05)	3.64 (±0.08)	3.71 (±0.09)
0.02	332.95 (±0.02)	334.00 (±0.04)	335.29 (±0.04)	336.51 (±0.02)	3.53 (±0.06)	3.70 (±0.13)	3.74 (±0.12)	3.77 (±0.07)
0.03	332.99 (±0.01)	334.05 (±0.01)	335.34 (±0.02)	336.53 (±0.01)	3.69 (±0.02)	4.12 (±0.04)	3.83 (±0.07)	4.13 (±0.04)

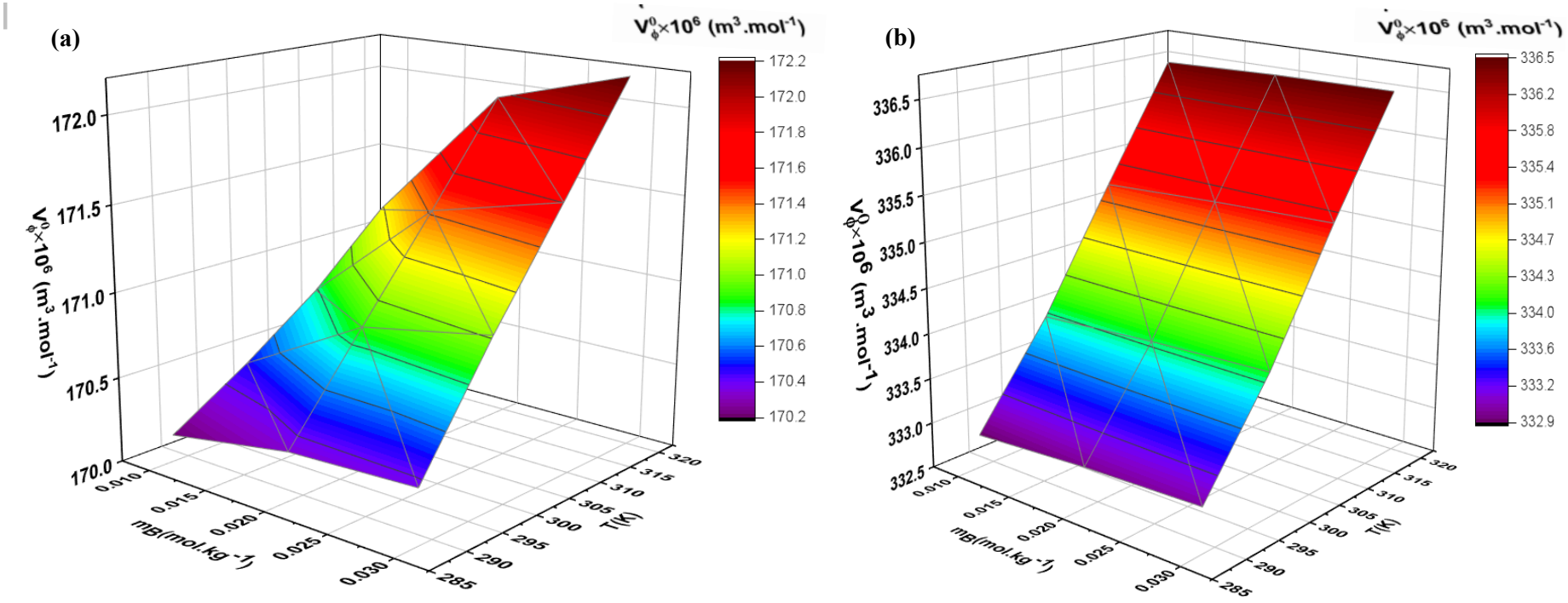

Figure 4.9 Variations in V_ϕ^0, of PEG-200 and PEG-400 in LBA corresponding to various concentrations and temperature in (a) and (b) respectively.

Temperature-Dependent Partial Molar Volume

The V_ϕ^0 are affected by temperature as stated by the formula given in equation **4.8**. The empirical factors, denoted as $a, b,$ and $c,$ for PEG-200/400 in aqueous lactobionic acid solutions are provided in **Table 4.11**. The computed and experimental data of V_ϕ^0 are used to attain deviations known as ARD (σ) that are determined using these empirical constants ($a, b,$ and $c,$). To obtain these deviations (ARD) or σ, the equations **4.9** and **4.10** are employed. In the current study, the R^2 values show that the deviation values are quite small and perfectly fit into the polynomial equation [41]. The goal of studying V_ϕ^0 is to arrive at the limiting apparent molar expansibilities, E_ϕ^0. The E_ϕ^0 values are determined using the relation given in equation **4.11.** The solute-solvent contacts in the ternary combination are significantly revealed by the expansibility (E_ϕ^0) whether the solute acts as a structure former or disrupter is determined by its partial difference regarding temperature [60-61]. From Eq. **4.8**, the differential is computed and expansibility (E_ϕ^0) is obtained by equation **4.11**. The sign of $\partial E_\phi^0/\partial T$ is used to denote if the solute strengthens or weakens the construction in the solvent since it can do either [62]. **Table 4.12** shows the various expansibilities E_ϕ^0 and its differential ($\partial E_\phi^0/\partial T$) at different T and m_B. All the E_ϕ^0 data for the mixture of aqueous lactobionic acid and PEG 200/PEG 400 are positive for complete range of temperatures and concentrations. Also, all the values of double derivative of V_ϕ or $\partial E_\phi^0/\partial T$ comes out to be positive corresponding to both the PEGs at all concentrations of LBA aqueous mixture which indicates the structure-making capability of the sample. The E_ϕ^0 numbers go up as the temperature goes up because of the packaging effect [49, 63]. Additionally, even though the positive numbers of E_ϕ^0 are irregular in nature and correlate to the LBA's concentration, they suggest that the solutes can form structures because lactobionic acid molecules concentrate in the spaces between molecules of the mixture. [64]

Table 4.11

a, b, c (Empirical parameters) of the ternary mixture of lactobionic acid with PEG-200/400 at various m_B and temperatures at the fixed pressure.

$^{a}m_B/$ $(mol.kg^{-1})$	$a \times 10^6$ $/ (m^3.mol^{-1})$	$b \times 10^6$ $/ (m^3.mol^{-1}K^{-1})$	$c \times 10^6$ $/ (m^3.mol^{-1}K^{-2})$	ARD	R^2
			PEG-200		
0.01	170.430	0.030	0.000	0.00003	0.999
0.02	170.838	0.056	0.000	0.00002	0.999
0.03	170.970	0.063	0.000	0.00004	0.999
			PEG-400		
0.01	333.968	0.116	0.000	0.00008	0.999
0.02	334.046	0.116	0.000	0.00011	0.999
0.03	334.096	0.116	0.000	0.00010	0.999

Table 4.12

Expansibilities, E_{ϕ}^{0}, of the blend of lactobionic acid with PEG-200/400 at various m_B and temperatures at 0.1 MPa pressure.

$^{a}m_B/(mol.kg^{-1})$	$E_{\phi}^{0} \times 10^{6}/(m^{3}.mol^{-1}.K^{-1})$				$\left(\frac{\partial E_{\phi}^{0}}{\partial T}\right)_{P}$ $/(m^{3}.mol^{-1}.K^{-2})$
	288.15K	298.15K	308.15K	318.15K	
			Poly(ethylene glycol)-200		
0.01	0.024	0.030	0.036	0.042	0.001
0.02	0.055	0.056	0.056	0.057	0.000
0.03	0.066	0.063	0.060	0.058	0.000
			Poly(ethylene glycol)-400		
0.01	0.107	0.116	0.126	0.136	0.001
0.02	0.110	0.116	0.123	0.129	0.001
0.03	0.109	0.116	0.122	0.129	0.001

Ultrasonic Properties

Apparent Molar Isentropic Compression ($K_{\phi,S}$)

The expression given in eq. **4.3** is utilized to govern the $K_{\phi,S}$ of PEGs- in the water based lactobionic acid solutions:

The isentropic compression is computed utilizing the Laplace formula [49] stated in equation **4.2. The Table 4.13** lists the experimental results for the ultrasonic speed (v) and computed ($K_{\phi,S}$) values with uncertainty $\mathrm{u}(K_{\phi,s})=\pm 0.25\times10^{6}/(m^{3}.mol^{-1}GPa^{-1})$. For ($H_2O$ + PEG-200/400), the values of ultrasonic speed (v) are obtained directly from the scientific literature [54]. All $K_{\phi,S}$ values are determined to be negative and its negativism upsurges with increasing polyethylene glycol molality at a certain LBA concentration but falls as temperature rises. Additionally, when lactobionic acid concentration increases, $K_{\phi,S}$ values become less negative, as seen by the linear expression in **Figure 4.10**. This pattern implies that H_2O particles are much lesser squeezable than water particles in bulk. As a result, water loses its ability to compress structurally, which causes water molecules to reorganize themselves over the solute [17-18]. The PEGs and LBA molecules produce compacted constructions by H-bonding amongst the molecules, which lowers the compressibility. Substantial interactions occur, as shown by the (dipole-dipole) contacts between H_2O particles nearby and the polyethylene glycols -OH clusters [19-20, 65].

Partial Molar Isentropic Compression ($K^{0}_{\phi,S}$)

The $K^{0}_{\phi,S}$ is obtained from the equation **4.5**, which also resolves the molality-related deviation of $K_{\phi,S}$. In **Table 4.14**, the experimental slope (S^{*}_{k}) and partial isentropic compression ($K^{0}_{\phi,S}$) having uncertainty $\pm0.24\times10^{6}/(\mathrm{m^{3}.mol^{-2}GPa^{-1}})$ and $\pm\,0.01\times10^{6}/(\mathrm{m^{3}.mol^{-1}GPa^{-1}})$ respectively are also presented and their graphical variation is shown in **Figure 4.11**. The values of $K^{0}_{\phi,S}$, S^{*}_{K}, and their associated errors are derived straight from the previous works for (H_2O + PEG-200/400) [54]. The estimated values of S^{*}_{k} show that the solute interactions are evidently tiny due to their slight size. As **Table 4.14** clearly demonstrates, the negative $K^{0}_{\phi,S}$ values become less negative as the temperature rises, indicating that water and polyethylene glycols have significant attractive interactions and the liquid mixture's solute-solvent interactions are

confirmed to persist by the negative numbers of S_K^* [66]. The dehydration of polyethylene glycols, resulting from the attractive interactions amid LBA ions and water molecules, leads to a diminution in the negative values of $K_{\phi,S}^0$ as temperature rises [67]. Consequently, the compressibility of water molecules surrounding PEGs is higher at high concentrations compared to low concentrations.

Table 4.13

Speed, v and $K_{\phi,S}$ of mixture of aqueous lactobionic acid with PEG-200/400 at various concentrations and temperatures at the 0.1 MPa pressure.

Molality m_A/ $(mol.kg^{-1})$	$v/(m.s^{-1})$				$K_{\phi,s} \times 10^6/\ (m^3.mol^{-1}.GPa^{-1})$			
	288.15K	298.15K	308.15K	318.15K	288.15K	298.15K	308.15K	318.15K
0.00 (mol. kg^{-1}) Lactobionic Acid + PEG-200								
0.00000	1466.59 [b]	1495.85 [b]	1519.14 [b]	1536.02 [b]				
0.10009	1477.01 [b]	1506.54 [b]	1529.35 [b]	1544.22 [b]	– 46.17 [b]	– 44.38 [b]	– 43.03 [b]	– 42.09 [b]
0.20044	1486.41 [b]	1516.04 [b]	1537.95 [b]	1553.92 [b]	– 46.54 [b]	– 44.74 [b]	– 43.37 [b]	– 42.43 [b]
0.30136	1496.73 [b]	1526.26 [b]	1548.14 [b]	1563.27 [b]	– 46.74 [b]	– 44.93 [b]	– 43.57 [b]	– 42.62 [b]
0.40026	1506.23 [b]	1534.26 [b]	1556.14 [b]	1572.27 [b]	– 46.90 [b]	– 45.08 [b]	– 43.72 [b]	– 42.76 [b]
0.49999	1515.44 [b]	1544.73 [b]	1567.02 [b]	1581.57 [b]	– 47.04 [b]	– 45.22 [b]	– 43.85 [b]	– 42.89 [b]
0.01 (mol. kg^{-1}) Lactobionic Acid + PEG-200								
0.00000	1470.42	1498.32	1522.3	1538.9				
0.10043	1480.6	1508.83	1532.14	1547.99	– 45.93	– 44.24	– 42.85	– 41.93
0.20062	1491.45	1518.76	1540.63	1556.83	– 46.29	– 44.59	– 43.19	– 42.26
0.29985	1501.32	1527.9	1549.7	1566.04	– 46.49	– 44.78	– 43.38	– 42.45
0.39982	1512.25	1536.87	1558.07	1574.67	– 46.65	– 44.93	– 43.53	– 42.59
0.50120	1521.95	1547.06	1569.59	1583.77	– 46.79	– 45.06	– 43.66	– 42.72
0.02 (mol. kg^{-1}) Lactobionic Acid + PEG-200								
0.00000	1473.37	1501.20	1525.26	1542.51				
0.10025	1484.50	1510.64	1534.39	1551.12	– 45.75	-43.63	-42.68	-41.73

0.20017	1494.98	1520.50	1542.84	1560.14	– 46.10	-43.97	-43.02	-42.06
0.29993	1505.90	1529.64	1551.64	1568.74	– 46.30	-44.16	-43.20	-42.24
0.39956	1516.55	1538.95	1560.48	1577.89	– 46.45	-44.31	-43.34	-42.38
0.49999	1526.65	1548.54	1571.62	1585.65	– 46.59	-44.43	-43.46	-42.50
0.03 (mol. kg^{-1}) Lactobionic Acid + PEG-200								
0.00000	1476.28	1503.70	1527.37	1544.70				
0.10035	1487.79	1512.89	1536.50	1553.94	– 45.57	– 43.92	– 42.56	– 41.61
0.20053	1498.57	1522.68	1545.41	1562.56	– 45.92	– 44.26	– 42.89	– 41.93
0.29972	1509.88	1531.94	1554.34	1571.23	– 46.11	– 44.44	– 43.07	– 42.11
0.39985	1520.37	1541.30	1563.20	1579.75	– 46.26	– 44.58	– 43.21	– 42.24
0.50007	1531.06	1551.18	1574.15	1588.03	– 46.39	– 44.70	– 43.32	– 42.36
0.00 (mol. kg^{-1}) Lactobionic Acid + PEG-400								
0.00000	1466.59 [b]	1495.85 [b]	1519.14 [b]	1536.02 [b]				
0.10015	1487.57 [b]	1517.76 [b]	1539.62 [b]	1558.49 [b]	-46.35 [b]	- 44.55 [b]	– 43.19 [b]	– 42.24 [b]
0.20004	1507.37 [b]	1537.69 [b]	1559.79 [b]	1578.91 [b]	- 46.86 [b]	- 45.04 [b]	– 43.67 [b]	– 42.71 [b]
0.29995	1527.36 [b]	1556.84 [b]	1578.93 [b]	1598.35 [b]	- 47.20 [b]	- 45.36 [b]	– 43.98 [b]	– 43.02 [b]
0.40100	1547.96 [b]	1576.84 [b]	1599.32 [b]	1617.80 [b]	- 47.48 [b]	- 45.63 [b]	– 44.24 [b]	– 43.27 [b]
0.50006	1569.69 [b]	1595.78 [b]	1617.05 [b]	1635.80 [b]	- 47.73 [b]	- 45.87 [b]	– 44.47 [b]	– 43.50 [b]
0.01 (mol. kg^{-1}) Lactobionic Acid + PEG-400								
0.00000	1469.82	1499.32	1523.3	1540.4				
0.09989	1492.6	1520.55	1544.09	1561.71	– 46.13	– 44.34	– 42.95	– 42.01

0.20029	1514.74	1543.35	1566.02	1583.08	– 46.63	– 44.82	– 43.42	– 42.48
0.29999	1536.35	1563.61	1585.41	1602.93	– 46.97	– 45.13	– 43.73	– 42.78
0.39959	1557.54	1582.94	1605.91	1622.58	– 47.25	– 45.40	– 43.99	– 43.03
0.50046	1578.43	1602.47	1624.79	1642.6	– 47.50	– 45.63	– 44.22	– 43.25
0.02 (mol. kg^{-1}) Lactobionic Acid + PEG-400								
0.00000	1472.37	1502.71	1526.26	1543.81				
0.09998	1495.02	1523.53	1546.69	1563.97	– 45.97	– 44.13	– 42.84	– 41.82
0.20018	1517.34	1545.39	1566.30	1584.00	– 46.47	– 44.61	– 43.30	– 42.28
0.29984	1538.24	1566.14	1586.63	1604.00	– 46.80	– 44.92	– 43.60	– 42.57
0.40025	1559.20	1586.92	1607.32	1625.06	– 47.08	– 45.18	– 43.86	– 42.82
0.50040	1579.46	1605.92	1626.75	1644.11	– 47.33	– 45.42	– 44.10	– 43.04
0.03 (mol. kg^{-1}) Lactobionic Acid + PEG-400								
0.00000	1475.28	1505.77	1529.37	1546.7				
0.10011	1496.97	1527.09	1548.35	1566.01	– 45.81	– 43.96	– 42.60	– 41.67
0.19995	1517.39	1547.13	1568.66	1586.52	– 46.30	– 44.43	– 43.05	– 42.11
0.29987	1539.29	1568.63	1588.13	1605.42	– 46.63	– 44.73	– 43.36	– 42.41
0.40004	1559.8	1588.79	1608.52	1625.4	– 46.91	– 45.00	– 43.61	– 42.65
0.49968	1579.61	1608.2	1627.18	1644.68	– 47.16	– 45.22	– 43.84	– 42.88

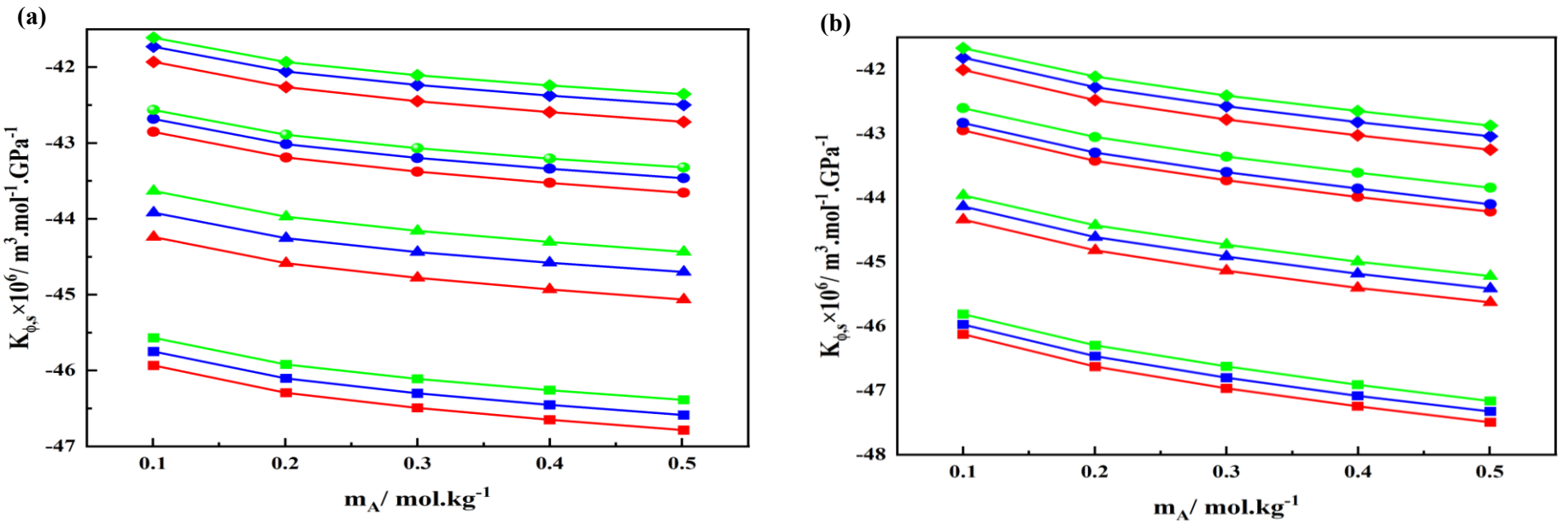

Figure 4.10 Variation of the $K_{\phi,s}$, of (a) PEG-200 and (b) PEG-400 against the m_A [Red, 0.01 lactobionic acid; blue, 0.02 lactobionic acid; green, 0.03 lactobionic acid] at various temperatures [square, $288.15K$; triangle, $298.15K$; circle, $308.15K$; diamond, $318.15K$].

Table 4.14

Calculated K_{ϕ}^{0}, and S_{K}^{*}, of the aqueous lactobionic acid with PEG-200/400 at various m_B and temperatures at the fixed 0.1 MPa pressure.

[a]m_B/ $mol.kg^{-}$	$K_{\phi,S}^{0} \times 10^{6}/(m^{3}.mol^{-1}.GPa^{-1})$				$S_{K}^{*} \times 10^{6}/(kg.m^{3}.mol^{-2}.GPa^{-1})$			
	$288.15K$	$298.15K$	$308.15K$	$318.15K$	$288.15K$	$298.15K$	$308.15K$	$318.15K$
				PEG-200				
0.00	-46.05 (±0.08)[b]	-44.26 (±0.08)[b]	-42.91 (±0.07)[b]	-41.97(±0.07)[b]	-2.09(±0.25)[b]	-2.02 (±0.24)[b]	-1.97 (±0.23)[b]	-1.95(±0.23)[b]
0.01	-45.81 (±0.08)	-44.12 (±0.08)	-42.74 (±0.08)	-41.82 (±0.08)	-2.06 (±0.25)	-1.99 (±0.24)	-1.94 (±0.24)	-1.91 (±0.23)
0.02	-45.63 (±0.08)	-43.82 (±0.08)	-42.57 (±0.08)	-41.62 (±0.08)	-2.03 (±0.25)	-1.94 (±0.24)	-1.89 (±0.24)	-1.85 (±0.23)
0.03	-45.46 (±0.08)	-43.61 (±0.08)	-42.46 (±0.08)	-41.51 (±0.08)	-1.97 (±0.25)	-1.89 (±0.24)	-1.83 (±0.24)	-1.80 (±0.23)
				PEG-400				
0.00	-46.11 (±0.09)[b]	-44.32 (±0.09)[b]	-42.97 (±0.09)[b]	-42.03 (±0.09) [b]	-3.38 (±0.29)[b]	-3.23 (±0.28)[b]	-3.13 (±0.27)[b]	-3.07 (±0.27)[b]
0.01	-45.89 (±0.10)	-44.12 (±0.09)	-42.73 (±0.09)	-41.80 (±0.09)	-3.36 (±0.29)	-3.15 (±0.28)	-3.09 (±0.27)	-3.03 (±0.28)
0.02	-45.73 (±0.09)	-43.91 (±0.09)	-42.61 (±0.08)	-41.61 (±0.09)	-3.32 (±0.28)	-3.13 (±0.27)	-3.08 (±0.25)	-2.99 (±0.27)
0.03	-45.57 (±0.09)	-43.74 (±0.09)	-42.38 (±0.08)	-41.46 (±0.08)	-3.32 (±0.26)	-3.08 (±0.27)	-3.04 (±0.25)	-2.95 (±0.25)

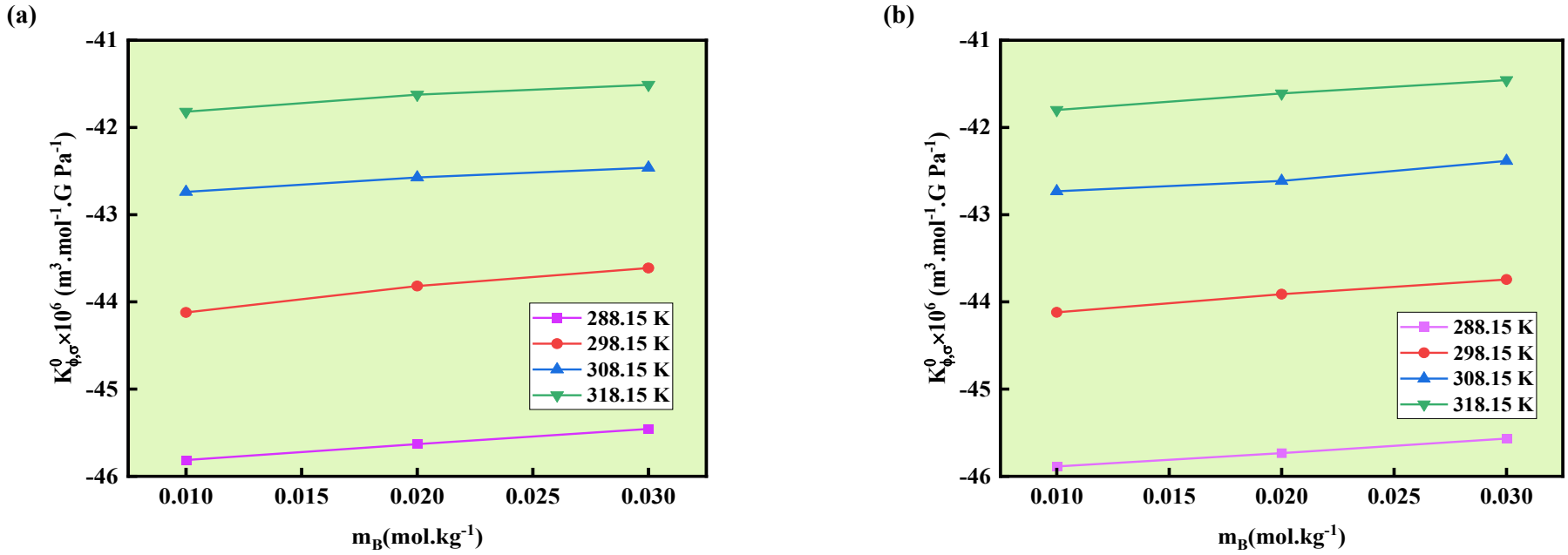

Figure 4.11 Variation of $K^0_{\phi,S}$, of PEG-200 and PEG-400 in LBA with respect to concentration at different temperatures in (a) and (b) respectively.

Partial Molar Transfer Properties:

Transfer Properties of Partial Molar Volume (ΔV_{ϕ}^{0})

Due to the fact that at extremely low concentrations the interactions between each solute and the number of molecules are negligible, limiting transfer characteristics can provide information on their association amongst the particles. Therefore, ΔV_{ϕ}^{0} is devoid of solute and solute interactions and offers insightful data on interactions amongst solute and cosolute. ΔV_{ϕ}^{0} is found by the eq. **4.6**. The **Table 4.15** lists the "ΔV_{ϕ}^{0} " values, which can be either positive or negative in magnitude and show no discernible pattern in relation to the LBA concentrations and various temperatures. **Table 4.15** demonstrates that for PEG-200 and PEG-400, respectively, except for concentrations 0.01 $mol.kg^{-1}$ of LBA at temperatures. (298.15K, 308.15K and 318.15K) and for 0.02 mol/kg at temperatures (308.15K and 318.15K) V_{ϕ}^{0} are positive. According to Pauling's [68,69] model for the structure of pure water, clathrates are empty spaces inside the water structures. Because other organic solvent molecules may easily enter these gaps, a little percentage of glycol molecules manage to position themselves in the water structure's cages, preventing the network of cages from being eliminated. Due to the development of a novel structure and the production of hydrogen bonds between water and organic molecules, it is possible that a larger glycol content damages the cage arrangement of water. For. The data demonstrates that there are positive and negative values for ΔV_{ϕ}^{0} indicating that multiple interactions, stated in 1st problem, are conceivable in molecules of lactobionic acid and glycols. But for both PEG-200 and PEG-400, hydrophilic type of associations will predominate due to most positive values of ΔV_{ϕ}^{0} . Additionally, this discloses any weak solute-solute interactions present in the combination. [42, 70-71]

Partial Molar Transfer Properties of Isentropic Compression ($\Delta K_{\phi,S}^{0}$)

Using the relation in equation **4.7**, it is feasible to calculate the $\Delta K_{\phi,S}^{0}$ of polyethylene glycols in water to lactobionic acid (aqueous) solution. The **Table 4.15** contains the computed values for $\Delta K_{\phi,S}^{0}$. The values decrease as the temperature rises and are positive at selected concentrations and temperatures [72]. The positive $\Delta K_{\phi,S}^{0}$ results imply that when lactobionic acid concentration rises, additionally, the electrostriction reduces and the interaction between the polyethylene glycols and lactobionic acid's

zwitterionic centre increases [73-74]. At lower temperatures, the PEGs interact with lactobionic acid and water molecules more strongly as a result of the estimated negative $K^0_{\phi,S}$ values and positive $\Delta K^0_{\phi,S}$ values. Because of the huge number of water molecules that connect with solvent molecules, the interactions keep growing.

Interaction Coefficients

The equations **4.13** and **4.14** yield the (V_{AB}, K_{AB}) and (V_{ABB}, K_{ABB}) interaction constants for the mixtures. 'A' stands for polyethylene glycols in equations **4.13** and **4.14**, 'B' stands for lactobionic acid, and m_B stands for the molality of lactobionic acid (aqueous) solutions. Volume and isentropic compression pair interaction coefficients are denoted by (V_{AB} and K_{AB}) and triplet(V_{ABB} and K_{ABB}) coefficients are (respectively. The properties of binary and triplet interactions may be retrieved using these interaction coefficients, whose derivation derives from McMillan-Mayer concept [50] and was further illuminated by Friedman and Krishnan [52]. According to **Table 4.16**, these coefficients were considered using the values of ΔV^0_ϕ and ΔK^0_ϕ [75]. The V_{AB} is observed to be positive for both glycols for complete range of T, with exception of PEG-400 at 318.15 K, and K_{AB} is observed to be positive for both PEG-200 and PEG-400 at various temperatures, with the exception of PEG-200 at 288.15 K, demonstrating that interactions between polyethylene glycols and lactobionic acid solution are primarily pairwise. This paired interaction results in some electrostricted water returning to the bulk solvent, which is more organized, and this positive volume change is what causes the hydration co-sphere to overlap. The triplet constants V_{ABB} and K_{ABB} show both positive and negative values with temperature. Pairwise interactions predominate in the current investigation, according to a complete examination of coefficients [63].

Table 4.15

Found values of ΔV_{ϕ}^{0}, and $\Delta K_{\phi,S}^{0}$ of the aqueous lactobionic acid with PEG-200/400 at various m_B and temperatures at the fixed 0.1 MPa pressure.

$^{a}\mathbf{m_B}/$ $\mathbf{mol.kg}$	$\Delta \mathbf{V}_{\phi}^{\mathbf{0}} \times \mathbf{10^6}/(\mathbf{m^3.mol^{-1}})$				$\Delta \mathbf{K}_{\phi,\mathbf{S}}^{\mathbf{0}} \times \mathbf{10^6}/(\mathbf{m^3.mol^{-1}.GPa^{-1}})$			
	$288.15K$	$298.15K$	$308.15K$	$318.15K$	$288.15K$	$298.15K$	$308.15K$	$318.15K$
Poly(ethylene) glycol-200								
0.01	0.20	0.24	0.27	0.30	0.24	0.14	0.17	0.15
0.02	0.32	0.64	0.91	1.11	0.42	0.44	0.34	0.35
0.03	0.36	0.78	1.10	1.33	0.59	0.65	0.45	0.46
Poly(ethylene) glycol-400								
0.01	0.19	-0.03	-0.03	-0.04	0.22	0.20	0.24	0.23
0.02	0.27	0.04	0.04	0.00	0.38	0.41	0.36	0.42
0.03	0.31	0.09	0.09	0.02	0.54	0.58	0.59	0.57

Table 4.16

V_{AB}, K_{AB}, V_{ABB} and K_{ABB} for the ternary mixture of the lactobionic acid with PEG-200/400 at various concentrations and temperatures at 0.1 MPa pressure.

$\boldsymbol{T/(K)}$	$\boldsymbol{V_{AB} \times 10^6}$ $\boldsymbol{/(m^3.mol^{-2}.kg)}$	$\boldsymbol{V_{ABB} \times 10^6}$ $\boldsymbol{/(m^3.mol^{-3}.kg^2)}$	$\boldsymbol{K_{AB} \times 10^6}$ $\boldsymbol{/(m^3.mol^{-2}.kgGPa^{-1})}$	$\boldsymbol{K_{ABB} \times 10^6}$ $\boldsymbol{/(m^3.mol^{-3}.kg^2GPa^{-1})}$
		PEG-200		
288.15	12.10	-135.20	12.30	-54.68
298.15	16.25	-63.62	7.98	67.93
308.15	20.64	-35.53	9.62	-46.74
318.15	23.95	-16.85	8.95	-26.35
		PEG-400		
288.15	10.57	-121.53	11.27	- 50.99
298.15	-1.71	72.74	10.72	- 23.65
308.15	-1.47	66.58	10.34	- 16.89
318.15	-1.66	45.55	12.46	- 64.87

Conclusion

The measurements of the volumetric and acoustical characteristics are carried out using the ρ and v values obtained from the DSA of PEG-200/400 in water based LBA solution at m_B (0.01, 0.02, and 0.03 $mol.kg^{-1}$) and within the same T range ($288.15K\ to\ 318.15\ K$). It was observed that V_ϕ values are positive, indicating a significant solute and cosolute association in the blend following the pattern of increasing interactions from in glycols from 200 to 400. The presence of hydrophobic effects and a robust H-bond amid the hydroxyl groups of glycols and the water molecules are indicated by these positive values of V_ϕ^0. At all temperatures and for all solution compositions, S_V^* values showed positive signs, showing pairwise interactions between the ions that make up the solute molecules. The partial double derivative of V_ϕ^0 or $\partial \mathrm{E}_\phi^0/\partial \mathrm{T}$ values and all the E_ϕ^0 values all have a positive sign, indicating that the solute is strengthening the structure in the solvent. Additionally, when the temperature increases, the negative $K_{\phi,S}^0$ values become less negative, showing that water and polyethylene glycols have strong attractive interactions. The negative values of S_K^* also reveal that the solute–cosolute relations in the system continue at infinite dilution. An overall analysis of coefficients of interaction indicates that pairwise interactions dominate in the current study.

References

[1] K. Kaur, K.C. Juglan and H. Kumar, J. Chem. Eng. Data, (2017).

[2] P. Kaur, N. Chakraborty, K.C. Juglan, H. Kumar and M. Singla, J. Mol. Liq. 329, 116810 (2021).

[3] S. Parveen, S. Singh, D. Shukla, M. Yasmin, M. Gupta and J.P. Shukla, J. Solution Chem. 41, 659 (2012).

[4] F.M. Sannaningannavar, B.S. Navati and N.H. Ayachit, J. Therm. Anal. Calorim. 113, 1217 (2013).

[5] M.S. Raman, M. Kesavan, K. Senthilkumar and V. Ponnuswamy, J. Mol. Liq. 204, 141 (2015).

[6] F. Ebner, A. Heller, F. Rippke and I. Tausch, Am. J. Clin. Dermatol. 3, 427 (2002).

[7] K. Kaur, K.C. Juglan and H. Kumar, J. Chem. Thermodyn. 124, 115 (2018).

[8] S. Chauhan, M.S. Chauhan, D. Kaushal, V.K. Syal and J. Jyoti, J. Solution Chem. 39, 1340 (2010).

[9] H. Kumar and I. Behal, J. Chem. Eng. Data 61, 2678 (2016).

[10] X. Jiang, C. Zhu and Y. Ma, J. Chem. Eng. Data 58, 2826 (2013).

[11] R. Rani, A. Kumar, T. Sharma and R.K. Bamezai, J. Chem. Thermodyn. 135, 58 (2019).

[12] X. Ren, C. Zhu and Y. Ma, J. Chem. Thermodyn. 93, 40 (2016).

[13] A. Thakur, K.C. Juglan, H. Kumar and K. Kaur, Phys. Chem. Liq. 58, 78 (2020).

[14] H. Kumar, I. Behal and M. Singla, J. Chem. Thermodyn. 97, 181 (2016).

[15] P. Pradhan, R.S. Sah and M.N. Roy, J. Mol. Liq. 145, 71 (2009).

[16] S. Chauhan and K. Kumar, J. Mol. Liq. 195, 128 (2014).

[17] H. Kumar and I. Behal, J. Chem. Thermodyn. 97, 156 (2016).

[18] H. Kumar and K. Kaur, Thermochim. Acta 568, 1 (2013).

[19] M.S. Raman, V. Ponnuswamy, P. Kolandaivel and K. Perumal, J. Mol. Liq. 140, 39 (2008).

[20] N. Chakraborty, K.C. Juglan and H. Kumar, J. Chem. Thermodyn. 153, 106326 (2021).

[21] N. Chakraborty, K.C. Juglan and H. Kumar, J. Chem. Thermodyn. 160, 106584 (2021).

[22] S.K. Schnell, P. Englebienne, J.M. Simon, P. Krüger, S.P. Balaji, S. Kjelstrup, D. Bedeaux, A. Bardow and T.J.H. Vlugt, Chem. Phys. Lett. 582, 154 (2013).

[23] S.I. Sandler, Chemical, Biochemical, and Engineering Thermodynamics, 4th ed., Wiley, New York (2006).

[24] M.J. Moran and H.N. Shapiro, Fundamentals of Engineering Thermodynamics, 5th ed., Wiley, Hoboken, NJ (2006).

[25] R.A. Alberty, Thermodynamics of Biochemical Reactions, 1st ed., Wiley, Hoboken, NJ (2003).

[26] T. Engel and P. Reid, Thermodynamics, Statistical Thermodynamics, and Kinetics, 3rd ed., Pearson, Boston, MA (2012).

[27] B.E. Poling, J.M. Prausnitz and J.P. O'Connell, The Properties of Gases and Liquids, 5th ed., McGraw-Hill Education, New York (2000).

[28] A. Podgorsek, J. Jacquemin, A.A.H. Pádua and M.F.C. Gomes, Chem. Rev. 116, 6075 (2016).

[29] M.B. Shiflett, B.A. Elliott, S.R. Lustig, S. Sabesan, M.S. Kelkar and A. Yokozeki, ChemPhysChem 13, 1806 (2012).

[30] D.S. Firaha, O. Hollóczki and B. Kirchner, Angew. Chem. Int. Ed. 54, 7236 (2015).

[31] R.C. Thakur, R. Sharma and M. Bala, J. Mater. Environ. Sci. 7, 3415 (2016).

[32] R.C. Thakur, R. Sharma, A. Kumar, S. Kumar and M.L. Parmar, Orient. J. Chem. 30, 1953 (2014).

[33] M. Iglesias, A. Torres, R. González-Olmos and D. Salvatierra, J. Chem. Thermodyn. 40, 119 (2008).

[34] J. Kulhavy, R. Andrade, S. Barros, J. Serra and M. Iglesias, J. Mol. Liq. 219, 1 (2016).

[35] T.S. Banipal, H. Singh, P.K. Banipal and V. Singh, Thermochim. Acta 555, 38 (2013).

[36] N. Chakraborty, K.C. Juglan and H. Kumar, ACS Omega 5, 27714 (2020).

[37] Z. Yan, J. Wang, H. Zheng and D. Liu, J. Solution Chem. 27, 1113 (1998).

[38] E. Ayranci and M. Sahin, J. Chem. Thermodyn. 40, 911 (2008).

[39] D. Das, B. Das and D.K. Hazra, J. Mol. Liq. 110, 5 (2004).

[40] H. Kumar and I. Behal, J. Mol. Liq. 221, 1050 (2016).

[41] A.K. Mishra and J.C. Ahluwalia, J. Phys. Chem. 88, 86 (1984).

[42] M.J. Iqbal and M.A. Chaudhry, J. Chem. Thermodyn. 42, 1375 (2010).

[43] P. Kaur, N. Chakraborty, K.C. Juglan and H. Kumar, J. Mol. Liq. 318, 113763 (2020).

[44] N. Chakraborty, K.C. Juglan and H. Kumar, J. Mol. Liq. 337, 116605 (2021).
[45] I. Gheorghe, C. Stoicescu and F. Sirbu, J. Mol. Liq. 285, 352 (2019).
[46] F. Soboleva and V. Iakubov, J. Mol. Liq. 305, 112806 (2020).
[47] L. Zheng, Y. Zhang and Y. Deng, New J. Chem. 27, 1421 (2003).
[48] M. Shahbaz, M.S. Shafiq, M. Moniruzzaman, I.M. Saeed, M. Irfan and M. Imran, J. Mol. Liq. 315, 113739 (2020).
[49] K. Sun, Z. Guo and H. Wang, J. Chem. Thermodyn. 105, 256 (2017).
[50] A. Hammouti, S. Kertit, M. Benchanaa and R. Salghi, Mater. Chem. Phys. 78, 122 (2003).
[51] F. Franks, M. Pedley and D.S. Reid, J. Chem. Soc. Faraday Trans. 1: Phys. Chem. Condensed Phases, 72, 359 (1976).
[52] C.V. Krishnan and H.L. Friedman, J. Solution Chem. 2, 81 (1973).
[53] R.K. Wadi and P. Ramasami, J. Chem. Soc. Faraday Trans. 93, 2267 (1997).
[54] N. Chakraborty, K.C. Juglan and H. Kumar, Braz. J. Chem. Eng. 38, 1 (2021).
[55] M.A. Jamal, M.K. Khosa, M. Rashad, I.H. Bukhari and S. Naz, Food Chem. 146, 460 (2014).
[56] H. Kumar and I. Behal, J. Chem. Thermodyn. 102, 48 (2016).
[57] N. Chakraborty, K. Kaur, H. Kumar and K.C. Juglan, J. Chem. Thermodyn. 126, 137 (2018).
[58] K. Klimaszewski, E. Stronka-Lewkowska, K. Abramczyk and A. Bald, J. Chem. Thermodyn. 89, 212 (2015).
[59] N.G. Tsierkezos and I.E. Molinou, J. Chem. Eng. Data 43, 989 (1998).
[60] T. Sharma, R. Rani, A. Kumar and R.K. Bamezai, J. Mol. Liq. 300, 111985 (2020).
[61] K.C. Juglan and H. Kumar, J. Chem. Thermodyn. 140, 105916 (2020).
[62] M.N. Roy, V.K. Dakua and B. Sinha, Int. J. Thermophys. 28, 1275 (2007).
[63] R. Rani, A. Kumar and R.K. Bamezai, J. Mol. Liq. 240, 642 (2017).
[64] N. Chakraborty, K.C. Juglan, H. Kumar and M. Singla, J. Chem. Thermodyn. 174, 106876 (2022).
[65] N. Chakraborty, K.C. Juglan and H. Kumar, J. Mol. Liq. 332, 115869 (2021).
[66] C.M. Romero and F. Negrete, Phys. Chem. Liq. 42, 261 (2004).
[67] S. Baluja and S. Oza, Fluid Phase Equilib. 178, 233 (2001).
[68] L. Pauling and R.E. Marsh, Proc. Natl. Acad. Sci. 38, 112 (1952).
[69] L. Pauling, The Nature of the Chemical Bond (Cornell University Press, Ithaca, New York, 1960).

[70] K. Kaur and K.C. Juglan, Der. Pharma. Chem. 7, 160 (2015).
[71] H. Kumar, M. Singla and R. Jindal, Monatsh. Chem. 145, 1063 (2014).
[72] M.T. Zafarani-Moattar and S. Sarmad, J. Chem. Thermodyn. 42, 1213 (2010).
[73] A. Salabat, L. Shamshiri and F. Sahrakar, J. Mol. Liq. 118, 67 (2005).
[74] R. Sadeghi and F. Ziamajidi, J. Chem. Eng. Data 52, 1037 (2007).
[75] H. Kumar, M. Singla and R. Jindal, J. Mol. Liq. 199, 385 (2014).
[76] A.K. Gill, N. Chakraborty, K.C. Juglan, Int. J. Thermophys. 46, 46 (2025).

Section II

Problem 3

An Investigation to Display Galactose's Physico-Chemical Behaviour with PEGs: A Thermo-Acoustical Study

In **Problem-3**, an extensive investigation of the volumetric characteristics of ternary solutions including water, galactose, and polyethylene glycols (400/600) was done through the investigation of ρ and v at four temperatures and at three variable compositions of (0.01, 0.02 and 0.03) $mol.kg^{-1}$ of galactose sol. with glycols.

Investigation of Density and Sound Velocity:

Density Examination

The determination of densities is made in a fluid mixture (water + galactose + PEG 400/PEG 600) at varied temperatures. An index of these investigational density values is provided in **Table 4.17**. The temperature-dependent density data were acquired while maintaining a constant Galactose concentration. But when the molality of polyethylene glycol grew, these density values tended to rise. Additionally, the density values are rising as we approach from PEG 400 to 600 with the rise in concentration. There is an increase in density, which causes the solute's chain length to grow. The data of densities and velocities, for (PEG400+water) and for PEG600+water at temperatures from 288.15 to 318.15K are taken from our previous publication [1 and 2] respectively.

Analysis of velocity

On the other hand, the sound speed rises with temperature and galactose content from 0.01 to 0.02 to 0.03) mol.kg^{-1}. The three-dimensional hydrogen bonding structures that make up the structure of water are the reason of this behavior [3-5]. The enhanced velocity of sound for the glycol-galactose system is owing to the formation of both intramolecular and intermolecular H-bonds amid the particles of the cosolute and the solute, which indicates a faster pace of molecular aggregation in solutions [6]. Furthermore, **Table 4.17** clearly shows that the reason for the enhancement of the data of sound speed as a function of glycol molality is that the presence of the aqueous gluconolactone molecule renders the H-bond network insoluble. Moreover, when the glycol's molar mass intensifies from PEG-400 to 600, new hydrogen interactions are created between the galactose molecules and PEGs, and the hydrogen connection amongst the water particles and galactose weakens and breaks [7].

Table 4.17 Determined densities, ρ, and sound velocity, v, of PEGs in a galactose solution at varying temperatures and 0.1 MPa fixed pressure.

Molality m_A/ $(mol.kg^{-1})$	$\rho \times 10^6/(kg.m^{-3})$				$v/(m.s^{-1})$			
	$288.15K$	$298.15K$	$308.15K$	$318.15K$	$288.15K$	$298.15K$	$308.15K$	$318.15K$
0.00 $(mol.kg^{-1})$ Galactose+ PEG-400								
0.00000	0.99926[a]	0.99705[a]	0.99404[a]	0.99036[a]	1466.59[a]	1495.85[a]	1519.14[a]	1536.02[a]
0.10015	1.00577[a]	1.00349[a]	1.00044[a]	0.99673[a]	1487.57[a]	1517.76[a]	1539.62[a]	1558.49[a]
0.20004	1.01179[a]	1.00945[a]	1.00636[a]	1.00264[a]	1507.37[a]	1537.69[a]	1559.79[a]	1578.91[a]
0.29995	1.01739[a]	1.01499[a]	1.01188[a]	1.00813[a]	1527.36[a]	1556.84[a]	1578.93[a]	1598.35[a]
0.40100	1.02267[a]	1.02019[a]	1.01705[a]	1.01330[a]	1547.96[a]	1576.84[a]	1599.32[a]	1617.80[a]
0.50006	1.02747[a]	1.02496[a]	1.02180[a]	1.01804[a]	1569.69[a]	1595.78[a]	1617.05[a]	1635.80[a]
0.01 $(mol.kg^{-1})$ Galactose+ PEG-400								
0	0.99984	0.99779	0.99477	0.99095	1469.37	1498.2	1522.2	1539.81
0.10005	1.006292	1.004182	1.001114	0.997268	1490.51	1520.35	1542.15	1561.8
0.20008	1.012324	1.010137	1.007013	1.0031444	1510.76	1540.44	1562.27	1582.5
0.29952	1.017915	1.015654	1.012489	1.0085958	1531.55	1560.18	1581.87	1601.54
0.39898	1.02308	1.020757	1.017553	1.0136344	1551.61	1579.88	1602	1621.24
0.49966	1.027848	1.02547	1.022243	1.0183577	1574.18	1598.29	1619.66	1639.51
0.02 $(mol.kg^{-1})$ Galactose+ PEG-400								
0	1.000434	0.998311	0.995379	0.991479	1470.89	1500.2	1524.8	1542.99
0.10018	1.006873	1.004695	1.001715	0.997786	1493.21	1522.72	1544.9	1565.2

0.199924	1.012834	1.010579	1.007552	1.003607	1514.25	1542.95	1564.68	1585.81
0.299689	1.018383	1.016041	1.012987	1.009032	1535.01	1562.34	1585.14	1604.72
0.399464	1.023544	1.021122	1.018032	1.014061	1556.4	1582.53	1604.5	1624.64
0.49921	1.028331	1.025878	1.022713	1.018774	1576.53	1600.58	1622.87	1643.66
0.03 ($mol.kg^{-1}$) Galactose+ PEG-400								
0	1.001064	0.998995	0.995957	0.992114	1472.78	1502.47	1526.3	1545.79
0.100053	1.007469	1.005345	1.00226	0.998391	1497.04	1525.15	1546.85	1568.61
0.199937	1.013403	1.011203	1.008089	1.0042	1518.6	1545.3	1567.04	1589.18
0.300244	1.018941	1.016672	1.013519	1.009616	1539.46	1565.76	1587.56	1608.13
0.399551	1.024049	1.0217	1.018504	1.014591	1560.49	1585.65	1606.98	1627.84
0.499157	1.028835	1.026413	1.023188	1.019263	1579.91	1603.92	1626.21	1647
0.00 ($mol.kg^{-1}$) Galactose+ PEG-600								
0	0.99926	0.99705	0.99404	0.99036	1466.59	1495.85	1519.14	1536.02
0.10411	1.00609[b]	1.00337[b]	1.00087[b]	0.99813[b]	1498.65[b]	1514.11[b]	1527.98[b]	1544.04[b]
0.19978	1.01318[b]	1.01047[b]	1.00797[b]	1.00521[b]	1525.77[b]	1540.09[b]	1555.04[b]	1569.04[b]
0.30099	1.02018[b]	1.01749[b]	1.01499[b]	1.01205[b]	1551.45[b]	1565.42[b]	1581.19[b]	1594.48[b]
0.40249	1.02676[b]	1.02410[b]	1.02160[b]	1.01837[b]	1579.92[b]	1592.94[b]	1607.62[b]	1621.00[b]
0.50775	1.03318[b]	1.03052[b]	1.02805[b]	1.02442[b]	1608.06[b]	1619.92[b]	1633.97[b]	1648.50[b]
0.01 ($mol.kg^{-1}$) Galactose+ PEG-600								
0	0.99984	0.99779	0.99477	0.99095	1469.37	1498.2	1522.2	1539.81
0.10005	1.008291	1.00612	1.00299	0.999162	1517.83	1532.24	1546.48	1558.89

0.20008	1.01701	1.014724	1.011372	1.007431	1546.22	1560.54	1573.31	1584.83
0.29952	1.02567	1.023314	1.019939	1.015812	1574.06	1588.5	1598.98	1610.78
0.39898	1.034413	1.031891	1.028473	1.024441	1603.21	1616.07	1624.55	1635.84
0.49966	1.04331	1.040717	1.037404	1.033657	1632.18	1644.72	1652.42	1662.39
0.02 ($mol.kg^{-1}$) Galactose+ PEG-600								
0	1.00043	0.99831	0.99538	0.99148	1470.89	1500.2	1524.8	1542.99
0.100058	1.00871	1.006405	1.003286	0.999318	1525.25	1540.69	1555.91	1569.32
0.199331	1.017145	1.014622	1.011303	1.007172	1553.34	1568.56	1583.22	1594.65
0.300115	1.025714	1.022952	1.019479	1.015236	1582.16	1597.53	1608.96	1620.77
0.399091	1.034031	1.031254	1.027589	1.023176	1611.31	1625.18	1634.77	1645.19
0.499604	1.042609	1.03965	1.036132	1.031498	1641.09	1654.53	1662.15	1672.07
0.03 ($mol.kg^{-1}$) Galactose+ PEG-600								
0	1.00106	0.99900	0.99596	0.99211	1472.78	1502.47	1526.3	1545.79
0.099959	1.00908	1.006647	1.003462	0.999407	1533.96	1550.4	1565.61	1579.01
0.199486	1.017014	1.014397	1.010996	1.006671	1562.3	1578.54	1593.23	1604.68
0.299088	1.024928	1.022078	1.018442	1.013944	1590	1606.38	1618.81	1630.54
0.399685	1.033052	1.030153	1.026387	1.021696	1620.3	1635.16	1644.73	1655.16
0.500966	1.041495	1.038282	1.034576	1.029518	1650.02	1664.34	1672.85	1682.66

Apparent Molar Properties

A characteristic of a solution component in a mixture is a measure employed to delineate the contribution of each element to the non-ideality of the amalgamation. Using investigational data of ρ and c, we have computed two parameters: V_ϕ and $K_{\phi,s}$ to investigate the interactions between the mixture's molecules.

Apparent Molar Volume

It is the characteristic property of the combination. It's a feature that varies when the complete chemical is added. Utilizing the density, ρ value and equation (**4.1**) we can compute the V_ϕ values [8]. The **Table 4.18** shows the various values of V_ϕ of the both the glycols with the combination of aqueous solution of Galactose at 3 range of concentration varying from 0.01 to 0.03 $mol.kg^{-1}$ at 4 temperatures with uncertainty of u(V_ϕ)= ± (0.05-0.07)×10^6/($m^3.mol^{-1}$). The values are depicted visually in **Figure 4.12**. The V_ϕ values for PEG-400 to 600 exhibit a rising trend with both temperature and concentration growth as obvious from **Figure 4.12**. The rise in the values with molality as well with the temperature is caused due to the process of mixing and high attraction towards the solvent. The Positive V_ϕ shows the presence of stronger solute-cosolute associations and electrostriction relations that preponderate in the mixture. [9] The composition's molecular interaction is elucidated by the robust linear correlation between $V_\phi$values and temperature, in addition to the poly (ethylene glycol) molality. [10] Values are shown to tend to rise when PEG's experimental molality (400) increases. Because of the solute molecules' high affinity for the solvent molecules, this increase in values causes more interactions between them [1]. However, the V_ϕ of water, PEG 600, galactose, and PEGs all decline with molality, suggesting the presence of attractive interactions like hydrogen bonds or other intermolecular forces inside the blend. The outcome of these linkages form smaller clusters than solute or solvent particles [2]. The **Figure 4.13** shows this trend, which rises from PEG 400 to 600 as their weight grows. This suggests a rise in the same order of molecular interaction.

Table 4.18 Apparent molar properties, V_ϕ, and $K_{\phi,S}$, of the ternary mixture of galactose with PEGs at 0.1 MPa fixed pressure.

m_A/ $(mol.kg^{-1})$	$V_\phi \times 10^6/(m^3.mol^{-1})$				$K_{\phi,S} \times 10^6/(m^3.mol^{-1}.GPa^{-1})$			
	$288.15K$	$298.15K$	$308.15K$	$318.15K$	$288.15K$	$298.15K$	$308.15K$	$318.15K$
0.01 $(mol.kg^{-1})$ Galactose+ PEG-400								
0.10005	333.4275	334.5986	335.923	337.1729	-46.172	-44.408	-43.014	-42.034
0.20008	333.4991	334.7757	336.152	337.425	-46.681	-44.896	-43.486	-42.497
0.29952	333.6745	334.9933	336.3435	337.6391	-47.015	-45.214	-43.794	-42.797
0.39898	334.04	335.3551	336.6969	338.0105	-47.292	-45.479	-44.050	-43.047
0.49966	334.6245	335.9298	337.2353	338.4296	-47.539	-45.714	-44.278	-43.272
0.02 $(mol.kg^{-1})$ Galactose+ PEG-400								
0.10018	333.4593	334.5914	335.8824	337.2537	-46.077	-44.290	-42.867	-41.860
0.19992	333.7207	334.9908	336.2873	337.597	-46.581	-44.773	-43.335	-42.319
0.29969	333.9933	335.3607	336.6	337.8731	-46.914	-45.089	-43.642	-42.619
0.39946	334.303	335.7078	336.9519	338.2264	-47.190	-45.352	-43.895	-42.867
0.49921	334.6613	335.9902	337.329	338.498	-47.434	-45.585	-44.119	-43.087
0.03 $(mol.kg^{-1})$ Galactose+ PEG-400								
0.100053	333.564	334.6786	335.9876	337.3033	-45.958	-44.155	-42.782	-41.708
0.199937	333.877	335.1239	336.3521	337.6543	-46.460	-44.635	-43.248	-42.164
0.300244	334.1912	335.4708	336.7184	337.9949	-46.790	-44.951	-43.554	-42.462
0.399551	334.4895	335.828	337.1015	338.3594	-47.063	-45.210	-43.804	-42.707

0.499157	334.7693	336.1373	337.4013	338.6543	-47.306	-45.440	-44.027	-42.924
				0.01 ($mol.kg^{-1}$) Galactose+ PEG-600				
0.10005	511.3069	513.4418	515.9021	517.5846	-46.281	-44.502	-43.099	-42.114
0.20008	505.5875	507.7168	510.7973	513.0557	-46.910	-45.108	-43.680	-42.681
0.29952	500.9009	502.8818	505.4608	508.1922	-47.385	-45.564	-44.124	-43.110
0.39898	496.2617	498.4518	500.8332	502.991	-47.827	-45.984	-44.530	-43.512
0.49966	491.6985	493.7972	495.6924	497.0156	-48.261	-46.399	-44.939	-43.926
				0.02 ($mol.kg^{-1}$) Galactose+ PEG-600				
0.100058	512.854	515.6697	518.9058	521.3344	-46.181	-44.377	-42.942	-41.928
0.199331	507.5007	510.5682	513.9303	516.8899	-46.792	-44.960	-43.503	-42.473
0.300115	502.8717	506.1398	509.4009	512.3524	-47.262	-45.405	-43.928	-42.886
0.399091	498.8764	501.6362	504.9842	508.1185	-47.683	-45.810	-44.313	-43.257
0.499604	494.548	497.3937	499.9845	503.355	-48.101	-46.205	-44.704	-43.630
				0.03 ($mol.kg^{-1}$) Galactose+ PEG-600				
0.09996	515.2095	519.92	522.8071	526.7685	-46.054	-44.227	-42.844	-41.756
0.19949	511.4296	515.2939	518.604	522.9606	-46.638	-44.786	-43.381	-42.272
0.29909	507.6423	511.4532	515.0184	519.1931	-47.076	-45.198	-43.772	-42.649
0.39969	503.4133	506.6881	510.095	514.2414	-47.486	-45.592	-44.150	-43.011
0.50097	498.6862	502.2712	505.1326	509.697	-47.897	-45.974	-44.524	-43.362

I(a)

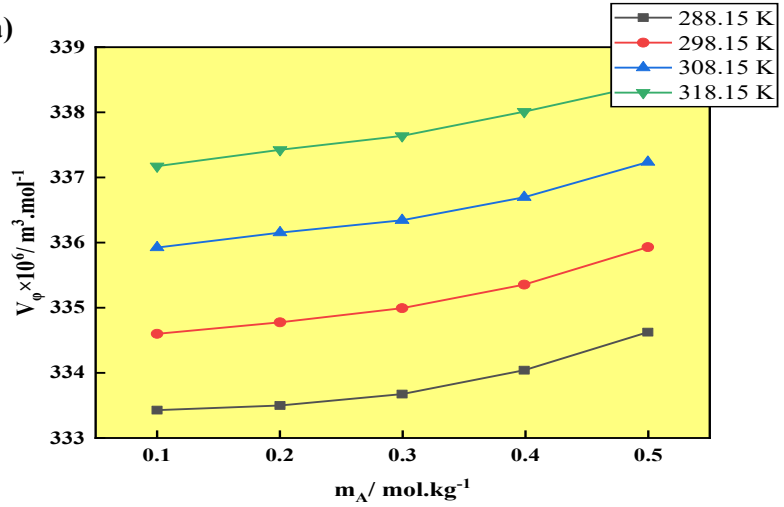
288.15 K
298.15 K
308.15 K
318.15 K
339
338
337
336
335
334
333
0.1
0.2
0.3
0.4
0.5
$V_\varphi \times 10^6$/ m^3.mol^{-1}
m_A/ mol.kg^{-1}

I(b)

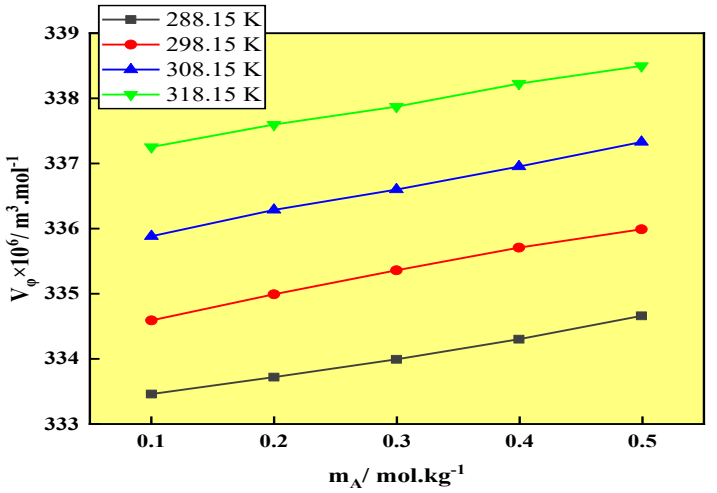
288.15 K
298.15 K
308.15 K
318.15 K
339
338
337
336
335
334
333
0.1
0.2
0.3
0.4
0.5
$V_\varphi \times 10^6$/ m^3.mol^{-1}
m_A/ mol.kg^{-1}

I(c)

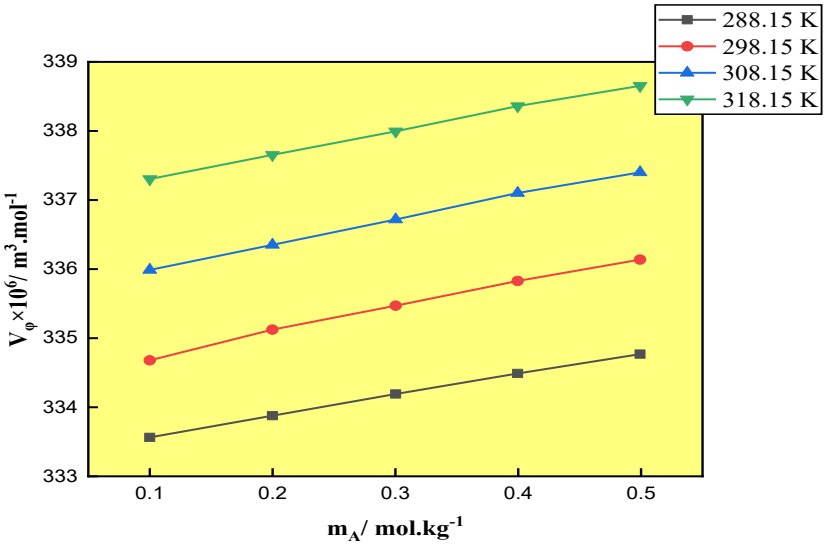
288.15 K
298.15 K
308.15 K
318.15 K
339
338
337
336
335
334
333
0.1
0.2
0.3
0.4
0.5
$V_\varphi \times 10^6$/ m^3.mol^{-1}
m_A/ mol.kg^{-1}

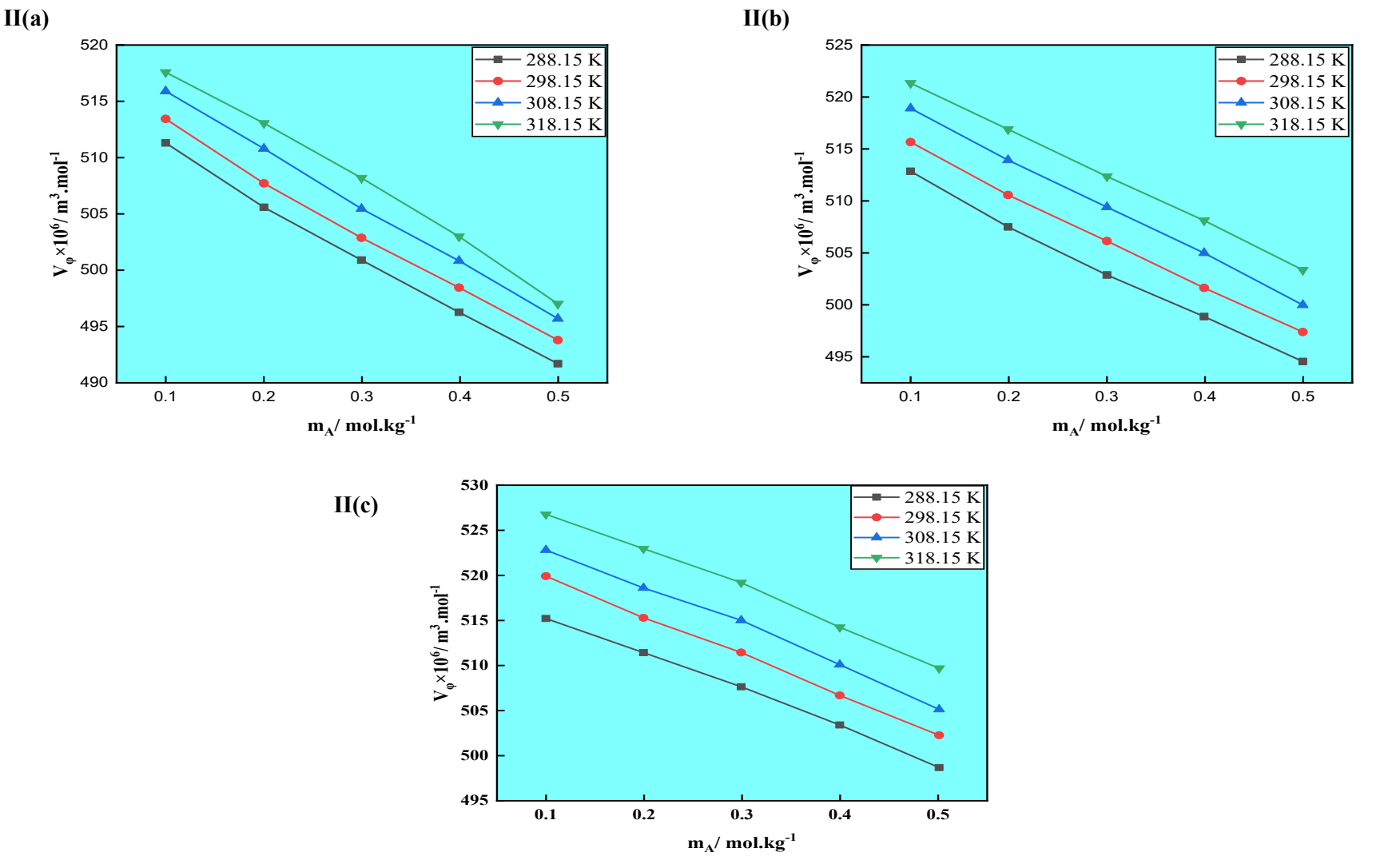

Figure 4.12 Changing temperatures effect on of V_ϕ (I) PEG-400 and (II) PEG-600 in aqueous solutions of galactose at concentrations of 0.01 $mol.kg^{-1}$ galactose, 0.02 $mol.kg^{-1}$ galactose, and 0.03 $mol.kg^{-1}$ galactose in (a), (b) and (c) respectively

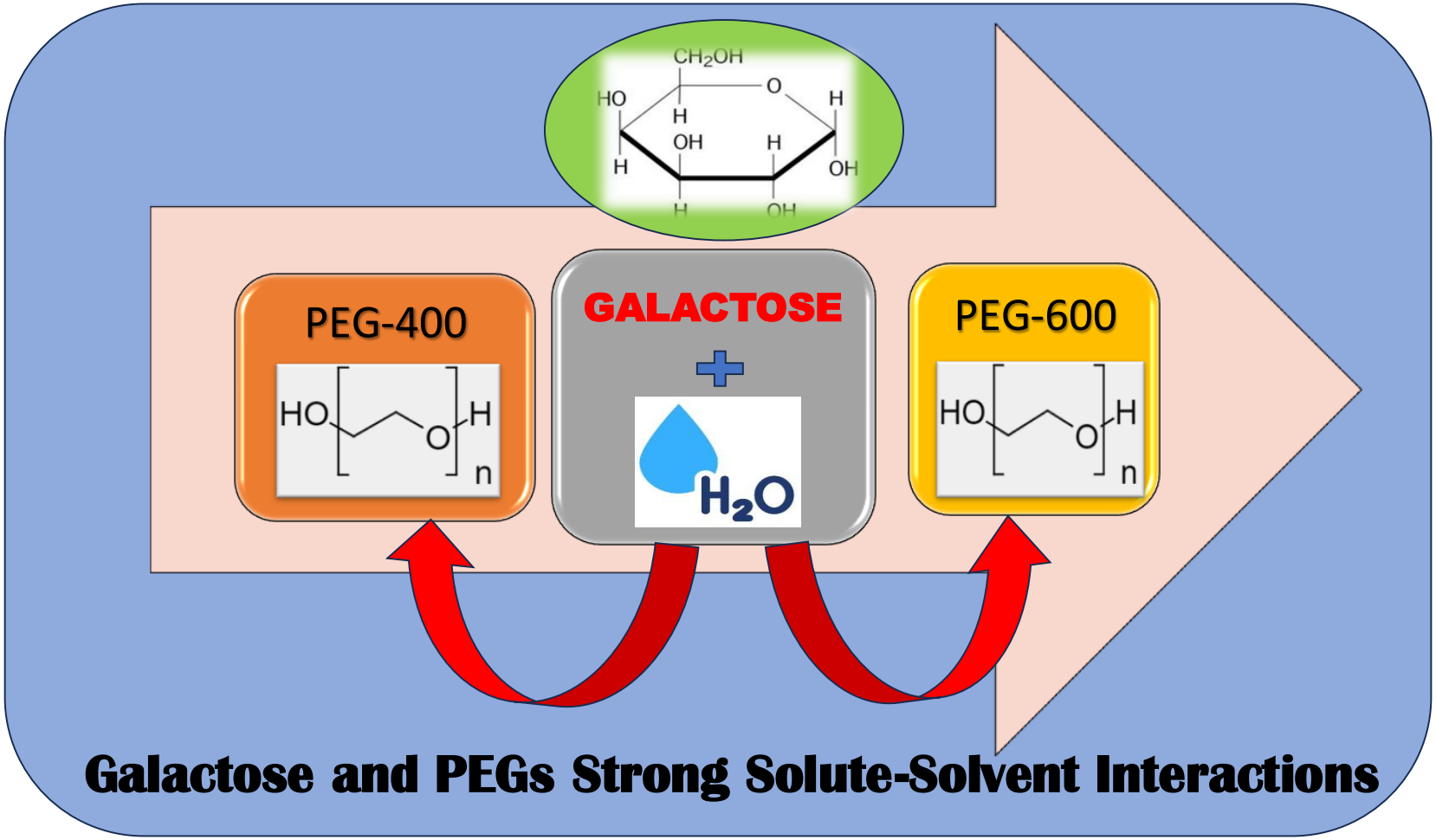

Figure 4.13 Trend of Interactions between Galactose & PEG-400 and Peg-600.

Apparent molar isentropic compressibility, $K_{\phi,S}$

$K_{\phi,S}$ depends on the variables such as k_S- solution's isentropic compression, $k_{S,0}$- pure solvent's isentropic compression, ρ- solution's density, ρ_0- density of the pure solvent, M- solute's molar mass.

Where k_S is calculated by using the Equation **4.2** given by Newton and Laplace [9]. The k_s values were used to estimate the $K_{\phi,S}$ by the stated equation **4.3**. The fact that all the $K_{\phi,S}$ values are negative advocates that the H_2O particles surrounding solute are typically harder to compress than the water molecules in the overall solution. Together with the V_ϕ data, these are shown in **Table 4.18** and are certain within the limits u($K_{\phi,S}$)=±0.25×10^6/($m^3.mol^{-1}.GPa^{-1}$). The fluctuation of the mixture's $K_{\phi,S}$ with temperature and molality is shown in **Figure 4.14**, demonstrating how these variables vary linearly with molality. According to **Table 4.18**, for every combination, the molality and temperature have an increasing effect on the size of $K_{\phi,S}$. Additionally, it has been noted that negative $K_{\phi,S}$ values imply that water's structural compressibility results in a larger loss and that the solute has a larger aligning influence on the solvent [11–13].

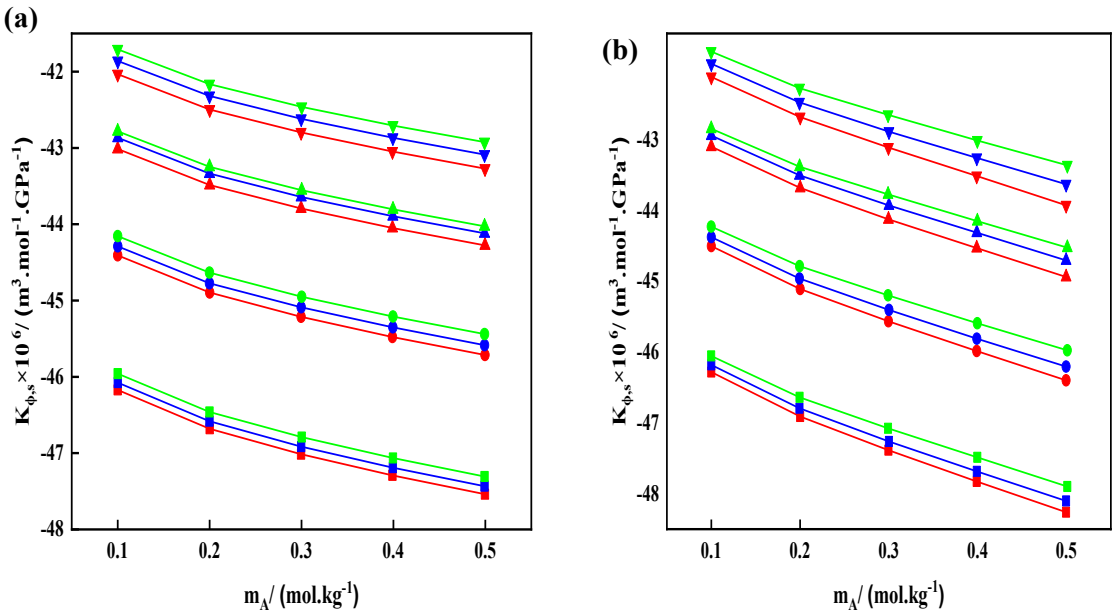

Figure 4.14 Variation of $K_{\phi,S}$ of (a) PEG-400 and (b) PEG-600 against the molality [Red, 0.01 galactose; blue, 0.02 galactose; green, 0.03 galactose] at various temperatures [square, 288.15K; circle, 298.15K; upper triangle, 308.15K; down triangle, 318.15K].

Partial molar properties

When temperature and pressure are held constant, variables that show how much they fluctuate with changes in molar content are known as partial molar characteristics. To investigate the sample's thermodynamics, we have computed two properties:

(i) V_ϕ^0 and

(ii) $K_{\phi,S}^0$

Partial Molar Volumes V_ϕ^0,

The one mole of the solute's apparent molar volume may be found by fitting the curve V_ϕ against m_A using the least squares fit approach. You may accomplish this by plugging the numbers into this formula given in equation **4.4**. We have used above equation to find the value of V_ϕ^0, here the molality of the solute is indicated by m_A and the slope is shown by S_V^*, also called the volumetric pair-wise interaction coefficient. Together with the calculated standard deviation values (S_V^*), the V_ϕ^0 values and their typical errors are listed in the **Table 4.19** it is evident that there are substantial solute-solvent associations since all of the V_ϕ^0 values in the water-based galactose solution are positive. The values of V_ϕ^0 and S_V^* for PEG-400 and 600 are discussed below:

PEG-400 – The S_V^* values are all modest and positive, while the V_ϕ^0 data data exhibits growth with T and m_B. PEG-600 – In relation to both temperature and concentration, the V_ϕ^0 values tend to be positive, but the S_V^* values are consistently negative. The V_ϕ^0 values rise with T due to the hydrophobic aspect of the chain of poly glycols, which enhances electrostriction association at sites of terminal charges. These positive values of V_ϕ^0 suggest the rate of occurrence of aquaphobic bonds and a stronger H-connection within the OH-groups of PEGs and the water particles. Positive S_V^* in case of PEG-400 suggesting pairwise interactions among the ions that comprise the solute molecules, with charged functional groups being the most prevalent. The volumetric properties of the liquid mixture are established by the solute-solvent association, which is dominant in the solution because of S_V^* values being lower than V_ϕ^0 values. The reduction in volume caused by ion-nonpolar contact in PEG-600 leads to negative S_V^* values. A decrease in S_V^* values indicates that solute-cosolute interactions outweigh solute-solute connections. Graphical variation of V_ϕ^0 values for concentration and temperature are shown in **Figure 4.15** which shows that partial molar volume increases steadily with increasing molality at all temperatures. This rise indicates strengthening solute–solvent

interactions and tighter molecular packing as more solute molecules enter the system. For each concentration, V_ϕ^0 is highest at 318.15 K and lowest at 288.15 K, demonstrating that temperature enhances thermal agitation, reduces viscosity, and allows faster propagation of sound waves. The consistent upward trend across all temperatures suggests structure-making behaviour of the solute and increased hydrogen bonding/association at higher concentrations. [14-18]

Table 4.19

V_ϕ^0 and S_V^* of the ternary mixture of Galactose in PEG mixture at same temperatures and pressure = 0.1 MPa.

m_B	$V_\phi^0 \times 10^6/\ (m^3.mol^{-1})$				$S_V^* \times 10^6\ /(m^3.kg.mol^{-2})$			
$/mol.kg^{-1}$	$288.15K$	$298.15K$	$308.15K$	$318.15K$	$288.15K$	$298.15K$	$308.15K$	$318.15K$
				PEG-400				
0.00	332.68(±0.01)[a]	333.96(±0.02)[a]	335.25(±0.01)[a]	336.51(±0.02)[a]	3.34 (± 0.03)[a]	3.41 (± 0.06)[a]	3.14 (± 0.05)[a]	3.00 (± 0.07)[a]
0.01	332.97(±0.20)	334.16(±0.15)	335.52(±0.13)	336.80(±0.08)	2.94(±0.60)	3.25(±0.47)	3.18(± 0.40)	3.11(± 0.25)
0.02	333.13(±0.04)	334.27(±0.04)	335.54(±0.03)	336.95(±0.02)	2.99(± 0.12)	3.52(± 0.13)	3.57(± 0.08)	3.13(± 0.07)
0.03	333.27(±0.01)	334.36(±0.04)	335.64(±0.03)	336.97(±0.02)	3.03(± 0.04)	3.63(± 0.13)	3.58(± 0.08)	3.41(± 0.06)
				PEG-600				
0.00	518.11(±0.04)[b]	519.12(±0.05)[b]	520.14(±0.03)[b]	521.14(±0.03)[b]	-9.81(±0.12)[b]	-9.89(±0.15)[b]	-9.92(±0.09)[b]	-9.89(±0.10)[b]
0.01	515.72(±0.43)	517.83(±0.47)	520.86(±0.20)	523.14(±0.52)	-48.63(±1.31)	-48.64(±1.41)	-50.48(±0.59)	-51.30(±1.56)
0.02	516.90(±0.49)	519.93(±0.30)	523.48(±0.20)	525.83(±0.12)	-45.29(±1.46)	-45.53(±0.90)	-46.84(±0.60)	-44.78(±0.36)
0.03	519.56(±0.36)	524.26(±0.23)	527.46(±0.50)	531.40(±0.45)	-40.98(±1.08)	-43.81(±0.70)	-43.77(±1.51)	-42.78(±1.36)

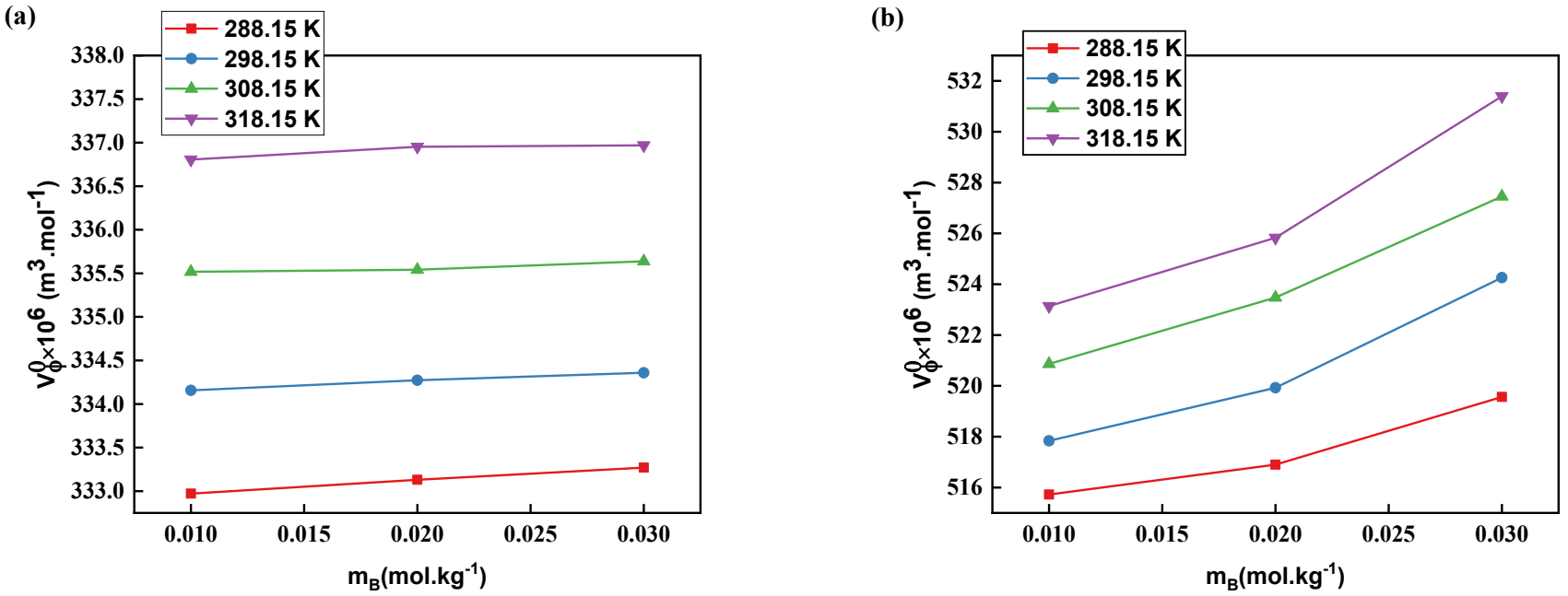

Figure 4.15 Variation in V_ϕ^0 of PEG-400/600 with molality at same temperature range in (a) and (b) respectively.

Partial molar isentropic compressibility

The $K_{\phi,S}^{0}$ and S_k^* is the experimental slope may be found by using the subsequent method given in **4.5** equation**.** The **Figure 4.16** shows a visual depiction of the discovered values of $K_{\phi,S}^{0}$. The data is recorded in **Table 4.20** sideways with their average errors in brackets. The data of $K_{\phi,S}^{0}$ and S_k^* exhibit a linear trend of increase and follows the uncertainty pattern of $\pm 0.01\times10^{6}/(m^3.mol^{-1}.GPa^{-1})$ for u($K_{\phi,S}^{0}$) and $\pm 0.24\times10^{6}/(kg.m^3.mol^{-2}.GPa^{-1})$ for u(S_K^*). It is understood that the negative values upsurge with temperature and galactose concentration, while the negative values decline with an upsurge in the molar weight of polyethylene glycols from 400 to 600. The powerful bond amongst the H_2O molecules and galactose in the PEGs origins the H_2O particles to be unconstrained into bulk, which makes it less compressible, surrounding the polyglycols, increasing the dehydration of the polyethylene glycols. Additionally, the negative S_k^* values exhibit a symmetrical pattern matching to the temperatures and concentrations of galactose, signifying that solute–cosolute connections prevail in the system. [19-20]

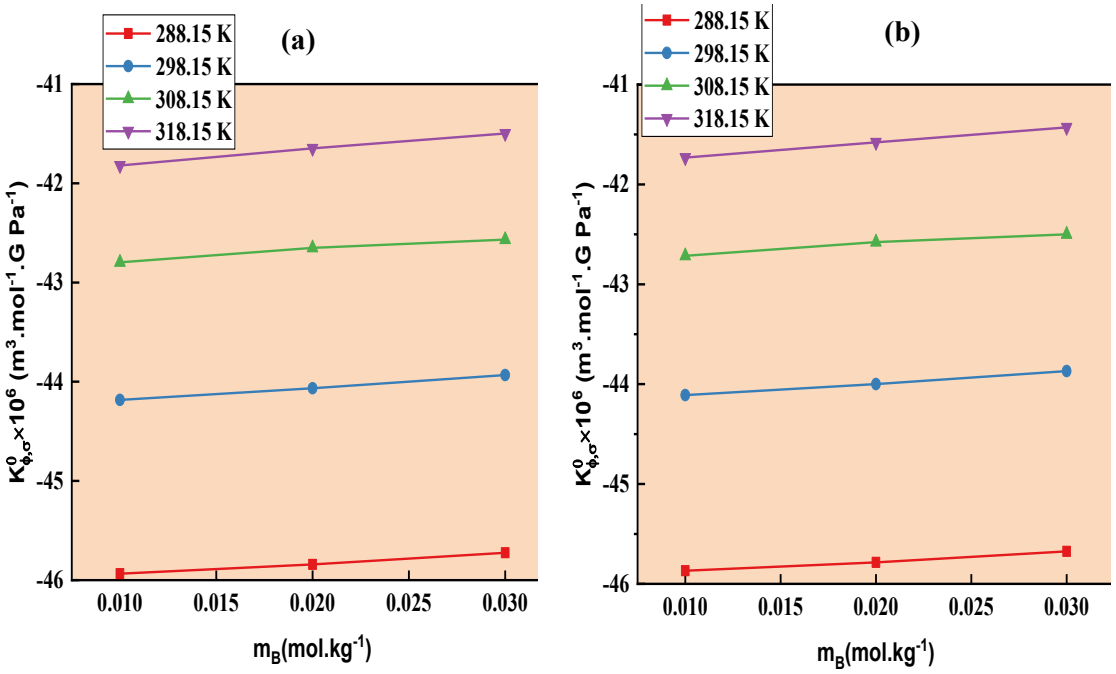

Figure 4.16 $K_{\phi,S}^{0}$ for (a) PEG-400 and (b) PEG-600 in varying temperatures in galactose containing m_B.

Table 4.20

Experimental $K^0_{\phi,S}$ and S^*_K, of aqueous galactose in PEG-400 and 600 at same temperatures and m_B at 0.1 MPa.

m_B/ $mol.kg^{-1}$	$K^0_{\phi,S} \times 10^6/(m^3.mol^{-1}.GPa^{-1})$				$S^*_K \times 10^6/(kg.m^3.mol^{-2}.GPa^{-1})$			
	$288.15K$	$298.15K$	$308.15K$	$318.15K$	$288.15K$	$298.15K$	$308.15K$	$318.15K$
PEG-400								
0.00	-46.11(±0.09)	-44.32 (±0.09)	- 42.97(±0.09)	-42.03(±0.09)	-3.38 (± 0.29)	-3.23 (± 0.28)	-3.13 (± 0.27)	-3.07 (± 0.27)
0.01	-45.94(±0.10)	-44.18 (±0.09)	-42.80(±0.09)	-41.82(±0.09)	-3.36(± 0.30)	-3.20(± 0.29)	-3.10(± 0.28)	-3.04(± 0.27)
0.02	-45.84(±0.10)	-44.07(±0.09)	-42.65(±0.09)	-41.65(±0.09)	-3.33(± 0.29)	-3.18(± 0.28)	-3.07(± 0.28)	-3.01(± 0.27)
0.03	-45.72(±0.10)	-43.93(±0.09)	-42.57(±0.09)	-41.50(±0.09)	-3.31(± 0.29)	-3.15(± 0.28)	-3.05(± 0.28)	-2.98(± 0.27)
PEG-600								
0.00	−46.02(±0.09)	−45.07(±0.09)	−44.17(±0.09)	−43.21(±0.09)	3.92(±0.29)	3.86(±0.28)	3.80(±0.28)	3.63(±0.29)
0.01	-45.87(±0.07)	-44.11(±0.07)	-42.71(±0.07)	-41.73(±0.06)	-4.89(± 0.22)	-4.68(± 0.22)	-4.54(± 0.21)	-4.46(± 0.19)
0.02	-45.78(±0.08)	-44.00(±0.07)	-42.58(±0.07)	-41.58(±0.07)	-4.74(± 0.23)	-4.51(± 0.22)	-4.34(± 0.20)	-4.19(± 0.20)
0.03	-45.67(±0.07)	-43.87(±0.07)	-42.50(±0.06)	-41.43(±0.06)	-4.52(± 0.21)	-4.29(± 0.21)	-4.12(± 0.19)	-3.94(± 0.19)

Properties of Partial Molar Transfer: -

Partial Molar Volume of Transfer

Understanding intermolecular interactions and the liquid's microscopic structure may be gained by studying the transfer characteristics of liquid mixtures. The ΔV_{ϕ}^{0} was computed with the formula which determines the ΔV_{ϕ}^{0} of PEGs transferred from water to galactose aqueous solutions at infinite dilution stated in **4.6** equation.

The ΔV_{ϕ}^{0} data is stated in **Table 4.21** are all positive for PEG-400. For PEG-600, most values are positive, but a few are negative. These results can be explained using the co-sphere overlap model, which helps us understand whether the solution expands or shrinks due to solute–solute interactions. According to this model, the interactions between PEG-400 or PEG-600 and galactose can be of four types:
i) ion–hydrophilic, ii) hydrophilic–hydrophilic, iii) ion–hydrophobic,and iv) hydrophobic–hydrophobic.

The first two types (i and ii) usually increase the transfer volume because they support better hydration. The last two types (iii and iv) reduce the transfer volume because they disturb the hydration around the solute [16–18]. From the data, it is clear that ion–hydrophilic and hydrophilic–hydrophilic interactions are the main types present in the PEG-400/PEG-600 + galactose + water system.

Transfer parameter of Partial Molar Isentropic Compression

It is determined by means of the equation **4.7** in the case of an infinitely diluted galactose concentration in water. The **Table 4.21** indicates that for all m_B of galactose and trial T, the $\Delta K_{\phi,S}^{0}$ values seem to be positive. As the galactose concentration increases, the $\Delta K_{\phi,S}^{0}$, values rise at a certain temperature; nonetheless, they show uneven pattern that matches the specific experimental temperatures. At increasing m_B, polyethylene glycols' zwitterionic core interacts more tightly with galactose, lowering electrostriction and modifying solute framework. As the concentration of galactose rises, the compressibility of the electrostriction water diminishes, resulting in positive $\Delta K_{\phi,S}^{0}$, values for PEG400/PEG600) at numerous temperatures and concentrations of galactose and negative $K_{\phi,S}^{0}$, values for the bulk. [21-25].

Table 4.21

ΔV_{ϕ}^{0} and $\Delta K_{\phi,S}^{0}$ of the ternary mixture of water and Galactose with PEGs at same temperatures and m_B at 0.1 MPa.

m_B/ $(mol.kg^{-1})$	$\Delta V_{\phi}^{0} \times 10^{6}/(m^{3}.mol^{-1})$				$\Delta K_{\phi,S}^{0} \times 10^{6}/(m^{3}.mol^{-1}.GPa^{-1})$			
	$288.15K$	$298.15K$	$308.15K$	$318.15K$	$288.15K$	$298.15K$	$308.15K$	$318.15K$
PEG-400								
0.01	0.29	0.20	0.27	0.29	0.18	0.14	0.17	0.21
0.02	0.45	0.31	0.29	0.44	0.27	0.25	0.32	0.38
0.03	0.59	0.40	0.39	0.46	0.39	0.39	0.40	0.53
PEG-600								
0.01	-2.39	-1.29	0.72	2.00	0.15	0.96	1.46	1.48
0.02	-1.21	0.81	3.34	4.69	0.24	1.07	1.59	1.63
0.03	1.45	5.14	7.32	10.26	0.35	1.20	1.67	1.78

Interaction coefficients

Liquid mixture interaction coefficients are found using the McMillan–Mayer concept [19]. The separation of effects acceptable by the coefficients is the consequence of interactions that occur among multiple solute molecules. Friedman and Krishnan provide more explanation for this hypothesis [26]. In this problem the interaction coefficients are found by using the equations **4.13** and **4.14** that contains the expression for the ΔV_{ϕ}^{0} and ΔK_{ϕ}^{0}. Where A=PEGs (PEG-400/600) and B= Galactose, m_B= molality of aqueous galactose; V_{AB} and K_{AB}; V_{ABB} and K_{ABB}. The values of ΔV_{ϕ}^{0} and ΔK_{ϕ}^{0} were entered into these equations to determine these coefficients, which are shown in **Table 4.22**. The pair-wise coefficients K_{AB} are all positive for PEG-400 and 600, whereas V_{AB} is positive for PEG-400/600 at all temperatures except for 318.15 K for PEG-600. In addition, all triplet coefficients (V_{ABB} and K_{ABB}) at all temperatures are negative for PEG-400, positive and negative for PEG-600. This illustrates that galactose solution and polyethylene glycols interact mostly pairwise. The hydration co-sphere overlaps because of the positive volume change that occurs from some electrostricted water returning to the more ordered bulk solvent because of this paired interaction. Most interactions in this study are pairwise. [27]

Table 4.22

V_{AB}, K_{AB}, V_{ABB}, and K_{ABB} for the ternary blend of galactose with PEGs.

T/(K)	$V_{AB} \times 10^6/(m^3.mol^{-2}.kg)$	$V_{ABB} \times 10^6/(m^3.mol^{-3}.kg^2)$	$K_{AB} \times 10^6/(m^3.mol^{-2}.kgGPa^{-1})$	$K_{ABB} \times 10^6/(m^3.mol^{-3}.kg^2GPa^{-1})$
		PEG-400		
288.15	15.66	-131.76	8.77	-54.05
298.15	10.83	-93.75	6.69	-6.08
308.15	13.26	-157.30	10.09	-74.67
318.15	18.12	-232.66	11.17	-51.72
		PEG-600		
288.15	-167.38	4298.39	7.39	-38.07
298.15	-126.34	4733.50	52.08	-729.59
308.15	-0.72	2735.66	80.88	-1203.09
318.15	39.57	2877.17	81.00	-1166.05

Partial molar volume depending upon temperature

The multinomial's eq. stated in equation **4.8** can be used to represent the V_ϕ^0 in terms of absolute temperature. These parameters and deviations R^2 and ARD are shown in **Table 4.23**. The examined V_ϕ^0 values are utilized to calculate σ deviations using equation **4.9** [28].

The primary goal of studying the V_ϕ^0 is to determine the molar expansibilities that restrict the system. The E_ϕ^0, of the solute are obtained from the derivative of Eq. **4.8** w.r.t. T keeping the P constant. The solute-solvent effect that exists in the solution is shown by the values of E_ϕ^0 [29]. Having all E_ϕ^0 values positive indicates that the PEG-400/PEG-600 interaction in aqueous galactose solution causes the volume to decrease [30]. The basic thermodynamic equation by Hepler [31] determines the solute's capacity to build and breakdown structures in a mixture. The capacity to produce and disruption structures in the co-solute medium is shown by the sign of the $\left(\partial E_\phi^0/\partial \mathrm{T}\right)_P$ values. Structure-making by the solute is designated by majority positive values of $\left(\partial E_\phi^0/\partial \mathrm{T}\right)_P$,although structure-disrupting is shown by fewer negative values of $\left(\partial E_\phi^0/\partial \mathrm{T}\right)_P$ [32]. The expansibilities E_ϕ^0 and $\left(\partial E_\phi^0/\partial \mathrm{T}\right)_P$ are shown in **Table 4.24**. It is observed that no consistent pattern for E_ϕ^0 values is observed with changes in concentration and temperature.

Table 4.23

Values of empirical parameters, a, b, c in equation (8), along with R^2 and ARD of the ternary mixture of galactose with PEGs at same temperatures and m_B at pressure = 0.1 MPa.

m_B/ $(mol.kg^{-1})$	$a \times 10^6/(m^3.mol^{-1})$	$b \times 10^6/(m^3.mol^{-1}.K^{-1})$	$c \times 10^6/(m^3.mol^{-1}K^{-2})$	R^2	ARD
		PEG-400			
0.01	334.195	0.126	0.000	0.9999	0.000075
0.02	334.270	0.121	0.001	0.9999	0.000872
0.03	334.380	0.118	0.001	0.9999	0.000956
		PEG-600			
0.01	518.085	0.2486	0.000419	0.9999	0.000321
0.02	520.1843	0.320212	-0.00168	0.9999	0.000331
0.03	523.9231	0.405852	-0.00189	0.9999	0.000428

Table 4.24

E_{ϕ}^{0}, for the ternary mixture Galactose with PEGs at fixed pressure = 0.1 MPa.

m_B/ $(mol.kg^{-1})$	$E_{\phi}^{0} \times 10^{6}/(m^{3}.mol^{-1}.K^{-1})$				$\left(\frac{\partial E_{\phi}^{0}}{\partial T}\right)_{P}/(m^{3}.mol^{-1}.K^{-2})$
	T=288.15K	T=298.15K	T=308.15K	T=318.15K	
			PEG-400		
0.01	0.121	0.126	0.131	0.136	0.00051
0.02	0.107	0.121	0.134	0.148	0.00135
0.03	0.106	0.118	0.130	0.142	0.00121
			PEG-600		
0.01	0.240	0.249	0.257	0.265	0.00084
0.02	0.354	0.320	0.287	0.253	-0.00337
0.03	0.444	0.406	0.368	0.330	-0.00377

Conclusion

his study provides a comprehensive analysis of the volumetric and acoustic behavior of aqueous mixtures containing polyethylene glycols (PEG-400 and PEG-600) and galactose. The evaluation of apparent and partial molar properties, including transfer volumes, reveals the presence of strong solute–solvent interactions. These interactions become more significant with increasing temperature, galactose concentration, and PEG molecular weight. The consistently positive values of partial molar volumes support the presence of favorable ion-related interactions between PEGs and galactose in solution. Furthermore, the thermodynamic properties results showed that the dominant interactions in the ternary mixes are those between hydrophilic and ion-hydrophilic substances. The pairwise association of galactose and PEGs is predicted by the values of V_{AB} and K_{AB}. The ability to create structures is shown by the values of $(\partial\phi_E^0/\partial \mathrm{T})_P$. Furthermore, the FTIR spectra of binary mixtures have been documented which offers insights into the molecular scale interactions that are predominant in the system. The examination of spectroscopic data suggests that interactions took place at the microscopic level in the systems of galactose and water under investigation

Problem 4

An Investigation of the Effects of Glycols on the Thermodynamic and Acoustic Parameters of Polyhydroxy Acid at Different Temperatures

Problem 4 makes it feasible to gauge the ρ and v of glycols (polyethylene glycol 200/400) in a well-known polyhydroxy acid, Lactobionic acid solutions, at concentrations range from 0.01, 0.02 to 0.03 mol/kg and constant experimental pressures of 0.1 MPa over various temperatures via DSA 5000 M.

To comprehend the interactions and effects of concentration and temperature, acoustic parameters are employed within the same temperature range and at varying concentration of Lactobionic acid (LBA).

Specific Acoustic Impedance (Z)

The effective sound pressure to effective particle velocity ratio at a place is known as the acoustic impedance. The sum of the repulsive, ionic, dipolar, and dispersion forces is used to calculate pressure [33]. Following formula **4.15** is used to calculate the specific acoustic impedance,

$$Z = v \times \rho \qquad \textbf{(4.15)}$$

The computed values of Z are tabulated in **Table 4.25**. As seen from the values the acoustic impedance is rising with the increase in molality and temperature. In ternary liquid mixes, changes in Z show the absence of interactions such as complex formation. The acoustic impedance grows with increasing concentration and increases with temperature in a linear fashion as shown in **Figure 4.17**. This linear fluctuation alone demonstrates that no complex development has occurred in this combination [34-36].

Adiabatic Compressibility

It is possible to measure intermolecular attachment or dissociation using the adiabatic compressibility (β) parameter. In the absence of heat transfer, β represents the proportional decrease in volume for each unit increase in pressure. The molecules' structure impacts both their adiabatic compressibility and how they are oriented in relation to the liquid molecules. It is evaluated with the Laplace equation given in eq. **4.16** [37] as determined from the sound speed (v) and the medium's density (ρ):

$$\beta = \frac{1}{v^2 \rho} \quad \textbf{(4.16)}$$

As seen from **Table 4.25**, when the temperature rises and the concentration of the co-solvent increases, the adiabatic compressibility decreases, indicating structural changes in the solute-solvent interaction that are reflected in the system [38]. This is because when concentration of lactobionic acid increases at a particular temperature, the experimental density of the mixture decreases, whereas the velocity increases, hence adiabatic compressibility decreases as shown in **Figure 4.18** proposing the formation and dissolution of H-bonding [39]. These variations in adiabatic compressibility indicate variation in the molecular forces with concentration and temperature [28].

Table 4.25 Impedance, Z and Compressibility, β of PEGs in water based Lactobionic acid at diverse temperatures.

Molality m_A $/(mol/kg)$	$Z/(kg/m^2/s)$				$\beta \times 10^{-10}/\,(N/m^2)$			
	$288.15K$	$298.15K$	$308.15K$	$318.15K$	$288.15K$	$298.15K$	$308.15K$	$318.15K$
0.01 mol/kg Lactobionic acid + PEG 200								
0.00000	1471.220	1495.605	1514.944	1525.732	4.6225	4.4625	4.3361	4.2590
0.10043	1485.736	1510.522	1529.244	1539.310	4.5459	4.3877	4.2680	4.1967
0.20062	1500.797	1524.719	1542.050	1552.476	4.4676	4.3184	4.2092	4.1375
0.29985	1514.716	1537.959	1555.252	1565.834	4.3974	4.2556	4.1491	4.0780
0.39982	1529.615	1550.940	1567.661	1578.507	4.3231	4.1954	4.0941	4.0231
0.50120	1543.217	1565.095	1583.171	1591.588	4.2577	4.1300	4.0243	3.9671
0.02 mol/kg Lactobionic acid + PEG 200								
0.10025	1491.431	1514.199	1533.44	1544.169	4.5167	4.3718	4.2501	4.1750
0.20017	1506.066	1528.229	1546.061	1557.362	4.4414	4.3035	4.1923	4.1157
0.29993	1521.013	1541.387	1558.873	1569.976	4.3659	4.2413	4.1343	4.0603
0.39956	1535.579	1554.606	1571.59	1582.998	4.2941	4.1798	4.0776	4.0035
0.49999	1549.494	1568.011	1586.545	1594.548	4.2274	4.1184	4.0105	3.9551
0.03 mol/kg Lactobionic acid + PEG 200								
0.00000	1480.642	1504.986	1524.005	1535.350	4.5749	4.4188	4.2961	4.2165
0.10035	1496.446	1518.459	1537.429	1548.891	4.4916	4.3530	4.2332	4.1548
0.20053	1511.328	1532.328	1550.413	1561.590	4.4153	4.2859	4.1736	4.0982
0.29972	1526.539	1545.439	1563.204	1574.113	4.3386	4.2238	4.1157	4.0432
0.39985	1540.811	1558.544	1575.787	1586.366	4.2688	4.1629	4.0596	3.9903
0.50007	1555.152	1572.011	1590.324	1598.212	4.1999	4.1009	3.9946	3.9401

0.01 mol/kg Lactobionic acid + PEG 400								
0.00000	1470.620	1496.603	1515.939	1527.219	4.6263	4.4566	4.3305	4.2508
0.09989	1503.027	1527.522	1546.436	1558.226	4.4575	4.3054	4.1879	4.1093
0.20029	1534.418	1559.624	1577.665	1588.885	4.3025	4.1545	4.0475	3.9756
0.29999	1564.827	1588.686	1605.858	1617.517	4.1595	4.0256	3.9278	3.8569
0.39959	1594.404	1616.380	1634.724	1645.512	4.0268	3.9083	3.8092	3.7454
0.50046	1623.446	1644.001	1661.682	1673.583	3.9024	3.7958	3.7039	3.6377
0.02 mol/kg Lactobionic acid + PEG 400								
0.00000	1474.997	1501.936	1520.961	1532.495	4.6046	4.4307	4.3078	4.2268
0.09998	1507.265	1532.438	1551.093	1562.358	4.4378	4.2832	4.1683	4.0925
0.20018	1538.799	1563.536	1579.924	1591.628	4.2829	4.1386	4.0410	3.9665
0.29984	1568.456	1593.051	1609.003	1620.356	4.1448	4.0081	3.9171	3.8476
0.40025	1597.849	1622.269	1638.125	1649.853	4.0139	3.8844	3.7980	3.7298
0.50040	1626.126	1649.323	1665.569	1676.859	3.8935	3.7755	3.6908	3.6272
0.03 mol/kg Lactobionic acid + PEG 400								
0.00000	1479.639	1507.057	1526.001	1537.338	4.5811	4.4067	4.2848	4.2056
0.10011	1510.941	1538.065	1554.671	1566.35	4.4212	4.2576	4.1543	4.0768
0.19995	1540.495	1567.281	1584.163	1596.036	4.2780	4.1241	4.0241	3.9492
0.29987	1571.15	1597.544	1612.361	1623.649	4.1349	3.9905	3.9053	3.8364
0.40004	1600.026	1626.077	1641.124	1651.967	4.0069	3.8707	3.7882	3.7243
0.49968	1627.777	1653.409	1667.705	1679.108	3.8892	3.7608	3.6851	3.6211

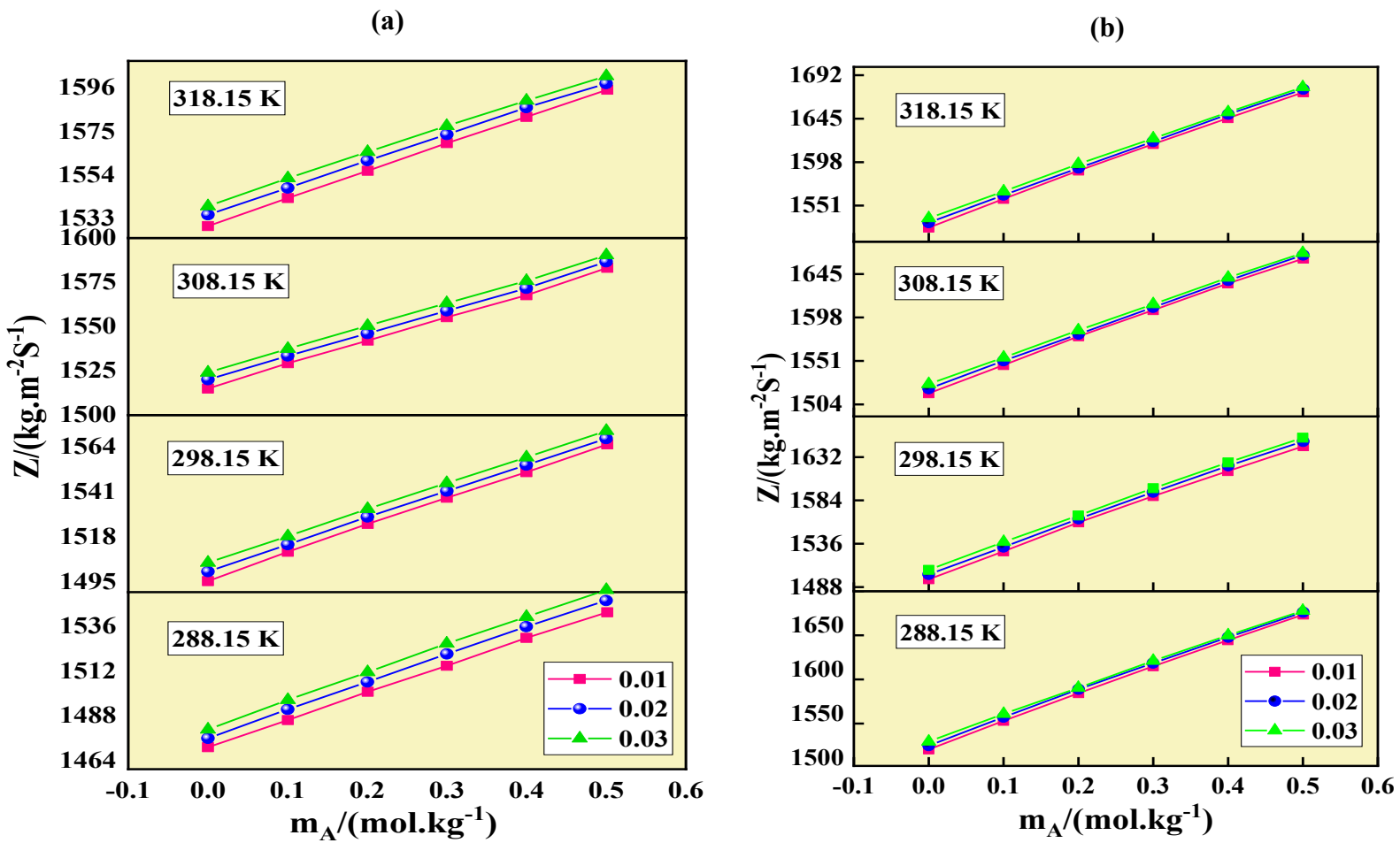

Figure 4.17 Stack graph between the Z, and m_A of PEG-200/400 in LBA shown as (a) and (b) respectively [pink, 0.01 mol/kg lactobionic acid; blue, 0.02 mol/kg lactobionic acid; green, 0.03 mol/kg lactobionic acid at several temperatures [square, 288.15 K; circle, 298.15 K; up triangle, 308.15 K; down triangle, 318.15K]

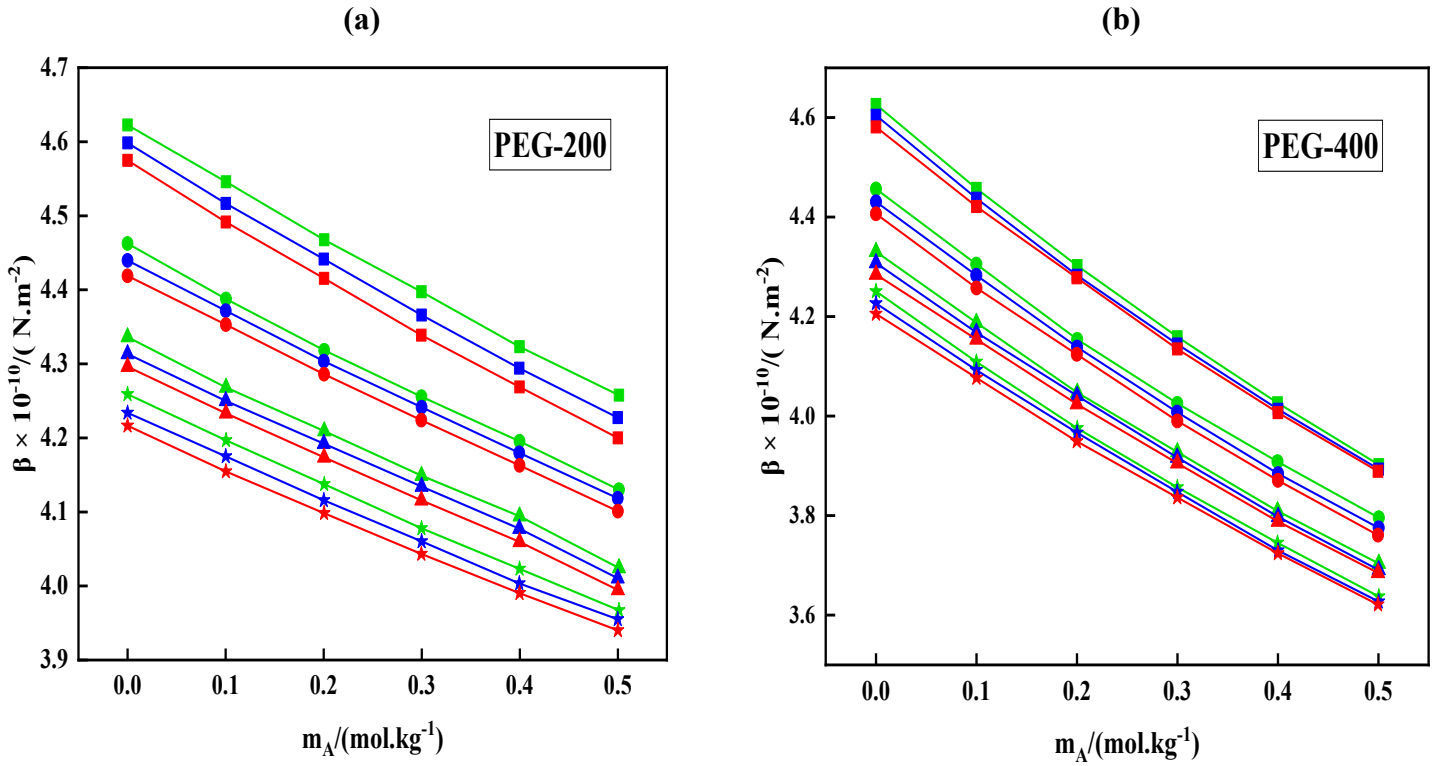

Figure 4.18 Change in Adiabatic Compressibility, β with respect to m_A of glycols (a) PEG-200 and (b) PEG-400 in lactobionic acid aqueous solution [green, 0.01 mol/kg lactobionic acid; blue, 0.02 mol/kg lactobionic acid; red, 0.03 mol/kg lactobionic acid at diverse temperatures [square, 288.15 K; circle, 298.15 K; up triangle, 308.15 K; star, 318.15 K].

Wada's Constant (W)

The following relation **4.17** can be used to get the Wada's constant.

$$W = (\beta)^{1/7} \frac{M_{eff}}{\rho} \quad \textbf{(4.17)}$$

Here β stands for adiabatic compressibility, and M_{eff} for the solution's effective molecular weight. W falls with an intensification in m_A and lactobionic acid concentration, as is evident from **Table 4.26**, but it surges on the growth of T temperature, as seen in **Figure 4.19**. The distance between the molecules narrows as density and sound velocity rise with concentration [40]. The W fluctuates with T, according to composition and molality in According to Table 4.26, the solute and co-solute particles are moving closer together**.** This suggests that the molecules are getting nearer to one another demonstrating the existence of robust solute solvent relations inside the solution [41-43].

Rao's Constant (R)

Equation (**4.18**) describes the relationship between mixture density (ρ), molecular weight (M), and speed (v)

$$R = v^{1/3} \frac{M}{\rho} \quad \textbf{(4.18)}$$

Rao's constant increases as temperature rises while seeing a decline in value as concentration grows. **Table 4.26** provides a description of the Rao's constant value, and **Figure 4.20** displays it graphically. In a solution where the components are tightly packed together, the number of components rises and interactions do too [44-45].

Table 4.26 Constants W and R of PEGs in water based Lactobionic acid.

Molality m_A /(mol /kg)	$W/(m^3/mol)(Pa^{1/7})$				$R/\ (m^3/mol)(m/s)^{1/3}$			
	$288.15K$	$298.15K$	$308.15K$	$318.15K$	$288.15K$	$298.15K$	$308.15K$	$318.15K$
0.01 mol/kg Lactobionic acid + PEG 200								
0.00000	160.62	161.82	162.97	164.01	2273.04	2292.73	2311.89	2328.98
0.10043	160.54	161.73	162.86	163.86	2271.64	2291.34	2310.03	2326.63
0.20062	160.49	161.65	162.73	163.74	2270.84	2289.95	2307.79	2324.49
0.29985	160.43	161.56	162.63	163.64	2269.85	2288.47	2306.18	2322.85
0.39982	160.41	161.48	162.52	163.53	2269.58	2287.10	2304.41	2321.15
0.50120	160.37	161.44	162.52	163.45	2268.84	2286.47	2304.36	2319.83
0.02 mol/kg Lactobionic acid + PEG 200								
0.00000	160.55	161.72	162.87	163.94	2271.75	2291.22	2310.23	2327.92
0.10025	160.50	161.62	162.75	163.80	2270.91	2289.44	2308.22	2325.57
0.20017	160.44	161.54	162.63	163.69	2270.04	2288.18	2306.21	2323.76
0.29993	160.42	161.46	162.54	163.59	2269.65	2286.85	2304.66	2322.05
0.39956	160.40	161.40	162.46	163.52	2269.34	2285.82	2303.39	2320.88
0.49999	160.38	161.36	162.46	163.41	2268.96	2285.13	2303.43	2319.19
0.03 mol/kg Lactobionic acid + PEG 200								
0.00000	160.48	161.61	162.76	163.83	2270.59	2289.35	2308.35	2326.03
0.10035	160.44	161.50	162.65	163.71	2269.99	2287.55	2306.45	2324.10
0.20053	160.40	161.43	162.55	163.60	2269.38	2286.42	2304.84	2322.27
0.29972	160.40	161.37	162.47	163.52	2269.40	2285.43	2303.61	2320.85

0.39985	160.39	161.33	162.41	163.44	2269.24	2284.69	2302.60	2319.59
0.50007	160.40	161.32	162.43	163.37	2269.41	2284.50	2302.89	2318.50
0.01 mol/kg Lactobionic acid + PEG 400								
0.00000	321.21	323.69	326.01	328.10	4545.47	4586.48	4624.79	4659.47
0.09989	320.86	323.22	325.49	327.60	4539.60	4578.68	4616.27	4651.18
0.20029	320.57	322.96	325.16	327.22	4534.89	4574.31	4610.79	4644.85
0.29999	320.37	322.66	324.80	326.87	4531.56	4569.41	4604.77	4639.07
0.39959	320.24	322.41	324.61	326.62	4529.47	4565.30	4601.62	4634.83
0.50046	320.16	322.25	324.39	326.46	4528.17	4562.59	4598.06	4632.21
0.02 mol/kg Lactobionic acid + PEG 400								
0.00000	321.03	323.54	325.81	327.96	4542.46	4583.97	4621.47	4657.14
0.09998	320.68	323.05	325.28	327.40	4536.63	4575.92	4612.75	4647.84
0.20018	320.42	322.75	324.83	326.95	4532.34	4570.91	4605.29	4640.43
0.29984	320.18	322.50	324.54	326.63	4528.49	4566.72	4600.49	4635.06
0.40025	320.04	322.33	324.36	326.45	4526.13	4563.98	4597.44	4632.06
0.50040	319.95	322.15	324.19	326.25	4524.64	4560.92	4594.71	4628.83
0.03 mol/kg Lactobionic acid + PEG 400								
0.00000	320.89	323.35	325.64	327.78	4540.15	4580.80	4618.72	4654.06
0.10011	320.48	322.90	325.04	327.17	4533.46	4573.39	4608.72	4644.05
0.19995	320.12	322.50	324.64	326.77	4527.54	4566.84	4602.20	4637.44
0.29987	319.96	322.30	324.31	326.39	4524.84	4563.53	4596.70	4631.12
0.40004	319.81	322.12	324.12	326.17	4522.29	4560.45	4593.61	4627.42
0.49968	319.71	321.99	323.93	326.01	4520.62	4558.27	4590.45	4624.77

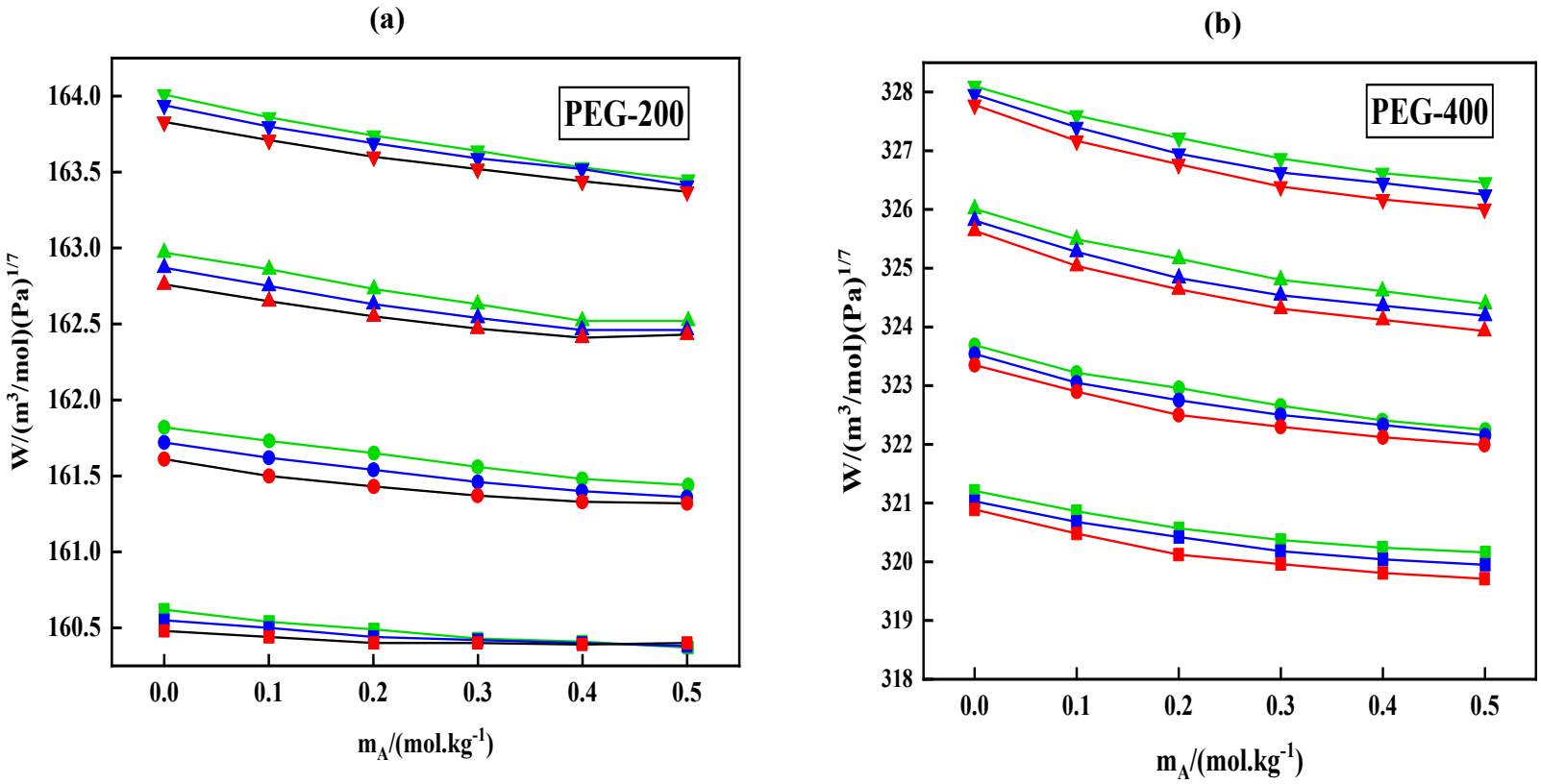

Figure 4.19. Variation of Wada's Constant, W, with respect to m_A of (a) PEG-200 and (b) PEG-400 in lactobionic acid [green, 0.01 mol/kg lactobionic acid; blue, 0.02 mol/kg lactobionic acid; red, 0.03 mol/kg lactobionic acid at temperatures [square, 288.15 K; circle, 298.15 K; up triangle, 308.15 K; down triangle, 318.15 K].

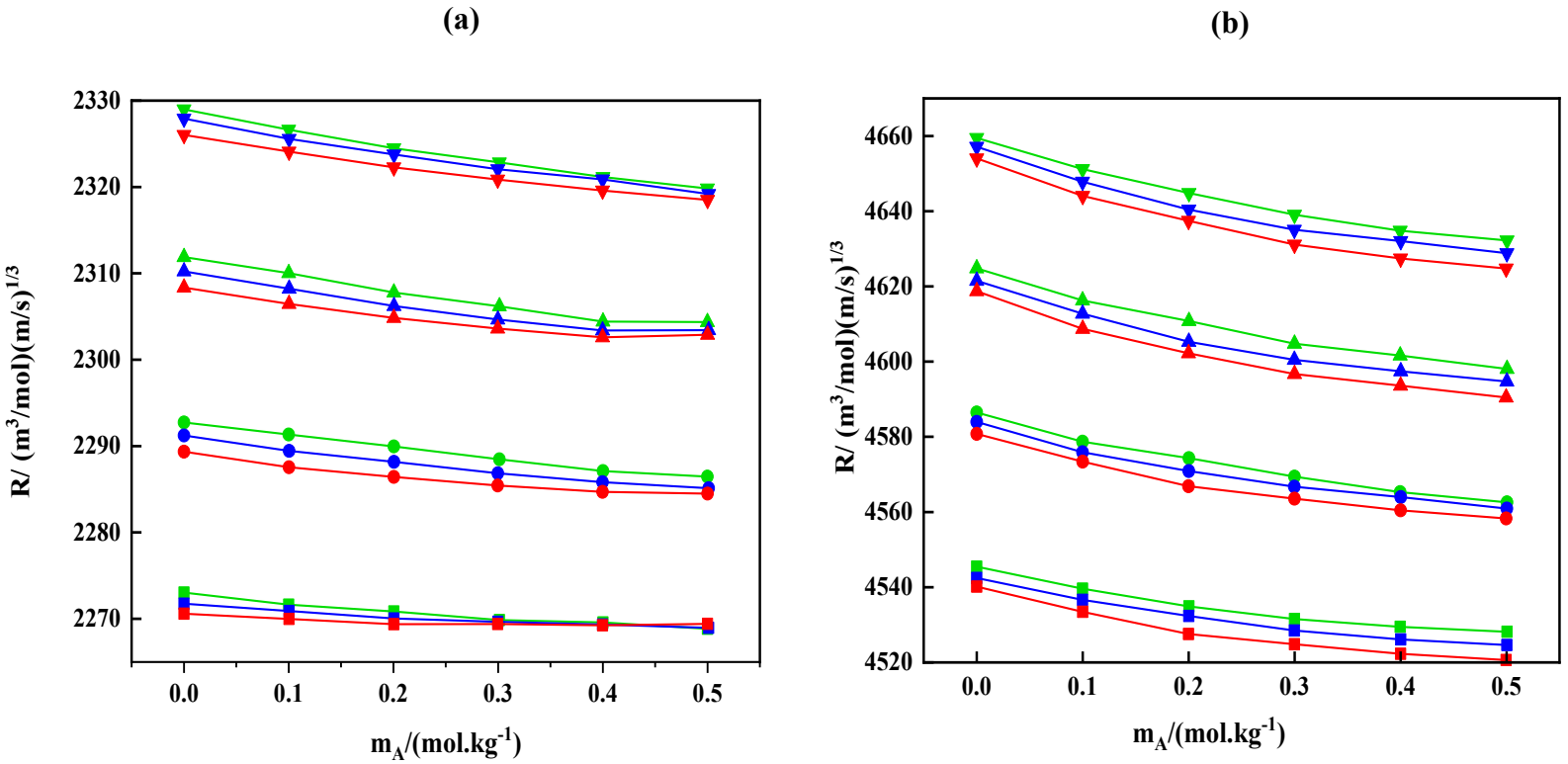

Figure 4.20. Variation of Rao's Constant, R, with respect to m_A of (a) PEG-200 and (b) PEG-400 in lactobionic acid [green, 0.01 mol/kg lactobionic acid; blue, 0.02 mol/kg lactobionic acid; red, 0.03 mol/kg lactobionic acid at temperatures [square, 288.15 K; circle, 298.15 K; up triangle, 308.15 K; down triangle, 318.15 K].

Intermolecular Free Length (L_f)

The separation amongst the boundaries of adjacent molecules is known as the intermolecular free length. The given relation **4.19** is used to compute it. [46]

$$L_f = K_T \beta^{1/2} \quad \textbf{(4.19)}$$

Where 'β' is the adiabatic compressibility and K_T is the temperature dependent constant. With increasing concentration and molality, the free length decreases. The fluctuation in intermolecular free length is shown in **Figure 4.21** and is caused by liquid compression. Values are stated in **Table 4.27** and show that the molecules are interacting with one another. Due to reduced adiabatic compressibility, which results in tighter packing of the molecules, the free length has decreased. Strong molecular connections arise from greater intermolecular cohesion, as may be observed clearly in **Figure 4.21.** The constant reduction in free length is what leads to the combination's increased sound velocity. On the other side, the free length lengthens as the temperature rises. [47-48]

Vander Waal's constant (b)

The Vander Waal's constant is found by using the quantities, M = molecular weight, R=the gas constant, ρ = density, T= temperature as per the equation **4.20.**

$$b = (M/\rho).[1 - (RT/Mv^2)\{(1 + \left(\frac{Mv^2}{3RT}\right))^{1/2} - 1\}] \quad \textbf{(4.20)}$$

Figure 4.22 illustrates the fluctuation of Vander Waal's constant, b, which is comparable to m_A of glycols in an LBA solution. It shows that the value of b decreases as molality and concentration increase, while it increases as temperature rises. The intensifying values of Vander Waal's coefficients in **Table 4.27** are evidence of the high binding forces between solute and solvent present inside the liquid combination. [49-52]

Table 4.27 L_f and b of PEGs in water based Lactobionic acid at different temperatures.

Molality	$L_f/(\text{Å})$				$b/(m^3/mol)$			
$m_A/(mol/kg)$	288.15K	298.15K	308.15K	318.15K	288.15K	298.15 K	308.15 K	318.15K
				0.01 mol/kg Lactobionic acid + PEG 200				
0.0000	4.3403	4.3438	4.3599	4.3984	395.28	396.2	397.38	398.84
0.1004	4.3042	4.3072	4.3255	4.3660	394.16	395.08	396.24	397.68
0.2006	4.2670	4.2730	4.2956	4.3351	393.10	394	395.16	396.59
0.2999	4.2333	4.2419	4.2648	4.3039	392.09	392.99	394.14	395.56
0.3998	4.1974	4.2117	4.2365	4.2748	391.13	392.02	393.16	394.57
0.5012	4.1655	4.1788	4.2002	4.2450	390.20	391.08	392.21	393.62
				0.02 mol/kg Lactobionic acid + PEG 200				
0.0000	4.3290	4.3326	4.3485	4.3853	394.80	395.70	396.85	398.35
0.1003	4.2903	4.2994	4.3164	4.3548	393.70	394.60	395.75	397.24
0.2002	4.2544	4.2657	4.2870	4.3237	392.66	393.56	394.71	396.20
0.2999	4.2181	4.2347	4.2572	4.2945	391.68	392.57	393.72	395.21
0.3996	4.1833	4.2039	4.2279	4.2644	390.74	391.63	392.79	394.27
0.5000	4.1507	4.1729	4.1930	4.2385	389.83	390.73	391.89	393.36
				0.03 mol/kg Lactobionic acid + PEG 200				
0.0000	4.3179	4.3224	4.3397	4.3763	394.35	395.17	396.36	397.85
0.1004	4.2784	4.2901	4.3079	4.3442	393.26	394.08	395.27	396.76
0.2005	4.2419	4.2569	4.2774	4.3145	392.25	393.07	394.26	395.75
0.2997	4.2049	4.2260	4.2476	4.2855	391.30	392.14	393.32	394.80

0.3999	4.1709	4.1954	4.2186	4.2573	390.40	391.24	392.43	393.90
0.5001	4.1371	4.1641	4.1847	4.2305	389.55	390.40	391.60	393.06
0.01 mol/kg Lactobionic acid + PEG 400								
0.0000	4.3421	4.3409	4.3570	4.3941	790.56	792.41	794.77	797.68
0.0999	4.2621	4.2666	4.2847	4.3204	785.65	787.50	789.86	792.76
0.2003	4.1874	4.1912	4.2123	4.2495	781.12	782.99	785.35	788.23
0.3000	4.1172	4.1257	4.1496	4.1856	776.99	778.87	781.23	784.10
0.3996	4.0510	4.0651	4.0864	4.1246	773.22	775.10	777.47	780.31
0.5005	3.9880	4.0062	4.0295	4.0649	769.68	771.58	773.95	776.80
0.02 mol/kg Lactobionic acid + PEG 400								
0.0000	4.3319	4.3283	4.3456	4.3817	789.60	791.41	793.71	796.72
0.1000	4.2527	4.2556	4.2747	4.3115	784.73	786.53	788.84	791.82
0.2002	4.1778	4.1832	4.2089	4.2446	780.25	782.08	784.38	787.33
0.2998	4.1099	4.1167	4.1439	4.1805	776.16	778.01	780.32	783.25
0.4003	4.0445	4.0526	4.0804	4.1160	772.38	774.25	776.55	779.47
0.5004	3.9834	3.9954	4.0224	4.0590	768.92	770.77	773.09	776.00
0.03 mol/kg Lactobionic acid + PEG 400								
0.0000	4.3208	4.3165	4.3340	4.3707	788.70	790.34	792.72	795.71
0.1001	4.2448	4.2428	4.2675	4.3032	783.85	785.51	787.88	790.85
0.2000	4.1755	4.1758	4.2001	4.2354	779.42	781.10	783.47	786.43
0.2999	4.1050	4.1076	4.1376	4.1744	775.37	777.07	779.44	782.37
0.4000	4.0410	4.0455	4.0751	4.1130	771.63	773.36	775.72	778.64
0.4997	3.9812	3.9876	4.0193	4.0556	768.22	769.97	772.31	775.24

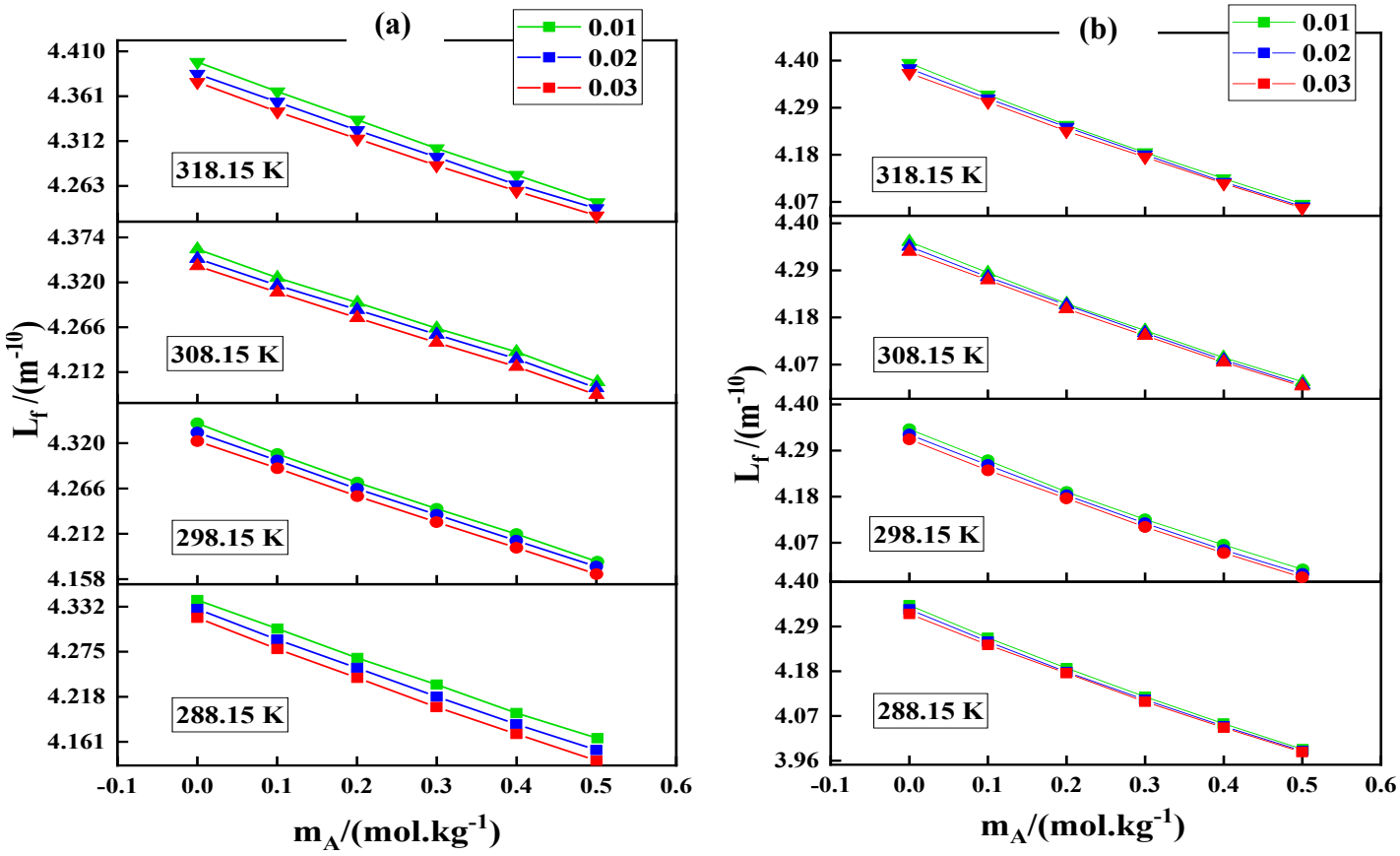

Figure 4.21 Stack graph between the intermolecular free length, L_f and the molality, m_A of glycols (a) PEG-200 and (b) PEG-400 in lactobionic acid solution [green, 0.01 mol/kg lactobionic acid; blue, 0.02 mol/kg lactobionic acid; red, 0.03 mol/kg lactobionic acid at temperatures [square, 288.15 K; circle, 298.15 K; up triangle, 308.15 K; down triangle, 318.15 K].

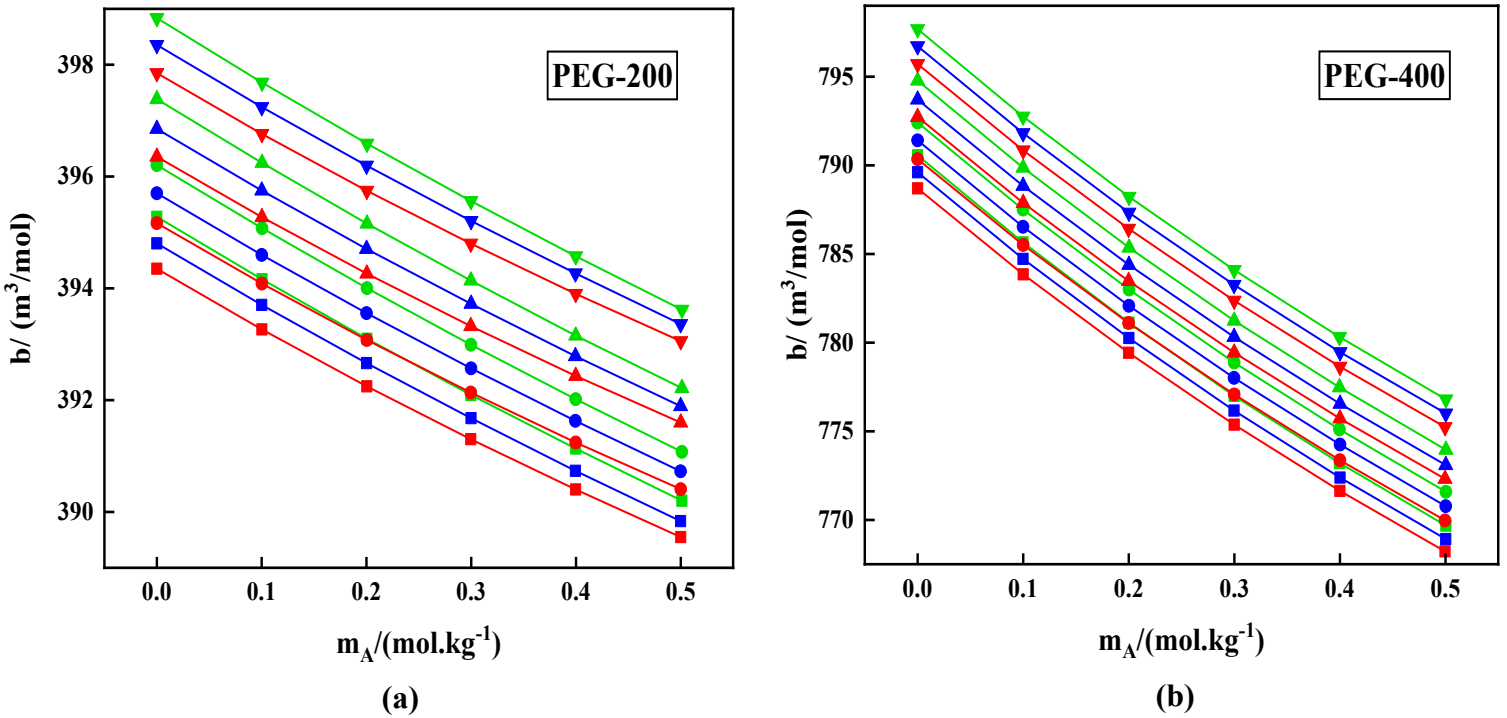

Figure 4.22 Change in Vander Waal's constant, b, with respect to m_A of PEGs (a) PEG-200 and (b) PEG-400 in lactobionic acid solution [green, 0.01 mol/kg lactobionic acid; blue, 0.02 mol/kg lactobionic acid; red, 0.03 mol/kg lactobionic acid at diverse temperatures [square, 288.15 K; circle, 298.15 K; up triangle, 308.15 K; down triangle, 318.15 K]

Conclusion

In the taken blend consisting of lactobionic acid, H_2O, and (PEG200/400), the thermodynamic and acoustic properties were explored at atmospheric pressure using a range of parameters over LBA compositions of (0.01-0.03) $mol.kg^{-1}$. This investigation's result were presented in the form of experimental data. An interaction between the lactobionic acid solution and polyethylene glycols can be observed on a molecular level, as demonstrated by the values that were experimentally measured and derived. It is possible to observe a linear pattern in the parameters that were acquired. It appears that there are no complicated interactions present, as indicated by the linear trend of the results. In response to changes in temperature and concentration, acoustic impedance displays a linear rise. At low concentrations, the Vander Waal constant has a significant interaction, whereas at large concentrations, it exhibits a modest impact. The significant binding forces are existing inside the liquid system are demonstrated by the fact that the values of $'b'$ will increase as the T increases. Both the free length and the compressibility of the water solution demonstrate that the solute and the fluid are located in close proximity to one another on a molecular level.

References

[1] N. Chakraborty, K.C. Juglan, H. Kumar, Braz. J. Chem. Eng. 38, 1–16 (2021).

[2] A.A. Firdaus, N. Chakraborty, K.C. Juglan, Chem. Thermodyn. Therm. Anal. 13, 100127 (2024).

[3] F.M. Sannaningannavar, B.S. Navati, N.H. Ayachit, J. Therm. Anal. Calorim. 112, 1573–1578 (2013).

[4] S. Parveen, S. Singh, D. Shukla, M. Yasmin, M. Gupta, J.P. Shukla, J. Solut. Chem. 41, 156–172 (2012).

[5] M. Lamba, N. Chakraborty, K.C. Juglan, R. Sharma, M. Singla, J. Chem. Eng. Data 69, 171–184 (2024).

[6] M.S. Raman, M. Kesavan, K. Senthilkumar, V. Ponnuswamy, J. Mol. Liq. 202, 115–124 (2015).

[7] F. Ebner, A. Heller, F. Rippke, I. Tausch, Am. J. Clin. Dermatol. 3, 427–433 (2002).

[8] S. Chauhan, M.S. Chauhan, D. Kaushal, V.K. Syal, J. Jyoti, J. Solut. Chem. 39, 622–638 (2010).

[9] H. Kumar, I. Behal, J. Chem. Eng. Data 61, 3740–3751 (2016).

[10] P. Pradhan, R.S. Sah, M.N. Roy, J. Mol. Liq. 144, 149–154 (2009).

[11] A.K. Mishra, J.C. Ahluwalia, J. Phys. Chem. 88, 86–92 (1984).
[12] L. Pauling, R.E. Marsh, Proc. Natl. Acad. Sci. 38, 112–118 (1952).
[13] M. Iqbal, M.A. Chaudhary, J. Chem. Thermodyn. 42, 951–956 (2010).
[14] H. Kumar, I. Behal, J. Chem. Thermodyn. 102, 48–62 (2016).
[15] K. Kaur, K.C. Juglan, H. Kumar, J. Chem. Eng. Data 62, 3769–3782 (2017).
[16] K. Belibagli, E. Aryanci, J. Solut. Chem. 19, 867–882 (1990).
[17] B.D.N. Rao, P. Venkateswarlu, A.S.N. Murthy, C.N.R. Rao, Can. J. Chem. 40, 963–965 (1962).
[18] A. Pal, Y.P. Singh, J. Chem. Eng. Data 41, 425–427 (1996).
[19] W.G. Mcmillan, J.E. Mayer, J. Chem. Phys. 13, 276–305 (1945).
[20] A.K. Nain, Fluid Phase Equilibr. 259, 218–227 (2007).
[21] H. Kumar, I. Behal, M. Singla, J. Chem. Thermodyn. 95, 1–14 (2016).
[22] A. Salabat, L. Shamshiri, F. Sahrakar, J. Mol. Liq. 118, 67–70 (2005).
[23] R.K. Wadi, P. Ramasami, J. Chem. Soc. Faraday Trans. 93, 243–247 (1997).
[24] R. Sadeghi, F. Ziamajidi, J. Chem. Eng. Data 52, 1037–1044 (2007).
[25] M. Lamba, N. Chakraborty, K.C. Juglan, M. Singla, Chem. Thermodyn. Therm. Anal. 13, 100129 (2024).
[26] C.V. Krishnan, H.L. Friedman, J. Solut. Chem. 2, 37–51 (1973).
[27] R. Rani, A. Kumar, R.K. Bamezai, J. Mol. Liq. 240, 642–655 (2017).
[28] K. Bhakri, M. Lamba, K.C. Juglan, N. Chakraborty, J. Mol. Liq. 125117 (2024).
[29] M.N. Roy, V.K. Dakua, B. Sinha, Int. J. Thermophys. 28, 1275–1284 (2007).
[30] F.J. Millero, Structure and Transport Process in Water and Aqueous Solutions, Wiley, New York (1972).
[31] L.G. Helper, Can. J. Chem. 47, 4613–4617 (1969).
[32] P.R. Misra, B. Das, M.L. Parmar, D.S. Banyal, Ind. J. Chem. A 44, 1582–1588 (2005).
[33] M.K. Praharaj, P.R. Mishra, S. Mishra, A. Satapathy, Arch. Phys. Res. 3, 192–200 (2012).
[34] N. Chakraborty, M. Rani, K.C. Juglan, Plant Arch. 20, 2825–2829 (2020).
[35] B. Kaur, K.C. Juglan, J. Polym. Eng. 33, 851–856 (2013).
[36] N. Santhi, J. Madhumitha, Int. J. Adv. Chem. 2, 12–16 (2014).
[37] D.N. Rao, A. Krishnaiah, P.R. Naidu, Acta Chim. Acad. Sci. Hung. 107, 49–55 (2022).
[38] A. Tadkalkar, P. Pawar, G.K. Bichile, J. Chem. Pharm. Res. 3, 165–168 (2011).
[39] N.P. Mohabansi, J. Sci. Res. 64, 352–358 (2020).

[40] S. Devi, M. Kumar, N. Sawhney, U. Syal, A.K. Sharma, M. Sharma, J. Chem. Thermodyn. 154, 106321 (2021).

[41] K. Kaur, K.C. Juglan, Der Pharma Chem. 7, 160–167 (2015).

[42] A. Kumar, V. Sharma, Int. J. ChemTech Res. 8, 438–443 (2015).

[43] R.C. Thakur, R. Sharma, M. Kumar, S. Kumar, Orient. J. Chem. 31, 363–369 (2015).

[44] M. Sohail, H.M. Rahman, M.N. Asghar, J. Surfactants Deterg. 24, 327–342 (2021).

[45] H. Eyring, J.F. Kincaid, J. Chem. Phys. 6, 620–629 (1938).

[46] P.S. Nikam, M. Hasan, Asian J. Chem. 5, 319–321 (1993).

[47] K. Kaur, A.S. Ghosh, T.K. Ghosh, T.S. Banipal, P.K. Banipal, J. Chem. Thermodyn. 159, 106477 (2021).

[48] V. Gajghate, A. Kanwar, J. Sci. Res. 13, 483–493 (2021).

[49] V. Sharma, V. Thakur, A. Kumar, Int. J. Pharm. Pharm. Sci. 8, 318–321 (2016).

[50] V. Sharma, P.C. Lopez, O.Y. Osses, A. Kumar, J. Chem. Eng. Data 63, 3083–3096 (2018).

[51] V. Sharma, P.C. Lopez, O.Y. Osses, C. Rojas-Fuentes, A. Kumar, J. Mol. Liq. 271, 443–451 (2018).

[52] N. Chakraborty, K.C. Juglan, H. Kumar, Plant Arch. 20, 3089–3091 (2020).

Section-III

Problem-5

Exploration of the Molecular Interactions between Polyhydroxy acid: Gluconolactone and Glycols: A Thermoacoustic Method''

In the Problem 5, the experiments were conducted via Density Speed Analyzer 5000M at a fixed 0.1 MPa pressure at 3 MHz to determine the ρ and v values for the ternary mixes of one of the Polyhydroxy acid: Gluconolactone and Polyethylene glycol-400/4000 at different doses of Gluconolactone (0.08, 0.09, and 0.10) $mol \cdot kg^{-1}$.

Apparent Molar Volume

Various characteristics were examined using the field work of density and speed of sound readings. The equation **4.1** was used to calculate V_ϕ by using density values. The **Table 4.28** shows the density and calculated V_ϕ values. The uncertainty of V_ϕ is u (V_ϕ) = 0.59×10^6/ ($m^3.mol^{-1}$) Every density number in the table goes down as the temperature goes up, molality and concentration go up. The graph in **Figure 4.23** compares experimental density values for the binary combination of water and gluconolactone at different temperatures with values found in the literature [1]. This makes clear that the results obtained from the experiment and those reported in the literature are correlated from **Figure 4.23.** In contrast, **Figure 4.24** reveals that all $V_\phi$values are positive and tend to increase when Gluconolactone concentration, molality, and temperature rise. On top of that, it sheds light on how solutes act when mixed with water [2]. The solute molecules take up more room in the solution than they would in their pure form, according to all the positive data of apparent molar volume. This further provides evidence that the solute expands and increases in volume when immersed in solvent [3–4]. In addition, the interactions between the molecules get stronger with concentration rise as the volume also rises. **Figure 4.25** illustrates the impact of increasing PEG masses (400-4000) on the chemical relationship of glycols and gluconolactone in a solution consisting of water. The apparent molar volume increases by interactions between solutes and solvents as concentration increases. In a water-rich environment, the increase in V_ϕ value could be explained by many physical phenomena, like hydrophilicity, dipole-induced-dipole phenomenon [5]. The values for the ρ and V_ϕ for PEGs with 0.00 $mol \cdot kg^{-1}$ Gluconolactone are taken from the previous publication. [6]

Table 4.28 Experimental (ρ) and calculated (V_ϕ) for solutions of PEGs in water based Gluconolactone at $p = 0.1\ MPa$ and different temperatures.

[a]$m_A/(mol \cdot kg^{-1})$	$\rho \times 10^{-3}\ /\ (kg.m^{-3})$				$V_\phi \times 10^6/(m^3.mol^{-1})$			
	$288.15K$	$298.15K$	$308.15K$	$318.15K$	$288.15K$	$298.15K$	$308.15K$	$318.15K$
PEG-400+ 0.00 $mol \cdot kg^{-1}$ Gluconolactone								
0.00000	0.99953 [b]	0.99748 [b]	0.99447 [b]	0.99065 [b]				
0.01000	0.99997 [b]	0.99774 [b]	0.99471 [b]	0.99101 [b]	328.890 [b]	331.370 [b]	334.340 [b]	336.930 [b]
0.01992	1.00064 [b]	0.99839 [b]	0.99534 [b]	0.99162 [b]	330.160 [b]	332.780 [b]	335.910 [b]	338.560 [b]
0.03006	1.00130 [b]	0.99903 [b]	0.99595 [b]	0.99222 [b]	331.510 [b]	334.260 [b]	337.450 [b]	340.090 [b]
0.03992	1.00191 [b]	0.99961 [b]	0.99651 [b]	0.99277 [b]	332.910 [b]	335.650 [b]	338.890 [b]	341.460 [b]
0.05009	1.00252 [b]	1.00020 [b]	0.99707 [b]	0.99331 [b]	334.060 [b]	336.830 [b]	340.060 [b]	342.780 [b]
PEG-400+ 0.08 $mol \cdot kg^{-1}$ Gluconolactone								
0.00000	1.00584	1.00367	1.00056	0.99665				
0.01000	1.00653	1.00432	1.00118	0.99725	329.670	334.090	337.593	340.585
0.02002	1.00717	1.00493	1.00177	0.99781	331.710	335.893	339.267	342.500
0.02977	1.00778	1.00551	1.00232	0.99835	332.841	336.816	340.208	343.314
0.03992	1.00838	1.00608	1.00289	0.99890	333.896	337.771	340.707	343.671
0.05013	1.00895	1.00665	1.00344	0.99944	335.415	338.575	341.543	344.225
PEG-400+ 0.09 $mol \cdot kg^{-1}$ Gluconolactone								
0.00000	1.00655	1.00437	1.00125	0.99733				
0.00998	1.00723	1.00500	1.00185	0.99791	330.536	335.696	339.164	342.312

0.02009	1.00787	1.00558	1.00241	0.99845	332.286	337.945	341.403	344.674
0.02995	1.00846	1.00611	1.00290	0.99893	333.964	339.916	343.660	346.566
0.04016	1.00904	1.00665	1.00342	0.99943	335.524	341.278	344.675	347.707
0.05242	1.00973	1.00729	1.00407	1.00006	336.600	342.029	344.871	347.764
PEG-400+ 0.10 $mol \cdot kg^{-1}$ Gluconolactone								
0.00000	1.00677	1.00461	1.00153	0.99767				
0.00987	1.00743	1.00522	1.00209	0.99821	331.415	336.775	341.994	345.785
0.02019	1.00807	1.00582	1.00264	0.99874	333.127	338.340	343.840	347.560
0.03014	1.00864	1.00635	1.00313	0.99920	335.335	340.397	345.606	349.478
0.04022	1.00919	1.00684	1.00360	0.99964	337.127	342.416	347.285	351.069
0.05011	1.00968	1.00728	1.00400	1.00003	338.943	344.370	349.257	352.866
PEG-4000+ 0.00 $mol \cdot kg^{-1}$ Gluconolactone								
0.00000	0.99953 [b]	0.99748 [b]	0.99447 [b]	0.99065 [b]				
0.01003	1.00568 [b]	1.00350 [b]	1.00055 [b]	0.99694 [b]	3340.480 [b]	3342.640 [b]	3344.860 [b]	3347.260 [b]
0.02001	1.01164 [b]	1.00950 [b]	1.00661 [b]	1.00307 [b]	3341.820 [b]	3343.890 [b]	3345.900 [b]	3348.390 [b]
0.02929	1.01684 [b]	1.01474 [b]	1.01189 [b]	1.00841 [b]	3343.020 [b]	3345.020 [b]	3347.230 [b]	3349.630 [b]
0.03994	1.02243 [b]	1.02037 [b]	1.01758 [b]	1.01416 [b]	3344.260 [b]	3346.110 [b]	3348.320 [b]	3350.750 [b]
0.05012	1.02745 [b]	1.02542 [b]	1.02267 [b]	1.01931 [b]	3345.290 [b]	3347.170 [b]	3349.420 [b]	3351.840 [b]
PEG-4000+ 0.08 $mol \cdot kg^{-1}$ Gluconolactone								
0.00000	1.00584	1.00367	1.00056	0.99665				
0.00998	1.01204	1.00990	1.00685	1.00301	3342.701	3345.593	3347.801	3350.485

0.01998	1.01782	1.01569	1.01269	1.00893	3344.486	3348.234	3350.759	3352.975
0.03000	1.02323	1.02114	1.01819	1.01450	3345.921	3349.180	3351.801	3354.367
0.03999	1.02829	1.02623	1.02332	1.01968	3347.150	3350.152	3353.077	3355.907
0.04999	1.03303	1.03100	1.02814	1.02459	3348.575	3351.357	3354.085	3356.606
PEG-4000+ 0.09 $mol \cdot kg^{-1}$ Gluconolactone								
0.00000	1.00655	1.00437	1.00125	0.99733				
0.01006	1.01276	1.01060	1.00753	1.00367	3344.244	3347.862	3350.773	3354.844
0.02001	1.01845	1.01632	1.01328	1.00948	3347.527	3350.804	3354.830	3359.033
0.02992	1.02376	1.02161	1.01863	1.01487	3349.263	3353.852	3357.043	3362.213
0.04002	1.02880	1.02667	1.02371	1.02001	3351.216	3355.625	3359.529	3364.236
0.05002	1.03350	1.03136	1.02840	1.02473	3352.440	3357.466	3362.388	3367.418
PEG-400+ 0.10 $mol \cdot kg^{-1}$ Gluconolactone								
0.00000	1.00677	1.00461	1.00153	0.99767				
0.00996	1.01288	1.01073	1.00769	1.00390	3346.957	3351.981	3356.494	3360.104
0.01989	1.01852	1.01638	1.01338	1.00964	3350.865	3355.786	3359.747	3364.384
0.02986	1.02377	1.02163	1.01866	1.01500	3354.670	3359.885	3364.280	3367.847
0.03995	1.02869	1.02654	1.02362	1.02000	3358.655	3364.222	3368.174	3372.303
0.04969	1.03311	1.03094	1.02806	1.02453	3362.161	3368.184	3372.269	3375.424

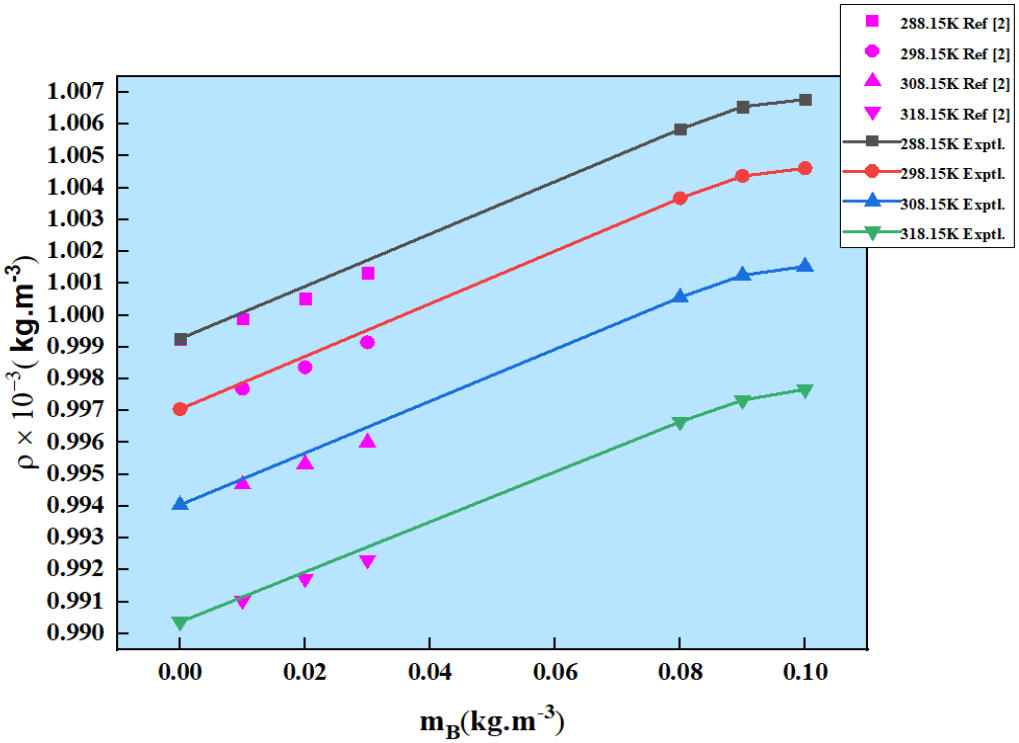

Figure 4.23 Comparison graph of literature [1] and experimental Gluconolactone's densities in water related to the concentration of Gluconolactone.

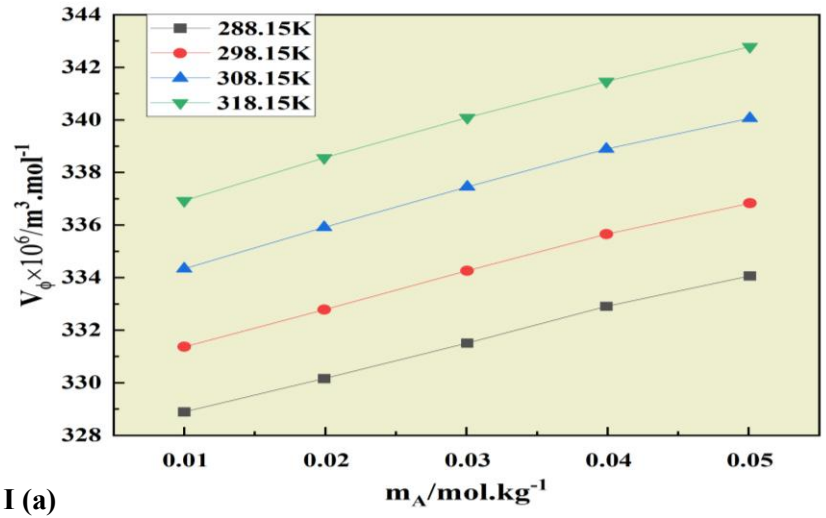
288.15K
298.15K
308.15K
318.15K
$V_\phi \times 10^6/m^3.mol^{-1}$
$m_A/mol.kg^{-1}$

I (a)

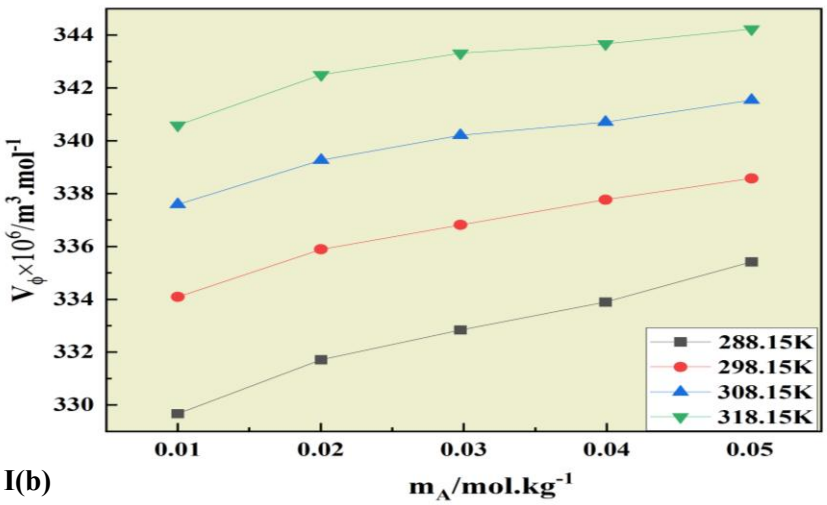
288.15K
298.15K
308.15K
318.15K
$V_\phi \times 10^6/m^3.mol^{-1}$
$m_A/mol.kg^{-1}$

I(b)

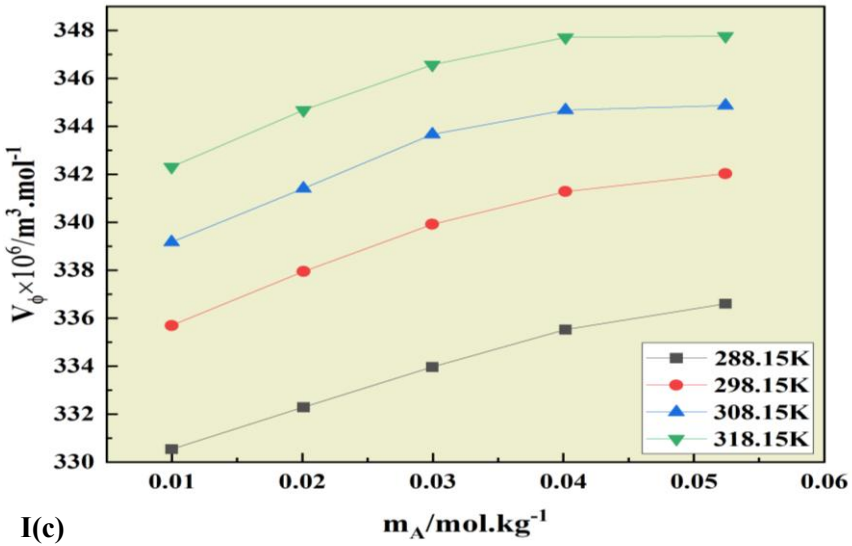
288.15K
298.15K
308.15K
318.15K
$V_\phi \times 10^6/m^3.mol^{-1}$
$m_A/mol.kg^{-1}$

I(c)

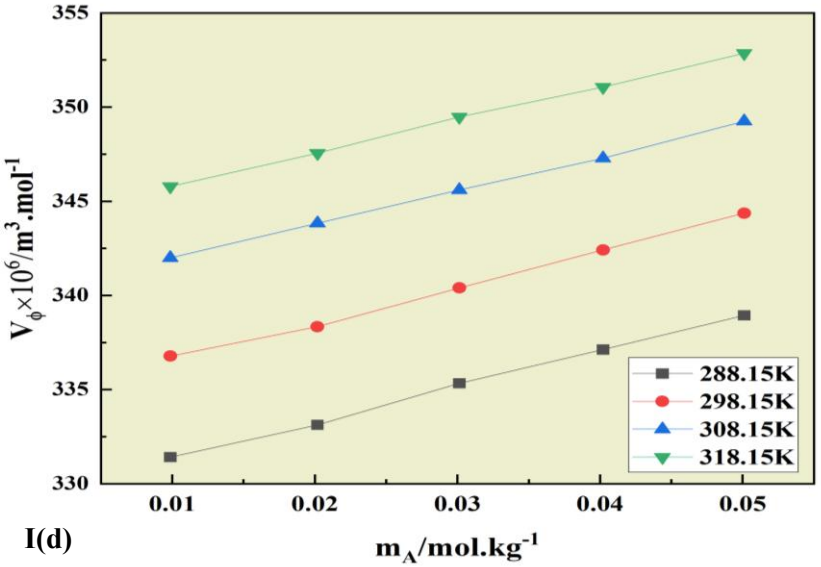
288.15K
298.15K
308.15K
318.15K
$V_\phi \times 10^6/m^3.mol^{-1}$
$m_A/mol.kg^{-1}$

I(d)

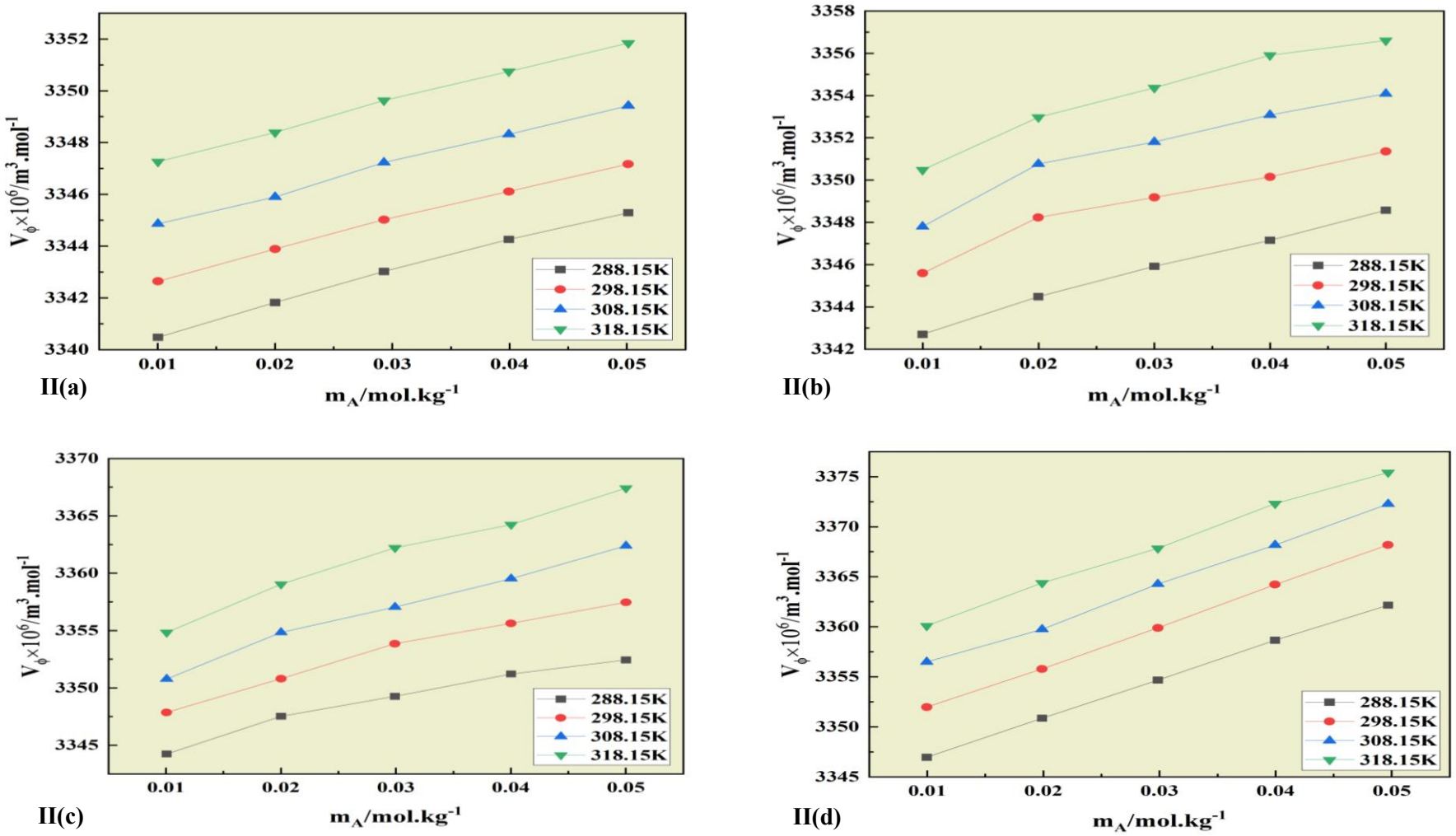

Figure 4.24 V_ϕ v/s molality of (I) PEG-400 and (II) PEG-4000 of Gluconolactone: 0.00, 0.08, 0.09 and 0.10 ($mol \cdot kg^{-1}$) GLA in (a), (b), (c) and (d) respectively.

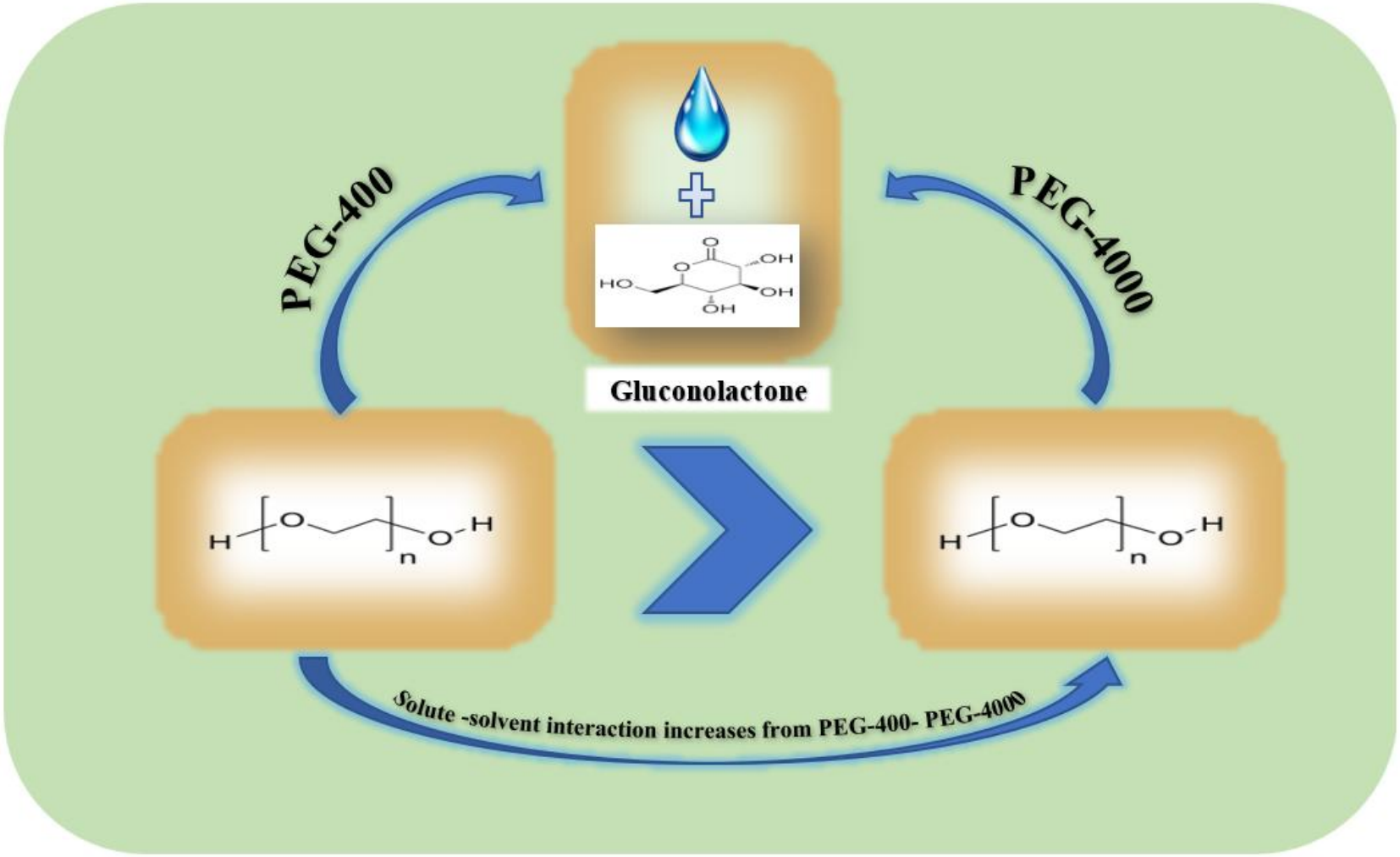

Figure 4.25 PEG-400/PEG4000 Interactions with Gluconolactone.

Limiting apparent molar volume ($\boldsymbol{V_\phi^0}$)

Utilizing the least square approach, we can determine the data of the V_ϕ^0 of the system comprising PEG-400/PEG-4000 + gluconolactone using the equation **4.4**. The computed values of V_ϕ^0 are stated in **Table 4.29** accompanied by experimental slope (S_V^*) with the uncertainties *u*(V_ϕ^0)= *0.38* $\times 10^6(m^3.mol^{-1})$ and *u*(S_V^*) =*1.07* $\times 10^6(m^3.kg.mol^{-2})$. The positive values of V_ϕ^0 are increasing with upsurge in T and m_B of GLA. The V_ϕ^0 are represented graphically in **Figure 4.26.** Additionally, V_ϕ^0 is an invaluable tool for analyzing the dynamics of solutions along with their ingredients, and (S_V^*)offers details regarding the features of solute-solute mixings [7,8]. Because of the packing effect and the dominance of ion- aquaphobic and aquaphobic-aquaphobic contacts over ion-aquaphilic association, positive values of V_ϕ^0 were found. Robust H-bonding connections between the O-atoms of polyethylene glycols and the H-atoms of H_2O are present in this combination [9-10]. Furthermore, the values of experimental slope (S_V^*) at each temperature at different concentration of Gluconolactone are positive. The (S_V^*) values represent the existence of solute connections with itself in the system, whereas its magnitude is very small as compare to the values of V_ϕ^0 [11-12]. This tells us that in this system, solute interacts with solvent more than a solute interacts with solute itself.

Table 4.29 V_ϕ^0 and S_V^*, along with deviations of PEG-400/4000 in water based Gluconolactone at 0.1 MPa pressure and 4 variable temperatures.

$^a m_B$/ $(mol \cdot kg^{-1})$	$V_\phi^0 \times 10^6 (m^3.mol^{-1})$				$S_V^* \times 10^6 (m^3.kg.mol^{-2})$			
	$288.15K$	$298.15K$	$308.15K$	$318.15K$	$288.15K$	$298.15K$	$308.15K$	$318.15K$
PEG-400								
0.08	328.61(±0.32)	333.38(±0.36)	337.07(±0.41)	340.33(±0.58)	129.5(±9.68)	108.3(±10.95)	93.2(±12.39)	84.2(±17.41)
0.09	329.34(±0.37)	334.76(±0.69)	338.55(±0.97)	341.81(±0.96)	145.6(±10.8)	151.0(±20.3)	137.9(±28.7)	130.8(±28.2)
0.10	329.48(±0.15)	334.79(±0.19)	340.22(±0.09)	344.06(±0.09)	189.5(±4.39)	191.6(±5.34)	178.7(±2.69)	175.8(±2.65)
PEG-4000								
0.08	3341.44(±0.18)	3344.87(±0.60)	3347.04(±0.70)	3349.52(±0.58)	3.44(±0.06)	3.71(±0.05)	3.64(±0.08)	3.71(±0.09)
0.09	3342.91(±0.69)	3345.91(±0.61)	3348.53(±0.57)	3352.90(±0.70)	3.53(±0.06)	3.70(±0.13)	3.74(±0.12)	3.77(±0.07)
0.10	3343.20(±0.11)	3347.75(±0.15)	3352.19(±0.34)	3356.44(±0.35)	3.69(±0.02)	4.12(±0.04)	3.83(±0.07)	4.13(±0.04)

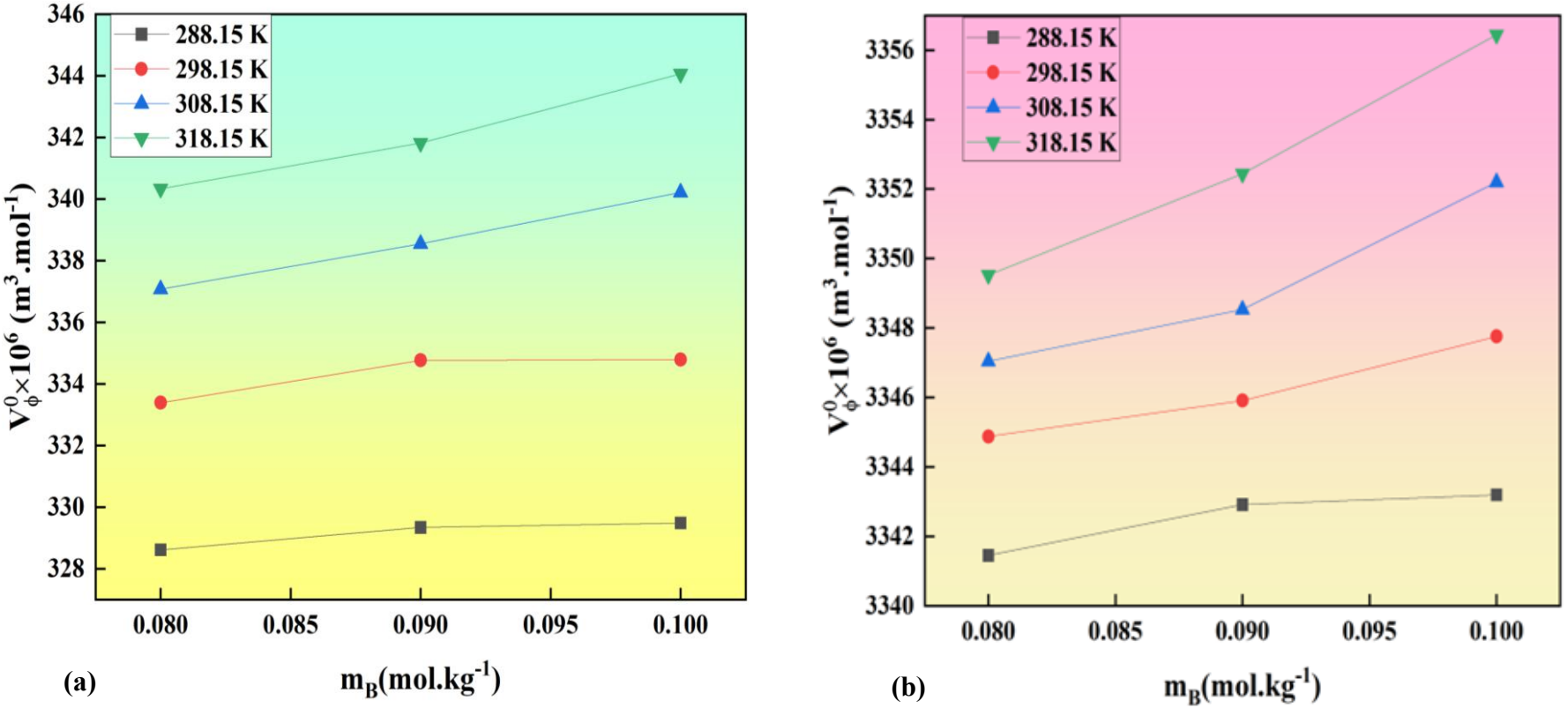

Figure 4.26 V_ϕ^0 v/s Concentrations for PEGs within a Gluconolactone solution at various temperatures: (a) and (b) represents PEG-400 and 4000 respectively.

Limiting apparent molar volume of transfer

The ΔV_{ϕ}^{0} for polyethylene glycols from water to Gluconolactone solution is calculated with the equation **4.6.** Calculated values of ΔV_{ϕ}^{0} at several temperatures are provided in **Table 4.30** with uncertainty of $u(\Delta V_{\phi}^{0})$=0.05 ×$10^{6}/(m^{3}.mol^{-1})$ Except at temperature of 298.15 K for 0.08 mol/kg of Gluconolactone in PEGs and 288.15 K at all concentrations, all other values for ΔV_{ϕ}^{0} for PEG-400 and PEG-4000, respectively, are positive. So, the interactions with positive ΔV_{ϕ}^{0} values will include (i) ionic-hydrophilic and (ii) hydrophilic-hydrophilic associations. Whereas, interactions with negative ΔV_{ϕ}^{0} values will include (iii) ionic-aquaphobic and (iv) aquaphobic-aquaphobic connections. The data shows that " ΔV_{ϕ}^{0}" can have both positive and negative values, suggesting that the gluconolactone and glycol (PEG-400/PEG-4000) molecules could potentially undergo a variety of interactions. The bulk of the interactions for both PEG-400 and PEG-4000 will be of the (i) and (ii) type since majority of ΔV_{ϕ}^{0} is positive. Therefore, the positive results indicate that the molecular connections between gluconolactone and PEGs are less strong than those between water and PEGs [13-14]. Moreover, as per co-sphere overlap modal, the ΔV_{ϕ}^{0} data indicates that solute-solute are negligible and it provides the strong interactions. Additionally, as per the model of co-sphere, positive ΔV_{ϕ}^{0} values indicate a structure arrangement. [15].

Table 4.30 ΔV_{ϕ}^{0}, of PEG-400/4000 in Gluconolactone.

[a]$m_B/(mol \cdot kg^{-1})$	$\Delta V_{\phi}^{0} \times 10^{6}(m^3.mol^{-1})$			
	$288.15K$	$298.15K$	$308.15K$	$318.15K$
PEG-400				
0.08	-4.07	-0.58	1.82	3.82
0.09	-3.34	0.80	3.30	5.30
0.10	-3.20	0.73	4.97	7.55
PEG-4000				
0.08	2.29	3.45	3.39	3.52
0.09	3.75	4.49	4.88	6.44
0.10	4.04	6.33	8.54	10.44

Partial molar volume depending on Temperature

To examine the temperature-dependent changes of V_ϕ^0 at infinite dilution, the equation **4.8** relationship is used. Here, T_{ref} is 298.15 K, representing the reference temperature on the Kelvin scale. The constants a, b, and c are empirical values listed in **Table 4.31.** Furthermore, expansibility coefficient, E_ϕ^0, has been derived using the equation **4.11**. The prevalence of solvent-solute contact is designated by the data of E_ϕ^0 in a solution. Regardless of the temperature or solution composition, the positive values of E_ϕ^0 point to the collaboration between the PEG-400/ PEG-4000 in the Gluconolactone solution and the reduction in volume. The E_ϕ^0 and $(\partial E_\phi^0/\partial T)_p$ data is enumerated in **Table 4.32** with uncertainty of [a]$u(E_\phi^0)$=0.023×$10^6/(m^3.mol^{-1}.K^{-1})$ *and* $u(\partial E_\phi^0/\partial T)_p$= 0.0014/$(m^3.mol^{-1}.K^{-2})$. Although the value of E_ϕ^0 decreases with temperature (except for PEG4000, at m_B of 0.09 mol/kg of GLA), there is no regular pattern for E_ϕ^0 and concentration. The E_ϕ^0, is beneficial parameter for evaluating the bonds in the blend. Solute activity in systemic structure formation and breakdown was quantified using the thermodynamic equation **4.12.** The expansibility shows how the behavior of interactions from its values. At all temperatures and solution compositions, the presence of a positive E_ϕ^0 value indicates that the PEG-400/PEG-4000 in the Gluconolactone solution effectively reduces the volume.

The partial derivative of E_ϕ^0 function's sign shows whether the solute is likely to form a structure or discontinuity one in the solvent. The solute is likely to operate as a structure creator if $(\partial E_\phi^0/\partial T)_p$ is positive or slightly negative. Conversely, the ability to shatter structures is indicated by negative numbers. The introduction of solutes into a solvent can cause the creation of new structures or the disruption of existing ones. The development of novel structures is indicated by positive values. **Table 4.32** gives useful information that sheds light on the behavior of glycols in water-based GLA that whether they make structures or break structures by the value of $(\partial E_\phi^0/\partial T)_p$. As per values of Table **4.32**, although the negative values of partial derivative of E_ϕ^0 indicates the distorting structure behaviour but the values are extremely small and on the other side we have all positive values of E_ϕ^0 that are correlated with the gluconolactone concentrations suggests that the occurrence of interactions is obvious from the positive values. The packing effect of GLA molecules in the mixture's voids could yield positive

readings, demonstrating bonding. So somehow, the internal structures of the system are formed by these interactions. The complex interconnections within the system are illuminated by these effects, which show how complex solute-solvent interactions are. Numerous academic disciplines rely on a thorough comprehension of the solutes' structural-forming and -breaking capabilities in ternary solutions [16, 17].

Table 4.31 Empirical numbers a, b and c, R^2 and ARD (deviations) for glycols in water based Gluconolactone at diverse temperatures and investigational pressure of 0.1Mpa.

[a]$m_B/(mol \cdot kg^{-1})$	a$\times 10^6(m^3.mol^{-1})$	$b \times 10^6(m^3.mol^{-1}.K^{-1})$	$c \times 10^6(m^3.mol^{-1}.K^{-2})$	R^2	*ARD*
PEG-400					
0.08	333.286	0.426	-0.004	0.9999	0.00020
0.09	334.595	0.466	-0.005	0.9999	0.00034
0.10	334.991	0.527	-0.003	0.9999	0.00059
PEG-4000					
0.08	3344.637	0.288	-0.002	0.9999	0.00005
0.09	3345.658	0.289	0.002	0.9999	0.00005
0.10	3347.765	0.449	-0.001	0.9999	0.00000

Table 4.32 E_ϕ^0 for PEG-400/4000 in aqueous Gluconolactone at diverse temperatures.

[a]$m_B\ (mol \cdot kg^{-1})$	$E_\phi^0 \times 10^6 (m^3.mol^{-1}.K^{-1})$				$(\partial E_\phi^0/\partial T)_p/(m^3.mol^{-1}.K^{-2})$
	$288.15K$	$298.15K$	$308.15K$	$318.15K$	
PEG-400					
0.08	0.501	0.426	0.351	0.275	-0.008
0.09	0.574	0.466	0.358	0.250	-0.011
0.10	0.595	0.527	0.458	0.390	-0.007
PEG-4000					
0.08	0.335	0.288	0.240	0.193	-0.005
0.09	0.244	0.289	0.335	0.380	0.005
0.10	0.465	0.449	0.434	0.418	-0.002

Apparent molar isentropic compression

The investigational data of sound's speed is mentioned in Table **4.33** and shows the similar trend of growth while both the molality and temperature rise. Empirically measured (ρ) and (v) are put in eq. **4.2** to estimate the, K_S. The $K_{\phi,s}$ parameter, calculated by equation **4.3**, permits accurate monitoring of changes in the solute's hydration layer, appears to be a more sensitive measure for measuring structural changes in solution than the V_ϕ parameter. We can find the numbers of $K_{\phi,s}$ in **Table 4.33** with uncertainty of $u(K_{\phi,S}) = 0.18 \times 10^6/(m^3.mol^{-1}.Gpa^{-1})$.

Notably, **Figure 4.27** consistently show negativity with respect to PEG molality in the aqueous Gluconolactone solution. The values of $K_{\phi,s}$ are decreasing with the content of polyethylene glycols as shown in **Figure 4.27**. Whereas, as the temperature rises the values of $K_{\phi,s}$ is increasing which means it is becoming less negative. Also, the values of $K_{\phi,s}$ are increasing with concentration. This effect shows that water near glycol's group of ions is less compressible than in more dilute solutions. Since the water molecules are now rearranged around the solute, its compressibility is diminished. The establishment of hydrogen bonds facilitates reorganization by reducing compressibility and creating dense arrangements between glycol and gluconolactone molecules. A further effect of increasing temperature is an upsurge in compressibility, since the regular distance amid molecules expands with increasing temperature. In addition, there are substantial solvent-molecule interactions because the glycols groups (-OH) of engage in dipole-dipole interactions with neighboring H_2O molecules. The results show that at various temperatures and concentrations of GLA, the compressibility behavior of glycol solutions is controlled by a web of molecular interactions. [18-22]

Table 4.33 v and $K_{\phi,S}$ of PEG-400 and PEG-4000 in water based Gluconolactone at pressure, p = 0.1 MPa.

[a]$m_A/(mol \cdot kg^{-1})$	$v/(m.s^{-1})$				$K_{\phi,S} \times 10^6/(m^3.mol^{-1}.Gpa^{-1})$			
	288.15K	298.15K	308.15K	318.15K	288.15K	298.15K	308.15K	318.15K
PEG-400 + 0.08 $mol \cdot kg^{-1}$ Gluconolactone								
0.00000	1472.24	1501.63	1524.06	1540.21				
0.01000	1474.27	1503.30	1525.69	1542.81	-41.62	-39.99	-38.79	-37.95
0.02002	1477.09	1505.73	1527.54	1544.86	-43.94	-42.22	-40.97	-40.10
0.02977	1479.56	1507.85	1529.34	1546.69	-44.71	-42.97	-41.70	-40.82
0.03992	1482.09	1509.99	1531.16	1548.52	-45.13	-43.37	-42.09	-41.20
0.05013	1484.46	1512.01	1532.87	1550.36	-45.39	-43.62	-42.33	-41.44
PEG-400 + 0.09 $mol \cdot kg^{-1}$ Gluconolactone								
0.00000	1472.82	1502.14	1524.50	1540.58				
0.00998	1474.98	1503.97	1526.06	1543.14	-41.59	-39.96	-38.77	-37.93
0.02009	1477.39	1506.01	1527.81	1545.43	-43.92	-42.20	-40.96	-40.09
0.02995	1479.80	1508.08	1529.56	1547.30	-44.69	-42.95	-41.68	-40.80
0.04016	1482.33	1510.22	1531.38	1549.25	-45.10	-43.34	-42.07	-41.18
0.05242	1485.20	1512.67	1533.45	1551.20	-45.40	-43.63	-42.34	-41.46
PEG-400 + 0.10 $mol \cdot kg^{-1}$ Gluconolactone								
0.00000	1473.09	1502.30	1524.65	1540.76				
0.00987	1475.71	1504.55	1526.61	1543.64	-41.53	-39.90	-38.71	-37.88
0.02019	1478.41	1506.83	1528.48	1545.87	-43.91	-42.21	-40.96	-40.09

0.03014	1480.85	1508.94	1530.28	1547.89	-44.68	-42.95	-41.68	-40.80
0.04022	1483.31	1511.11	1532.13	1549.76	-45.08	-43.33	-42.06	-41.17
0.05011	1485.45	1512.88	1533.65	1551.35	-45.33	-43.57	-42.28	-41.39
PEG-4000 + 0.08 $mol \cdot kg^{-1}$ Gluconolactone								
0.00000	1472.24	1501.63	1524.06	1540.21				
0.00998	1498.20	1523.74	1542.86	1560.03	-42.06	-40.39	-39.17	-38.33
0.01998	1521.45	1543.50	1562.47	1579.90	-44.60	-42.84	-41.58	-40.70
0.03000	1544.11	1562.63	1581.58	1599.29	-45.60	-43.81	-42.53	-41.64
0.03999	1564.91	1583.08	1603.06	1620.22	-46.20	-44.40	-43.10	-42.21
0.04999	1587.29	1602.77	1623.58	1640.95	-46.64	-44.82	-43.52	-42.63
PEG-4000 + 0.09 $mol \cdot kg^{-1}$ Gluconolactone								
0.00000	1472.82	1502.14	1524.50	1540.58				
0.01006	1502.17	1527.21	1545.83	1565.57	-42.09	-40.42	-39.20	-38.38
0.02001	1528.48	1548.88	1567.14	1586.11	-44.58	-42.83	-41.56	-40.70
0.02992	1549.11	1569.11	1587.61	1604.97	-45.56	-43.78	-42.50	-41.62
0.04002	1570.39	1588.69	1609.95	1626.50	-46.16	-44.36	-43.07	-42.18
0.05002	1590.56	1608.50	1631.80	1647.57	-46.59	-44.78	-43.48	-42.59
PEG-4000 + 0.10 $mol \cdot kg^{-1}$ Gluconolactone								
0.00000	1473.09	1502.30	1524.65	1540.76				
0.00996	1504.11	1529.09	1549.69	1569.42	-42.04	-40.38	-39.17	-38.34
0.01989	1532.02	1553.97	1574.03	1591.60	-44.56	-42.81	-41.55	-40.68

0.02986	1554.93	1576.17	1596.09	1614.07	-45.54	-43.77	-42.49	-41.61
0.03995	1575.44	1596.96	1618.50	1634.45	-46.13	-44.34	-43.06	-42.17
0.04969	1594.13	1615.28	1637.74	1653.83	-46.55	-44.74	-43.45	-42.56

(I)

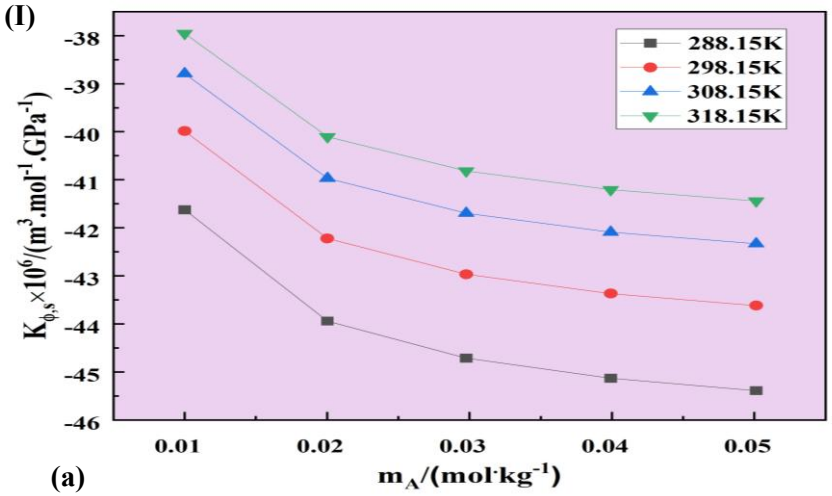
288.15K
298.15K
308.15K
318.15K
$K_{\phi,s}\times10^6/(m^3.mol^{-1}.GPa^{-1})$
$m_A/(mol\cdot kg^{-1})$

(a)

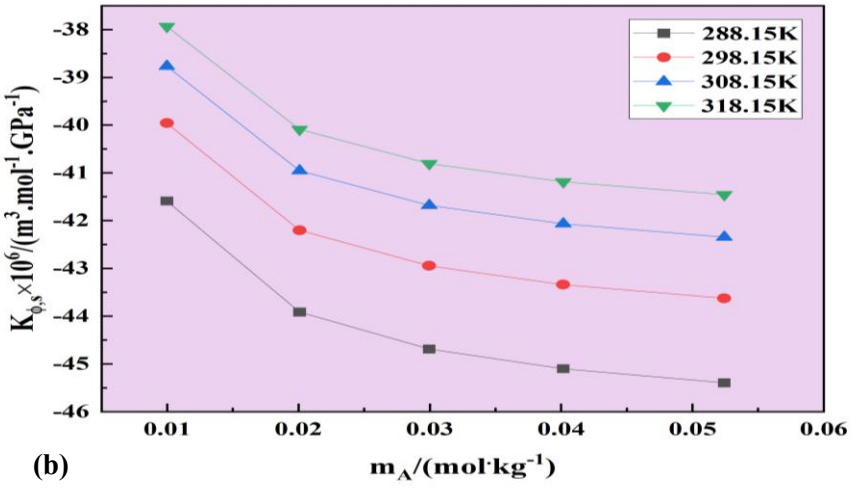
288.15K
298.15K
308.15K
318.15K
$K_{\phi,s}\times10^6/(m^3.mol^{-1}.GPa^{-1})$
$m_A/(mol\cdot kg^{-1})$

(b)

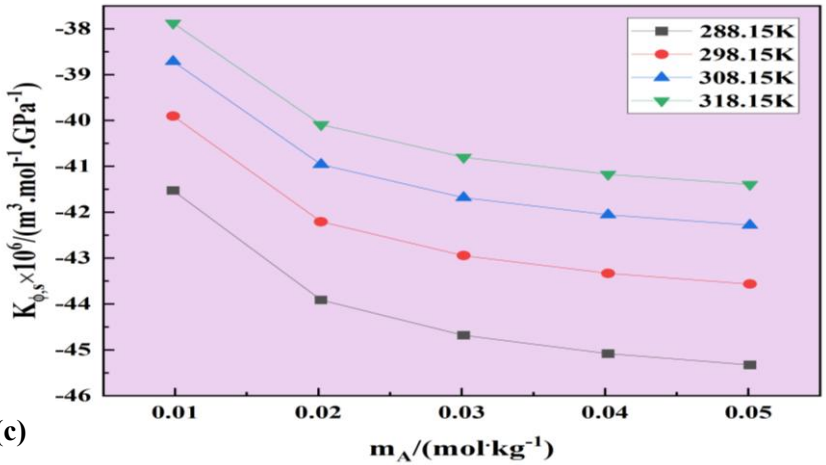
288.15K
298.15K
308.15K
318.15K
$K_{\phi,s}\times10^6/(m^3.mol^{-1}.GPa^{-1})$
$m_A/(mol\cdot kg^{-1})$

(c)

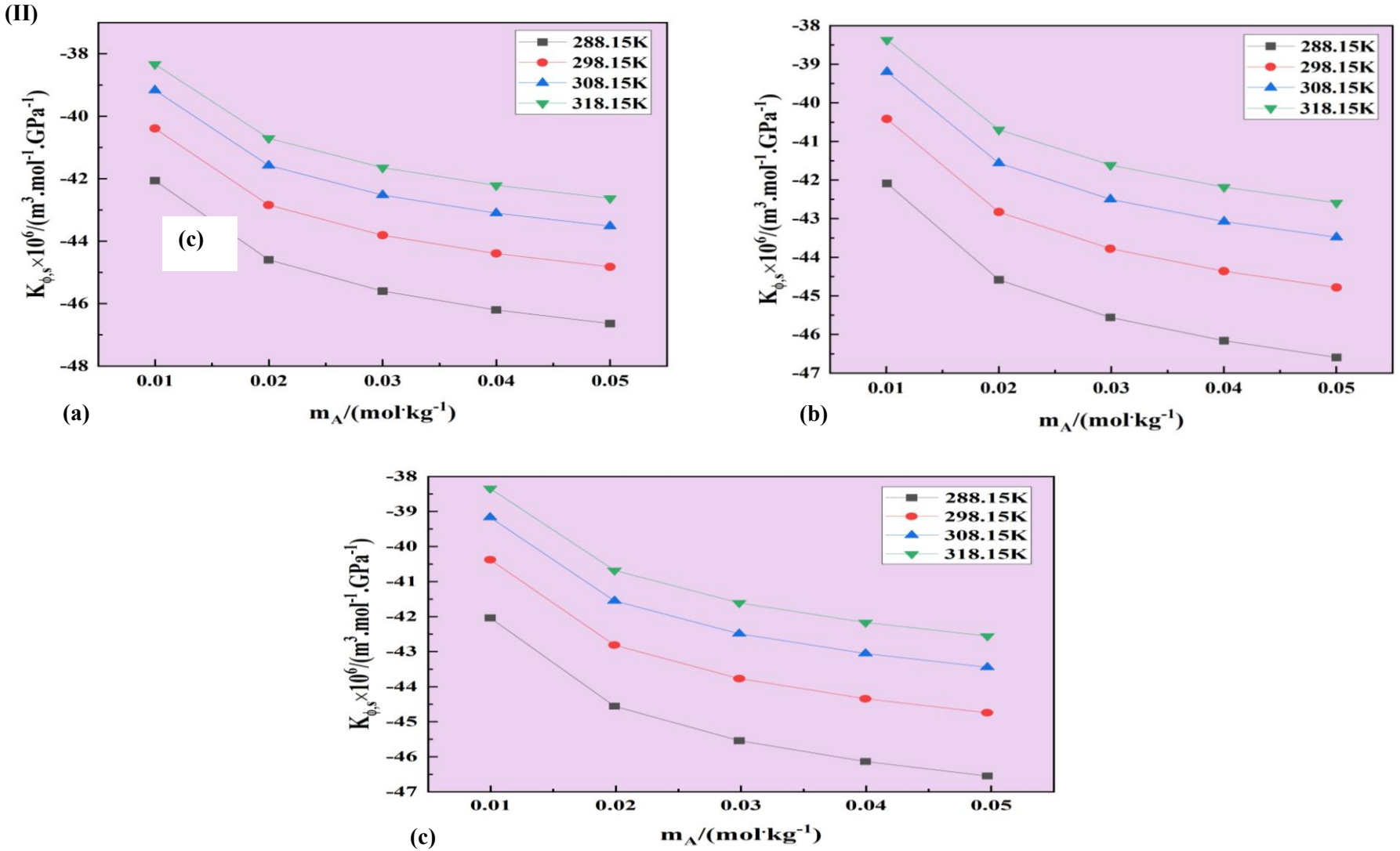

Figure 4.27 $K_{\phi,s}$, v/s molality, for (I) PEG-400 and (II) PEG-4000, (a) 0.08 Gluconolactone, (b) 0.09 Gluconolactone, (c) 0.10 Gluconolactone ($mol \cdot kg^{-1}$). (squares: $288.15K$, circles: $298.15K$, upward triangles: $308.15K$, and downward triangles: $318.15K$).

Partial molar isentropic compression ($K^{0}_{\phi,s}$)

The $K^{0}_{\phi,s}$ was calculated by the equation **4.5**, where S^{*}_{K} represents experimental slope. **Table 4.34** compiles the computed values and any associated uncertainty gained from least square fitting method with the uncertainty of $u(\kappa^{0}_{\phi,s}) = 0.38\times10^{6}/(m^{3}.mol^{-1}.Gpa^{-1})$ and $u(S^{*}_{K}) = 0.39\times10^{6}/(kg.m^{3}.mol^{-2}.Gpa^{-1})$. As illustrated in **Figure 4.28**, all $K^{0}_{\phi,s}$ values are negative and are increasing as temperature increases. However, there is no consistent trend with concentration. When the solution is endlessly diluted, the solute-solvent interactions become insignificant owing to their low magnitude, as demonstrated by the computed acoustic virial coefficient. The cohesive forces between solutes and water molecules are increased when the temperature upsurges because the negativity of $K^{0}_{\phi,s,}$ values decrease. Consistent with the concepts defined in Kirkwood's model, this mechanism encourages the displacement of water molecules in the bulk phase. Two major effects play a role in determining the main components of the partial molar isentropic compression $K^{0}_{\phi,s,}$. A rise in intermolecular free space causes the solution to be more compressible, which has a beneficial effect that is typically associated with the solvent's inherent compressibility. On the flip side, the detrimental impact of solvent diffusion happens when molecules of the solvent fill the empty spaces within ions as a result of interactions amongst the solute and the solvent. It might be deduced that the bonds among the solute molecules in the mixture are practically non-existent because the values of S^{*}_{K} are significantly smaller than the values of ($K^{0}_{\phi,s,}$). This suggests that the solute-solvent bonds inside the solution are more noticeable in the solution itself [23-26]

Table 4.34 $K^0_{\phi,S}$ and S^*_K, with standard deviations of PEG-400 and PEG-4000 in water based Gluconolactone.

[a]$m_B/(mol \cdot kg^{-1})$	$K^0_{\phi,S} \times 10^6/(m^3.mol^{-1}.Gpa^{-1})$				$S^*_K \times 10^6(kg.m^3.mol^{-2}.Gpa^{-1})$			
	$288.15K$	$298.15K$	$308.15K$	$318.15K$	$288.15K$	$298.15K$	$308.15K$	$318.15K$
PEG-400								
0.08	-41.56(±0.78)	-39.92(±0.75)	-38.73(±0.73)	-37.89(±0.72)	-86.9(±23.53)	-83.8(±22.70)	-81.7(±22.16)	-80.5(±21.83)
0.09	-41.72(±0.80)	-39.99(±0.77)	-38.79(±0.75)	-37.96(±0.74)	-82.6(±23.44)	-79.6(±22.62)	-77.6(±22.08)	-76.5(±21.78)
0.10	-41.47(±0.79)	-39.85(±0.77)	-38.66(±0.75)	-37.83(±0.74)	-87.5(±23.83)	-84.3(±23.02)	-82.2(±22.47)	-80.9(±22.16)
PEG-4000								
0.08	-41.79(±0.79)	-40.13(±0.76)	-38.91(±0.75)	-38.07(±0.74)	-107.5(±23.8)	-104.1(±23.0)	-102.3(±22.5)	-101.2(±22.2)
0.09	-41.82(±0.78)	-40.16(±0.75)	-38.94(±0.74)	-38.12(±0.73)	-105.9(±23.5)	-102.6(±22.7)	-100.8(±22.3)	-99.2(±21.9)
0.10	-41.78(±0.79)	-40.12(±0.76)	-38.92(±0.75)	-38.09(±0.73)	-106.5(±23.9)	-103.5(±22.1)	-101.1(±22.6)	-99.6(±22.2)

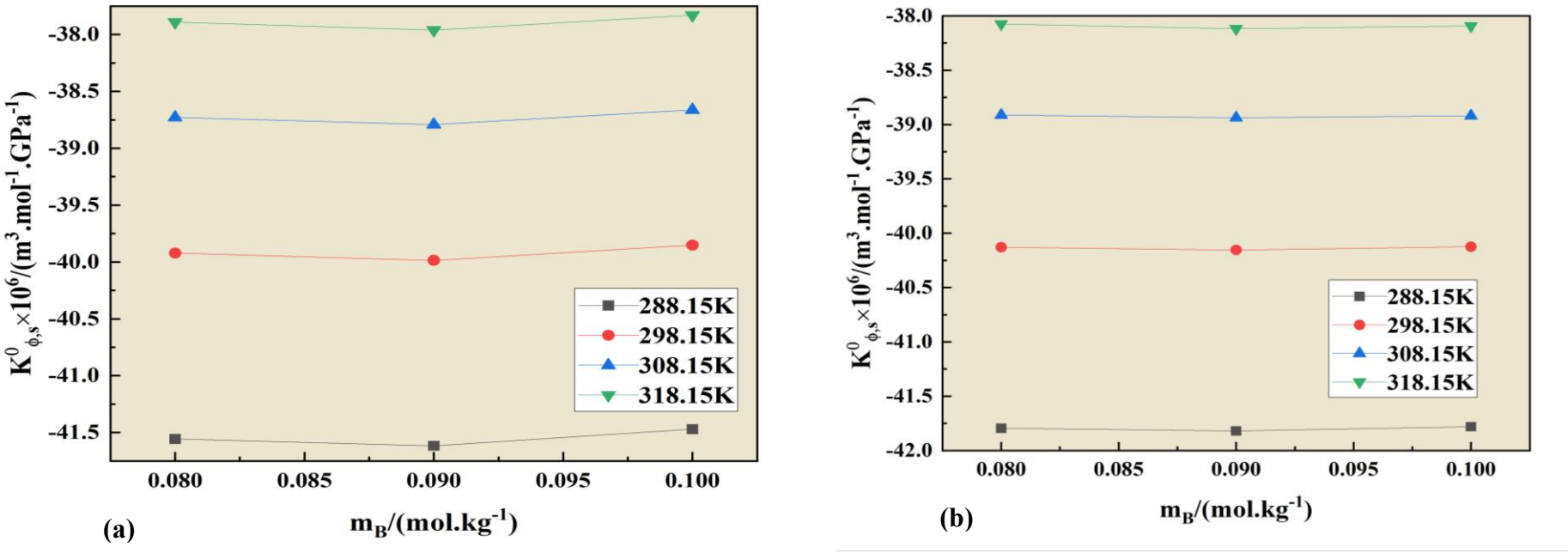

Figure 4.28 Graph showing how $K^0_{\phi,s}$ is changing with molality, for (a) PEG-400 and (b) PEG-4000 in Gluconolactone at various temperatures.

Transfer of Partial molar isentropic compression

The ΔK_ϕ^0 for PEGs in aqueous Gluconolactone was calculated using the **4.7** equation. **Table 4.35** presents the values of ΔK_ϕ^0 with uncertainty of $u\,(\Delta K_\phi^0) = 0.70 \times 10^6\,/(m^3.mol^{-1})$, which consistently show positive values for PEG-400 and negative values for PEG-4000. There is no trend with increase in concentrations. Values of ΔK_ϕ^0 are decreasing with increase in temperature. This observation can be elucidated by the model proposed by Krishnan and Friedman which describes the effects of volume expansion due to associations amid solute molecules. The ΔK_ϕ^0 suggest that volume expansion is occurring because of the displacement of water molecules at hydrophilic centers, indicating strong solute-solvent interactions [27-29].

Coefficients of interactions

To clarify the transfer characteristics of a solute in a water-based Gluconolactone solution, Friedman and Krishnan [30] revised the model of the hypothesis put forth by McMillian and Mayer [31]. They put out a procedure for finding the coefficients of interaction between solutes and co-solutes. According to their method, the equation **4.13** and **4.14** are the relationship between ΔV_ϕ^0, and ΔK_ϕ^0 of water to aqueous gluconolactone solution and Pair and triplet interaction coefficients**.** There, A- polyethylene glycols and B- co-solvent, Gluconolactone. See **Table 4.36** for the V_{AB} and V_{ABB}; $K_{AB} and\ K_{ABB}$- coefficients values. Coefficients of pair and triplet interactions are epitomized by V_{AB} and V_{ABB} ; $K_{AB} and\ K_{ABB}$. The Pair coefficients from both volume and adiabatic compressibility have majority of negative values for both PEGs and on the other hand the majority of values are positive for triplet coefficients of volume and adiabatic compressibility as observed from **Table 4.36**. So, the triplet wise interactions are more favorable. Also, the magnitude of triplet coefficients is much larger than the pair hence the triplet interactions are dominating in both the mixtures [32-33].

Table 4.35 $\Delta K_{\phi,s}^{0}$ of PEG-400/4000 in Gluconolactone at four temperatures.

$m_B/(mol \cdot kg^{-1})$	$\Delta K_{\phi}^{0} \times 10^{6}(m^{3}.mol^{-1})$			
	$288.15K$	$298.15K$	$308.15K$	$318.15K$
		PEG-400		
0.08	4.55	4.40	4.24	4.14
0.09	4.49	4.33	4.18	4.07
0.10	4.64	4.47	4.31	4.20
		PEG-4000		
0.08	-2.45	-2.35	-2.32	-2.33
0.09	-2.48	-2.38	-2.35	-2.38
0.10	-2.44	-2.34	-2.33	-2.35

Table 4.36 Pair (V_{AB}, K_{AB}) and triplet (V_{ABB}, K_{ABB}) interaction coefficients of PEGs in aqueous Gluconolactone.

$T/(K)$	$V_{AB} \times 10^6$ $(m^3.mol^{-2}.kg)$	$V_{ABB} \times 10^6$ $(m^3.mol^{-3}.kg^2)$	$K_{AB} \times 10^6$ $(m^3.mol^{-2}.kg.GPa^{-1})$	$K_{ABB} \times 10^6$ $(m^3.mol^{-3}.kg^2.GPa^{-1})$
		PEG-400		
$288.15K$	-60.936	303.470	48.648	-171.209
$298.15K$	-28.095	219.577	47.209	-167.267
$308.15K$	-42.182	447.077	45.584	-161.757
$318.15K$	-32.869	468.361	44.495	-158.090
		PEG-4000		
$288.15K$	-5.626	178.427	-27.895	104.603
$298.15K$	-20.487	344.667	-26.524	98.686
$308.15K$	-69.829	741.670	-25.954	95.458
$318.15K$	-100.115	1012.976	-25.890	94.075

Conclusion

In the current work, volumetric and acoustic studies of PEGs (400/4000) in Gluconolactone water-based solutions are provided. The experiments were conducted at different concentrations (0.08, 0.09, and 0.10 $mol \cdot kg^{-1}$) and temperature range of $288.15K \ to \ 318.15K$. The results discovered that an increase in both T and Gluconolactone composition (m_B) led to greater solute-solvent interactions. Density measurements are beneficial for the computation of both V_ϕ and V_ϕ^0, respectively. In corresponding, experimental data of v allowed for the determination of acoustic numbers such as $K_{\phi,s,}^0$ and $K_{\phi,s}^0$, respectively. The study found that $(\partial E_\phi^0/\partial T)_p$ provided understanding of system's capacity to form and breakdown the arrangements and indicating that the liquid system exhibited strong solute-solvent interactions. These interactions were further evidenced by the analysis of transfer characteristics (ΔV_ϕ^0 and $\Delta K_{\phi,S}^0$), which suggested that hydrophilic-hydrophilic interactions dominated within the mixture. Additionally, it was noted that the ternary mixture demonstrated greater compressibility compared to its pure components, with all $K_{\phi,s}^0$ values being negative. These findings have important implications for understanding the behaviours of such ternary systems.

Problem-6

Exegesis of molecular interactions of mixes comprising Polyethylene glycol-4000 and Polyhydroxy acids (PHAs) with spectroscopic analysis

Densities and Sound velocities

The numerous thermodynamic and acoustic properties are explored via measured data of Density and ultrasonic velocity in the mixture by experimentation. **Table 4.37** displays the findings of a study that examined the density (ρ) and sound's velocity (v) of PHAs (gluconolactone, galactose, and LBA) in several combinations with aqueous solutions glycol-PEG-4000 at various temperatures. The quantities of the substances were altered between 0.05 and 0.07 $mol.kg^{-1}$ of PHAs. The general uncertainties are as follows: $u(T) = 0.001K, u(m) = 1\%, u(V_\phi) = \pm(0.05 - 0.07) \times 10^6/(m^3 \cdot mol^{-1})$, and $u(K_{\phi,s}) = \pm 0.25 \times 10^6/(m^3 \cdot mol^{-1} \cdot GPa^{-1})$. Density vs. molality for various Polyhydroxyacids (PHAs: Gluconolactone, Lactobionic acid and galactose) and PEG-4000 combinations for diverse temperatures are shown in **Figure 4.29**. The outcomes shown that density drops with rising temperature and density climbs with rising molality. The densities of gluconolactone and lactobionic acid with water that were obtained at all temperatures agree with the known data of the liquid combination [1, 34] as shown in **Figure 4.30**. This consensus lends credence to the idea that the two datasets are nearly indistinguishable. When it comes to understanding how ions, solutes, and solvents interact with one another, the data on sound speeds is invaluable [35]. At an unchanged pressure, as documented in **Table 4.37**, the ultrasonic velocity grows with increasing molality of PHAs, as long as the concentration of PHAs stays the same. 3D H-bond networks between solvent and solute molecules might be one reason why the sound speed data upsurges when the solute molality does [36-38]. Water and PEG-4000's density, sound speed and other statistics were culled from the reference [15] denoted as subscript [b] in the **Table 4.37**.

Table 4.37

Values of (V_ϕ) and ($K_{\phi,s}$) corresponding to particular density and velocity values at different temperatures and concentration combination of PHAs (gluconolactone, galactose, and LBA) in water with PEG 4000.

T/K	$^{a}m_A$/ $(mol.kg^{-1})$	$\rho \times 10^{-3}$/ $(kg.m^{-3})$	$V_\phi \times 10^{6}$/ $(m^{-3}.mol^{-1})$	v/ $(m.s^{-1})$	$K_{\phi,s} \times 10^{15}$/ $(m^{3}.mol^{-1}.Pa^{-1})$
		0.00 $mol.kg^{-1}$ gluconolactone + PEG-4000			
288.15	0.00000 [b]	0.999528 [b]		1466.89 [b]	
	0.00979 [b]	1.006162 [b]	3301.97 [b]	1490.78 [b]	-42.24 [b]
	0.01995 [b]	1.012565 [b]	3304.65 [b]	1521.5 [b]	-44.97 [b]
	0.02996 [b]	1.018438 [b]	3307.57 [b]	1545.14 [b]	-46.00 [b]
	0.04002 [b]	1.023918 [b]	3311.08 [b]	1570.75 [b]	-46.64 [b]
	0.05000 [b]	1.028995 [b]	3314.30 [b]	1591.28 [b]	-47.10 [b]
298.15	0.00000 [b]	0.997479 [b]		1496.82 [b]	
	0.00979 [b]	1.004137 [b]	3304.75 [b]	1517.44 [b]	-40.53 [b]
	0.01995 [b]	1.010561 [b]	3307.66 [b]	1543.27 [b]	-43.16 [b]
	0.02996 [b]	1.016449 [b]	3310.76 [b]	1563.19 [b]	-44.16 [b]
	0.04002 [b]	1.021957 [b]	3314.05 [b]	1584.69 [b]	-44.78 [b]
	0.05000 [b]	1.027049 [b]	3317.40 [b]	1603.27 [b]	-45.22 [b]
308.15	0.00000 [b]	[b]0.994467 [b]		1519.79 [b]	
	0.00979 [b]	1.001167 [b]	3308.23 [b]	1537.22 [b]	-39.28 [b]
	0.01995 [b]	1.007620 [b]	3311.75 [b]	1558.99 [b]	-41.84 [b]
	0.02996 [b]	1.013541 [b]	3314.92 [b]	1575.71 [b]	-42.82 [b]
	0.04002 [b]	1.019083 [b]	3318.18 [b]	1593.58 [b]	-43.42 [b]
	0.05000 [b]	1.024200 [b]	3321.67 [b]	1611.93 [b]	-43.86 [b]
318.15	0.00000 [b]	[b]0.990646 [b]		1536.39 [b]	
	0.00979 [b]	0.997408 [b]	3311.65 [b]	1551.1 [b]	-38.39 [b]
	0.01995 [b]	1.003920 [b]	3315.35 [b]	1569.18 [b]	-40.91 [b]
	0.02996 [b]	1.009896 [b]	3318.58 [b]	1583.08 [b]	-41.88 [b]
	0.04002 [b]	1.015490 [b]	3321.90 [b]	1597.79 [b]	-42.48 [b]
	0.05000 [b]	1.020664 [b]	3325.29 [b]	1615.05 [b]	-42.91 [b]
		0.05 $mol.kg^{-1}$ gluconolactoe + PEG-4000			
288.15	0.00000	1.00296		1470.28	

	0.010021	1.00965	3303.17	1494.69	-42.19
	0.020257	1.01598	3306.63	1523.03	-44.80
	0.030274	1.02171	3310.69	1550.18	-45.81
	0.040032	1.02690	3314.78	1575.32	-46.41
	0.050013	1.03187	3318.06	1599.87	-46.86
298.15	0.00000	1.00085		1499.76	
	0.010021	1.00754	3307.46	1521.69	-40.51
	0.020257	1.01388	3311.14	1547.06	-43.03
	0.030274	1.01962	3315.44	1567.39	-44.00
	0.040032	1.02481	3319.72	1588.06	-44.58
	0.050013	1.02979	3322.87	1606.84	-45.01
308.15	0.00000	0.997793		1522.33	
	0.010021	1.00453	3310.86	1540.15	-39.27
	0.020257	1.01090	3315.18	1562.9	-41.74
	0.030274	1.01667	3319.58	1581.1	-42.69
	0.040032	1.02189	3323.91	1596.6	-43.25
	0.050013	1.02691	3326.98	1614.06	-43.68
318.15	0.00000	0.993945		1538.6	
	0.010021	1.00074	3315.02	1553.63	-38.40
	0.020257	1.00716	3320.07	1571.67	-40.83
	0.030274	1.01297	3324.55	1587.8	-41.77
	0.040032	1.01825	3328.39	1601	-42.34
	0.050013	1.02327	3332.52	1618.81	-42.76
		0.07 $mol.kg^{-1}$gluconolactone + PEG-4000			
288.15	0.00000	1.004493		1471.18	
	0.010006	1.01107	3308.67	1496.96	-42.14
	0.020017	1.01722	3310.31	1525.34	-44.71
	0.030023	1.02292	3313.22	1555.44	-45.73
	0.04007	1.02818	3317.87	1579.09	-46.35
	0.050069	1.03307	3321.90	1603.67	-46.79
298.15	0.00000	1.002372		1500.61	
	0.010006	1.00893	3316.96	1525.87	-40.48
	0.020017	1.01504	3318.57	1549.78	-42.95

	0.030023	1.02071	3321.80	1571.95	-43.93
	0.04007	1.02599	3325.59	1591.09	-44.52
	0.050069	1.03090	3328.64	1610.11	-44.95
308.15	0.00000	0.999321		1523.14	
	0.010006	1.00589	3323.09	1543.25	-39.24
	0.020017	1.01203	3324.80	1565.56	-41.66
	0.030023	1.01772	3327.92	1583.97	-42.62
	0.04007	1.02305	3330.66	1598.87	-43.19
	0.050069	1.02798	3333.95	1617.86	-43.62
318.15	0.00000	0.995496		1539.4	
	0.010006	1.00212	3327.80	1556.65	-38.37
	0.020017	1.00831	3329.32	1574.34	-40.76
	0.030023	1.01405	3332.57	1589.91	-41.70
	0.04007	1.01940	3335.92	1604.01	-42.28
	0.050069	1.02436	3339.62	1622.2	-42.70
		0.05 $mol.kg^{-1}$ Galactose + PEG-4000			
288.15	0.00000	1.00274		1470.2	
	0.010002	1.00933	3312.04	1496.76	-42.19
	0.020008	1.01544	3315.94	1524.34	-44.76
	0.03001	1.02113	3318.82	1549.17	-45.78
	0.040003	1.02641	3322.06	1574.45	-46.40
	0.050054	1.03135	3325.66	1595.85	-46.85
298.15	0.00000	1.00064		1500	
	0.010002	1.00721	3319.82	1522.6	-40.48
	0.020008	1.01330	3323.45	1547.67	-42.97
	0.03001	1.01894	3327.44	1567.88	-43.95
	0.040003	1.02419	3331.17	1588.36	-44.55
	0.050054	1.02908	3335.24	1607.36	-44.98
308.15	0.00000	0.997592		1522.6	
	0.010002	1.00418	3326.03	1542.08	-39.25
	0.020008	1.01030	3329.00	1562.47	-41.68
	0.03001	1.01597	3332.76	1578.92	-42.63
	0.040003	1.02124	3336.67	1596.79	-43.22

	0.050054	1.02619	3339.92	1615.12	-43.64
318.15	0.00000	0.993737		1538.96	
	0.010002	1.00036	3332.22	1555.28	-38.37
	0.020008	1.00652	3335.28	1572.455	-40.77
	0.03001	1.01225	3338.27	1586.76	-41.72
	0.040003	1.01757	3341.79	1600.69	-42.29
	0.050054	1.02255	3345.29	1618.44	-42.72
		0.07 $mol.kg^{-1}$Galactose + PEG-4000			
288.15	0.00000	1.004146		1471.91	
	0.00999	1.01065	3316.29	1499.97	-42.10
	0.020017	1.01671	3319.40	1526.79	-44.66
	0.029994	1.02230	3323.03	1552.94	-45.67
	0.039883	1.02745	3326.86	1577.68	-46.27
	0.049927	1.03237	3329.31	1598.08	-46.72
298.15	0.00000	1.002022		1501.4	
	0.00999	1.00850	3324.73	1525.82	-40.42
	0.020017	1.01453	3328.13	1549.9	-42.89
	0.029994	1.02009	3332.03	1569.82	-43.86
	0.039883	1.02520	3335.89	1590.78	-44.45
	0.049927	1.03009	3338.53	1609.1	-44.88
308.15	0.00000	0.99895		1523.95	
	0.00999	1.00544	3331.40	1545.16	-39.19
	0.020017	1.01148	3334.99	1565.56	-41.61
	0.029994	1.01707	3338.32	1582.16	-42.55
	0.039883	1.02219	3342.39	1599.609	-43.12
	0.049927	1.02708	3345.45	1618.47	-43.55
318.15	0.00000	0.995077		1540.2	
	0.00999	1.00161	3337.88	1558.53	-38.32
	0.020017	1.00769	3341.22	1575.72	-40.71
	0.029994	1.01330	3344.89	1589.38	-41.64
	0.039883	1.01846	3348.86	1603.3	-42.20
	0.049927	1.02337	3352.07	1620.46	-42.62
		0.05 $mol.kg^{-1}$ LBA + PEG-4000			

288.15	0.00000	1.006448		1471.85	
	0.010013	1.01286	3320.64	1497.98	-42.12
	0.020002	1.01878	3324.75	1523.79	-44.65
	0.030026	1.02430	3328.49	1548.82	-45.66
	0.040037	1.02943	3331.59	1573.45	-46.26
	0.050184	1.03424	3335.56	1594.64	-46.70
298.15	0.00000	1.004301		1501.38	
	0.010013	1.01072	3326.44	1523.67	-40.43
	0.020002	1.01663	3330.75	1545.56	-42.88
	0.030026	1.02212	3335.30	1566.67	-43.85
	0.040037	1.02724	3338.67	1587.53	-44.44
	0.050184	1.03206	3341.98	1606.86	-44.86
308.15	0.00000	1.001207		1523.91	
	0.010013	1.00763	3333.52	1542.85	-39.20
	0.020002	1.01357	3337.10	1563.23	-41.60
	0.030026	1.01909	3341.25	1579	-42.54
	0.040037	1.02423	3344.68	1596.97	-43.12
	0.050184	1.02908	3347.88	1614.42	-43.54
318.15	0.00000	0.997322		1540.12	
	0.010013	1.00378	3340.91	1556.08	-38.34
	0.020002	1.00974	3344.83	1573.46	-40.70
	0.030026	1.01531	3348.15	1587.21	-41.64
	0.040037	1.02046	3351.93	1603.45	-42.20
	0.050184	1.02537	3354.41	1618.59	-42.62
		0.07 $mol.kg^{-1}$ LBA + PEG-4000			
288.15	0.00000	1.008987		1473.4	
	0.010017	1.015319	3322.60	1503.17	-42.07
	0.02001	1.021169	3326.23	1526.5	-44.56
	0.030014	1.026589	3330.23	1552.65	-45.56
	0.040035	1.031605	3334.68	1575.4	-46.15
	0.050248	1.036384	3338.17	1598.52	-46.59
298.15	0.00000	1.006813		1502.76	
	0.010017	1.013113	3331.60	1528.23	-40.39

	0.02001	1.018934	3335.21	1548.67	-42.81
	0.030014	1.024324	3339.31	1569.49	-43.76
	0.040035	1.029343	3342.97	1589.23	-44.34
	0.050248	1.034096	3346.60	1609.76	-44.76
308.15	0.00000	1.003723		1525.17	
	0.010017	1.010038	3338.41	1546.87	-39.17
	0.02001	1.015888	3341.21	1567.43	-41.54
	0.030014	1.021321	3344.52	1583.79	-42.47
	0.040035	1.026349	3348.72	1599.56	-43.03
	0.050248	1.031116	3352.54	1618.44	-43.45
318.15	0.00000	0.99984		1541.31	
	0.010017	1.006187	3345.55	1559.59	-38.31
	0.02001	1.012054	3349.11	1576.4	-40.64
	0.030014	1.017508	3352.55	1590.99	-41.57
	0.040035	1.022595	3355.73	1607.3	-42.13
	0.050248	1.027408	3359.21	1621.84	-42.54

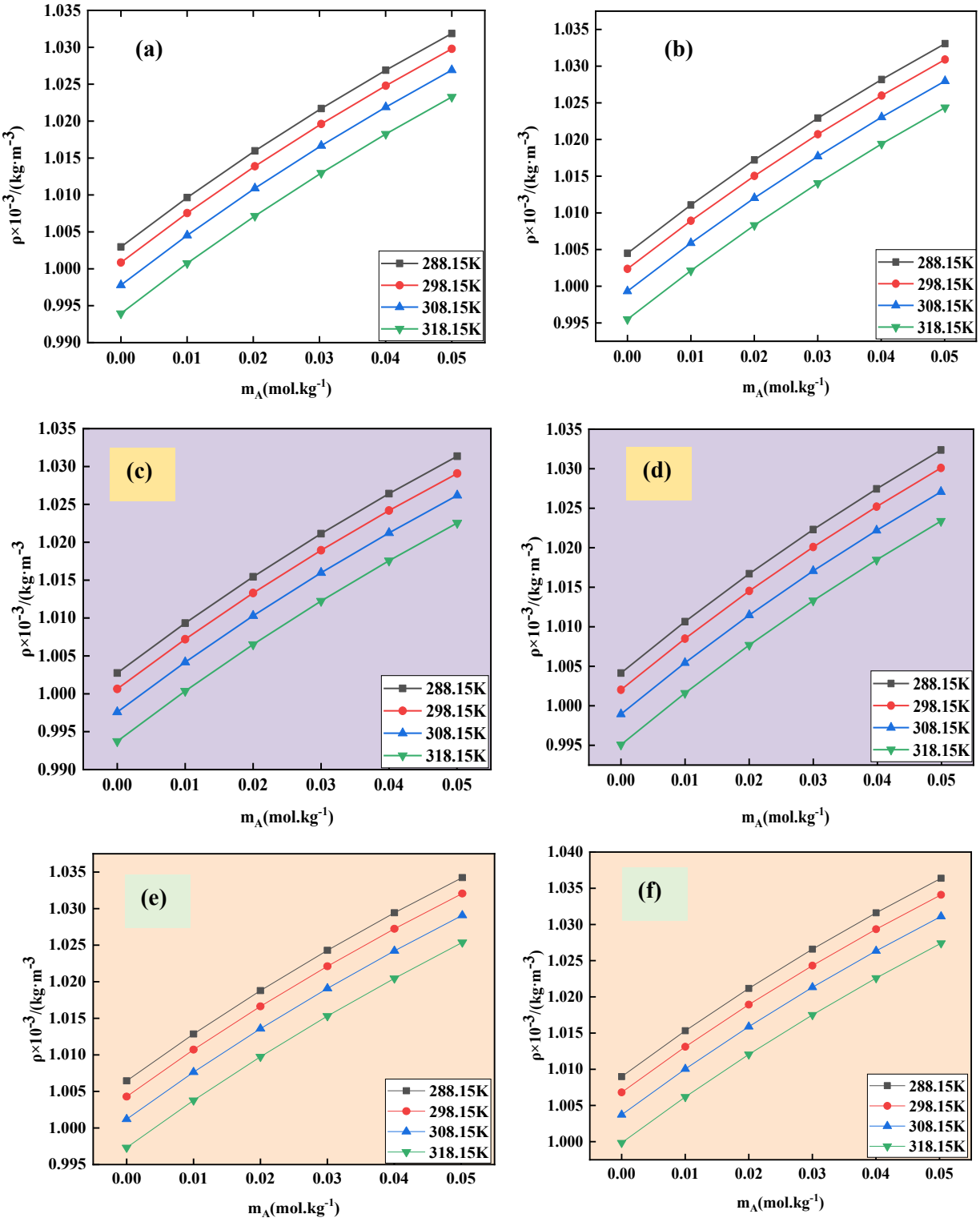

Figure 4.29 Graph showing how the density changes with molality of the water created PHAs with PEG-4000 at diverse temperatures and fixed atmospheric pressure, (a) 0.05 Gluconolactone with PEG-4000; (b) 0.07 Gluconolactone with PEG-4000; (c) 0.05 Galactose with PEG-4000; (d) 0.07 Galactose with PEG-4000; (e) 0.05 LBA with PEG-4000 and (f) 0.07 LBA with PEG-4000.

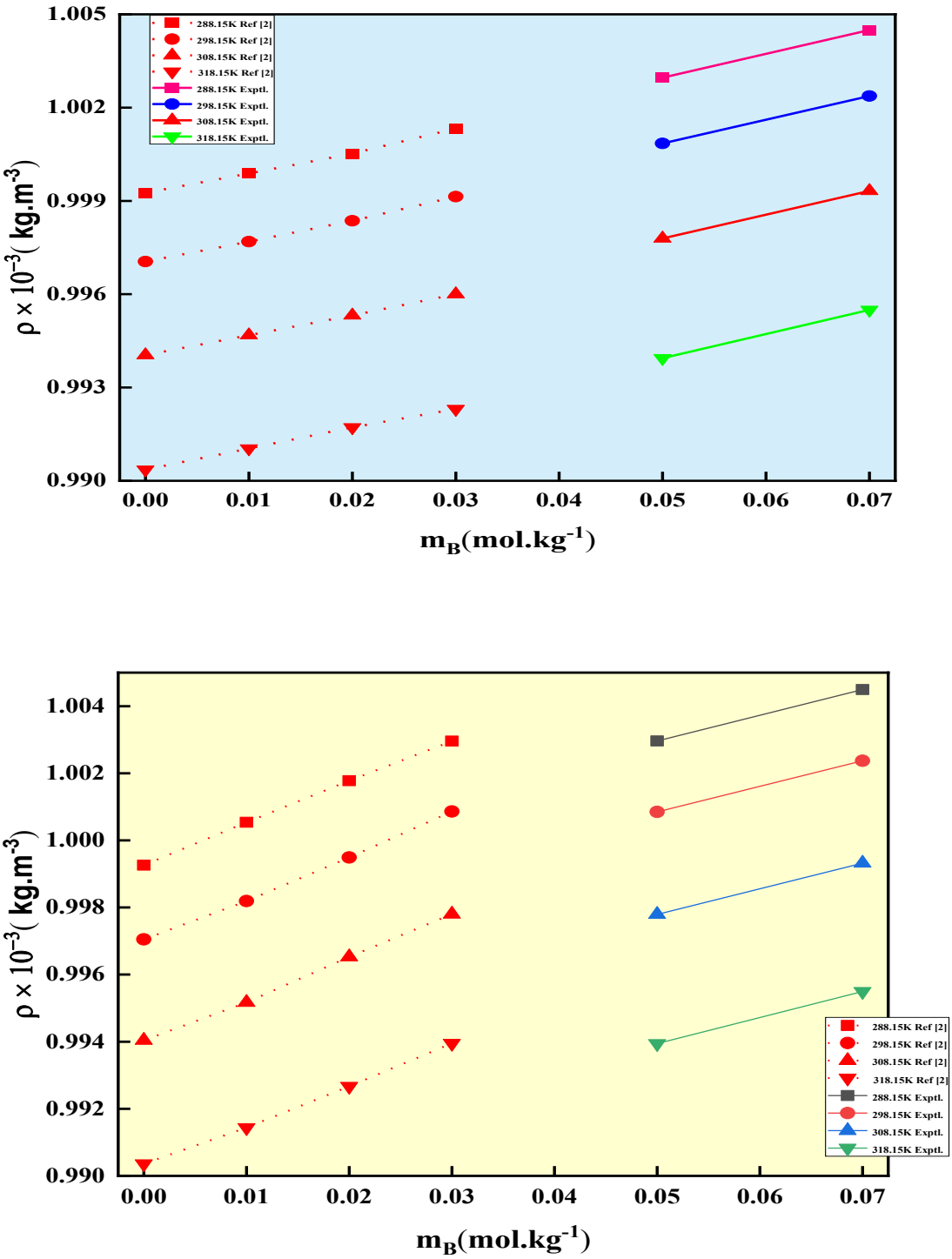

Figure 4.30 Density plot displaying literature and experimental data for a mixture of (a) aqueous Gluconolactone and (b) aqueous LBA at various temperatures referenced in [1,34] respectively.

Apparent Molar Properties:

Apparent Molar Volume

The density calculated by Anton Paar DSA 5000M is utilised to determine V_ϕ [39], by by means of the equation **(4.1).** Results for apparent molar volumes derived from density experiments are shown in **Table 4.37**. V_ϕ in ternary mixtures grow with temperature and PHAs content, according to the computed data. **Figure 4.31** provides a clear 2D visual depiction of the liquid system. Current liquid mixtures may exhibit high solute-solvent interactions, as shown by the large intrinsic volume of the solute, if all computed apparent molar volumes are positive. What happens inside a solution between a solute and a solvent may be learned from a lot of experience. **Figure 4.32** shows the growing molecular interaction between the PHAs and PEG-4000 and shows that it is actually growing the trend in the increasing order from Gluconolactone, galactose, and the lactobionic acid. The electrostrictive impact of water molecules decreases with increasing concentration due to connections among the particles, causing to a rise in V_ϕ. Some physical mechanisms, such as relations among dipoles, the water attracting effect, and dipole-induced-dipole connections, might be responsible for an increase in V_ϕ values in the water-rich area. The composition's molecular interactions are explained by the robust linear relationship with V_ϕ values and temperature, as well as by the molality of polyethylene glycol, which is a result of solvation and its high attraction in the solvent. Hydrophobic hydration, the hydrophobic effect, interparticle H-bonding, interactions amongst the dipoles are all established when water is present.

Low V_ϕ values indicate effective hydration of solute molecules, as hydrogen bonding in water promotes tighter molecular packing. Conversely, substantial solute-co-solute interactions are indicated by high V_ϕ values. [4-40]

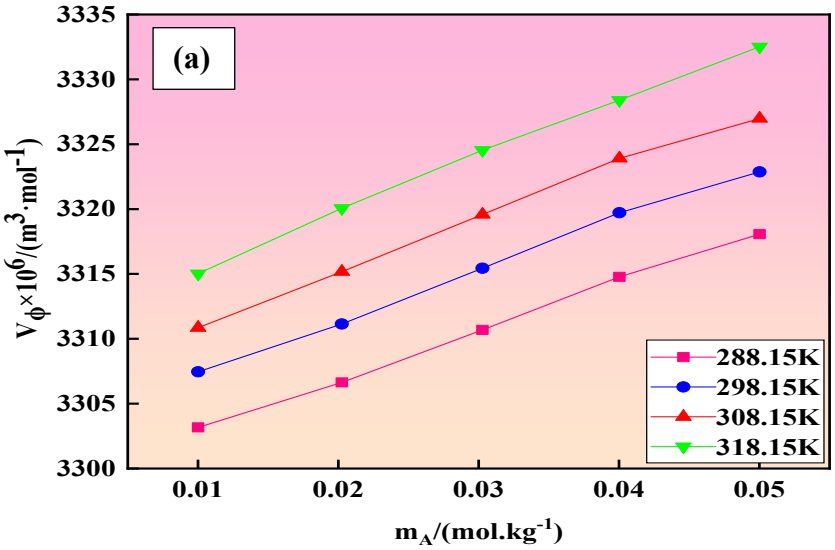
(a)
3335
3330
3325
3320
3315
3310
3305
3300
0.01
0.02
0.03
0.04
0.05
$V_\phi \times 10^6/(m^3 \cdot mol^{-1})$
$m_A/(mol.kg^{-1})$
288.15K
298.15K
308.15K
318.15K

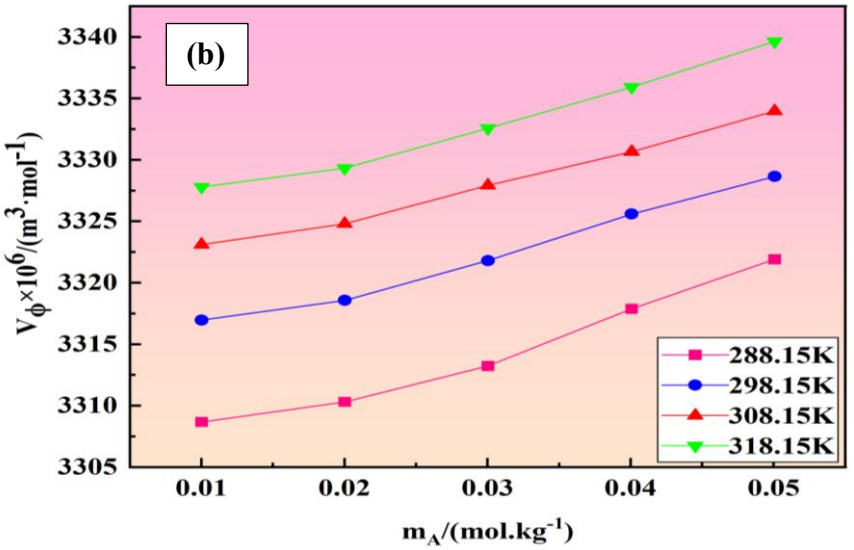
(b)
3340
3335
3330
3325
3320
3315
3310
3305
0.01
0.02
0.03
0.04
0.05
$V_\phi \times 10^6/(m^3 \cdot mol^{-1})$
$m_A/(mol.kg^{-1})$
288.15K
298.15K
308.15K
318.15K

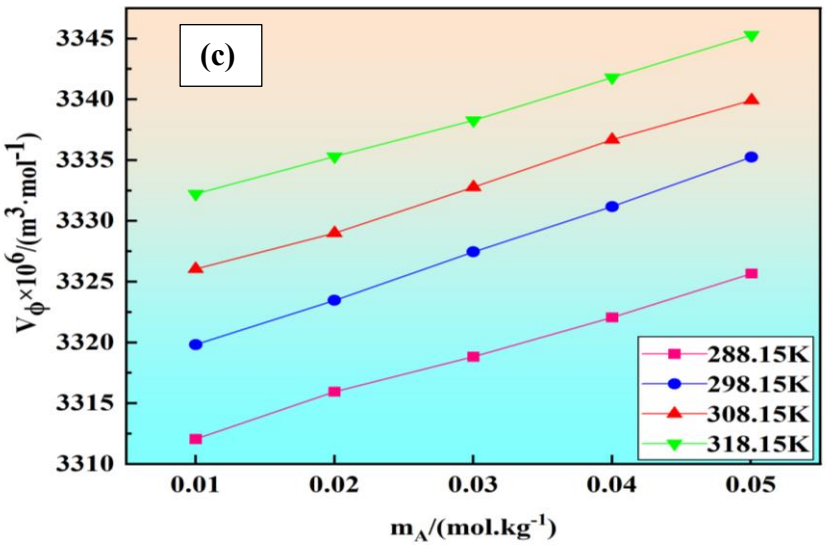
(c)
3345
3340
3335
3330
3325
3320
3315
3310
0.01
0.02
0.03
0.04
0.05
$V_\phi \times 10^6/(m^3 \cdot mol^{-1})$
$m_A/(mol.kg^{-1})$
288.15K
298.15K
308.15K
318.15K

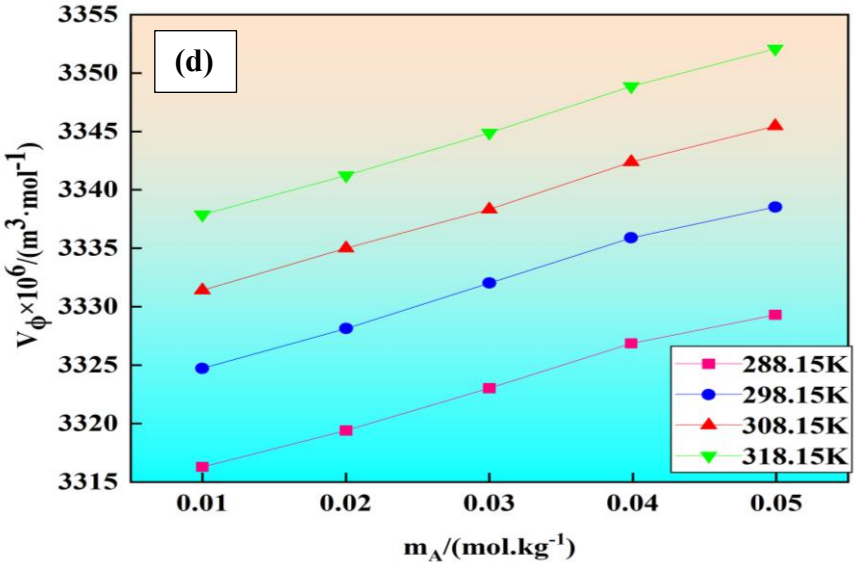
(d)
3355
3350
3345
3340
3335
3330
3325
3320
3315
0.01
0.02
0.03
0.04
0.05
$V_\phi \times 10^6/(m^3 \cdot mol^{-1})$
$m_A/(mol.kg^{-1})$
288.15K
298.15K
308.15K
318.15K

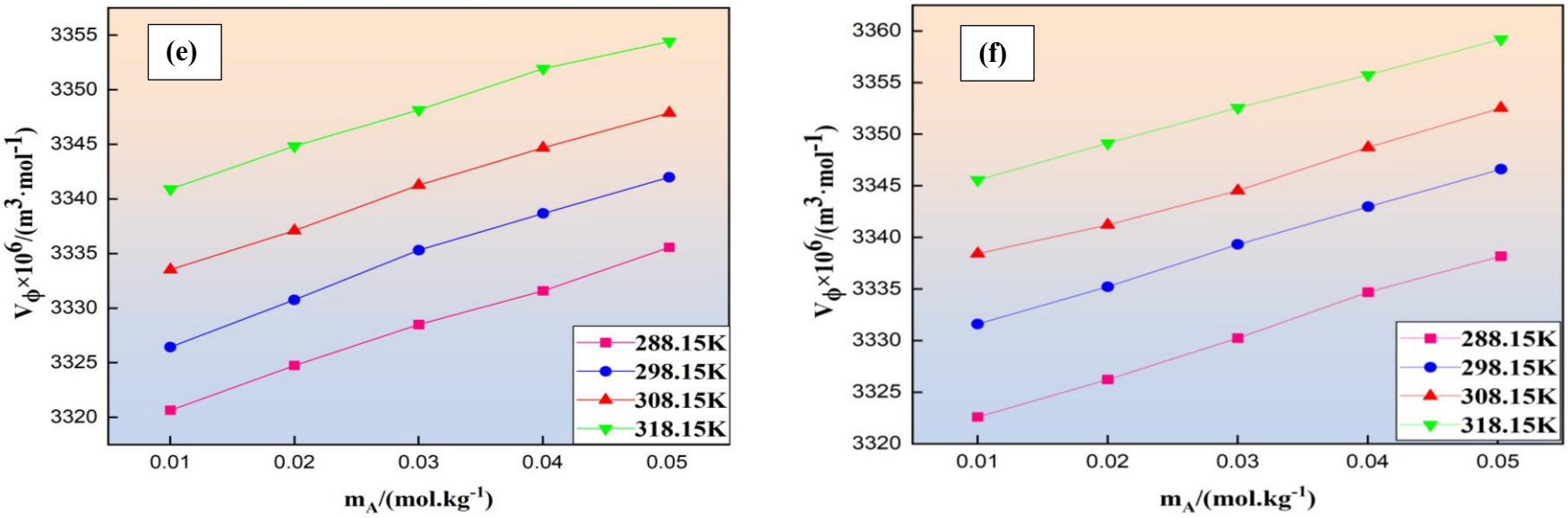

Figure 4.31 2-D plots showing the changes in the V_ϕ at diverse concentrations of PHAs and PEG-4000 with respect to molality at different temperatures. The plots are labelled as ((a) 0.05 and (b) 0.07 $mol.kg^{-1}$ gluconolactone, (c) 0.05 and (d) 0.07 $mol.kg^{-1}$ galactose, (e) 0.05 and (f) 0.07 $mol.kg^{-1}$ LBA) with PEG-4000.

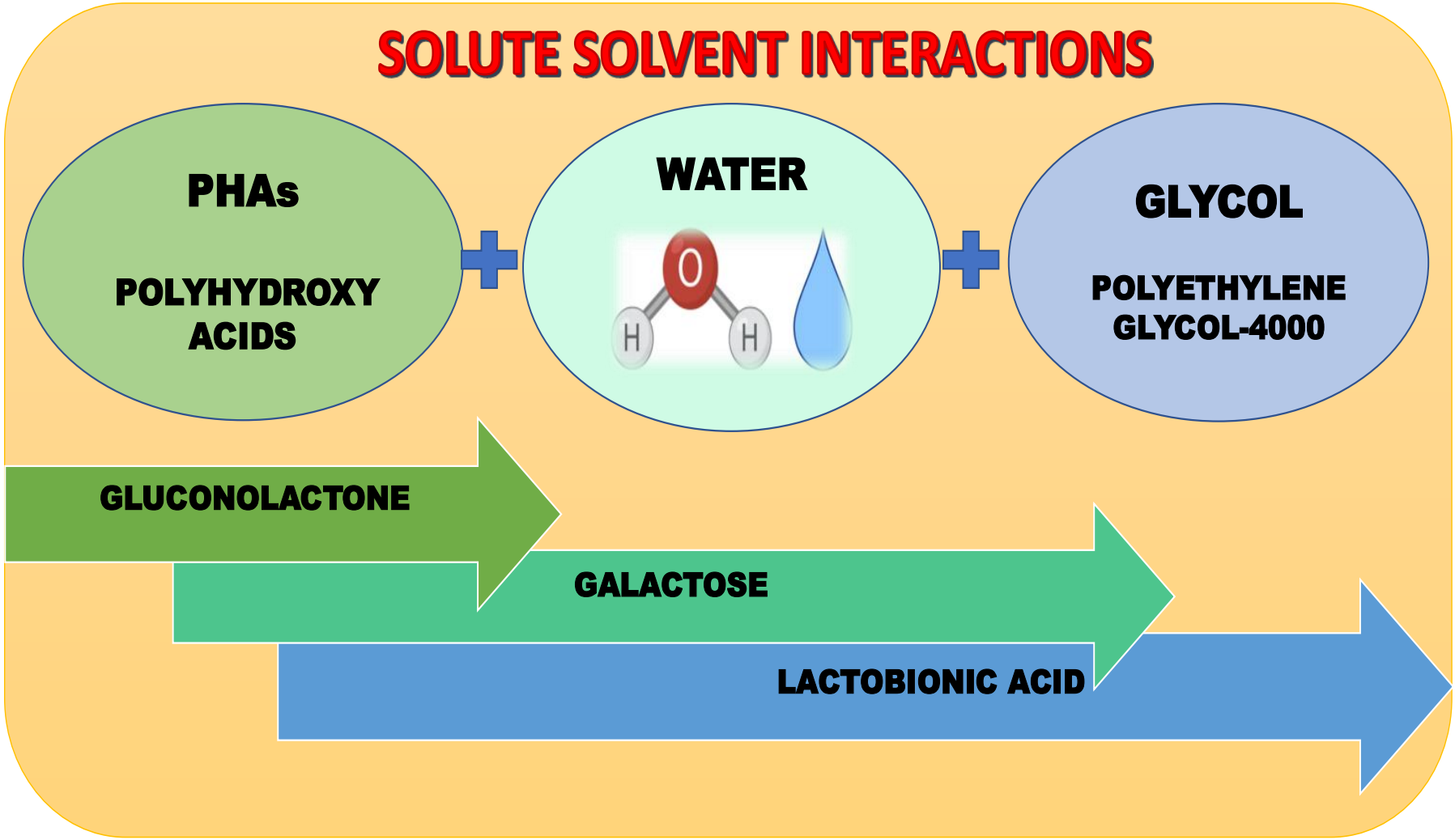

Figure 4.32 Trend of Molecular interactions amongst PHAs.

Apparent molar Isentropic compressibility

The isentropic compressibility, k_s may be calculated using the equation **4.2** stated as Laplace-Newton formula. Using that we have determined the data of $K_{\phi,s}$ of PHAs aqueous solutions containing polyethylene glycol 4000 Symbols are being used in equation **4.3** with their normal notations. **Figure 4.33** exhibits the calculated $K_{\phi,s}$ for different temperatures and concentrations of glycol 4000 in gluconolactone, galactose, and LBA aqueous solutions versus molality, while **Table 4.37** demonstrate all negative $K_{\phi,s}$ numbers which is dropping as the T is rising and shows an upsurge with the surge of PHA's composition. Glycol and ion charges fully compress water molecules, while PEG 4000 and ions remain unaffected by pressure. The negative $K_{\phi,s}$ indicates that H_2O near glycol's ionic groups is less squeezable than in more dilute solutions. This suggests that compression in the solution mainly occurs through pressure acting on bulk water molecules. Because PEG-4000 and PHA ions form strong solute-solvent interactions [41]. Thermal agitation, which increases the solvent's volume and compressibility, removes the solute molecules from the solvent, which also explains these negative results. In addition, the solute's hydration shells (PEG-4000) and the solvent molecules (PHAs) both impact the observed behaviour of $K_{\phi,s}$ values. Solutions of PEG-4000 and PHAs can build more compact structures, which lowers their compressibility, by forming intermolecular hydrogen bonds. [23, 42]

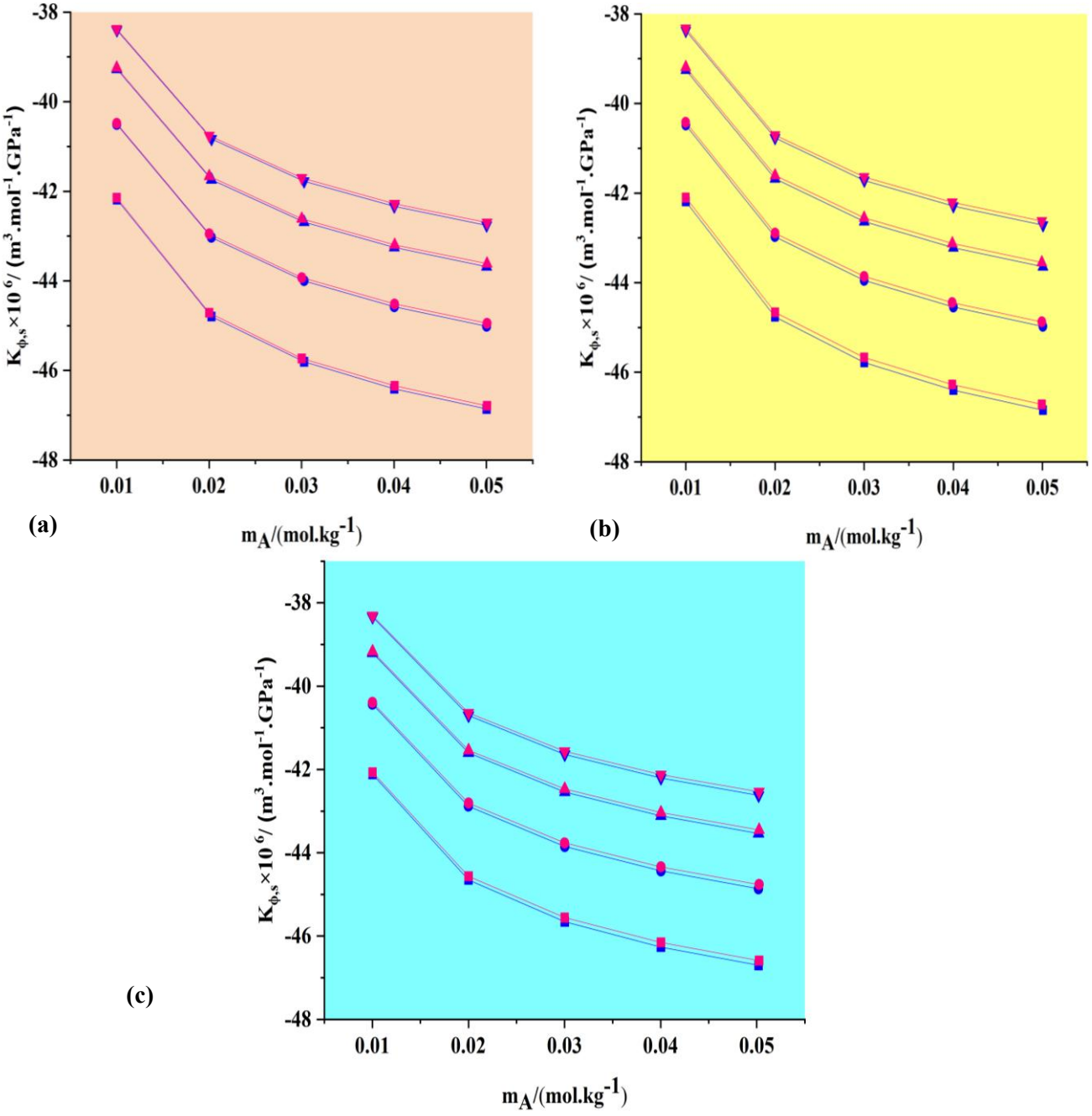

Figure 4.33 The dependence of apparent molar isentropic compression ($K_{\phi,s}$) of PEG-4000 on molality is illustrated for:

(a) Gluconolactone (pink: 0.05; blue: 0.07 $mol.kg^{-1}$)

(b) Galactose (pink: 0.05; blue: 0.07 $mol.kg^{-1}$)

(c) LBA (pink: 0.05; blue: 0.07 $mol.kg^{-1}$)

Different symbols denote temperatures: square ($288.15K$), circle ($298.15K$), up facing triangle ($308.15K$), and down facing triangle ($318.15K$).

Partial Molar Variables:

Limiting apparent molar' volume at infinite dilution

A ternary combination including PHAs sol. and PEG-4000 at infinite dilution can have its V_ϕ° determined by the formula provided in eq. **4.4.** [43] In **Table 4.38**, along with the experimental slopes (S_V^*), you can see the results for V_ϕ° within uncertainty of u(V_ϕ^0) = ±0.01 × 10^6 ($m^3 \cdot mol^{-1}$), u(S_V^*) = ±*0.03* × *10^6* $m^3.kg.mol^{-2}$). Values of V_ϕ^0, S_V for (PEG-4000 + water) are all taken from previous publication subscripted as [b] in **Table 4.38** [15]. It has been observed that for S_V^* has all positive values. The lack of regularity in S_V^* values suggests that factors other than solute concentrations impact these interactions [44]. No matter the temperature, the V_ϕ° is positively correlated and increases as the PHA concentration does. The improved solute-solvent interactions shown in **Figure 4.34** may have played a role in this. Thorough understanding of the many interactions, such as those between solutes and solvents, ions, and solvents, requires precise determination of the limiting partial molar volume [45, 46]. Co-sphere overlap causes volume expansion, hydrophobic and hydrophilic group overlap, and bulk decrease. Ion hydrophilic bonds are the main cause of positive V_ϕ° values, with interactions between solutes and solvents being more significant than solute molecules. The observed positive V_ϕ° values point toward significant hydrophobic interactions and strong hydrogen bonding between the –OH groups of PEGs and water molecules. This behavior is likely due to the release of structured water from the solvation shell of the solute into the bulk solution, enhancing molecular interactions. In addition, their temperature dependence reveals information on several processes including solvation layer molecular discharge, etc. [48-49]

Table 4.38

Values of (V_ϕ^0 and $K_{\phi,s}^0$) and their respective experimental slopes S_V^* and S_K^*, corresponding to temperature values at different concentration combination of PHAs (gluconolactone, galactose, and LBA) in water with PEG 4000 with the standard errors.

T/K	$V_\phi^0 \times 10^6/$ $(m^3.mol^{-1})$	$S_V^* \times 10^6/$ $(m^3.kg.mol^{-2})$	$K_{\phi,s}^0 \times 10^6/$ $(m^3.mol^{-1}.GPa^{-1})$	$S_K^* \times 10^6/$ $(kg.m^3.mol^{-2}.GPa^{-1})$
		0.00 mol·kg^{-1} Gluconolactone+ PEG 4000		
288.15	3298.65(±0.32) [b]	309.40(±9.54) [b]	-42.00(±0.84) [b]	-113.38(±25.41) [b]
298.15	3301.48(±0.19) [b]	315.47(±5.63) [b]	-40.29(±0.81) [b]	-109.47(±24.45) [b]
308.15	3305.02(±0.11) [b]	331.45(±3.42) [b]	-39.04(±0.79) [b]	-107.02(±23.82) [b]
318.15	3308.47(±0.12) [b]	336.71(±3.74) [b]	-38.15(±0.78) [b]	-105.74(±23.45) [b]
		0.05 mol·kg^{-1} Gluconolactone+ PEG 4000		
288.15	3299.21(±0.30)	380.27 (±9.12)	-41.89(±0.81)	-110.14(±24.23)
298.15	3303.43(±0.39)	394.91 (±11.85)	-40.23(±0.78)	-106.10(±23.37)
308.15	3306.93(±0.48)	410.74 (±14.42)	-39.00(±0.76)	-103.87(±22.88)
318.15	3311.03(±0.37)	434.32 (±11.22)	-38.13(±0.75)	-102.69(±22.50)
		0.07 mol·kg^{-1} Gluconolactone + PEG 4000		
288.15	3304.19(±1.13)	339.68 (±14.05)	-41.87(±0.80)	-109.06(±24.16)
298.15	3313.20(±0.72)	303.24 (±21.56)	-40.22(±0.77)	-104.79(±23.15)
308.15	3319.81(±0.52)	275.44(±15.65)	-38.98(±0.75)	-102.69(±22.69)
318.15	3323.97(±0.78)	301.00(±23.47)	-38.11(±0.74)	-101.52(±22.32)
		0.05 mol·kg^{-1} Galactose+ PEG 4000		
288.15	3308.90(±0.28)	333.22(±8.55)	-41.91(±0.80)	-109.41(±24.19)
298.15	3315.86(±0.13)	385.28(±3.90)	-40.22(±0.78)	-105.43(±23.39)
308.15	3322.25(±0.30)	354.08(±9.14)	-38.99(±0.76)	-103.14(±22.76)
318.15	3328.78(±0.24)	326.02(±7.29)	-38.11(±0.74)	-101.98(±22.44)
		0.07 mol·kg^{-1} Galactose + PEG 4000		
288.15	3312.92(±0.43)	335.74(±12.94)	-41.82(±0.80)	-108.82(±24.09)
298.15	3321.24(±0.43)	354.51(±12.95)	-40.16(±0.77)	-104.91(±23.25)
308.15	3327.85(±0.26)	355.91(±7.92)	-38.93(±0.75)	-102.58(±22.68)
318.15	3334.17(±0.24)	360.97(±7.19)	-38.06(±0.74)	-101.32(±22.36)
		0.05 mol·kg^{-1} LBA + PEG 4000		
288.15	3317.22(±0.31)	365.44(±9.30)	-41.85(±0.79)	-107.34(±23.86)

298.15	3322.95(±0.57)	388.47(±7.09)	-40.18(±0.76)	-103.66(±23.01)
308.15	3330.02(±0.33)	361.49(±9.88)	-38.95(±0.75)	-101.35(±22.50)
318.15	3337.84(±0.48)	339.70(±14.33)	-38.09(±0.74)	-100.21(±22.19)
		0.07 mol·kg^{-1} LBA + PEG 4000		
288.15	3318.54(±0.29)	393.90(±8.70)	-41.81(±0.78)	-105.68(±23.51)
298.15	3327.85(±0.17)	375.63(±5.23)	-40.14(±0.76)	-102.08(±22.71)
308.15	3334.38 (±0.50)	356.08(±5.07)	-38.93(±0.74)	-99.87(±22.30)
318.15	3342.28(±0.13)	337.62(±3.83)	-38.07(±0.73)	-98.84(±21.97)

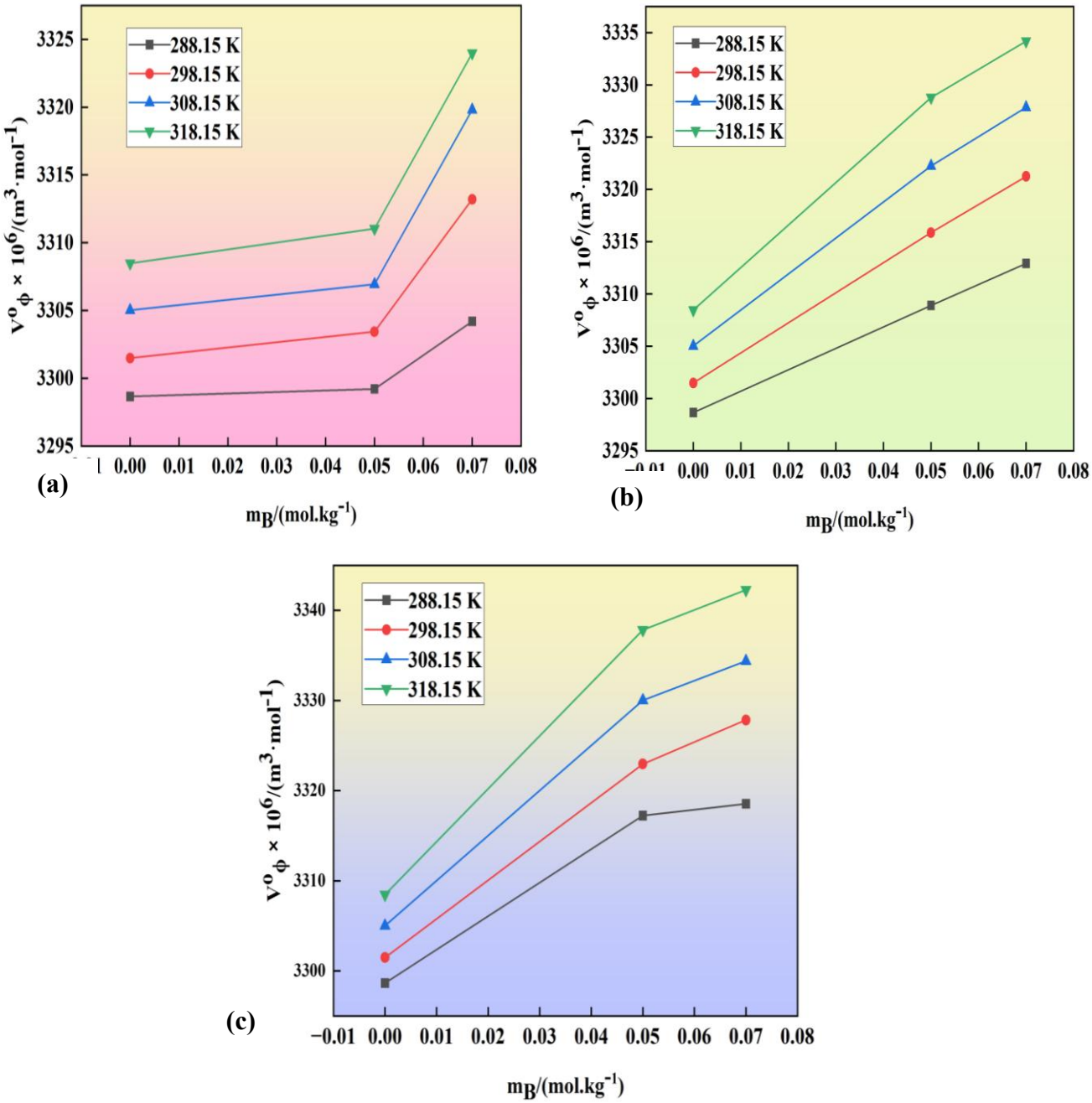

Figure 4.34 The linear plot represents the variations in V_{ϕ}^{0} of aqueous (a) gluconolactone, (b) galactose, (c) lactobionic acid at composition (0.00, 0.05 and 0.07) $mol.kg^{-1}$ and four diverse T.

Partial Molar Isentropic compressibility

The compression $K_{\phi,s}^{\circ}$, is found by technique of least square along with the determination of acoustic virial coefficient called S_K^* with their standard errors by the equation **4.5** obtained from our previous paper [1]. The data collected is organized in **Table 4.38**, which presents $K_{\phi,s}^{\circ}$, S_K^*, along with their respective standard errors with uncertainty of u($K_{\phi,s}^0$) = ±0.01×10⁶/($m^3.mol^{-1}.GPa^{-1}$) *and* *u*(S_K^*) = ±0.24×10⁶ ($kg.m^3.mol^{-2}.GPa^{-1}$). The table presented all the negative data for both $K_{\phi,s}^{\circ}$ and S_K^*. The results show that stronger connections between water molecules and solutes are achieved when the temperature escalates because the rate of negative $K_{\phi,s}^{\circ}$ values drop. These outcomes in the liberation of H_2O molecules into the surrounding solution. Model of Kirkwood provides a significant elucidation for this phenomenon [50–52]. These results are mostly responsible for the fundamental aspects that affect the $K_{\phi,s}^{\circ}$. This advantageous property, known as the solvent's inherent compressibility, comes into play as the amount of empty space inside solution molecules grows, leading to stronger contraction of the mixture [53]. When solvent molecules enter the spaces among ions as a consequence of association amid the solute and the solvent, it causes the undesirable effect known as solvent penetration [54]. **Figure 4.35** presents a visual depiction of a three-dimensional plot illustrating the relationship between $K_{\phi,s}^{\circ}$, concentration, and temperature within the ternary mixture.

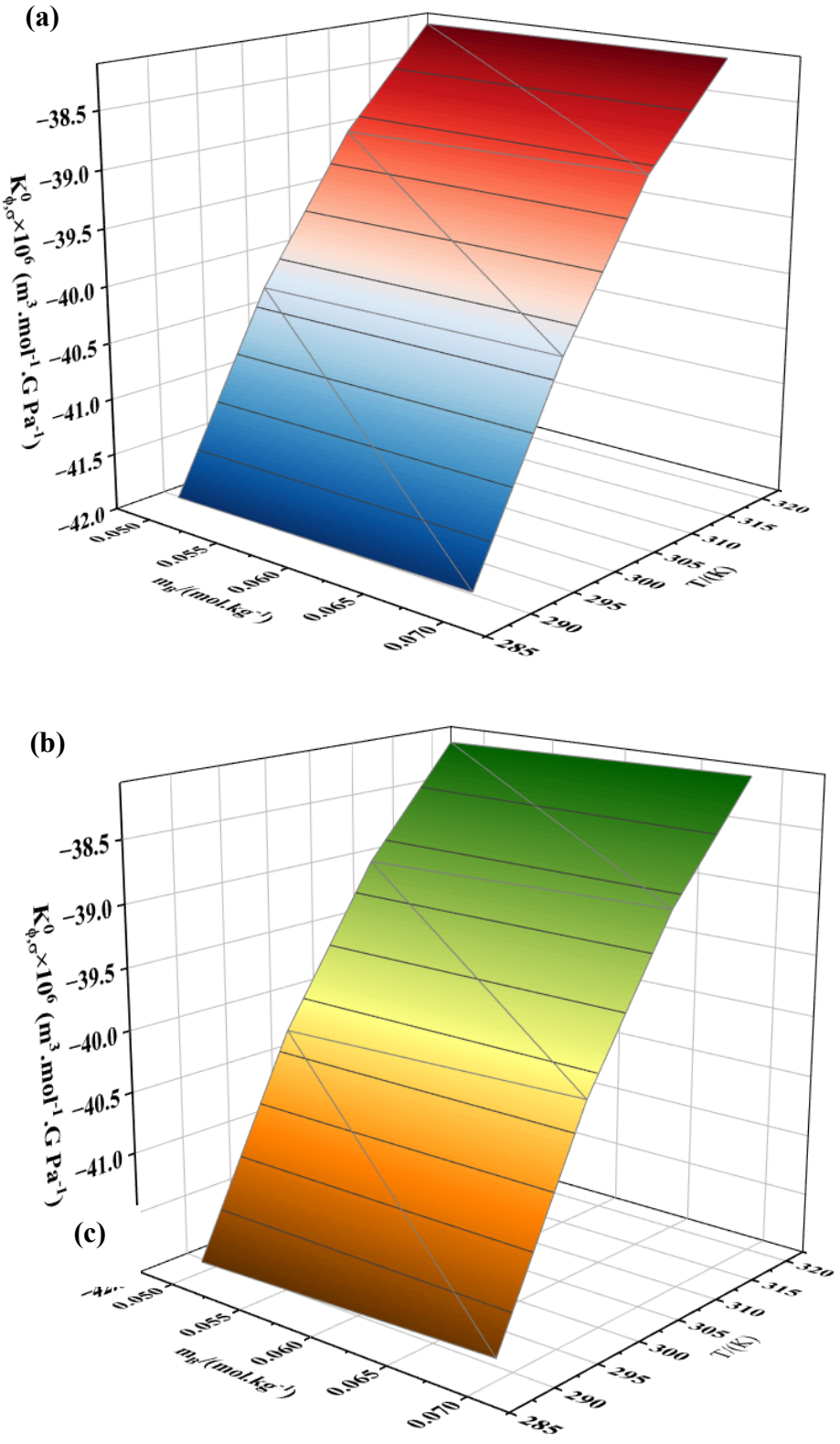
(a)
(b)
(c)
$K^0_{\phi,\sigma}\times10^6$ (m^3.mol^{-1}.G Pa^{-1})
−38.5
−39.0
−39.5
−40.0
−40.5
−41.0
−41.5
−42.0
0.050
0.055
0.060
0.065
0.070
m_{ly}/(mol.kg^{-1})
285
290
295
300
305
310
315
320
T/(K)

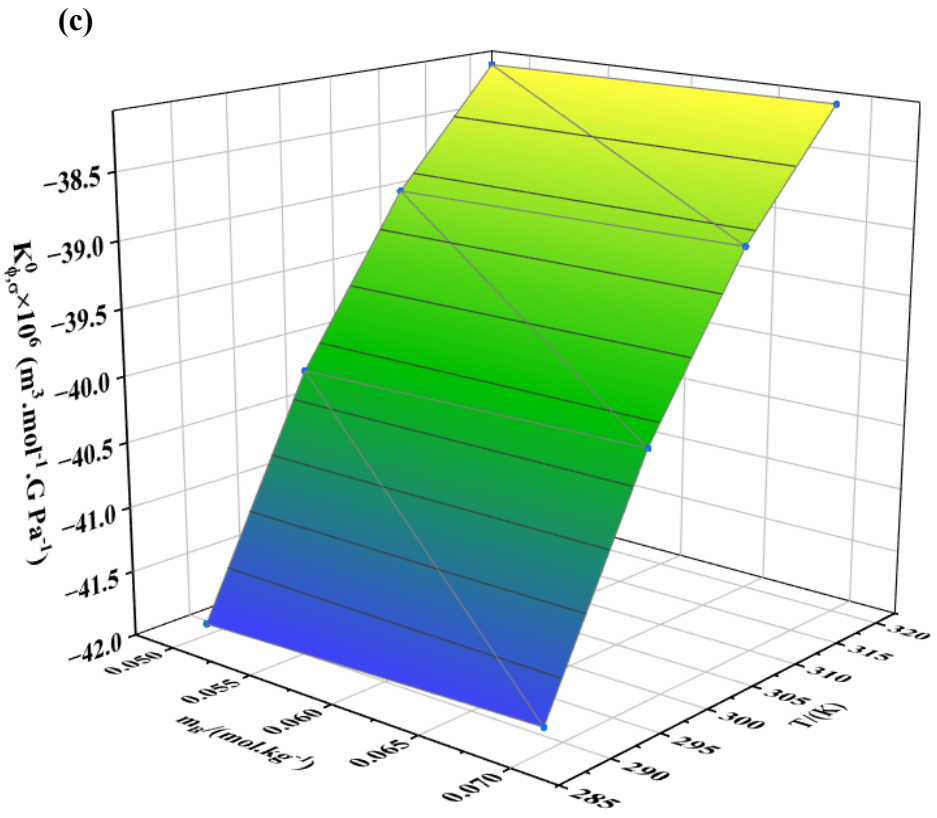

Figure 4.35 The 3D graphs showing how the $K^{\circ}_{\phi,s}$ changes with respect to temperature and m_B of (a) Gluconolactone, (b) galactose and (c) Lactobionic acid aqueous mixture in PEG-4000.

Properties of Transfer:

Transfer parameter of Partial molar Volume,

The measurement of the alteration in solution's volume upon transfer of a solute between two solvents (water and PHAs) is known as the transfer property of partial molar volume. It shows how the solute interacts with the solvent and gives information about the solute's behaviour under various conditions [48]. It is measured as per the equation **4.6**. The **Table 4.39** signifies that all of the ΔV°_{ϕ} values are positive and appear to increase as Gluconolactone, galactose and Lactobionic acid's concentrations climb. These positive numbers demonstrate PEG-4000's capacity for structure formation. It is clear from the values of ΔV°_{ϕ} and the co-sphere overlap model that there is very little interaction between the solute and itself [49]. The co-sphere overlap theory in the present study is linked to interactions like ion-hydrophilic, ion-ion, and hydrophilic-hydrophilic and is associated with positive values. The positive values of ΔV°_{ϕ} [50-52] specify that the solute and solvent bonds in the current ternary structures have been

identified. This suggests that the solute molecules have been successfully incorporated into the solution, which may have an impact on the general characteristics like the ability to dissolve, stability, and biological function in a range of applications, including formulations for food and medicine.

Transfer Property of Partial molar isentropic compression

It shows the intensity of the relationships between the solute along with the solvent and how the solute influences the degree of compression in the PHAs solution. A positive number indicates that the smaller component reduces the squeezability of the sol., indicating stronger interactions among the solvents. If it is negative, it means there are less interactions between the solute and the solution, which makes it more compressible [60]. The formula stated in Eq. **4.7** has been used to determine the quantity of PEG-4000 that is transferred through water to PHA mixtures at infinite dilutions.

The **Table 4.39** displays the results of the computations. In every temperature and LBA, gluconolactone, and galactose concentration, polyethylene glycol 4000 yields the same positive result. The solution's propensity to build structures is shown when $\Delta K_{\phi,s}^{\circ}$is positive, although this also highlights the abundance of zwitterionic connections between PHAs and glycols molecules. With an upsurge in PHAs concentration, the electrostriction diminishes, making structure building easier [61]. As the PHA concentration rises, the solution mixture becomes less compressible compared to the pure solvent, which triggers the solutes' tendency to form structures. This is why, as the concentration of PHA increases, the compressibility decreases noticeably [62, 63]. On the other hand, when the $\Delta K_{\phi,s}^{\circ}$ values are positive, the water molecules engage with the glycol’s ions. Because of these molecular interactions, the solvent increases, and the water molecules of the solutes join with it [64].

Table 4.39 Obtained data of (ΔV_{ϕ}^{0} and $\Delta K_{\phi,S}^{0}$) corresponding to temperature values at different concentration combination of PHAs (gluconolactone, galactose, and LBA) in water with glycols.

T/K	$\Delta V_{\phi}^{0} \times 10^{6}/$ $(m^{3}.mol^{-1})$	$\Delta K_{\phi,S}^{0} \times 10^{6}/$ $(m^{3}.mol^{-1}.GPa^{-1}))$
	0.05 Gluconolactone and PEG-4000	
288.15	0.56	0.10
298.15	1.95	0.06
308.15	1.90	0.04
318.15	2.56	0.02
	0.07 Gluconolactone and PEG-4000	
288.15	5.54	0.13
298.15	11.72	0.07
308.15	14.79	0.05
318.15	15.51	0.03
	0.05 Galactose and PEG-4000	
288.15	10.25	0.08
298.15	14.38	0.07
308.15	17.22	0.05
318.15	20.32	0.03
	0.07 Galactose and PEG-4000	
288.15	14.27	0.17
298.15	19.76	0.14
308.15	22.82	0.11
318.15	25.70	0.08
	0.05 LBA and PEG-4000	
288.15	18.57	0.14
298.15	21.47	0.11
308.15	25.00	0.08
318.15	29.37	0.06
	0.07 LBA and PEG-4000	
288.15	19.89	0.19
298.15	26.37	0.15
308.15	29.35	0.11
318.15	33.81	0.08

Temperature-dependent limiting apparent molar volume

The thermal dynamics of solute-solvent connections, influenced by temperature, are crucial for understanding the stability, dissolved ability, and behavior of solutions under different conditions, influenced by molecular bond nature [65,66]. The expression given in Eq. **4.8** can be used to express the relationship between T and V_{ϕ}°. [67]

For PEG 4000 in water-based PHA solutions, **Table 4.40** provides the reference temperature, T_r=298.15K. To get the ARD (Average Relative Deviation) values, we have applied the equation **4.9** [68] which are also stated in **Table 4.40.**

With these empirical constants, we can calculate the discrepancies between the measured ($Y_{Exp.}$.) and determined (Y_{calc}) parameters. Here 'Y' represents V_{ϕ}°. Determining V_{ϕ}° is essential for knowing the connections in the blend [69–71], and the goal of the inquiry is to analyze the expansibilities. To find the expansibility, we can differentiate Eq. (**4.11**) w.r.t temperature and get Eq. (**4.12**).

A system's solute-solvent linkages are measured by E_{ϕ}^{0} The architectures of solutes and solvents are described by Hepler's thermodynamic equation. The volume apparent molar property is validated by positive results of E_{ϕ}^{0} as shown in **Table 4.41**, which establish solute and solvent relationships. Solute-solvent interactions are enhanced by the packaging/caging effect. [72-75]. The parameter $\left(\frac{\partial E_{\phi}^{0}}{\partial T}\right)_{P}$ defines the propensity of the solute that dissolve to produce or break formations in a solvent.

The capability of the solute to build structures is shown by a positive value for $\left(\frac{\partial E_{\phi}^{0}}{\partial T}\right)_{P}$, as stated in reference [76], whereas the possibility of structure breaking is indicated by a negative value. The values, designated as E_{ϕ}^{0} and $\left(\frac{\partial E_{\phi}^{0}}{\partial T}\right)_{P}$, are listed in **Table 4.41**. The positive $\left(\frac{\partial E_{\phi}^{0}}{\partial T}\right)_{P}$ value shown by PEG 4000 in its aqueous PHAs solution demonstrates its capability to create structures.

Table 4.40

Determined values of empirical parameters, a, b and c of a triple liquid mixture of PHAs in aqueous solutions with PEG 4000 with their respective Average relative deviations, (ARD) at different concentrations.

	T_r=298.15K				
$^{a}m_B/(mol.kg^{-1})$	$a \times 10^6/$ $(m^3.mol^{-1})$	$b \times 10^6/$ $(m^3.mol^{-1}K^{-1})$	$c \times 10^6/$ $(m^3.mol^{-1}K^{-2})$	R^2	ARD
		Gluconolactone			
0.05	3303.232	0.392	-0.0003	0.9999	0.000040
0.07	3313.209	0.781	-0.0121	0.9999	0.000001
		Galactose			
0.05	3315.752	0.671	-0.0010	0.9999	0.000022
0.07	3321.026	0.754	-0.0050	0.9999	0.000043
		LBA			
0.05	3323.041	0.637	0.0052	0.9999	0.000018
0.07	3327.223	0.813	-0.0035	0.9999	0.000125

$^{a}m_B$ represents the concentration of various PHAs solution. T_r is the reference temperature.

Table 4.41

Values of E_ϕ^0, Partial molar expansibilities of a triple liquid mixture of PHAs in aqueous solutions with PEG 4000 and double partial derivative of V_ϕ^0 with respect to temperature at different concentrations.

$^a m_B/$ $(mol \cdot kg^{-1})$	$E_\phi^0 \times 10^6/$ $(m^3.mol^{-1}.K^{-1})$				$(\partial^2 V_\phi^0/\partial T^2)_P/$ $(m^3.mol^{-1}.K^{-2})$
	$288.15K$	$298.15K$	$308.15K$	$318.15K$	
			Gluconolactone		
0.05	0.398	0.392	0.386	0.381	0.773
0.07	1.023	0.781	0.538	0.296	1.08
			Galactose		
0.05	0.692	0.671	0.650	0.629	-0.0021
0.07	0.854	0.754	0.653	0.553	-0.01
			LBA		
0.05	0.533	0.637	0.741	0.846	0.010
0.07	0.883	0.813	0.743	0.672	-0.01

Pair and triplet coefficients

To comprehend the type and intensity of the connections in a solution, the pair and triplet coefficients are used. When two molecules interact with one another, as in a solute with solvent or solute and solute pair, the resulting pair coefficient describes the way they interact. In contrast, three molecules or ions' interactions are considered concurrently by the triplet coefficient [31]. The volumetric interaction and isentropic compression coefficients were determined by McMillian and Mayer [80]. This interaction's transfer parameters (V_{AB}, K_{AB}; V_{ABB}, K_{ABB}) are shown in the following equation:

$$\Delta V_{\phi}^{\circ}(\text{Water to aqueous PHA}) = 2V_{AB}m_B + 3V_{ABB}{m_B}^2 \quad (13)$$

$$\Delta K_{\phi,s}^{\circ}(\text{Water to aqueous PHA}) = 2K_{AB}m_B + 3K_{ABB}{m_B}^2 \quad (14)$$

Here we define the molality of aqueous PHAs (m_B), and we use the symbols (A) for glycols and (B) for PHAs. The constants that were found by fitting the values of ΔV_{ϕ}° and $\Delta K_{\phi,s}^{\circ}$ given in the preceding equations are listed in **Table 8**. Pairs of interactions have a positive V_{AB}value at all temperatures, while triplet pairs of interactions have a positive value for all PEG 4000 values except 288.15 K. As the values of triplet coefficients have larger values than pairwise coefficients so this indicates the dominance of triplet interactions. There are three positive compressibility coefficients for PEG 4000: K_{AB} and K_{ABB}. This discovery emphasizes the importance of the molecular contacts between these components in the current analysis, suggesting persistent and beneficial interactions between them. The results show that at different temperatures, the liquid mixtures with lactic and malic acids had better structural stability and cohesiveness [81]. Also, in the case of isentropic compression the triplet interactions are more popular due to higher values of triplet interactions than the pair wise values.

Table 4.42

The pair (V_{AB}, K_{AB}) and triplet (V_{ABB}, K_{ABB}) coefficients of PHAs aqueous solution with PEG 4000.

T/K	$V_{AB} \times 10^6/$ $(m^3 \cdot mol^{-2} \cdot kg)$	$V_{ABB} \times 10^6/$ $(m^3 \cdot mol^{-3} \cdot kg^2)$	$K_{AB} \times 10^6/$ $(m^3 \cdot mol^{-2}.kg.GPa^{-1})$	$K_{ABB} \times 10^6/$ $(m^3 \cdot mol^{-3}.kg^2.GPa^{-1})$
		PEG-4000		
288.15	106.56	-114.59	0.94	2.05
298.15	96.71	390.72	0.70	1.40
308.15	116.17	411.99	0.33	2.85
318.15	162.98	148.84	0.11	3.50

Conclusion

This study investigates the behavior of PEG-4000 in aqueous polyhydroxy acid (PHA) solutions by measuring densities and sound velocities at concentrations of 0.05 and 0.07 mol·kg^{-1} over the temperature range of 288.15–318.15 K. The PHAs examined include gluconolactone, galactose, and lactobionic acid. Volumetric and acoustic analyses reveal strong solute–solvent interactions, which intensify with increasing PHA concentration and molecular weight. Transfer property data suggest that ion–hydrophilic, ion–ion, and hydrophilic–hydrophilic interactions dominate over hydrophobic effects. An increase in apparent molar volume with solute concentration, along with supporting compressibility data, indicates that hydrogen bonding between the –OH groups of PEG and PHAs disrupts the water structure and increases structural rigidity. These findings deepen our understanding of solute–solvent interactions in aqueous systems and highlight their relevance in stabilizing pharmaceutical and cosmetic formulations by reducing free water and enhancing shelf life.

References

1. K. Bhakri, N. Chakraborty, K.C. Juglan, H. Kumar, R. Sharma, J. Therm. Anal. Calorim. 147, 1234 (2023).

2. H. Kaur, N. Chakraborty, K.C. Juglan and A. Upmanyu, J. Mol. Liq. 387, 123403 (2023).

3. H. Kumar, I. Behal and M. Singla, J. Chem. Thermodyn. 97, 201 (2016).

4. T. Sharma, R. Rani, A. Kumar and R.K. Bamezai, J. Mol. Liq. 304, 111985 (2020).

5. T. Sharma, R. Rani, A. Kumar and R.K. Bamezai, J. Mol. Liq. 304, 111985 (2020).

6. N. Chakraborty, K.C. Juglan and H. Kumar, J. Chem. Eng. Data 66, 246 (2021).

7. P. Kaur, N. Chakraborty, K.C. Juglan and H. Kumar, J. Mol. Liq. 318, 113763 (2020).

8. S.K. Lomesh, M. Bala, D. Kumar and I. Kumar, J. Mol. Liq. 276, 220 (2019).

9. R.C. Thakur, R. Sharma and M. Bala, J. Mater. Environ. Sci. 7, 3904 (2016).

10. R.C. Thakur, R. Sharma, A. Kumar, S. Kumar and M.L. Parmar, Orient. J. Chem. 30, 2299 (2014).

11. I. Banik and M.N. Roy, J. Mol. Liq. 211, 988 (2015).

12. M.N. Roy, B. Sinha, R. Dey and A. Sinha, Int. J. Thermophys. 26, 1543 (2005).

13. D. Brahman and B. Sinha, J. Chem. Thermodyn. 74, 156 (2014).

14. M.J. Iqbal and M.A. Chaudhry, J. Chem. Thermodyn. 42, 787 (2010).

15. M. Lamba, N. Chakraborty, K.C. Juglan, R. Sharma and M. Singla, J. Chem. Eng. Data 69, 932 (2024).

16. B. Naseem, I. Arif and M.A. Jamal, Arab. J. Chem. 14, 103405 (2021).

17. K.C. Juglan and H. Kumar, J. Chem. Thermodyn. 141, 105916 (2020).

18. M.N. Roy, V.K. Dakua and B. Sinha, Int. J. Thermophys. 28, 776 (2007).

19. H. Kumar, M. Singla and R. Jindal, J. Mol. Liq. 199, 289 (2014).

20. R. Sadeghi and A. Gholamireza, J. Chem. Thermodyn. 43, 1641 (2011).

21. S.S. Dhondge, R.L. Paliwal and N.S. Bhave, J. Chem. Thermodyn. 58, 296 (2013).

22. A.K. Nain and R. Pal, J. Chem. Thermodyn. 64, 108 (2013).

23. H.S. Frank and M.W. Evans, J. Chem. Phys. 13, 507 (1945).

24. N. Chakraborty, H. Kumar, K. Kaur and K.C. Juglan, J. Chem. Thermodyn. 126, 85 (2018).

25. K. Kaur, K.C. Juglan and H. Kumar, J. Mol. Liq. 266, 895 (2018).

26. J.G. Kirkwood, Chem. Rev. 19, 275 (1939).
27. P. Ramasami and R. Kakkar, J. Chem. Thermodyn. 38, 753 (2006).
28. R. Sadeghi and F. Ziamajidi, J. Chem. Eng. Data 52, 2676 (2007).
29. U. Gazal, Am. J. Anal. Chem. 14, 34 (2023).
30. C.V. Krishnan and H.L. Friedman, J. Solution Chem. 2, 685 (1973).
31. W.G. McMillan Jr. and J.E. Mayer, J. Chem. Phys. 13, 276 (1945).
32. A. Pal, H. Kumar, R. Maan and H.K. Sharma, J. Solution Chem. 42, 657 (2013).
33. M.J. Iqbal and M.A. Chaudhry, J. Chem. Thermodyn. 42, 787 (2010).
34. K. Bhakri, M. Lamba, K.C. Juglan and N. Chakraborty, J. Mol. Liq. 125117 (2024).
35. Bahadur and N. Deenadayalu, J. Solut. Chem. 40, 1528 (2011).
36. S. Parveen, S. Singh, D. Shukla, M. Yasmin, M. Gupta and J.P. Shukla, J. Solut. Chem. 41, 156 (2012).
37. F.M. Sannaningannavar, B.S. Navati and N.H. Ayachit, J. Therm. Anal. Calorim. 112, 1573 (2013).
38. M.S. Raman, M. Kesavan, K. Senthilkumar and V. Ponnuswamy, J. Mol. Liq. 202, 115 (2015).
39. H.S. Harned, B.B. Owen and C.V. King, J. Electrochem. Soc. 106, 15C (1959).
40. K. Kaur, K.C. Juglan and H. Kumar, J. Mol. Liq. 268, 700 (2018).
41. N. Chakraborty, K. Kaur, K.C. Juglan and H. Kumar, J. Chem. Eng. Data 65, 1435 (2020).
42. H. Kumar, K. Kaur, S. Arti and M. Singla, J. Mol. Liq. 221, 526 (2016).
43. D.O. Masson, Lond. Edinb. Dubl. Philos. Mag. J. Sci. 8, 218 (1929).
44. Thakur, K.C. Juglan and H. Kumar, Results Chem. 2, 100049 (2020).
45. R.C. Thakur, R. Sharma, A. Kumar, S. Kumar and M.L. Parmar, Orient. J. Chem. 30, 2037 (2014).
46. Z. Yan, J. Wang, H. Zheng and D. Liu, J. Solut. Chem. 27, 473 (1998).
47. E. Ayranci and M. Sahin, J. Chem. Thermodyn. 40, 1200 (2008).
48. M.T. Zafarani-Moattar and H. Shekaari, J. Chem. Thermodyn. 37, 1029 (2005).
49. H. Kumar and I. Behal, J. Chem. Thermodyn. 102, 48 (2016).
50. J.G. Kirkwood, Chem. Rev. 24, 233 (1939).
51. N. Chakraborty, K.C. Juglan and H. Kumar, J. Chem. Thermodyn. 154, 106326 (2021).
52. S. Baluja and S. Oza, Fluid Phase Equilib. 200, 11 (2002).

53. J. Wang, D. Zhang, Q. Chu and J. Ye, Chin. J. Chem. 28, 313 (2010).

54. S. Panda, V. Singh, N. Islam and R.L. Gardas, Fluid Phase Equilib. 445, 35 (2017).

55. A.K. Mishra and J.C. Ahluwalia, J. Phys. Chem. 88, 86 (1984).

56. H.L. Friedman and C.V. Krishnan, J. Solut. Chem. 2, 119 (1973).

57. A.K. Nain, J. Mol. Liq. 318, 114190 (2020).

58. T. Sharma, S.S. Shah and R.K. Bamezai, J. Solut. Chem. 50, 1363 (2021).

59. S. Li, W. Sang and R. Lin, J. Chem. Thermodyn. 34, 1761 (2002).

60. H. Kaur, N. Chakraborty and K.C. Juglan, J. Chem. Eng. Data 69, 2461 (2024).

61. N. Chakraborty, K.C. Juglan and H. Kumar, Braz. J. Chem. Eng. 1, 1 (2021).

62. A. Salabat, L. Shamshiri and F. Sahrakar, J. Mol. Liq. 118, 67 (2005).

63. R. Sadeghi and F. Ziamajidi, J. Chem. Eng. Data 52, 1037 (2007).

64. H. Kumar, M. Singla and R. Jindal, Monatsh. Chem. 145, 1063 (2014).

65. R. Xu, G. Tang, X.-L. Fu and Q.-L. Yan, Cryst. Growth Des. 22, 909 (2021).

66. E.L. Smith, A.P. Abbott and K.S. Ryder, Chem. Rev. 114, 11060 (2014).

67. F.J. Millero, J. Phys. Chem. 75, 3107 (1971).

68. K.R. Brower, J. Chem. Phys. 47, 4526 (1967).

69. S. Devi, M. Kumar, N. Sawhney, U. Syal, A.K. Sharma and M. Sharma, J. Chem. Thermodyn. 154, 106321 (2021).

70. I. Gheorghe, C. Stoicescu and F. Sirbu, J. Mol. Liq. 218, 515 (2016).

71. B. Sinha, A. Sarkar, P. Roy and D. Brahman, Int. J. Thermophys. 32, 2062 (2011).

72. L.G. Hepler, Can. J. Chem. 47, 4613 (1969).

73. T. Sharma, H. Singh, R.K. Bamezai and A. Kumar, J. Mol. Liq. 349, 118412 (2022).

74. X. Chen, Z. Huang, W. Hua, H. Castada and H.C. Allen, Langmuir 26, 18902 (2010).

75. M.N. Roy, V.K. Dakua and B. Sinha, Int. J. Thermophys. 28, 1275 (2007).

76. R. Gaba, A. Pal, D. Sharma and J. Kaur, J. Mol. Liq. 233, 38 (2017).

77. C.A. Zuritz et al., J. Food Eng. 71, 143 (2005).

78. D. Champion, M. Le Meste and D. Simatos, Trends Food Sci. Technol. 11, 41 (2000).

79. R. Gaba, A. Pal, H. Kumar, D. Sharma and R. Saini, J. Mol. Liq. 229, 417 (2017).

80. H. Kumar, M. Singla and R. Jindal, J. Mol. Liq. 208, 170 (2015).

81. S.A. Markarian, Z.K. Papanyan and G.A. Shahinyan, J. Solut. Chem. 49, 1094 (2020)

Section-IV

Problem -7

Molecular Dynamics of a Polyhydroxy acid's aqueous solution in Propylene glycol and Hexylene glycol by Volumetric and Acoustic approach

This problem presented the ρ and v of PG and HG in "(0.007, 0.008, 0.009) mol·kg^{-1} aqueous solutions of one of the polyhydroxy acids: Galactose at temperatures T = (288.15, 298.15, 308.15,318.15) K".

Apparent molar volume

The data of ρ data was utilized in the computation process to generate various volumetric properties. Propylene (PG) and Hexylene glycol (HG) densities in an aqueous galactose solution were scrutinized at four unlike temperatures with the range of concentration from 0.007, 0.008, to 0.009 mol/kg of galactose. The glycols (PG) and (HG) total mass values in relation to their molality inside aqueous galactose solutions are shown in **Table 4.43**. The densities of galactose and glycols are described in **Table 4.44**. The data of densities for (Water and both glycols) at the whole temperatures range is taken from our previous study [1]. The molecular mass of the PG and HG is represented by M $(mol.kg^{-1})$, the symbol $m_A(mol.kg^{-1})$, is used to denote the molality of PG and HG relative to the total mass of the solvent system (water + galactose), and the solution and solvent densities are denoted by ρ and ρ_0, respectively. The **Figure 4.36** shows the graphical representation of the density data of all the sample combinations. The **Table 4.44** shows that the density data increase with rising m_A of glycols in the galactose sol. and fall with growing T. As the m_A of glycol rises, the density data mostly increases due to the growth in the solution's molecular weight. The V_ϕ are derived from the measured ρ results from experimentation by the equation **4.1** [2-4]. By studying the changes in apparent molar volume, V_ϕ one can gain vision into the connections amongst the particles of blend [5-6]. **Table 4.45** displays the estimated values of V_ϕ derived from the investigated density data. In **Figure 4.37 (a)**, we can see a simple but clear three-dimensional representation of the liquid systems containing only water and glycols. **Figure 4.37 (b) to (g)** shows the plots of the possible values for the V_ϕ w.r.t. molality of PG and HG. The presence of PG and HG in galactose solutions in a ternary system indicates strong effects, as shown by the V_ϕ numbers that increase by growing galactose concentration and molality of solutes (PG/HG). An

increase in concentration leads to a reduction in the electrostrictive effect on water molecules, indicating a weakening of the solute-induced structural ordering. Molecular connections among the particles are mainly accountable for the upsurge in V_ϕ values [7-8].

Table 4.43 The molecular weight in grams of (PG) and (HG) as per its molality in water-based galactose solutions.

$^a m_A(mol.kg^{-1})$,	weight (g)	$m_A(mol.kg^{-1})$,	weight (g)
0.007 $(mol.kg^{-1})$ Galactose			
PG		**HG**	
0.102410	0.03120	0.104638	0.04960
0.199961	0.06087	0.200180	0.09462
0.301946	0.09230	0.300137	0.14187
0.399349	0.12174	0.400037	0.18911
0.505134	0.15420	0.500068	0.23650
0.008 $(mol.kg^{-1})$ **Galactose**			
PG		**HG**	
0.105037	0.03210	0.100615	0.04770
0.201472	0.06137	0.200318	0.09477
0.302532	0.09250	0.306506	0.14510
0.402644	0.12274	0.399470	0.18912
0.500274	0.15280	0.500356	0.23720
0.009 $(mol.kg^{-1})$ **Galactose**			
PG		**HG**	
0.110041	0.03360	0.103628	0.04900
0.204592	0.06233	0.202111	0.09554
0.299768	0.09131	0.305220	0.14500
0.404697	0.12331	0.400046	0.18912
0.502594	0.15370	0.500323	0.23653

Table 4.44 The densities of the ternary glycol mixture in water-based galactose solutions at four temperatures.

$^{a}m_A/$ $(mol.kg^{-1})$	$\rho \times 10^{-3}/(kg.m^{-3})$ T/(K)				$^{a}m_A/$ $(mol.kg^{-1})$	$\rho \times 10^{-3}/(kg.m^{-3})$ T/(K)			
	$288.15K$	$298.15K$	$308.15K$	$318.15K$		$288.15K$	$298.15K$	$308.15K$	$318.15K$
	0.007 Galactose and PG					**0.007 Galactose and HG**			
0.00000	0.999794	0.997825	0.994856	0.990995	0.00000	0.999794	0.997825	0.994856	0.990995
0.10241	1.000052	0.998093	0.995141	0.991302	0.10464	0.999981	0.99803	0.995092	0.991272
0.19996	1.000285	0.998335	0.995399	0.991579	0.20018	1.000142	0.99821	0.995299	0.991515
0.30195	1.000518	0.998576	0.995653	0.991856	0.30014	1.000305	0.998388	0.995505	0.991758
0.39935	1.000732	0.998797	0.995887	0.992107	0.40004	1.000459	0.998559	0.995703	0.991992
0.50513	1.000961	0.999029	0.996125	0.992367	0.50007	1.000596	0.998721	0.995884	0.992208
	0.008 Galactose and PG					**0.008 Galactose and HG**			
0.00000	0.999919	0.997958	0.994973	0.991188	0.00000	0.999919	0.997958	0.994973	0.991188
0.10504	1.000177	0.998226	0.995259	0.991497	0.10061	1.000095	0.998152	0.995196	0.99145
0.20147	1.000403	0.998461	0.995508	0.991766	0.20032	1.000259	0.998335	0.995407	0.991698
0.30253	1.000627	0.998694	0.995757	0.992036	0.30651	1.000425	0.998519	0.995625	0.991953
0.40264	1.000839	0.998916	0.995993	0.992293	0.39947	1.000563	0.998671	0.995804	0.992164
0.50027	1.001033	0.999122	0.996212	0.992532	0.50036	1.000699	0.998828	0.99598	0.992376
	0.009 Galactose and PG					**0.009 Galactose and HG**			
0.00000	0.999993	0.998129	0.995167	0.991385	0.00000	0.999993	0.998129	0.995167	0.991385
0.11004	1.00026	0.998405	0.99546	0.991703	0.10363	1.000171	0.998324	0.995392	0.991647

0.20459	1.000475	0.998628	0.995697	0.991962	0.20211	1.00033	0.998501	0.995594	0.991886
0.29977	1.000682	0.99884	0.995926	0.992213	0.30522	1.00049	0.998675	0.995797	0.992126
0.40470	1.000898	0.999067	0.996167	0.992475	0.40005	1.000624	0.998826	0.995973	0.992336
0.50259	1.001097	0.99927	0.99638	0.992709	0.50032	1.000755	0.998975	0.996144	0.992547

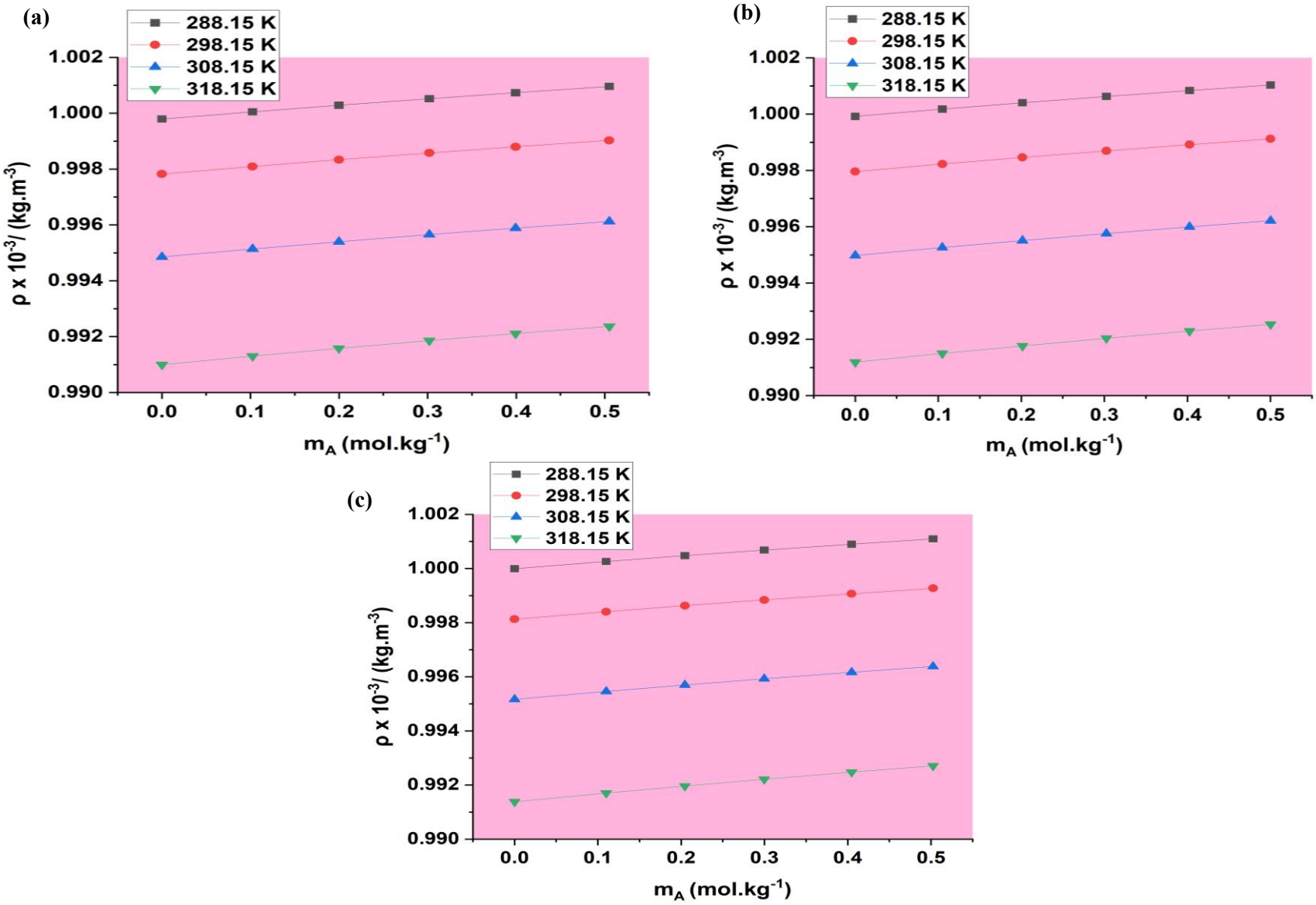
(a)
288.15 K
298.15 K
308.15 K
318.15 K
1.002
1.000
0.998
0.996
0.994
0.992
0.990
ρ x 10-3/ (kg.m-3)
0.0
0.1
0.2
0.3
0.4
0.5
mA (mol.kg-1)
(b)
288.15 K
298.15 K
308.15 K
318.15 K
1.002
1.000
0.998
0.996
0.994
0.992
0.990
ρ x 10-3/ (kg.m-3)
0.0
0.1
0.2
0.3
0.4
0.5
mA (mol.kg-1)
(c)
288.15 K
298.15 K
308.15 K
318.15 K
1.002
1.000
0.998
0.996
0.994
0.992
0.990
ρ x 10-3/ (kg.m-3)
0.0
0.1
0.2
0.3
0.4
0.5
mA (mol.kg-1)

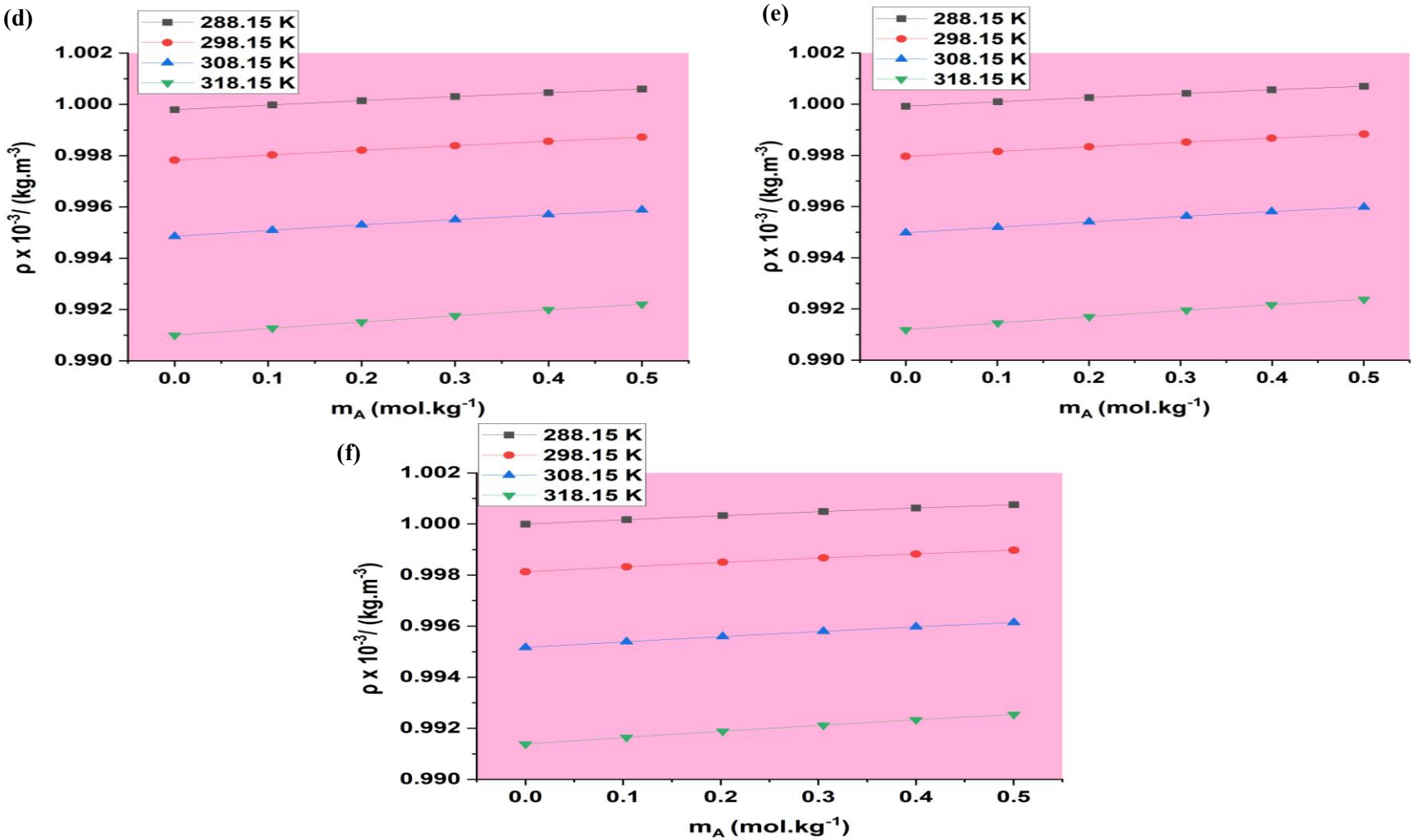

Figure 4.36 Density v/s molality of various ternary liquid solutions of galactose and glycols (a) 0.007 galactose + PG; (b) 0.008 galactose + PG; (c) 0.009 galactose + PG; (d) 0.007 galactose + HG; (e) 0.008 galactose + HG; (f) 0.009 galactose + HG at distinct temperatures. (concentrations in $mol.kg^{-1}$)

Table 4.45 Computed V_ϕ for both glycols at different compositions of galactose.

$^a m_A$/ $(mol.kg^{-1})$	$V_\phi \times 10^6/\ (m^3.mol^{-1})$ T/(K)				$^a m_A$/ $(mol.kg^{-1})$	$V_\phi \times 10^6/\ (m^3.mol^{-1})$ T/(K)			
	$288.15K$	$298.15K$	$308.15K$	$318.15K$		$288.15K$	$298.15K$	$308.15K$	$318.15K$
	0.007 Galactose and PG					**0.007 Galactose and HG**			
0.10241	73.57	73.61	73.65	73.70	0.10464	116.38	116.43	116.47	116.51
0.19996	73.61	73.66	73.70	73.76	0.20018	116.41	116.45	116.49	116.54
0.30195	73.65	73.70	73.76	73.81	0.30014	116.43	116.48	116.52	116.57
0.39935	73.69	73.74	73.80	73.86	0.40004	116.45	116.50	116.54	116.59
0.50513	73.71	73.77	73.85	73.91	0.50007	116.50	116.52	116.58	116.63
	0.008 Galactose and PG					**0.008 Galactose and HG**			
0.10504	73.62	73.66	73.70	73.75	0.10061	116.41	116.46	116.50	116.54
0.20147	73.66	73.70	73.75	73.80	0.20032	116.44	116.48	116.53	116.57
0.30253	73.70	73.75	73.80	73.85	0.30651	116.47	116.51	116.54	116.59
0.40264	73.74	73.79	73.84	73.89	0.39947	116.49	116.54	116.57	116.62
0.50027	73.79	73.82	73.88	73.93	0.50036	116.53	116.56	116.62	116.66
	0.009 Galactose and PG					**0.009 Galactose and HG**			
0.11004	73.65	73.69	73.75	73.78	0.10363	116.44	116.48	116.52	116.59
0.20459	73.70	73.75	73.80	73.84	0.20211	116.47	116.50	116.56	116.62

0.29977	73.74	73.80	73.85	73.88	0.30522	116.48	116.53	116.59	116.64
0.40470	73.79	73.84	73.89	73.93	0.40005	116.52	116.56	116.61	116.67
0.50259	73.81	73.87	73.93	73.97	0.50032	116.56	116.60	116.66	116.70

(a)

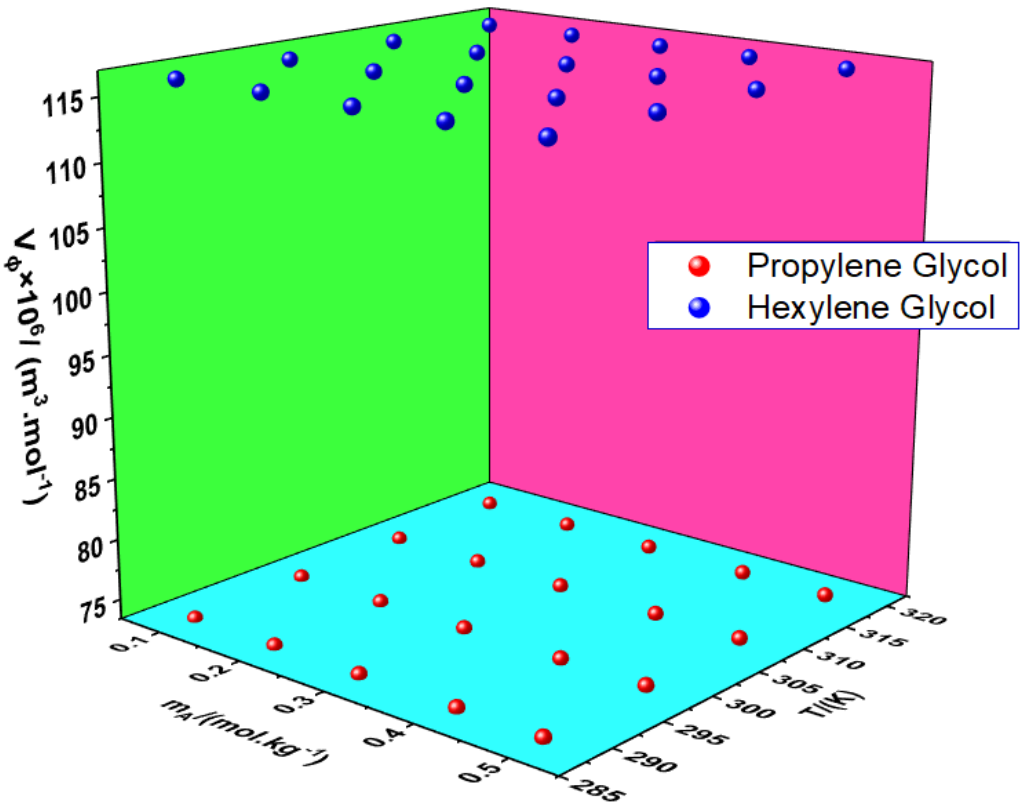

(b)

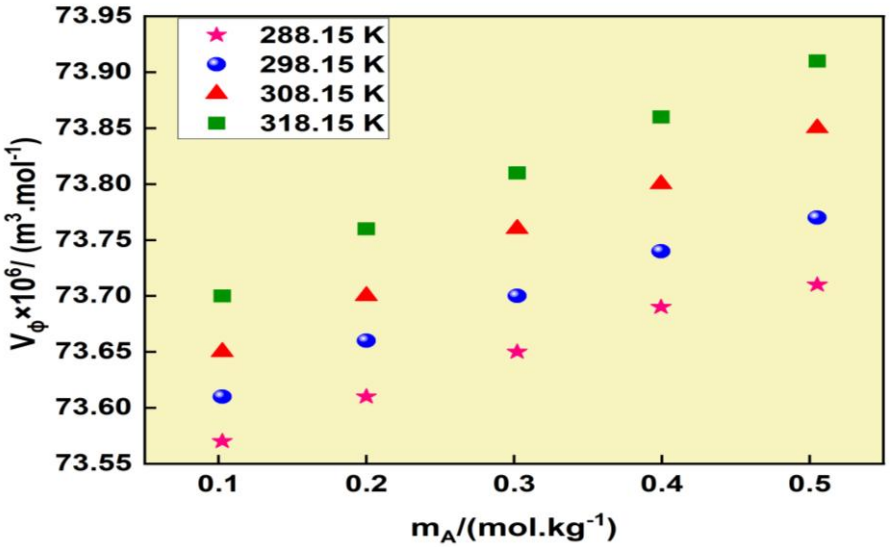
288.15 K
298.15 K
308.15 K
318.15 K
$V_\phi \times 10^6/(m^3.mol^{-1})$
$m_A/(mol.kg^{-1})$

(c)

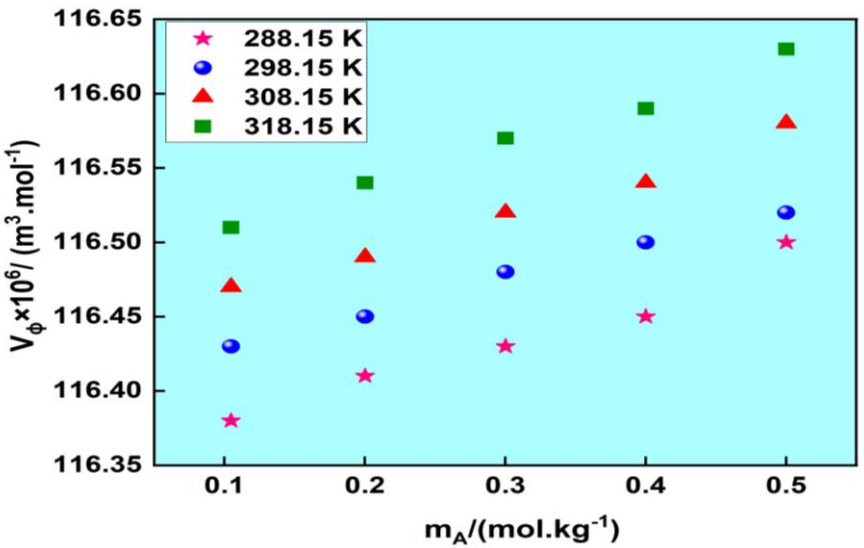
288.15 K
298.15 K
308.15 K
318.15 K
$V_\phi \times 10^6/(m^3.mol^{-1})$
$m_A/(mol.kg^{-1})$

(d)

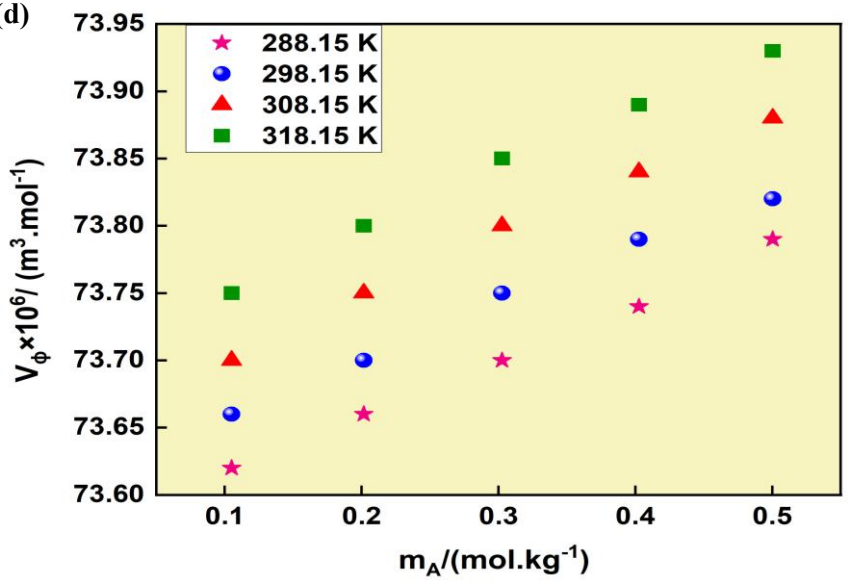
288.15 K
298.15 K
308.15 K
318.15 K
$V_\phi \times 10^6/(m^3.mol^{-1})$
$m_A/(mol.kg^{-1})$

(e)

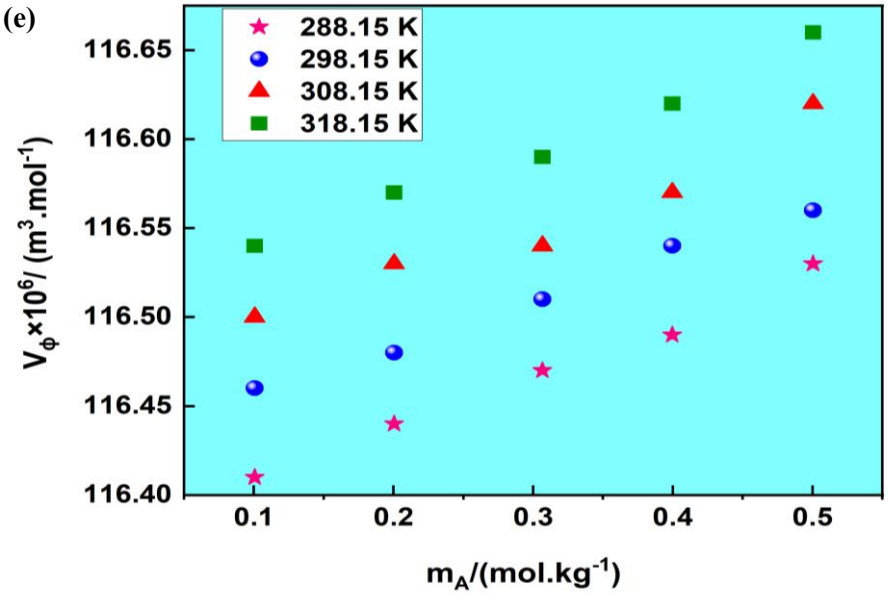
288.15 K
298.15 K
308.15 K
318.15 K
$V_\phi \times 10^6/(m^3.mol^{-1})$
$m_A/(mol.kg^{-1})$

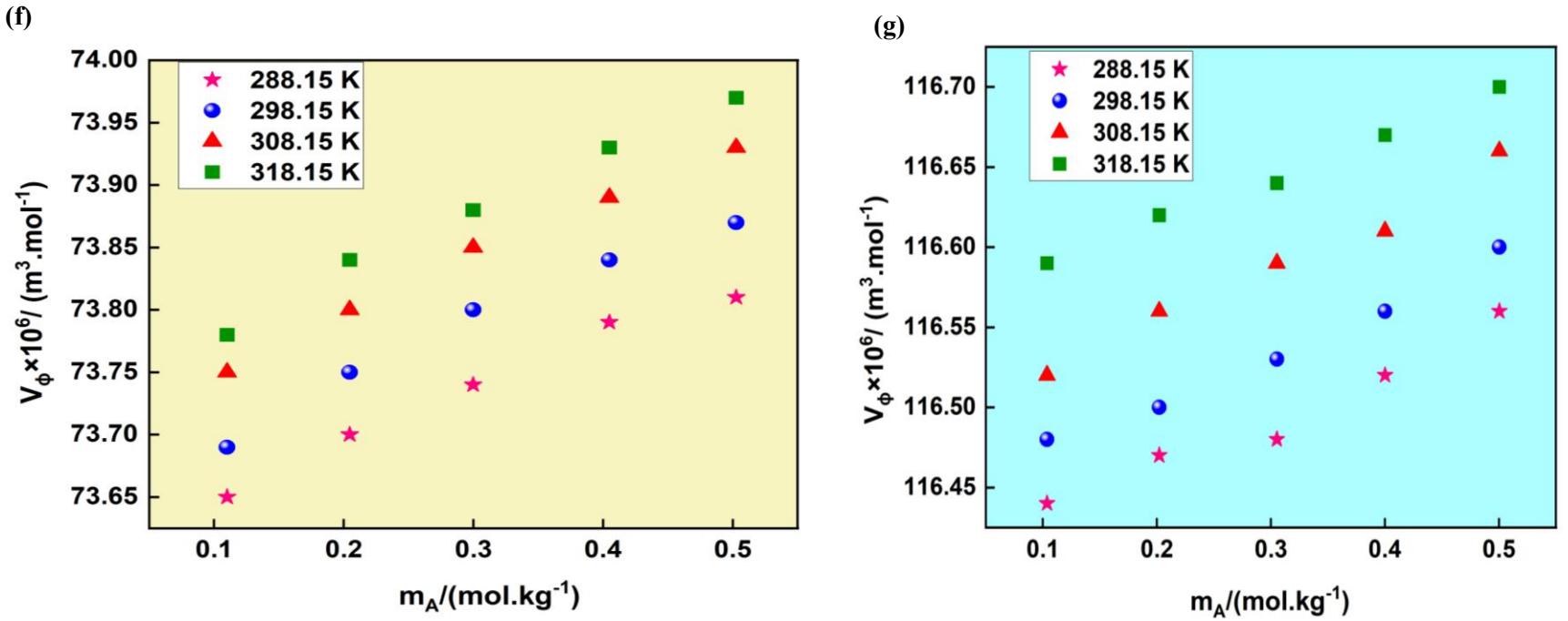

Figure 4.37 The plots show the possible values for (V_ϕ) as a function of m_A of PG and HG at diverse temperatures and concentrations in *mol.kg*$^{-1}$ of galactose: (yellow for PG/ blue for HG) (a) 0.00 for Galactose + PG/HG, (b) 0.007 for Galactose + PG, (c) 0.007 for Galactose + HG, and (d) 0.008 for Galactose + PG; (e) 0.008 for Galactose + HG; (f) 0.009 for Galactose + PG; and (g) 0.009 for Galactose + HG

Partial molar volume

Using the same formula as before [9] stated in Eq. **4.4** and fitting V_ϕ using least squares, we can determine V_ϕ^0 i.e. Partial molar volume and experimental slopes S_V^*. The results of V_ϕ^0 and S_V^* are displayed in **Table 4.46** and **Figure 4.38** illustrates the results graphically in relation to concentration of galactose in aqueous solutions. When the V_ϕ^0 values are positive, it means that the solute and solvent bonds are very important. These interactions become much more important as the temperature and galactose concentrations of PG and HG increase. This kind of interaction is described by the co-sphere model [10,11]. As per overlap model, ion-aquaphilic connections led to the computation of positive values V_ϕ^0. Hydrophobic and ion-hydrophobic molecule interactions are mostly governed by them. For both PG and HG, the V_ϕ^0 increases with rising temperature. This may be interpreted as a partial dissolution of the solute's solvation layer. Furthermore, it is more common for V_ϕ^0 values to increase as the molar mass of glycol does. The positive magnitude of S_V^* is evident at all temperatures and concentrations of galactose (as shown in **Table 4.46**). Since S_V^* values are much smaller than V_ϕ^0, it shows that solute–solvent relations are stronger in the blend [12,13].

Table 4.46
Computed V_{ϕ}^{0} and its experimental slopes, S_V^* , in water-based galactose for both glycols at different compositions and temperatures.

m_B /$mol.kg^{-1}$	$V_{\phi}^{0} \times 10^{6}/\ (m^3.mol^{-1})$				$S_V^* \times 10^6\ /(m^3.kg.mol^{-2})$			
	$288.15K$	$298.15K$	$308.15K$	$318.15K$	$288.15K$	$298.15K$	$308.15K$	$318.15K$
PG								
0.000	73.39(±0.004)[b]	73.46(±0.002)[b]	73.55(±0.001)[b]	73.62(±0.002)[b]	0.59(±0.014)[b]	0.58(±0.007)[b]	0.55(±0.004)[b]	0.55(±0.007[b]
0.007	73.54(±0.010)	73.57(±0.007)	73.60(±0.003)	73.66(±0.004)	0.35(±0.031)	0.41(±0.021)	0.49(±0.010)	0.51(±0.013)
0.008	73.57(±0.002)	73.62(±0.004)	73.66(±0.004)	73.71(±0.005)	0.43(±0.005)	0.41(±0.012)	0.44(±0.012)	0.45(±0.015)
0.009	73.61(±0.009)	73.65(±0.011)	73.70(±0.006)	73.74(±0.004)	0.42(±0.027)	0.45(±0.032)	0.46(±0.017)	0.47(±0.012)
HG								
0.000	116.35(±0.000)[b]	116.39(±0.000)[b]	116.43(±0.001)[b]	116.46(±0.000)[b]	0.23(±0.001)[b]	0.23(±0.001)[b]	0.24(±0.004)[b]	0.24(±0.003)[b]
0.007	116.35(±0.008)	116.41(±0.002)	116.44(±0.007)	116.48(±0.007)	0.27(±0.025)	0.23(±0.006)	0.27(±0.022)	0.29(±0.020)
0.008	116.38(±0.004)	116.42(±0.003)	116.47(±0.010)	116.50(±0.007)	0.30(±0.011)	0.28(±0.009)	0.28(±0.031)	0.31(±0.022)
0.009	116.40(±0.008)	116.44(±0.002)	116.49(±0.005)	116.56(±0.003)	0.30(±0.023)	0.30(±0.007)	0.33(±0.016)	0.26(±0.008)

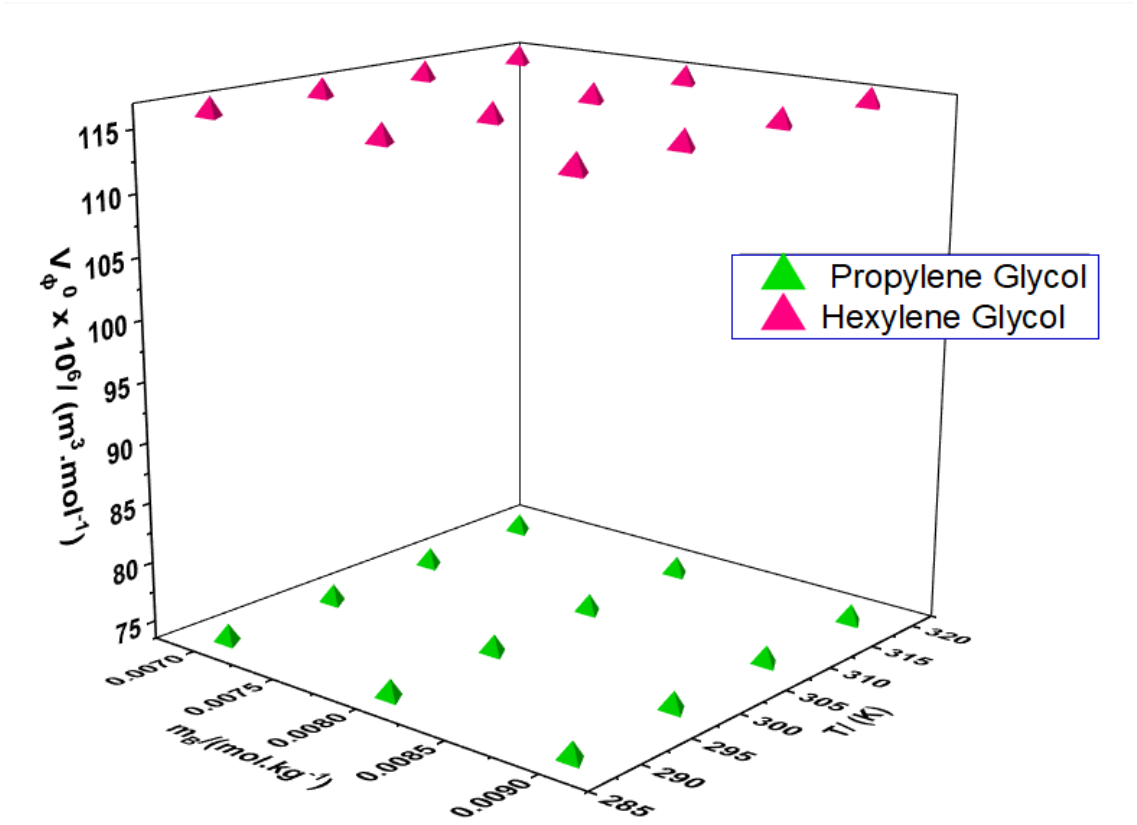

Figure 4.38 Graphical representation of V_ϕ^0 with respect to Concentrations for Galactose and distinct temperature range. (green tetrahedron-PG); (green tetrahedron-HG)

Transfer parameter of Partial molar volume

When a substance is moved from one phase to another, its partial volume changes, which is indicated by the partial molar volume (ΔV_ϕ^0). The **4.6** equation was used at infinite dilution to determine the values of ΔV_ϕ^0 for the taken blend. At various T, ΔV_ϕ^0 are presented in **Table 4.47**. You can see that all ΔV_ϕ^0 are positive from **Table 4.47**. The weaker interactions between glycol and galactose molecules seen in all ΔV_ϕ^0 values compare to the stronger interactions between water and glycols. As opposed to an infinite dilution, the solute takes up more space in the solution when all of the values of ΔV_ϕ^0 are positive [14]. Because of their solvophobic properties and structural interactions, as the co-sphere overlap model illustrates, solutes can take on the shape of certain parameters. TThe solute-solute interaction is determined to have an insignificant contribution to these values. When it comes to contacts, the model states that ion hydrophobic associations are the ones that cause negative contributions to the ΔV_ϕ^0 values, whilst the other two kinds of interactions are the ones that cause positive contributions to the ΔV_ϕ^0 values. So, looking at galactose with water and glycols, it's clear that hydrophilic effects are the most prevalent ones in our liquid combination. [15-19].

Table 4.47

The obtained results of (ΔV_ϕ^0) for temperature values at various galactose concentrations in water with PG/HG.

m_B/ $(mol.kg^{-1}$	$\Delta V_\phi^0 \times 10^6/(m^3.mol^{-1})$ $T/(K)$				m_B/ $(mol.kg^{-}$	$\Delta V_\phi^0 \times 10^6/(m^3.mol^{-1})$ $T/(K)$			
	288.15 K	**298.15 K**	**308.15 K**	**318.15 K**		**288.15 K**	**298.15 K**	**308.15 K**	**318.15 K**
		PG					**HG**		
0.007	0.15	0.11	0.05	0.04	**0.007**	0.00	0.02	0.01	0.02
0.008	0.18	0.16	0.11	0.09	**0.008**	0.03	0.03	0.04	0.04
0.009	0.22	0.19	0.15	0.12	**0.009**	0.05	0.05	0.06	0.10

Partial molar volume depending on temperature

This measure sheds light on the interactions by reflecting the change in solution volume with temperature. Whether molecular contacts strengthen or diminish with temperature is one example of how this property reveals the nature of interactions; understanding how solutions behave in different temperature circumstances, stability, and solubility depends on this information [20,21]. To find the difference between V_ϕ^0 and the temperature at infinite dilutions, we have used the formula stated in equation **4.8.**

In **Table 4.48**, we can see the variables $a, b \; and \; c$ representing the empirical coefficients of PG and HG in solutions of Galactose along with the standard errors. As an example, 298.15 K is the reference temperature, or T_{ref}.

A full satisfaction of the eq. is achieved in this study since the R^2 values show that the value variations are quite tiny. Finding expansibilities is essential for understanding interactions in a mixture, as seen below [22, 23]. Hepler derived the solute's structure-forming and breaking capabilities in a solvent, and the resulting equation is as stated in equation **4.12.** [24] The packaging or caging phenomena is the cause of positive E_Φ^0 values being more common [25-26]. For the solutions under consideration, the positive E_Φ^0 values suggest that, upon heating, some solvent molecules may be freed from their solvation layers. As seen in **Table 4.49**, $\left(\partial E_\Phi^0/\partial T\right)_P$ was found to be positive for 0.007 mol.kg-1 of aqueous galactose in PG and also 0.009 $mol.kg^{-1}$ of aqueous galactose in HG, indicating that the liquid systems behave in a way that makes structures, while it was found to be negative for 0.008 & 0.009 $mol.kg^{-1}$ of galactose in PG; 0.007 and 0.008 $mol.kg^{-1}$of galactose in HG, indicating that the combinations in this study break structures This constant. But the negative values of $\left(\partial E_\Phi^0/\partial T\right)_P$ are extremely small as compared to positive values of $\left(\partial E_\Phi^0/\partial T\right)_P$. All the positive E_Φ^0 values mean that the solute and solvent are interacting in the mixtures. [27,28]

Table 4.48
Average relative deviations (ARD) and standard errors for the $a, b, and\ c$ of a triple liquid blend of galactose solutions with PG and HG.

m_B/ $mol.kg^{-1}$	$a \times 10^6$ $/(m^3.mol^{-1})$	$b \times 10^6$ $/(m^3.mol^{-1}.K^{-1})$	$c \times 10^6$ $/(m^3.mol^{-1}K^{-2})$	R^2	Standard Error	ARD
			Propylene glycol			
0.007	73.569	0.003	0.00005	0.9999	0.004575	0.00004
0.008	73.619	0.005	-0.00001	0.9999	0.001809	0.00034
0.009	73.657	0.005	-0.00003	0.9999	0.003659	0.00003
			Hexylene glycol			
0.007	116.403	0.004	-0.00003	0.9999	0.003846	0.000020
0.008	116.425	0.004	-0.00002	0.9999	0.000225	0.000001
0.009	116.439	0.004	0.00009	0.9999	0.004394	0.000023

Table 4.49

The expansibilities, E_{ϕ}^{0} at various concentrations of galactose in aqueous solutions with PG/HG and its derivative shown against temperature.

m_B/ $(mol.kg^{-1})$	$E_{\phi}^{0} \times 10^{6}/(m^{3}.mol^{-1}.K^{-1})$				$\left(\frac{\partial E_{\phi}^{0}}{\partial T}\right)_{P}$ $/(m^{3}.mol^{-1}.K^{-2})$
	$288.15K$	$298.15K$	$308.15K$	$318.15K$	
			Propylene Glycol		
0.007	0.002	0.003	0.004	0.005	0.00010
0.008	0.005	0.005	0.004	0.004	-0.00001
0.009	0.005	0.005	0.004	0.003	-0.00006
			Hexylene Glycol		
0.007	0.005	0.004	0.004	0.003	-0.00006
0.008	0.005	0.004	0.004	0.003	-0.00005
0.009	0.003	0.004	0.006	0.008	0.00018

Apparent molar isentropic compression

At different temperatures, the $K_{\phi,S}$ for PG/HG in galactose aqueous solutions was determined using Equation (**4.3**) [1]

To calculate the isentropic compressibility, one uses the Laplace-Newton formula stated in Eq. **4.2. Table 4.50** shows the calculated '$K_{\phi,S}$' values and the sound speed values 'v' at several temperatures. In **Table 4.50**, we can see that, for a fixed concentration of galactose, the sound velocity increases or becomes more penetrating with m_A. This is supported by the sound speed measurements for (galactose + water) and (galactose + water + PG/HG) at different temperatures. All temperatures and galactose concentrations result in negative $K_{\phi,S}$ values, as shown in the **Figure 4.39**. This is because the glycol & charged ions and causes the H_2O particles to be compressed to their maximum degree. Since galactose and glycol ions interact strongly with one another as solutes and solvents [20]. Throughout the whole concentration range of PG/HG and galactose, the negative value of $K_{\phi,S}$ could be explained, in part, by the statistic that the hydration rings contain water molecules that are less easily squeezed than the bulk [29]. This makes hydration shells, which contain water molecules, easier to squeeze than plain water. Higher concentrations of PG and HG result in a greater loss of water molecules due to mass. The result is hydration rings. The process results in the loss of water molecules. Because of this, the bulk compressibility decreases and disparity among the bulk and liquid's compressibility increases [30].

Table 4.50 v and $K_{\phi,s}$ at the full range of temperature from $288.15K$ to $318.15K$ and various concentrations of galactose in PG/HG.

$^{a}m_A$/ $(mol.kg^{-1})$	v/ $(m.s^{-1})$ T /(K)				$K_{\phi,s}\times10^{15}$/ $(m^3.mol^{-1}.Pa^{-1})$ T /(K)			
	$288.15K$	$298.15K$	$308.15K$	$318.15K$	$288.15K$	$298.15K$	$308.15K$	$318.15K$
0.00 $mol.kg^{-1}$ Galactose and PG								
0.00000	1466.59[b]	1495.85[b]	1519.14[b]	1536.02[b]				
0.10028	1471.03[b]	1500.79[b]	1523.09[b]	1539.09[b]	-46.04[b]	-44.26[b]	- 42.91[b]	- 41.97[b]
0.20000	1475.50[b]	1504.61[b]	1526.29[b]	1542.06[b]	-46.29[b]	-44.49[b]	-43.14[b]	- 42.20[b]
0.30017	1479.61[b]	1508.02[b]	1529.50[b]	1545.03[b]	-46.38[b]	-44.58[b]	-43.22[b]	-42.28[b]
0.40905	1483.28[b]	1511.16[b]	1532.52[b]	1548.34[b]	- 46.43[b]	-44.63[b]	-43.27[b]	-42.33[b]
0.50000	1486.61[b]	1513.99[b]	1535.04[b]	1550.83[b]	-46.46[b]	-44.66[b]	-43.30[b]	-42.36[b]
0.007 $mol.kg^{-1}$ Galactose and PG								
0.00000	1468.14	1497	1520.97	1537.59				
0.10241	1472.5	1501.95	1524.82	1540.53	-45.96	-44.20	-42.82	-41.89
0.199961	1476.83	1505.78	1527.81	1543.46	-46.19	-44.42	-43.03	-42.11
0.301946	1481.24	1509.29	1531.22	1546.51	-46.28	-44.51	-43.12	-42.19
0.399349	1484.71	1512.45	1534.05	1549.53	-46.32	-44.56	-43.16	-42.24
0.505134	1488.88	1516.18	1537.02	1552	-46.36	-44.59	-43.20	-42.27
0.008 $mol.kg^{-1}$ Galactose and PG								
0.00000	1469.32	1498.17	1521.67	1538.86				

0.105037	1474.71	1503.59	1525.76	1541.68	-45.89	-44.14	-42.79	-41.83
0.201472	1478.83	1507.57	1528.94	1544.53	-46.12	-44.36	-43.00	-42.04
0.302532	1483.25	1510.91	1532.56	1547.67	-46.20	-44.44	-43.08	-42.12
0.402644	1487.34	1514.45	1535.56	1550.56	-46.25	-44.49	-43.13	-42.17
0.500274	1491.48	1517.96	1538.53	1553.05	-46.28	-44.52	-43.16	-42.20
0.009 $mol.kg^{-1}$ Galactose and PG								
0.00000	1471.11	1499.99	1522.99	1539.59				
0.110041	1476.41	1505.39	1527.58	1542.83	-45.80	-44.05	-42.73	-41.81
0.204592	1481.15	1509.45	1530.55	1545.73	-46.01	-44.25	-42.93	-42.00
0.299768	1485.36	1512.45	1533.99	1549	-46.09	-44.33	-43.00	-42.08
0.404697	1489.65	1516.35	1537.13	1552.15	-46.14	-44.38	-43.05	-42.13
0.502594	1493.57	1519.84	1540.64	1554.63	-46.17	-44.41	-43.08	-42.16
0.00 $mol.kg^{-1}$ Galactose and HG								
0.00000	1466.59 [b]	1495.85 [b]	1519.14 [b]	1536.02 [b]				
0.09976	1476.42 [b]	1504.09 [b]	1526.06 [b]	1542.03 [b]	-46.04 [b]	-44.26 [b]	-42.91 [b]	-41.97 [b]
0.20012	1485.99 [b]	1513.18 [b]	1532.68 [b]	1549.03 [b]	-46.28 [b]	-44.49 [b]	-43.14 [b]	-42.20 [b]
0.30214	1495.08 [b]	1521.73 [b]	1540.15 [b]	1555.44 [b]	-46.37 [b]	-44.57 [b]	-43.22 [b]	-43.22 [b]
0.39996	1503.80 [b]	1529.03 [b]	1545.50 [b]	1560.44 [b]	-46.41 [b]	-44.62 [b]	-43.26 [b]	-42.32 [b]
0.50067	1510.68 [b]	1536.10 [b]	1550.22 [b]	1565.35 [b]	-46.44 [b]	-46.44 [b]	-43.30 [b]	-42.36 [b]
0.007 $mol.kg^{-1}$ Galactose and HG								
0.00000	1468.14	1497	1520.97	1537.59				

0.104638	1489.08	1515.69	1541.06	1560.56	-45.97	-44.21	-42.83	-41.91
0.20018	1509.02	1533.65	1561.07	1579.89	-46.19	-44.43	-43.04	-42.12
0.300137	1528.43	1553.94	1580.03	1600.26	-46.28	-44.51	-43.12	-42.20
0.400037	1549.01	1573.64	1600.74	1619.14	-46.32	-44.55	-43.17	-42.24
0.500068	1571.59	1593.44	1619.29	1637.34	-46.35	-44.58	-43.20	-42.27
0.008 $mol.kg^{-1}$ Galactose and HG								
0.00000	1469.32	1498.17	1521.67	1538.86				
0.100615	1491.73	1518.19	1543.86	1562.33	-45.88	-44.13	-42.78	-41.83
0.200318	1512.2	1538.11	1564.9	1581.23	-46.12	-44.36	-43.00	-42.05
0.306506	1532.47	1557.85	1584.09	1603.3	-46.20	-44.44	-43.08	-42.13
0.39947	1551.34	1576.57	1603.46	1622	-46.25	-44.48	-43.13	-42.17
0.500356	1573.95	1594.77	1621.13	1640.99	-46.28	-44.51	-43.15	-42.20
0.009 $mol.kg^{-1}$ Galactose and HG								
0.00000	1471.11	1499.99	1522.99	1539.59				
0.103628	1494.13	1523.45	1547.1	1564.52	-45.78	-44.04	-42.72	-41.80
0.202111	1513.29	1542.87	1567.08	1584.03	-46.01	-44.25	-42.93	-42.01
0.30522	1534.83	1563.29	1587.27	1605.43	-46.09	-44.33	-43.01	-42.09
0.400046	1555.26	1579.06	1605.45	1624.03	-46.13	-44.38	-43.05	-42.13
0.500323	1575.02	1599.69	1624.33	1642.25	-46.16	-44.40	-43.08	-42.16

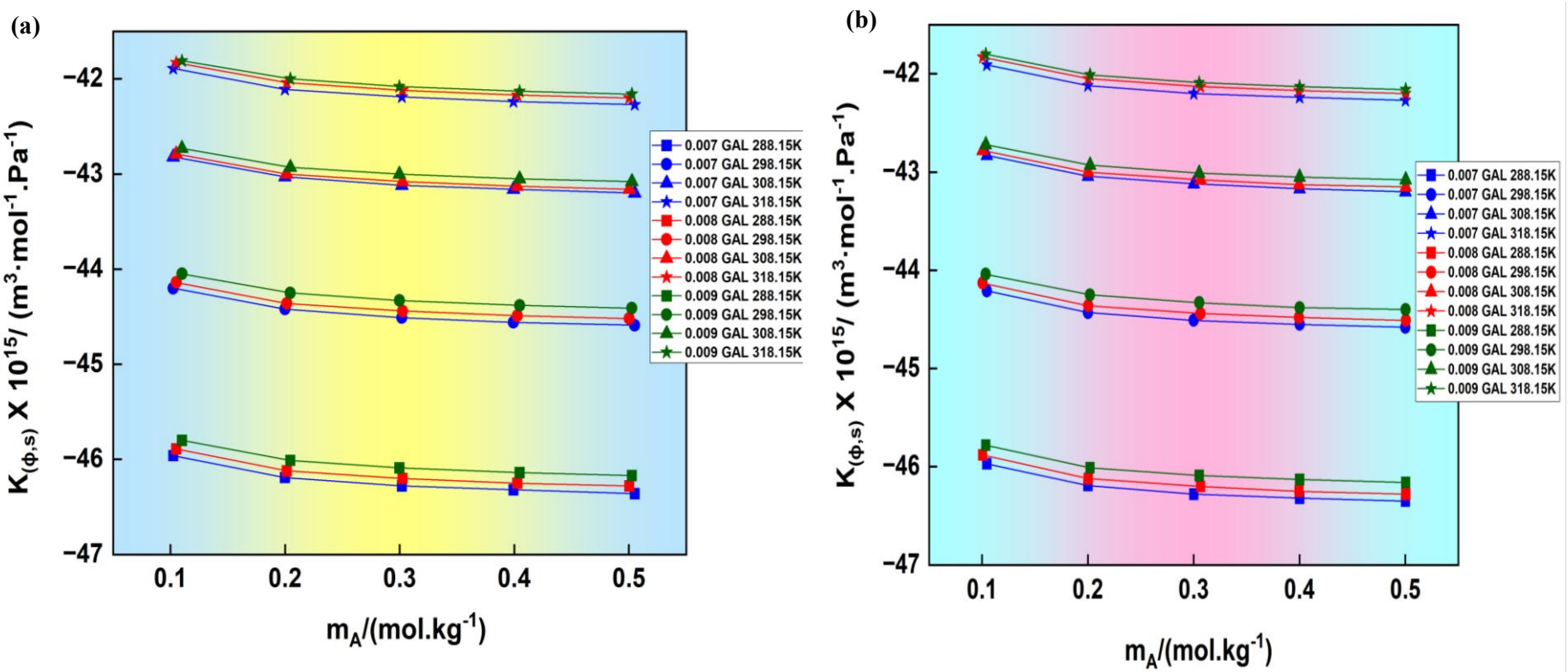

Figure 4.39 Plot shows the variation of $K_{\phi,S}$ with respect to molality at different m_B for (a) PG and (b) HG (blue-0.007 $mol.kg^{-1}$galactose; red-0.008 $mol.kg^{-1}$galactose; green-0.009 $mol.kg^{-1}$galactose) (square- 288.15K, circle- 298.15K, up triangle- 308.15 K and star- 318.15K)

Partial molar isentropic compression

Furthermore, the interaction behavior of the components at infinite dilution can be understood by applying the $K_{\phi,S}^{0}$. By visualizing $K_{\phi,S}$ v/s m_A for the solute in aqueous solvent from the relation stated in Eq. **4.5**, the $K_{\phi,S}^{0}$, and S_k^*, may be obtained using the linear regression approach.

The experimental slope, S_k^*, gives information on solute-solute interactions, and the intercept, $K_{\phi,S}^{0}$, is unrestricted from solute-solute associations and so measures solute-solvent interactions. In **Table 4.51**, you can see the values of $K_{\phi,S}^{0}$ and S_k^*. All negative $K_{\phi,S}^{0}$ which is further dropping as the T rises, is seen in **Figure 4.40**. If $K_{\phi,S}^{0}$ is negative, then the H_2O molecules near the glycol would be more resistant to compression than the bulk H_2O. Due to its more open structure, bulk water is better at compressibility than electrostricted water, according to various models [31-33]. There is an increase in the compression of the bulk solution because of the release of more H_2O molecules from the area around galactose as a result of electrostriction reduction, which occurs when the temperature rises. Addition of galactose also reduces the electrostriction effect, which improves solute-solvent interactions.

Table 4.51 Computed $K^0_{\phi,S}$ and its experimental slopes, S^*_K in water-based galactose for both glycols at different compositions and temperatures.

m_B /$mol.kg$	$K^0_{\phi,S} \times 10^6/(m^3.mol^{-1}.GPa^{-1})$				$S^*_K \times 10^6/(kg.m^3.mol^{-2}.GPa^{-1})$			
	$288.15K$	$298.15K$	$308.15K$	$318.15K$	$288.15K$	$298.15K$	$308.15K$	$318.15K$
PG								
0.007	-45.94(±0.08)	-44.18(±0.07)	-42.80(±0.07)	-41.87(±0.07)	-0.94(±0.23)	-0.90(±0.22)	-0.89(±0.22)	-0.88(±0.21)
0.008	-45.87(±0.07)	-44.12(±0.07)	-42.76(±0.07)	-41.81(±0.07)	-0.92(±0.22)	-0.89(±0.21)	-0.87(±0.21)	-0.87(±0.20)
0.009	-45.78(±0.07)	-44.03(±0.07)	-42.71(±0.06)	-41.79(±0.06)	-0.87(±0.20)	-0.84(±0.20)	-0.83(±0.19)	-0.83(±0.19)
HG								
0.007	-45.95 (±0.07)	-44.20(±0.07)	-42.81(±0.07)	-41.89(±0.07)	-0.89(±0.22)	-0.87(±0.21)	-0.86(±0.21)	-0.86(±0.21)
0.008	-45.87(±0.08)	-44.11(±0.08)	-42.76(±0.07)	-41.81(±0.07)	-0.92(±0.23)	-0.90(±0.23)	-0.89(±0.22)	-0.89(±0.22)
0.009	-45.77(±0.07)	-44.02(±0.07)	-42.70(±0.07)	-41.78(±0.07)	-0.89(±0.22)	-0.87(±0.22)	-0.86(±0.21)	-0.86(±0.21)

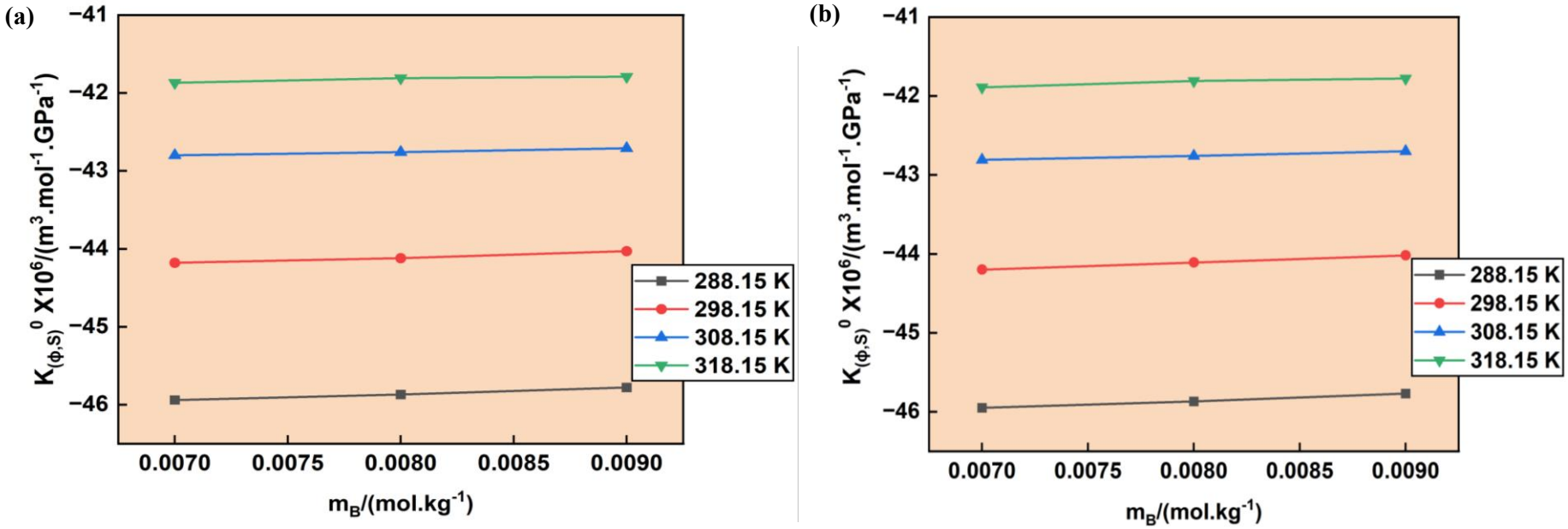

Figure 4.40 Graphical representation of $K_{\phi,S}^{0}$ with respect to Concentrations for Galactose and distinct temperature range. (a) PG; (b) HG

Partial molar isentropic compression of transfer

The partial molar isentropic compression of transfer, $\Delta K^0_{\phi,S}$ for glycol from water to aqueous galactose solutions at infinite dilution has been determined by using the equation **4.7.** A net volume decrease occurs when hydration co-spheres of hydrophobic-hydrophobic groups and ion-hydrophobic/hydrophilic-hydrophobic groups overlap, but volume inflation occurs when electrostricted water molecules are released into the bulk solution by combining hydration co-spheres of two ionic species [34]. The values of $\Delta K^0_{\phi,S}$ are tabulated in **Table 4.52**. The interactions among the co-spheres of glycol and galactose particles are dominant, as indicated by the positive $\Delta K^0_{\phi,S}$ values. As the molal concentration of the taken galactose increases, the estimated transfer values also increase, which means that the attractive interactions among the solute and the PHA particles are amplified, and the electrostriction of the water around the solute pieces is diminished. The outcome is an increase in the bulk solution's compressibility due to the diffusion of electrostricted water into its interior [35].

Table 4.52

Obtained data of ($\Delta K^0_{\phi,S}$) corresponding to temperature values at different concentrations of galactose in water with PG/HG.

m_B/ $(mol.kg^{-1}$	$\Delta K^0_{\phi,S} \times 10^6/(m^3.mol^{-1}.GPa^{-1})$ $T/(K)$				m_B/ $(mol.kg^{-1}$	$\Delta K^0_{\phi,S} \times 10^6/(m^3.mol^{-1}.GPa^{-1})$ $T/(K)$			
	288.15 K	**298.15 K**	**308.15 K**	**318.15 K**		**288.15 K**	**298.15 K**	**308.15 K**	**318.15 K**
	PG					**HG**			
0.007	0.09	0.06	0.09	0.08	**0.007**	0.08	0.04	0.08	0.06
0.008	0.16	0.12	0.13	0.14	**0.008**	0.16	0.13	0.13	0.14
0.009	0.25	0.21	0.18	0.16	**0.009**	0.26	0.22	0.19	0.17

Pair and Triplet interaction coefficient

Examining the solute and solvent in a pair is the major focus of interaction coefficient research. You can learn a lot about the chemistry of solutions from these coefficients. The (ΔV_ϕ^0 and ΔK_ϕ^0) acquired from volumetric and compressibility investigations are used to examine the interaction coefficients. The equations are **4.13** and **4.14** are used where the letters A and B stand for the solute and the solvent, respectively. In this context, m_B represents the solvent's molality, V_{AB} and V_{ABB} are the coefficients for volume, respectively. The K_{AB} and K_{ABB} are the coefficients for isentropic compression, respectively. The results of transfer (ΔV_ϕ^0 and ΔK_ϕ^0) are used to fit those equations, which yields these coefficients. The values acquired for both pair and triplet coefficients are tabulated in **Table 4.53**. Glycol interacts mostly through triplet interactions, as V_{ABB} and K_{ABB} are both positive for glycol in the presence of galactose. Also V_{AB} is positive for PG at just 288.15 K. Additionally, V_{AB}, V_{ABB} and K_{ABB} values that are positive indicate that contacts between hydrophilic and ion molecules, as well as hydrophobic and hydrophilic effects, are more common than aquaphobic connections. Yet, except for V_{AB} at 288.15 K, the K_{AB} and V_{AB} are all negative. These outcomes specify the supremacy of triplet over pairwise combinations amongst the system. Moreover, the stronger solute/solvent interactions were found in the combination when the present study's overall analysis of the interaction coefficients was performed. [36-38]

Table 4.53 V_{AB}, V_{ABB}, K_{AB}, K_{ABB} for the combination-water, PG/HG and galactose at same T range & concentrations, p constant.

T/(K)	$V_{AB} \times 10^6$ $/(m^3.mol^{-2}.kg)$	$V_{ABB} \times 10^6$ $/(m^3.mol^{-3}.kg^2)$	$K_{AB} \times 10^6$ $/(m^3.mol^{-2}.kgGPa^{-1})$	$K_{ABB} \times 10^6$ $/(m^3.mol^{-3}.kg^2GPa^{-1})$
		Propylene glycol		
288.15	5.56	485.35	-13.57	1913.23
298.15	-0.71	860.28	-16.31	1938.32
308.15	-12.07	1542.41	-2.77	883.64
318.15	-10.01	1239.3911	-7.06	1182.99
		Hexylene glycol		
288.15	-6.94	691.42	-19.85	2411.00
298.15	-3.85	477.02	-21.78	2378.08
308.15	-6.45	685.79	-8.31	1321.56
318.15	-8.87	984.46	-12.98	1644.52

Conclusion

By measuring density and sound speed with an extremely precise instrument known as a DSA from the Anton Paar Company (model number 5000 M), the molecular dynamics can be located and examined. Then, the type of interactions discovered in the mixture of three components—one PHA, galactose, and two glycols, either propylene glycol or hexylene glycol—with water—were analyzed by measuring the different parameters that had been determined. Using a stable pressure and same T range, three distinct doses of PHA—0.007, 0.008, and 0.009 $mol.kg^{-1}$— are employed. Each of the five glycols was tested at a concentration of 0.1–0.5 mol.kg-1, with a standard deviation of 0.1 $mol.kg^{-1}$. As the galactose m_A and m_B grow, the positive V_ϕ values demonstrate significant connections in the blend. It is also evident as S_V^* values are smaller than V_ϕ^0. Based on the positive ΔV_ϕ^0 values, it is evident that the most prominent interactions between galactose and water or glycols are ion-hydrophilic and hydrophilic-hydrophilic. The solutions investigated across the entire working temperature range show positive E_ϕ^0 values, suggesting the presence of significant ion-hydrophilic interactions between the solvent molecules and the solute. Throughout the whole concentration range of PG/HG and galactose, the negative $K_{\phi,S}$ values show that the solvent diffuses into the intra ionic free space of the organic molecules. Improved solute-solvent interactions are another benefit of adding galactose, which lowers the electrostriction effect. The majority of the interactions between galactose in water and glycol occur via triplet interactions.

Problem-8

Volumetric and acoustical studies of glycols with water-soluble lactobionic acid solutions at different temperatures

This problem presented the densities, ρ and sound speed v of PG and HG in "(0.007, 0.008, 0.009) mol·kg^{-1} aqueous solutions of one of the polyhydroxy acids: Lactobionic acid (LBA) at temperatures T = (288.15, 298.15, 308.15,318.15) K" and fixed pressure.

Volumetric parameters:

Density

The ρ measurements have been employed to calculate several volumetric properties. **Table 4.54** provides the investigational density data for propylene and hexylene glycols dissolved in water-soluble lactobionic acid solutions at several concentrations and across different temperatures. **Figure 4.41** presents a comparison between the investigated densities and those stated in the literature for aqueous lactobionic acid at various temperatures [39] The close alignment between our measurements and previously reported data confirms the accuracy and reliability of the present work. A consistent trend is observed where density decreases as temperature increases which can be accredited to the weakening of the hydrogen bonding network among molecules, leading to a more expanded molecular arrangement [5,8,40-41].

Apparent molar volume

The V_ϕ is found by using experimental ρ stated in **Table 4.54 with uncertainty of**, u (V_ϕ) = $(0.05 - 0.07) \times 10^6/(m^3.mol^{-1})$. V_ϕ data for propylene and hexylene glycols in water-soluble lactobionic acid solutions were evaluated at several temperatures. The already stated formula for V_ϕ in equation **4.1** is applied for these calculations. A consistent trend reveals that greater concentrations cause a minor rise in volume. The graphical data in **Figures 4.42** and **Figure 4.43** reveal that V_ϕ values progressively increase with both temperature and glycols (PG/HG) molality at a specified lactobionic acid concentration. This phenomenon arises mainly from the interactions between glycols and lactobionic acid, diminishing the electrostrictive influence of solute particles on water. Consequently, the apparent molar volume shows an upward trend. The enhanced V_ϕ values further imply the dominance of dipole-dipole and dipole-induced-dipole interactions, emphasizing a stronger hydrophilic

behavior [42–44].

The analysis reveals that chemical features such as polarity and the ability to form hydrogen bonds play a key role in solute-solvent interactions. Continued exploration of these aspects can deepen knowledge about solution properties and assist in optimizing pharmaceutical formulations, where these interactions contribute to the design of more stable and desired therapeutic effects [45].

Table 4.54 ρ and V_ϕ in the ternary blend of lactobionic acid with glycols (PG/HG) at several temperatures.

$^{a}m_A$/ $(mol.kg^{-1})$	$\rho \times 10^{-3}/(kg.m^{-3})$				$V_\phi \times 10^{6}/(m^{3}.mol^{-1})$			
	$288.15K$	$298.15K$	$308.15K$	$318.15K$	$288.15K$	$298.15K$	$308.15K$	$318.15K$
0.007 ($mol.kg^{-1}$) Lactobionic Acid + PG								
0.00000	0.99995	0.99777	0.99461	0.99090				
0.12187	1.00027	0.99809	0.99495	0.99126	73.48	73.56	73.64	73.73
0.19996	1.00045	0.99828	0.99515	0.99148	73.55	73.65	73.71	73.80
0.30539	1.00069	0.99853	0.99543	0.99176	73.60	73.69	73.74	73.83
0.39935	1.00089	0.99873	0.99565	0.99200	73.68	73.76	73.80	73.88
0.50787	1.00111	0.99897	0.99589	0.99226	73.72	73.79	73.86	73.96
0.008 ($mol.kg^{-1}$) Lactobionic Acid + PG								
0.00000	1.00003	0.99793	0.99478	0.99106				
0.11192	1.00032	0.99822	0.99508	0.99138	73.50	73.63	73.75	73.83
0.20147	1.00053	0.99843	0.99531	0.99163	73.58	73.69	73.81	73.89
0.30734	1.00077	0.99867	0.99556	0.99189	73.65	73.76	73.86	73.96
0.40592	1.00096	0.99887	0.99578	0.99212	73.73	73.84	73.94	74.04
0.52186	1.00120	0.99911	0.99603	0.99238	73.76	73.89	73.99	74.10
0.009 ($mol.kg^{-1}$) Lactobionic Acid + PG								
0.00000	1.00011	0.99813	0.99498	0.99125				
0.11007	1.00038	0.99841	0.99527	0.99156	73.61	73.71	73.79	73.92
0.20459	1.00060	0.99863	0.99550	0.99181	73.67	73.77	73.86	73.96
0.30060	1.00081	0.99884	0.99573	0.99204	73.70	73.82	73.91	74.02

0.40525	1.00102	0.99905	0.99595	0.99229	73.77	73.89	73.99	74.09
0.50853	1.00122	0.99925	0.99616	0.99251	73.82	73.95	74.05	74.16
0.007 ($mol.kg^{-1}$)Lactobionic Acid + HG								
0.00000	0.99995	0.99777	0.99461	0.99090				
0.09900	1.00012	0.99796	0.99483	0.99116	116.43	116.47	116.52	116.56
0.19998	1.00029	0.99814	0.99505	0.99141	116.45	116.50	116.55	116.60
0.30373	1.00045	0.99832	0.99526	0.99165	116.48	116.52	116.58	116.64
0.39993	1.00059	0.99848	0.99544	0.99187	116.50	116.56	116.61	116.67
0.49707	1.00072	0.99863	0.99561	0.99208	116.54	116.60	116.65	116.70
0.008 ($mol.kg^{-1}$)Lactobionic Acid + HG								
0.00000	1.00003	0.99793	0.99478	0.99106				
0.10084	1.00020	0.99812	0.99500	0.99132	116.46	116.51	116.56	116.61
0.19990	1.00036	0.99829	0.99521	0.99156	116.48	116.54	116.59	116.64
0.29912	1.00051	0.99846	0.99540	0.99179	116.51	116.58	116.63	116.68
0.39936	1.00065	0.99861	0.99559	0.99201	116.55	116.61	116.67	116.72
0.50689	1.00079	0.99877	0.99577	0.99223	116.59	116.65	116.71	116.75
0.009 ($mol.kg^{-1}$) Lactobionic Acid + HG								
0.00000	1.00011	0.99813	0.99498	0.99125				
0.09996	1.00028	0.99831	0.99519	0.99150	116.50	116.54	116.60	116.64
0.20027	1.00043	0.99848	0.99539	0.99174	116.53	116.58	116.64	116.68
0.29998	1.00058	0.99864	0.99558	0.99196	116.56	116.61	116.68	116.72
0.40005	1.00071	0.99880	0.99576	0.99217	116.59	116.64	116.71	116.76
0.49898	1.00083	0.99894	0.99593	0.99238	116.63	116.67	116.73	116.78

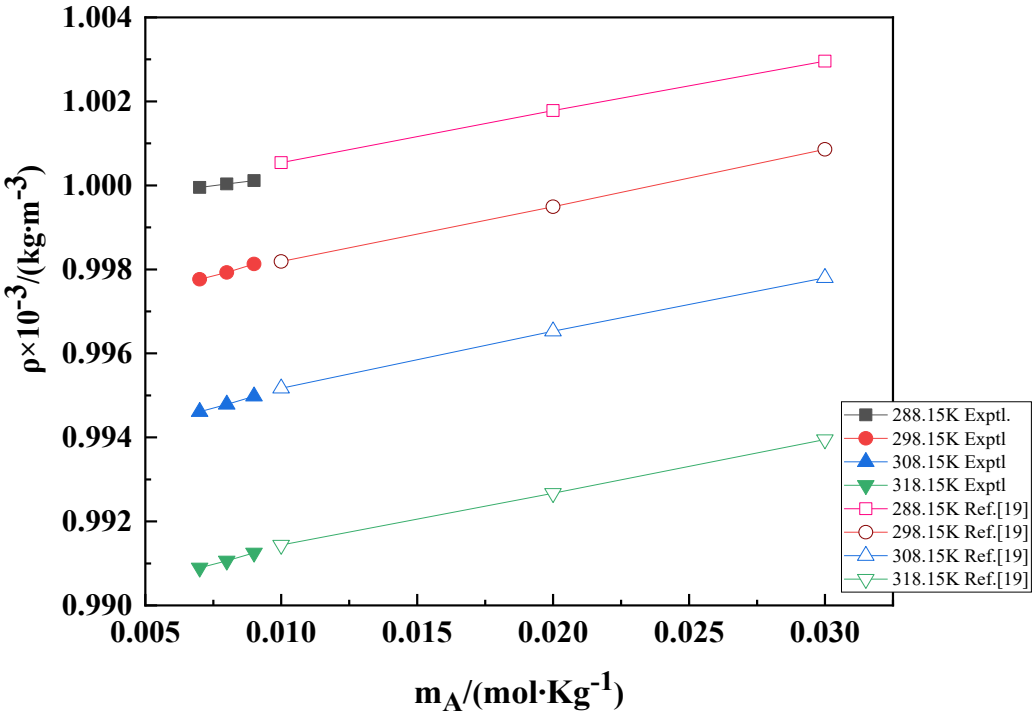

Figure 4.41 Assessment of densities for lactobionic acid with water between measured and literature values at different concentrations and temperatures [39].

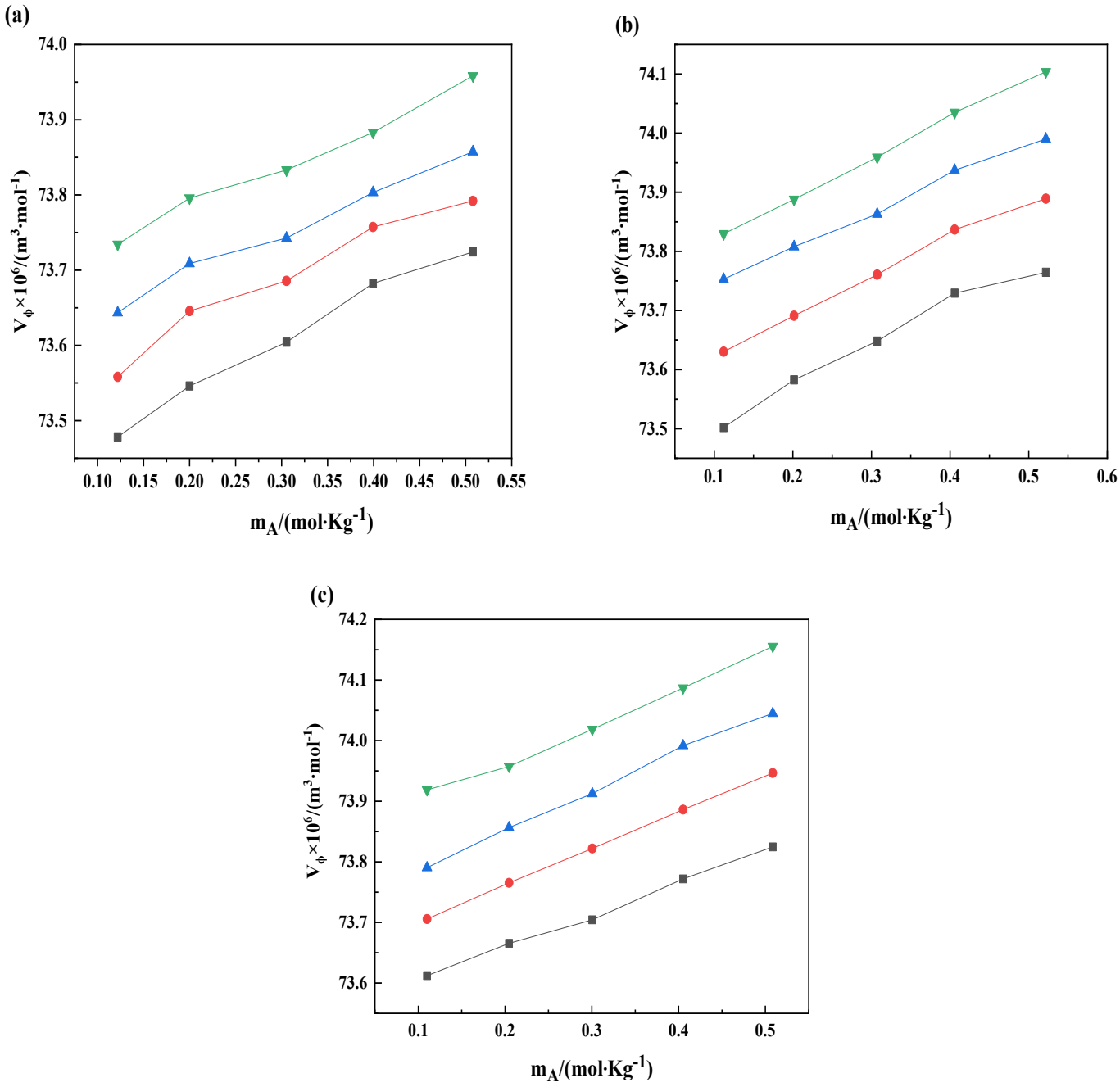

Figure 4.42 Plots demonstrate the changes in (V_ϕ) of 0.007, 0.008, and 0.009 $mol.kg^{-1}$ LBA with the molality of propylene glycol at varying temperatures in (a), (b) and (c) respectively [black square (288.5K); red circle (298.15K); blue upward triangle (308.15K); green downward triangle (318.15K)].

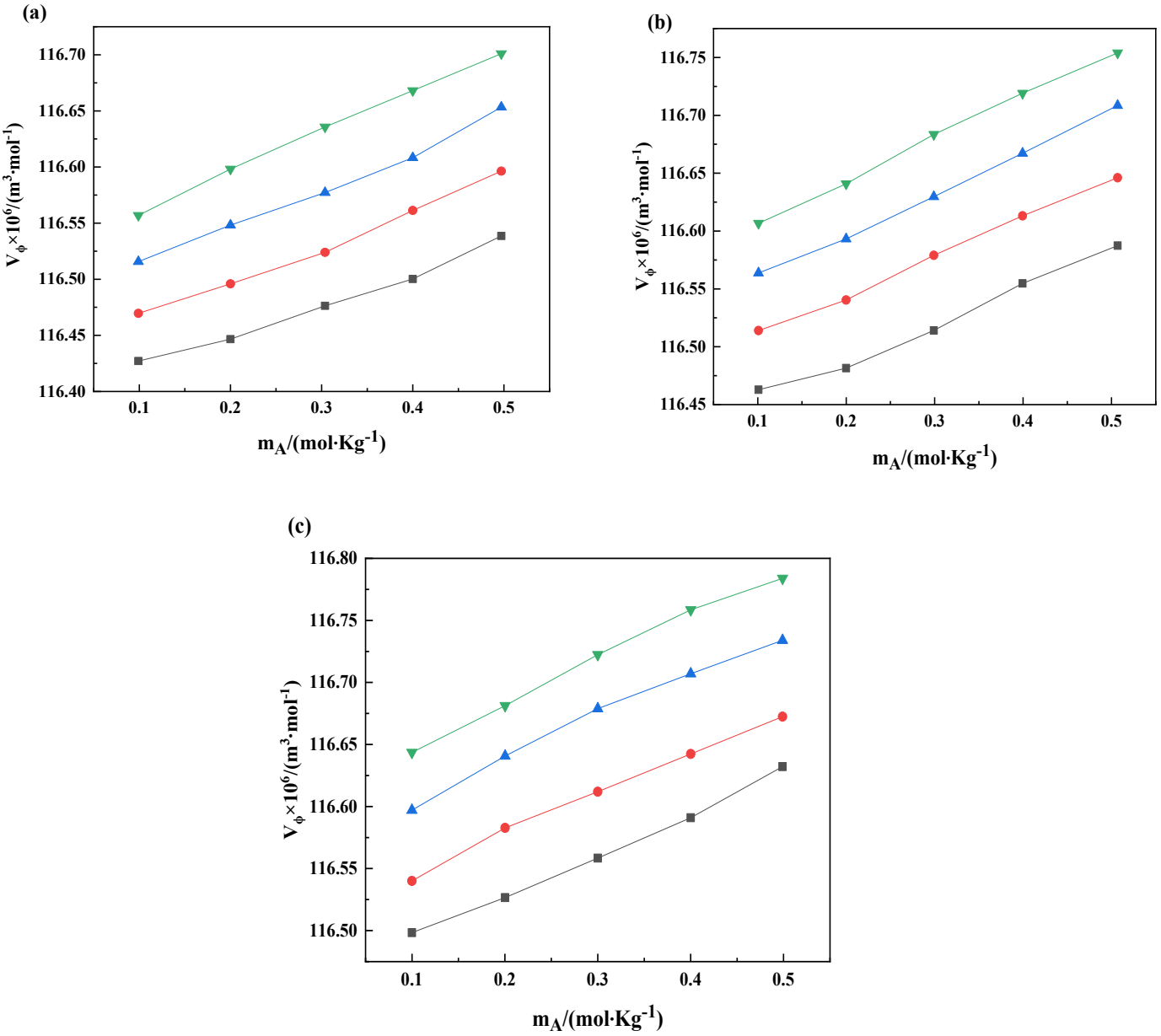

Figure 4.43 Plots demonstrate the changes in (V_ϕ) of (a) 0.007 LBA; (b) 0.008 LBA; (c) 0.009 LBA with the molality of hexylene glycol at varying temperatures [black square (288.5K); red circle (298.15K); blue upward triangle (308.15K); green downward triangle (318.15K)].

Partial molar volume

The addition of an infinitesimal quantity of a solute to a solution at persistent temperature and pressure leads to a measurable change in the total volume, which is quantified by this parameter [46]. The formula stated in equation **4.4,** combined with least-squares fitting analysis was employed to estimate the partial molar volumes of LBA and glycols (PG/HG) solutions. The magnitude of S_V^* is significantly smaller in comparison to the respective V_ϕ^0 values as recorded in **Table 4.55** with uncertainty of u (V_ϕ^0)= $0.01 \times 10^6/(m^3.mol^{-1})$ and u (S_V^*) = $\pm 0.03 \times /(m^3.kg.mol^{-2})$. The irregular patterns detected in values imply the influence of other factors on solute interaction mechanisms. The V_ϕ^0 values for both propylene and hexylene glycols were positive and demonstrated a steady increase with the enhancement of lactobionic acid concentration, as shown in **Figure 4.44**. The 'co-sphere overlap' scheme suggests that the interaction and overlap of ionic hydration shells within a solution contribute to a rise in the solution volume, resulting from the combination of ionic and hydration shell spaces[47,48]. The upward trend in V_ϕ^0 with increasing glycols molality reflects that the ions interact more effectively with hydrophilic groups than with hydrophobic groups in the solution. In this study, solute and solvent interactions are predominant, as evidenced by the significantly lower S_V^* values compared to the corresponding V_ϕ^0 values [49-50,22].

Transfer of partial molar volume

In thermodynamics, ΔV_ϕ^0 characterizes the volume shift occurring during the transition of a solute molecule transfers between two phases. This property was determined using the mathematical expression given in equation **4.6.** The **Table 4.56** lists the positive transfer parameter values observed for propylene and hexylene glycols when dissolved in lactobionic acid solutions with uncertainty of (ΔV_ϕ^0)= $\pm 0.06 \times 10^6/(m^3.mol^{-1})$. Based on Pauling's hypothesis, the clathrate structures in water are available for occupation by other molecules. While glycols are expected to occupy these voids, they instead disrupt the original water structure and may generate a new hydrogen-bonded arrangement with the water molecules [51,52]. This study involves a system where both solute and solvent components- propylene glycol, hexylene glycol, lactobionic acid, and water are electrolytic in nature. The resulting

ΔV_{ϕ}^{0} measurements, can be attributed to ion-ion associations in the aqueous medium. This work reveals that the solutes improve the structural organization of the solution, which is facilitated by ion-ion, ion-hydrophilic, and hydrophilic behavior of both glycols and lactobionic acid [11,53-54].

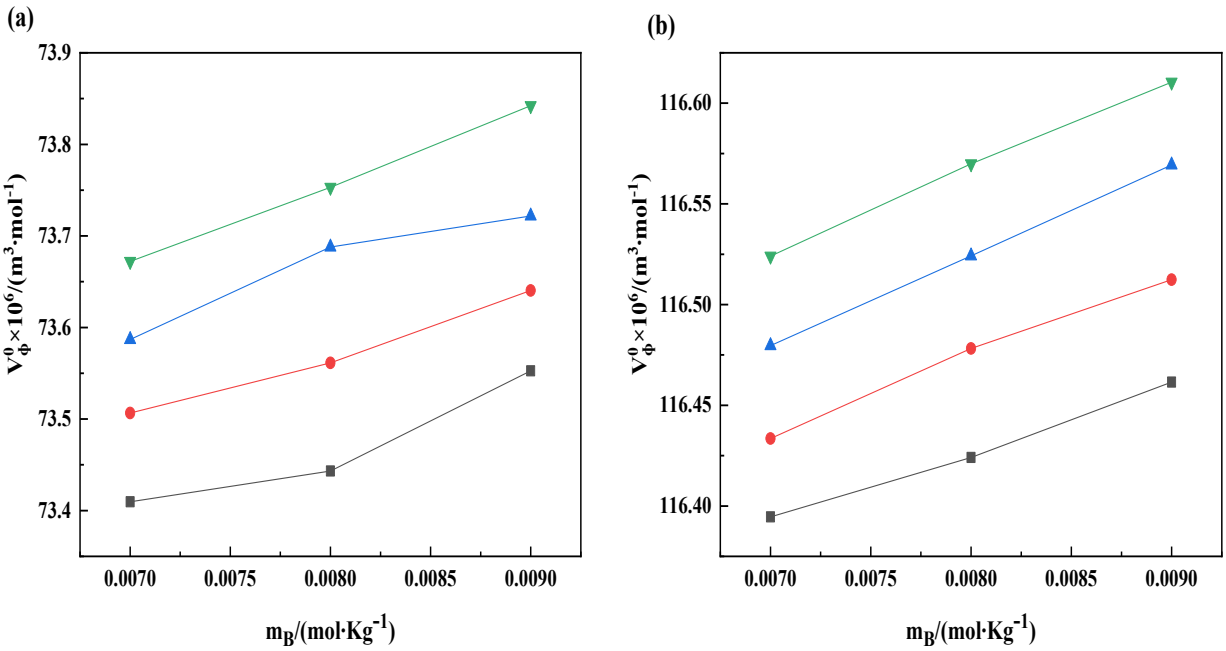

Figure 4.44 Plots representing the variations in V_{ϕ}^{0}, for (a) PG, (b) HG inside an LBA solution at numerous temperatures [black square (288.5K); red circle (298.15K); blue upward triangle (308.15K); green downward triangle (318.15K)].

Table 4.55 Calculated V_{ϕ}^{0} and S_{V}^{*} values of lactobionic acid in water-soluble solutions with PG/HG.

[a]m_B/ (mol·kg^{-1})	$V_{\phi}^{0} \times 10^{6}/(m^3.mol^{-1})$				$S_{V}^{*} \times 10^{6}\ /(m^3.kg.mol^{-2})$			
	$288.15K$	$298.15K$	$308.15K$	$318.15K$	$288.15K$	$298.15K$	$308.15K$	$318.15K$
				PG				
0.000	73.39(±0.00)	73.46(±0.00)	73.55(±0.00)	73.62(±0.00)	0.59(±0.01)	0.58(±0.00)	0.55(±0.00)	0.55(±0.00)
0.007	73.41(±0.01)	73.51(±0.02)	73.59(±0.01)	73.67(±0.01)	5.88(±0.11)	6.18(±0.09)	5.96(±0.04)	5.88(±0.09)
0.008	73.44(±0.02)	73.56(±0.01)	73.69(±0.01)	73.75(±0.00)	5.93(±0.04)	6.29(±0.11)	5.93(±0.11)	5.82(±0.12)
0.009	73.55(±0.01)	73.64(±0.00)	73.72(±0.01)	73.84(±0.01)	5.76(±0.04)	6.19(±0.10)	5.68(±0.25)	5.80(±0.31)
				HG				
0.000	116.35(±0.000)	116.39(±0.000)	116.43(±0.001)	116.46(±0.001)	0.23(±0.001)	0.23(±0.001)	0.24(±0.004)	0.24(±0.003)
0.007	116.39(±0.006)	116.43(±0.005)	116.48(±0.006)	116.52(±0.003)	0.277(±0.019)	0.320(±0.017)	0.336(±0.019)	0.360(±0.008)
0.008	116.42(±0.007)	116.48(±0.003)	116.52(±0.003)	116.57(±0.003)	0.319(±0.020)	0.333(±0.010)	0.360(±0.010)	0.368(±0.010)
0.009	116.46(±0.005)	116.51(±0.005)	116.57(±0.007)	116.61(±0.005)	0.333(±0.014)	0.325(±0.014)	0.341(±0.021)	0.359(±0.016)

Table 4.56 Transfer parameter of ΔV_{ϕ}^{0}, of PG/HG in the water-soluble solution of lactobionic acid at same temperatures and m_B.

[a]m_B/ (mol·kg^{-1})	$\Delta V_{\phi}^{0} \times 10^{6}/(m^3 \cdot mol^{-1})$			
	$288.15K$	$298.15K$	$308.15K$	$318.15K$
		PG		
0.007	0.02	0.05	0.04	0.05
0.008	0.05	0.10	0.14	0.13
0.009	0.16	0.18	0.17	0.22
		HG		
0.007	116.35	116.41	116.44	116.48
0.008	116.38	116.42	116.47	116.50
0.009	116.40	116.44	116.49	116.56

Partial molar volume relying on temperature T

By applying a thermodynamic relation given in Eq. **4.8** the temperature-dependent V_ϕ° can be determined which enables a deeper exploration into the molecular dynamics of the solution [55]. Here, the reference temperature, denoted by T_{ref}, is fixed at 298.15 K. The parameters labelled a, b, and c are coefficients extracted from the experimental observations. These coefficients for propylene and hexylene glycols dissolved in lactobionic acid solutions as represented in **Table 4.57**. The R^2 values recorded in this study indicate that the experimental data show very minor deviations and correspond well to the polynomial fitting [6,56]. The main purpose behind evaluating V_ϕ° is to derive the expansibilities, which can be computed as stated in Eq. **4.11**. The persistence of solute-solvent bonds, evidenced by the positive E_ϕ^0 values as represented in **Table 4.58** highlight the role of apparent molar volume which are attributed to the caging or packing mechanism. The structural behavior (structure creator or disruptor) of the solute in the solvent was determined through a thermodynamic relationship introduced by Hepler [24,57] given in Eq. **4.12.** Hepler's thermodynamic approach is widely utilized to assess whether glycols (PG/HG) in a lactobionic acid mixture act as a structure creator or disruptor [58]. The negative values of the $(\partial E_\phi^0 / \partial T)_P$ were observed for propylene glycol, except at 0.009 $mol.kg^{-1}$and for hexylene glycol, except 0.007 $mol.kg^{-1}$in all LBA aqueous mixtures as shown in **Table 4.58**. These findings imply the prevalence of structure-disrupting tendencies in the current study.

Acoustic parameters:

Sound speed: The sound speed is a crucial parameter for calculating various acoustic properties, providing valuable insight into the interactions inside the solution. Ultrasonic speed data for the combinations of water, lactobionic acid, and glycols (PG/HG) at varying compositions (0.007, 0.008, 0.009) $mol.kg^{-1}$ have been measured and are reported in **Table 4.59**. An intensification in both temperature and molality of propylene or hexylene glycol results in higher sound velocity. This phenomenon can be ascribed to the creation of hydrogen bonds inside solute and solvent, influenced by water's extensive hydrogen bonding framework. The lactobionic acid-glycols solution shows enhanced sound propagation due to these interactions. Furthermore, as the molecular mass rises from PG to HG, the original bonds

within water-lactobionic acid become weaker, allowing lactobionic acid to form new associations with the glycols [7, 59-60].

Table 4.57 Evaluation of a, b, c and Average relative deviations (ARD) of lactobionic acid in water-soluble solutions with PG and HG.

$m_B/(mol.kg^{-1})$	$a \times 10^6/$ $(m^3.mol^{-1})$	$b \times 10^6/$ $(m^3.mol^{-1}.K^{-1})$	$c \times 10^6/$ $(m^3.mol^{-1}.K^{-2})$	R^2	ARD
		PG			
0.007	73.50	0.009	0.000	0.9999	0.0000
0.008	73.57	0.012	0.000	0.9999	0.0000
0.009	73.63	0.009	0.000	0.9999	0.0000
		HG			
0.007	116.43	0.004	0.000	0.9999	0.0000
0.008	116.48	0.005	0.000	0.9999	0.0000
0.009	116.52	0.005	0.000	0.9999	0.0000

Table 4.58 Values of E_{ϕ}^{0} of LBA in water-soluble solutions with PG/HG at various temperatures and concentrations.

[a]m_B/ $(mol.kg^{-1})$	$E_{\phi}^{0} \times 10^{6}/(m^{3}.mol^{-1}.K^{-1})$				$\left(\frac{\partial E_{\phi}^{0}}{\partial T}\right)_P/(m^{3}.mol^{-1}.K^{-2})$
	$288.15K$	$298.15K$	$308.15K$	$318.15K$	
			PG		
0.007	0.010	0.009	0.008	0.008	-0.00006
0.008	0.015	0.012	0.009	0.007	-0.00026
0.009	0.007	0.009	0.010	0.012	0.00016
			HG		
0.007	0.004	0.004	0.004	0.005	0.00003
0.008	0.005	0.005	0.005	0.004	-0.00004
0.009	0.006	0.005	0.005	0.004	-0.00005

Table 4.59 v and $K_{\phi,s}$ of lactobionic acid in water-soluble solutions of PG/HG at several temperatures.

[a]m_A/ (mol·kg^{-1})	$v/(m.s^{-1})$				$K_{\phi,s} \times 10^6/(m^3.mol^{-1}.GPa^{-1})$			
	288.15K	298.15K	308.15K	318.15K	288.15K	298.15K	308.15K	318.15K
0.007 (mol·kg^{-1}) Lactobionic acid + PG								
0.00000	1467.54	1497.32	1520.25	1536.82				
0.12187	1473.54	1502.49	1524.64	1540.55	-46.07	-44.25	-42.93	-42.00
0.19996	1477.23	1505.78	1527.31	1543.06	-46.23	-44.41	-43.08	-42.15
0.30539	1482.92	1510.53	1531.46	1546.37	-46.32	-44.49	-43.16	-42.24
0.39935	1487.21	1513.95	1535.05	1549.03	-46.36	-44.54	-43.21	-42.28
0.50787	1491.36	1517.83	1537.74	1551.76	-46.40	-44.57	-43.24	-42.32
0.008 (mol·kg^{-1}) Lactobionic acid + PG								
0.00000	1468.09	1497.84	1520.72	1537.21				
0.11192	1473.73	1502.59	1524.68	1540.53	-46.00	-44.19	-42.87	-41.95
0.20147	1478.23	1506.57	1527.54	1543.23	-46.19	-44.38	-43.05	-42.13
0.30734	1483.19	1510.71	1531.6	1546.47	-46.28	-44.46	-43.14	-42.22
0.40592	1487.34	1514.45	1534.56	1549.56	-46.33	-44.51	-43.18	-42.26
0.52186	1493.44	1519.53	1539.14	1552.89	-46.37	-44.54	-43.21	-42.29
0.009 (mol·kg^{-1}) Lactobionic acid + PG								
0.00000	1468.86	1498.4	1521.49	1538.09				
0.11007	1473.98	1502.79	1525.31	1541.32	-45.94	-44.15	-42.82	-41.89
0.20459	1478.45	1506.45	1528.65	1544.23	-46.15	-44.35	-43.01	-42.09
0.30060	1482.83	1510.4	1531.6	1546.66	-46.23	-44.42	-43.09	-42.16

0.40525	1487.65	1514.65	1534.43	1549.15	-46.28	-44.47	-43.13	-42.21
0.50853	1491.81	1518.13	1538.02	1552.01	-46.31	-44.50	-43.17	-42.24
0.007 (mol·kg^{-1}) Lactobionic acid + HG								
0.00000	1467.54	1497.32	1520.25	1536.82				
0.09900	1479.51	1510.35	1530.15	1545.80	-45.83	-44.05	-42.74	-41.79
0.19998	1488.76	1520.44	1539.27	1556.50	-46.14	-44.35	-43.03	-42.08
0.30373	1498.55	1527.58	1547.87	1564.54	-46.22	-44.43	-43.10	-42.15
0.39993	1506.61	1535.88	1555.00	1572.24	-46.28	-44.48	-43.16	-42.21
0.49707	1514.18	1542.29	1562.66	1578.51	-46.31	-44.51	-43.19	-42.24
0.008 (mol·kg^{-1}) Lactobionic acid + HG								
0.00000	1468.09	1497.84	1520.72	1537.21				
0.10084	1482.21	1516.72	1535.90	1551.20	-45.72	-43.95	-42.63	-41.77
0.19990	1492.25	1526.95	1545.68	1562.91	-45.96	-44.18	-42.85	-42.00
0.29912	1502.01	1533.34	1555.14	1572.32	-46.05	-44.27	-42.94	-42.09
0.39936	1510.40	1541.53	1562.50	1579.64	-46.11	-44.32	-42.99	-42.14
0.50689	1518.53	1550.58	1569.87	1585.66	-46.14	-44.36	-43.03	-42.17
0.009 (mol·kg^{-1}) Lactobionic acid + HG								
0.00000	1468.86	1498.40	1521.49	1538.09				
0.09996	1485.04	1520.15	1539.85	1555.61	-45.52	-43.75	-42.52	-41.66
0.20027	1495.60	1531.30	1549.04	1565.18	-45.81	-44.03	-42.80	-41.94
0.29998	1505.46	1537.76	1558.56	1572.13	-45.89	-44.11	-42.88	-42.02
0.40005	1514.49	1547.65	1565.98	1579.84	-45.94	-44.15	-42.92	-42.06
0.49898	1521.91	1555.92	1575.21	1589.00	-45.97	-44.18	-42.95	-42.09

Apparent molar isentropic compression

The subsequent mathematical expression, known as the Laplace equation **4.2**, was utilized to derive the isentropic compressibility[62].The formula given in Eq. **4.3** is applied to ascertain the $K_{\phi,s}$values for PG and HG in aqueous solutions of LBA within uncertainty of $u\ (K_{\phi,S}) = 0.25 \times 10^6/(m^3.mol^{-1}.GPa^{-1})$. The computed $K_{\phi,s}$ values at varying levels of lactobionic acid and temperatures are provided in **Table 4.59** and their trends are illustrated in **Figures 4.44** and **4.45**. This table shows negative $K_{\phi,s}$ numbers are which suggests that water molecules farther from the ionic charges of the solute are more compressible than those closer to the solute, implying that the solute reduces water's overall structural compressibility [63-65]. It was observed that the compressibility of lactobionic acid declines with rising temperature, likely because of the creation of robust intermolecular H_2 bonds within lactobionic acid, propylene and hexylene glycols. Less negative $K_{\phi,s}$ values show that the solute changes how tightly water molecules are packed in the solution. This implies that the H_2O particles undergo some degree of reorganization near the solute, as indicated by the negative $K_{\phi,s}$ values. It can be inferred from these values that water molecules in proximity to the solute's charged ionic groups are more resistant to compression than those found in the bulk solution [66,67].

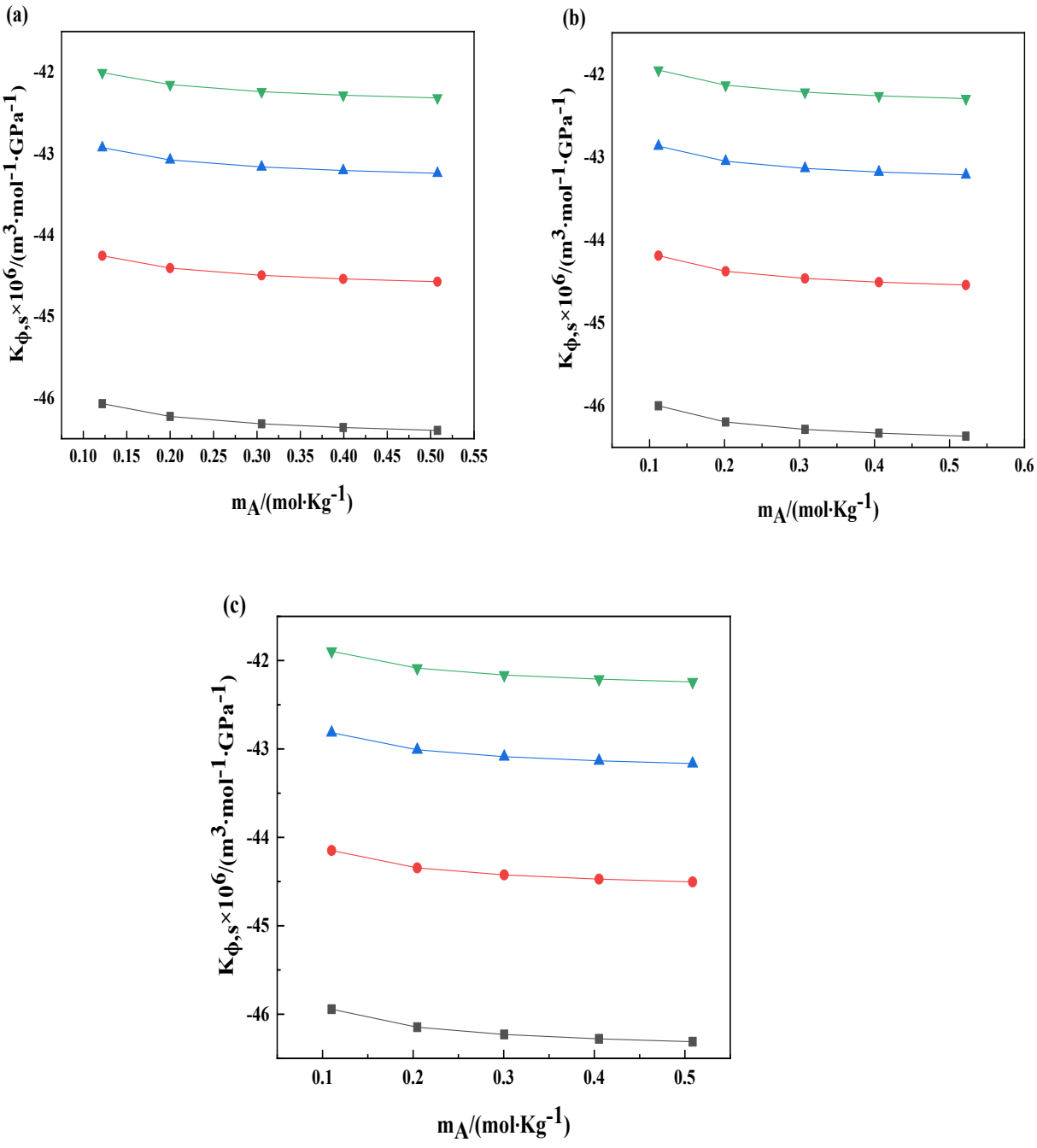

Figure 4.45 Changes in $K_{\phi,s}$, of PG in (a) 0.007 LBA; (b) 0.008 LBA; (c) 0.009 LBA for molality of propylene glycol solutions [black square (288.15K); red circle (298.15K); blue upward triangle (308.15K); green downward triangle (318.15K)].

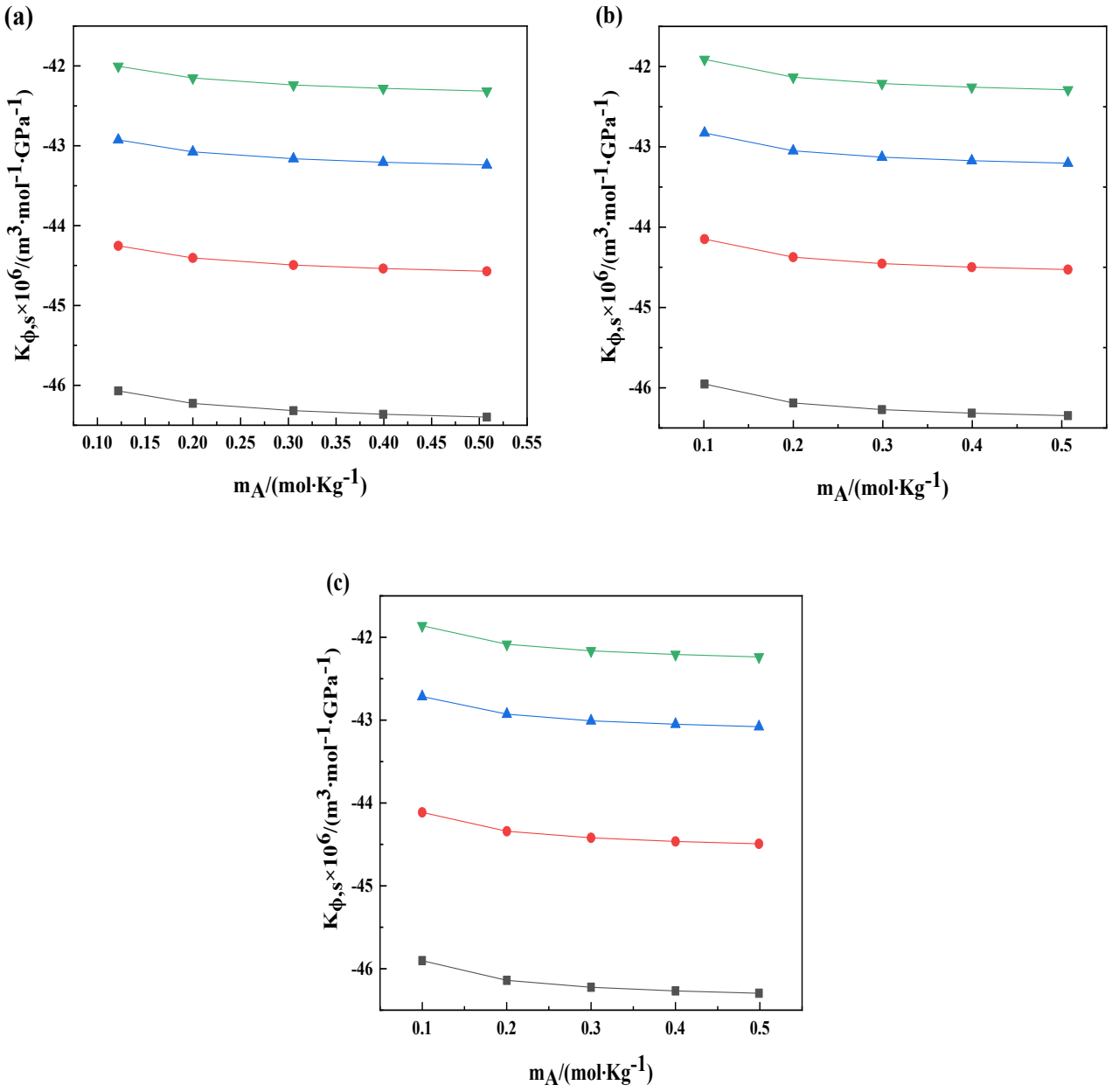

Figure 4.46 Changes of $K_{\phi,s}$, of hexylene glycol (HG) in of 0.007, 0.008, and 0.009 $mol.kg^{-1}$ LBA for molality of hexylene glycol solutions in (a), (b) and (c) respectively [black square (288.15K); red circle (298.15K); blue upward triangle (308.15K); green downward triangle (318.15K)].

Partial molar isentropic compression, $(K_{\phi,s}^{0})$

The computation of $K_{\phi,s}^{0}$ is carried out through Equation (**4.5**), which addresses variations in compressibility influenced by solute concentration. The S_K^* values at infinite dilution suggest limited interaction between the two components, likely resulting from the compactness of particles of solute. The reduction in the negativity of $K_{\phi,s}^{0}$with increasing temperature suggests intensified hydrogen bonding between water and the glycols (PG/HG) ions [18,68]. The computed acoustic virial coefficient (S_K^*) and $K_{\phi,s}^{0}$ values with their respective errors are shown in **Table 4.60** with uncertainty of u $(K_{\phi,S}^{0})$ = $0.01 \times 10^6/(m^3.\mathrm{mol}^{-1})$, u$(S_K^*)$= $\pm 0.24 \times 10^6$ /$(\mathrm{m}^3.\mathrm{kg}.\mathrm{mol}^{-2})$. This coefficient helps elucidate the interactions occurring among the solute particles. The graphical representation in **Figure 4.47** indicates a consistent decrease in the negativity of $K_{\phi,s}^{0}$ with rising temperature, implying intensified water-glycol interactions. As a result, the incorporation of propylene or hexylene glycols and water reduces electrostriction effects in the mixtures, thus strengthening the interaction between lactobionic acid and the varying molality of propylene and hexylene glycols, as interpreted through the Kirkwood model [31]. In this study, the observed negative values suggest enhanced binding between glycols and lactobionic acid, resulting in an ordered structuring of surrounding water molecules [69,70].

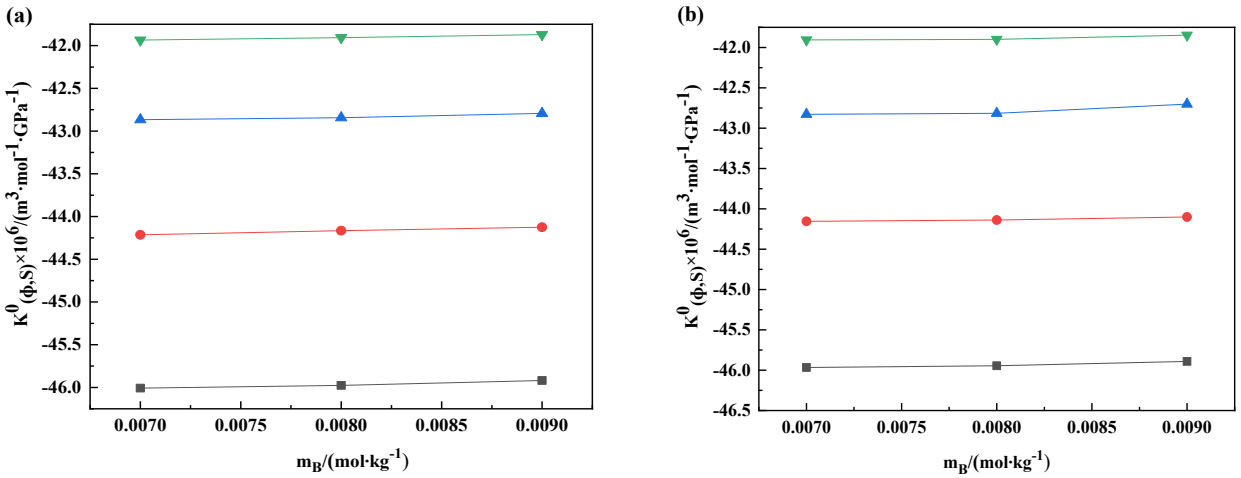

Figure 4.47 Plots representing $K_{\emptyset,S}^{0}$ for (a) PG and (b) HG in water-soluble lactobionic acid solution at varying temperatures [black square (288.5K); red circle (298.15K); blue upward triangle (308.15K); green downward triangle (318.15K)].

Table 4.60 Calculated $K^0_{\phi,S}$, and S^*_K, of the lactobionic acid with PG/HG at several temperatures.

$m_B/$ ($mol.kg^{-1}$)	$K^0_{\phi,s} \times 10^6/(m^3.mol^{-1})$				$S^*_K \times 10^6/(m^3.kg.mol^{-2})$			
	$288.15K$	$298.15K$	$308.15K$	$318.15K$	$288.15K$	$298.15K$	$308.15K$	$318.15K$
				PG				
0.000	-46.03 (±0.079)[b]	-44.24(±0.076)[b]	-42.89(±0.074)[b]	-41.95(±0.073)[b]	-0.96(±0.236)[b]	-0.93(±0.228)[b]	-0.91(±0.222)[b]	-0.91(±0.219)[b]
0.007	-46.01(±0.058)	-44.21(±0.055)	-42.87(±0.054)	-41.93(±0.054)	-0.80(±0.171)	-0.78(±0.165)	-0.77(±0.161)	-0.76(±0.159)
0.008	-45.98(±0.067)	-44.17(±0.065)	-42.84(±0.064)	-41.91(±0.063)	-0.84(±0.197)	-0.81(±0.190)	-0.79(±0.186)	-0.79(±0.184)
0.009	-45.92(±0.069)	-44.12(±0.067)	-42.79(±0.065)	-41.87(±0.064)	-0.86(±0.206)	-0.83(±0.198)	-0.82(±0.194)	-0.81(±0.191)
				HG				
0.000	-46.03(±0.079)[b]	-44.24(±0.077)[b]	-42.89(±0.075)[b]	-41.95(±0.074)[b]	-0.94(±0.240)[b]	-0.92(±0.232)[b]	-0.90(±0.226)[b]	-0.91(±0.223)[b]
0.007	-45.97(±0.080)	-44.05(±0.077)	-42.73(±0.076)	-41.78(±0.075)	-0.94(±0.241)	-0.91(±0.233)	-0.91(±0.228)	-0.91(±0.225)
0.008	-45.94(±0.079)	-43.92(±0.075)	-42.60(±0.074)	-41.59(±0.073)	-0.90(±0.236)	-0.87(±0.225)	-0.86(±0.222)	-0.87(±0.220)
0.009	-45.89(±0.079)	-43.74(±0.075)	-42.52(±0.070)	-41.66(±0.073)	-0.92(±0.238)	-0.88(±0.227)	-0.85(±0.210)	-0.88(±0.220)

Transfer of $K^0_{\phi,S}$

The relationship given in eq. **4.7** facilitates the evaluation of the variation in isentropic compressibility ($\Delta K^0_{\phi,S}$) for glycols in water containing lactobionic acid. The data with uncertainty of u ($\Delta K^0_{\phi,S}$) = $0.02 \times 10^6 (m^3.mol^{-1}.GPa^{-1})$ in **Table 4.61** reveals that $\Delta K^0_{\phi,S}$ remains positive at every temperature and concentration, though its magnitude reduces with increasing thermal conditions. The observed positive $\Delta K^0_{\phi,S}$ values reflect a reduction in electrostriction with increasing lactobionic acid concentration and greater affinity between its zwitterionic center and glycols. It is identified that water undergoing electrostriction exhibits lesser compressibility compared to bulk water with compressibility declining alongside increasing levels of lactobionic acid. The observed behavior can be ascribed to the overlap hypothesis suggested by Friedman and Krishnan, which highlights the influence of solute as well as solvent interactions have a direct significance on volume variations in solutions [71]. The negative $K^0_{\phi,S}$ and positive $\Delta K^0_{\phi,S}$ values at lower temperatures suggest that glycols establish stronger associations with lactobionic acid and water. The abundance of water molecules further amplifies these interactions through extensive hydrogen bonding [72-73].

Interaction coefficients

The interactions between pairs and triplets of components, represented by V_{AB}, V_{ABB}; K_{AB} K_{ABB}, can be obtained through the set of equations **4.13** and **4.14**. Here, the variables V_{AB} and V_{ABB} denote volumetric interaction terms for two and three-component systems. K_{AB} and K_{ABB} are used to describe their respective interactions for isentropic compressibilities as reported in **Table 4.62**. Propylene and hexylene glycols serve as the solute (A) while lactobionic acid acts as the solvent (B). The concept of interaction coefficients is based on the theoretical model developed by McMillan and Mayer[36] and later adapted by Krishnan and Friedman[37] to account for molecular contributions to solution behavior. At all examined temperatures, the pair interaction volume coefficients for the solutes (PG/HG) in aqueous LBA are negative which indicates that interactions between solute molecules result in contraction of the system volume. This behavior suggests that when two solute molecules interact, they likely promote tighter molecular packing or cause structural compression. However, V_{ABB} being positive for both glycols (PG/HG) across the entire temperature range imply that a third interacting entity

introduces an expansion effect. This may be attributed to structural disruption, leading to a reduced packing efficiency or the formation of less compact, possibly more hydrated. Negative K_{AB} values suggest that interactions between glycols reduce system compressibility by promoting tighter structuring. In contrast, positive values indicate that a third molecule disrupts this structure which enhances compressibility in the present investigation.

Table 4.61 Values of $\Delta K^0_{\phi,S}$, of the ternary system of lactobionic acid in water-soluble solutions with PG/HG at several temperatures and concentrations.

[a]m_B/ $(\boldsymbol{mol.kg^{-1}})$	$\Delta \boldsymbol{K^0_{\phi,S}} \times \boldsymbol{10^6}/(\boldsymbol{m^3.mol^{-1}.GPa^{-1}})$			
	$288.15K$	$298.15K$	$308.15K$	$318.15K$
		PG		
0.007	0.02	0.03	0.02	0.02
0.008	0.05	0.07	0.05	0.04
0.009	0.11	0.12	0.10	0.08
		HG		
0.007	0.06	0.08	0.06	0.04
0.008	0.09	0.10	0.07	0.05
0.009	0.14	0.14	0.19	0.10

Table 4.62 Interaction coefficients of water-soluble lactobionic acid with PG/HG at numerous temperatures.

$T/(K)$	$V_{AB} \times 10^6$ $/(m^3.mol^{-2}.kg)$	$V_{ABB} \times 10^6/$ $/(m^3.mol^{-3}.kg^2)$	$K_{AB} \times 10^6/$ $(m^3.mol^{-2}.kg.GPa^{-1})$	$K_{ABB} \times 10^6/$ $(m^3.mol^{-3}.kg^2.GPa^{-1})$
		PG		
$288.15K$	-27.25	2651.91	-10.38	1134.72
$298.15K$	-20.47	l2252.23	-11.23	1250.50
$308.15K$	-18.97	2160.74	-7.65	886.33
$318.15K$	-26.19	2860.44	-7.74	845.71
		HG		
$288.15K$	-5.98	842.93	-2.80	699.18
$298.15K$	-9.04	1123.91	2.44	344.74
$308.15K$	-9.55	1212.69	-7.90	1170.63
$318.15K$	-7.51	1118.60	-2.19	504.59

Conclusion

The last problem of our research focusses on the assessment of molecular behavior in ternary mixtures composed of a polyhydroxy acid (PHA-lactobionic acid) and two types of glycols-propylene or hexylene glycols in aqueous media. Several thermo-dynamic characteristics, such as apparent and partial molar properties, transfer characteristics, were evaluated under controlled experimental conditions and T varying from $288.15K$ to $318.15K$. The increase in solute molality and LBA content was found to enhance the magnitude of positive apparent molar volume, signifying stronger solute-solvent interactions. Lower values of the limiting slope compared to transfer partial molar volume further emphasized the supremacy of solvent-solute associations within the blend. Positive transfer volumes indicate a prevalence of mostly hydrophilic interactions between LBA, water, and the glycols. Across all examined temperatures, positive expansibilities were observed, reinforcing the role of ion and hydrophilic effects. The presence of negative apparent molar compression values throughout the range of glycols and LBA concentrations suggests that water molecules occupy the free spaces within the organic molecular structure. The inclusion of LBA is seen to diminish electrostriction, further enhancing solute-solvent interactions. Predominantly, ternary interactions among LBA, glycol, and water contribute to the structural behavior of the solutions. Collectively, the evaluated systems reveal pronounced solute–solvent interactions within the ternary mixtures of glycols, polyhydroxy acids, and water, as substantiated by detailed analyses of volumetric and acoustic parameters. These interactions are particularly relevant due to the widespread application of combined polyhydroxy acid–glycol systems in fields such as pharmaceutical formulation, cosmetic delivery systems, and biocompatible solvents, where understanding molecular interactions is critical for optimizing performance, stability, and bioavailability.

References

[1] M. Lamba, N. Chakraborty and K.C. Juglan, J. Chem. Eng. Data 70, 244-260 (2024)

[2] K.D. Amirchand, S. Kaur, T.S. Banipal and V. Singh, J. Mol. Liq. 334, 116077 (2021).

[3] R. Sharma, N.R. Kar, M. Ahmad et al., Community Pract. 21, 1812–1826 (2024).

[4] H.S. Harned, B.B. Owen and C.V. King, J. Electrochem. Soc. 106, 15C (1959).

[5] P. Kaur, K.C. Juglan, H. Kumar and M. Singla, Braz. J. Chem. Eng. 40, 1213–1226 (2023).

[6] A.K. Gill, N. Chakraborty and K.C. Juglan, Chem. Phys. Impact 10, 100843 (2025).

[7] Y. Marcus, Chem. Rev. 111, 2761–2783 (2011).

[8] H. Kaur, N. Chakraborty, K.C. Juglan and A. Upmanyu, J. Mol. Liq. 392, 123403 (2023).

[9] M. Lamba, N. Chakraborty, K.C. Juglan and M. Singla, Chem. Thermodyn. Therm. Anal. 13, 100129 (2024).

[10] A.K. Mishra and J.C. Ahluwalia, J. Phys. Chem. 88, 86–92 (1984).

[11] M. Iqbal and M.A. Chaudhary, J. Chem. Thermodyn. 42, 951–956 (2010).

[12] Z. Yan, J.J. Wang, H. Zheng and D. Liu, J. Sol. Chem. 27, 473–483 (1998).

[13] M. Lamba, N. Chakraborty and K.C. Juglan, J. Mol. Liq. 416, 126497 (2024).

[14] Y. Marcus, Chem. Rev. 109, 1346–1370 (2009).

[15] H. Kumar, R. Sharma, V. Kumar and N. AlMasoud, J. Chem. Thermodyn. 158, 106452 (2021).

[16] K. Kaur, K.C. Juglan and H. Kumar, J. Chem. Eng. Data. 62, 3769−3782 (2017).

[17] H. Kumar, M. Singla and R. Jindal, Monatsh. Chem. 145, 1063–1082 (2014).

[18] H. Kumar and I. Behal, J. Mol. Liq. 219, 756–764 (2016).

[19] H. Kaur, N. Chakraborty, K.C. Juglan and A. Upmanyu, J. Chem. Thermodyn. 204, 107446 (2025).

[20] R. Xu, G. Tang, X.-L. Fu and Q.-L. Yan, Cryst. Growth Des. 22, 909–936 (2021).

[21] E.L. Smith, A.P. Abbott and K.S. Ryder, Chem. Rev. 114, 11060–11082 (2014).

[22] N. Chakraborty, K.C. Juglan and H. Kumar, J. Chem. Thermodyn. 163, 106584 (2021).

[23] H. Kumar and I. Behal, J. Chem. Thermodyn. 99, 16–29 (2016).

[24] L.G. Hepler, Can. J. Chem. 47, 4613–4617 (1969).

[25] A. Apelblat and E. Manzurola, J. Chem. Thermodyn. 33, 581–595 (2001).

[26] A. Ghosh and K.S. Schweizer, Macromolecules 53, 4366–4380 (2020).

[27] K. Dhal, S. Singh and M. Talukdar, J. Mol. Liq. 361, 119578 (2022).

[28] P. Kaur, N. Chakraborty, H. Kumar, M. Singla and K.C. Juglan, J. Sol. Chem. 51, 1268–1291 (2022).

[29] N. Chakraborty, K. Kaur, K.C. Juglan and H. Kumar, J. Chem. Eng. Data 65, 1435–1446 (2020).

[30] R.K. Pradhan and S. Singh, J. Mol. Liq. 412, 125790 (2024).

[31] J.G. Kirkwood, Chem. Rev. 24, 233–251 (1939).

[32] P. Ramsami and R. Kakkar, J. Chem. Thermodyn. 38, 1385–1395 (2006).

[33] R. Rani, A. Kumar and R.K. Bamezai, J. Mol. Liq. 224, 1142–1153 (2016).

[34] H.L. Friedman and C.V. Krishnan, in: Aqueous Solutions of Simple Electrolytes, Springer, Boston, MA, 1–118 (1973).

[35] T. Sharma, A. Bandral, R.K. Bamezai and A. Kumar, Chem. Thermodyn. Therm. Anal. 6, 100043 (2022).

[36] W.G. McMillan and J.E. Mayer, J. Chem. Phys. 13, 276–305 (1945).

[37] C.V. Krishnan and H.L. Friedman, J. Solut. Chem. 2, 37–51 (1973).

[38] F. Franks, M. Pedley and D.S. Reid, J. Chem. Soc. Faraday Trans. 1 72, 359–367 (1976).

[39] K. Bhakri, M. Lamba, K.C. Juglan and N. Chakraborty, J. Mol. Liq. 406, 125117 (2024).

[40] N. Chakraborty, K.C. Juglan and H. Kumar, J. Mol. Liq. 337, 116605 (2021).

[41] Ashima, K.C. Juglan and H. Kumar, Results Chem. 2, 100049 (2020).

[42] S. Devi, M. Kumar, N. Sawhney, U. Syal, A.K. Sharma and M. Sharma, J. Chem. Thermodyn. 154, 106321 (2021).

[43] B. Sinha, A. Sarkar, P.K. Roy and D. Brahman, Int. J. Thermophys. 32, 2062–2078 (2011).

[44] M. Lamba, N. Chakraborty, K.C. Juglan, R. Sharma and M. Singla, J. Chem. Eng. Data 69, 171–184 (2024).

[45] A.K. Gill, N. Chakraborty and K.C. Juglan, in: P.K. Prabhakar, A. Prakash (Eds.), *Adv. Med. Diagn. Treat. Care*, IGI Global, pp. 450–459 (2023)

[46] A.K. Gill, N. Chakraborty and K.C. Juglan, Int. J. Thermophys. 46, 46 (2025).

[47] M. Natarajan, R.K. Wadi and H.C. Gaur, J. Chem. Eng. Data 35, 87–93 (1990).

[48] M.A. Cheema, S. Barbosa, P. Taboada, E. Castro, M. Siddiq and V. Mosquera, Chem. Phys. 328, 243–250 (2006).

[49] A. Salabat, L. Shamshiri and F. Sahrakar, J. Mol. Liq. 118, 67–70 (2005).

[50] R. Sadeghi and A. Gholamireza, J. Chem. Thermodyn. 43, 200–215 (2011).

[51] L. Pauling and R.B. Corey, Proc. Natl. Acad. Sci. U.S.A. 38, 86–93 (1952).

[52] L. Pauling and R.E. Marsh, Proc. Natl. Acad. Sci. U.S.A. 38, 112–118 (1952).

[53] T. Sharma, S.S. Shah and R.K. Bamezai, J. Solution Chem. 50, 1363–1390 (2021).

[54] A.K. Nain, J. Mol. Liq. 318, 114190 (2020).

[55] V. Abbot and P. Sharma, J. Mol. Liq. 328, 115489 (2021).

[56] Ashima, K.C. Juglan and H. Kumar, J. Chem. Thermodyn. 140, 105916 (2020).

[57] N. Chakraborty, K.C. Juglan and H. Kumar, J. Chem. Eng. Data 66, 2391–2400 (2021).

[58] Q.M. Omar, J.-N. Jaubert and J.A. Awan, Int. J. Chem. Eng. 2018, 8689534 (2018).

[59] M. Sethu Raman, M. Kesavan, K. Senthilkumar and V. Ponnuswamy, J. Mol. Liq. 202, 115–124 (2015).

[60] K. Dhal, P. Das, S. Singh and M. Talukdar, J. Mol. Liq. 376, 121413 (2023).

[61] D. Chawla, N. Chakraborty, K.C. Juglan and H. Kumar, Chem. Pap. 75, 1497–1506 (2021).

[62] S.S. Dhondge, R.L. Paliwal and N.S. Bhave, J. Chem. Thermodyn. 59, 158–165 (2013).

[63] N. Chakraborty, K.C. Juglan and H. Kumar, ACS Omega 5, 32357–32365 (2020).

[64] M.T. Zafarani-Moattar and S. Sarmad, J. Chem. Thermodyn. 42, 1213–1221 (2010).

[65] S.K. Sharma and A. Thakur, J. Mol. Liq. 322, 114527 (2021).

[66] T. Kondo, K. Nomura, M. Gemmei-Ide, H. Kitano, H. Noguchi, K. Uosaki and Y. Saruwatari, Colloids Surf. B Biointerfaces 113, 361–367 (2014).

[67] H. Kumar, K. Kaur, S. Arti and M. Singla, J. Mol. Liq. 221, 526–534 (2016).

[68] T.S. Banipal, H. Singh, P.K. Banipal and V. Singh, Thermochim. Acta 553, 31–39 (2013).

[69] A.K. Gill, N. Chakraborty and K.C. Juglan, Phys. Scr. 99, 115009 (2024).

[70] A. Thakur, K.C. Juglan, H. Kumar and K. Kaur, J. Mol. Liq. 288, 111014 (2019).

[71] H.L. Friedman and C.V. Krishnan, J. Solution Chem. 2, 119–140 (1973).

[72] N. Ammari, H. Shekaari, B. Golmohammadi, F. Ghaffari and M.T. Zafarani-Moattar, Sci. Rep. 15, 13867 (2025).

[73] K. Dhal, S. Singh and M. Talukdar, J. Mol. Liq. 352, 118659 (2022).

Summary and Conclusion

The physicochemical properties of a ternary mixture containing Gluconolactone, Lactobionic acid, and galactose, as well as various combinations of glycols spanning a wide molecular range, were studied in a thesis titled "Study of Acoustic and Volumetric Properties of Aqueous Polyhydroxy Acids and Glycols Mixtures at Different Temperatures Using Ultrasonic Technique." The study was conducted at various PHA concentrations and temperatures (288.15, 298.15, 308.15, and 318.15) K, while a constant pressure held at 0.1 MPa. This study sheds insight on crucial ternary system structural properties.

Polyhydroxy acids (PHAs) and glycols exhibit highly organized molecular behavior governed predominantly by extensive hydrogen-bonding interactions. PHAs, with their multiple hydroxyl and carbonyl groups, tend to form stable self-associated structures, whereas glycols develop flexible, dynamic hydrogen-bonded networks. In mixed systems, glycols effectively disrupt PHA self-association and establish stronger PHA–glycol linkages, leading to enhanced structural reorganization within the medium. The balance of these interactions is strongly influenced by temperature and solvent composition. Variations in thermodynamic and acoustic properties—reflected through changes in density and speed of sound—clearly demonstrate the cooperative effects of hydrogen bonding and solvation. Collectively, these interactions dictate the overall molecular organization, stability, and physicochemical behavior of PHA–glycol systems.

Across all eight problems, based on the apparent molar and partial molar properties, it is evident that there are strong solute-solvent interactions among the PHAs and glycols. Hydrophobic hydration effect, dipole-dipole, and dipole-induced dipole interactions are all examples of such interactions. The solute in the liquid system can form structures because all the E_ϕ^0 values are positive. The values of (V_{AB}, V_{ABB}, K_{AB} and K_{ABB}) and positive S_V^* values show that pairwise interactions are the most common in all the systems taken under study containing PHAs and Glycols. As the molecular mass of the glycols increases, the positive V_ϕ values show that there is a considerable solute-solvent relationship in the liquid system. The presence of a positive sign in the partial double derivative of V_ϕ^0 or $\partial E_\phi^0/\partial T$ values and all the E_ϕ^0 values, as well as all E_ϕ^0 values, suggests that the solute is enhancing the structure inside the solvent. When water molecules are close to glycol ionic charge groups, they are much less compressible than water molecules in bulk, as indicated by the negative $K_{\phi,S}$ values.

Pharmaceutical formulation, cosmetic delivery systems, and biocompatible solvents are just a few areas that extensively use combined polyhydroxy acid-glycol systems. In these areas, understanding molecular interactions is crucial for optimizing performance, stability, and bioavailability, making these interactions particularly relevant. Collaborating with glycols such as EG, DEG, TEG, PEGs, propylene glycol, or hexylene glycol, polyhydroxy acids (PHAs) like galactose, lactobionic acid, or gluconolactone can create multifunctional systems. These systems have several uses in cosmetics, medicines, food, and sustainable materials. Combinations like this have a variety of cosmetic applications, including exfoliation (PHAs) and moisturization (glycols). Glycols and PHAs are potential building blocks for polyester in the field of polymer chemistry. The high solubility, enhanced viscosity, moisture retention, and formulation stability of these mixes are primarily caused by the strong hydrogen bonding interactions that exist between the hydroxyl (-OH) groups in both the PHAs and the glycols. Gluconolactone, with its small molecular size and accessible carboxylic acid (-COOH) group, is the most reactive and interactive of the three PHAs. Lactobionic acid, on the other hand, has a carboxyl group as well, but its disaccharide structure causes it to react more slowly, and galactose, without a -COOH group, only forms non-covalent bonds. Because of this, gluconolactone is ranked higher in terms of reactivity and interaction than lactobionic acid and galactose. This results in a reactivity and interaction ranking of gluconolactone > lactobionic acid >> galactose.

Temperature plays a decisive role in shaping the molecular interactions and structural organization of polyhydroxy acid–glycol systems. At lower temperatures, the strength and stability of hydrogen-bonding interactions lead to tightly associated molecular assemblies and well-structured solvation environments. These conditions promote compact packing, reduced compressibility, and limited molecular mobility, reflecting a highly ordered solution structure. As the temperature rises, enhanced thermal motion weakens these intermolecular forces, progressively disrupting associated species and loosening solvation shells. This shift results in greater molecular freedom, increased compressibility, and larger apparent molar volumes, indicative of a more open and dynamically interacting system. Overall, temperature governs the transition from a strongly structured to a more dispersed molecular state, providing essential insight into the thermodynamic and acoustic behavior exhibited by these mixtures.

Pharmaceutics: PHA-glycol esterification allows for the preparation of controlled-release drug delivery vehicles; food systems: PHA-glycol esters solubilize and stabilize substances (such as gluconolactone, which is used as a preservative or tofu coagulant), and biodegradable polymers and packaging materials: PHAs in skincare offer gentle exfoliation and barrier repair, while glycols hydrate and stabilize formulations. Several United Nations Sustainable Development Goals (SDGs) are strongly supported by these applications. For example, SDG 3 (Good Health and Well-being) is addressed by their use in dermatology and medicine. SDG 12 (Responsible Consumption and Production) is extended through the creation of biodegradable alternatives to petrochemical plastics. SDG 13 (Climate Action) is addressed through the facilitation of green chemistry practices. And SDG 2 (Zero Hunger) is addressed through safer, longer-lasting food technologies. Taken as a whole, PHA-glycol mixtures are bio-based, sustainable, multifunctional materials that meet performance demands while also contributing to global sustainability goals. If we want to know how polyhydroxy acids (PHAs) and glycols behave in all their many functional contexts, we need to examine their molecular interactions in water. Hydrogen bonding, dipole-dipole attractions, and potential esterification, which can only occur under certain conditions, are the main interactions that influence important physicochemical qualities including solubility, viscosity, hydration capacity, and thermal stability. Researchers can improve the composition of cosmetic products, medications, food systems, and biodegradable materials by studying these interactions at the molecular level. For example, in cosmetics, higher hydrogen bonding between PHAs and glycols improves skin compatibility and moisture retention. In pharmaceuticals, it improves medication solubility and release profiles. And in the field of polymers, it helps build stable, environmentally acceptable materials. In product development, knowing these molecular characteristics also helps with rationally choosing component ratios, processing conditions, and functional aims. By supporting the use of renewable, biocompatible components that are in line with ecologically acceptable procedures, these investigations ultimately improve material performance while also contributing to sustainability goals and green chemistry.

Future Scope of the Study

The combined study of polyhydroxy acids and glycols using volumetric and acoustic techniques presents significant potential for advancing both theoretical understanding and practical applications in solution chemistry and material science. Future investigations can leverage these approaches to explore solute–solvent and solute–solute interactions at varying temperatures, concentrations, and pH conditions, enabling deeper insight into molecular association, hydration dynamics, and structural rearrangements in complex media. Volumetric properties such as apparent molar volume and excess molar volume, along with acoustic parameters like isentropic compressibility and acoustic impedance, provide non-invasive, sensitive tools for probing intermolecular forces and solvation behavior at the microscopic level. These studies can be extended to design optimized solvent systems for controlled drug delivery, bioresorbable formulations, and environmentally benign solvents. Moreover, understanding these interactions can inform the design of next-generation formulations in cosmetics and dermatology, where polyhydroxy acids are increasingly used for their gentle exfoliating and humectant properties, while glycols function as carriers and stabilizers. These acids are employed in chemical synthesis building blocks, monomers of different biopolymers and bioplastics, drug delivery, tissue engineering, and the manufacture of numerous commodity chemicals. In the hunt for new sustainable materials to replace petrochemical polymers in packaging applications, polyhydroxy acids have been garnering a lot of interest. Advanced computational modelling combined with experimental volumetric and acoustic data may also open avenues for predictive formulation science, aiding in the rational design of solvent systems tailored for specific industrial and biomedical applications.

List of Publications

1. Nabaparna Chakraborty, **Kanika Bhakri,** K.C. Juglan and Harsh Kumar, "**Physicochemical studies of polyethylene glycols in aqueous biotin solutions at different temperatures and constant pressure**" (2022) 012124 published in ***Journal of Physics: Conference Series*** **(IOP Publishing)** **https://doi.org/10.1088/1742-6596/2267/1/012124**
2. **Kanika Bhakri,** Nabaparna Chakraborty, K.C. Juglan and Harsh Kumar, "**Investigation of Volumetric and Acoustical Properties of Polyethylene Glycols in Niacin Solutions**" (2023) 81 is published in Journal **Letters in Applied NanoBioScience (Springer publications) https://doi.org/10.33263/LIANBS123.081**
3. **Kanika Bhakri**, Nabaparna Chakraborty, K. C. Juglan, Harsh Kumar, Ravinder Sharma, **"Thermodynamic behaviour and physicochemical characteristics of EG, DEG, TEG in aqueous gluconolactone solutions"** (2024) 1234 published in '***Journal of Thermal Analysis and Calorimetry'*** **(Springer publications)** with impact factor **3.2** **https://doi.org/10.1007/s10973-023-12223-z**
4. **Kanika Bhakri**, Manisha Lamba, Nabaparna Chakraborty, K. C. Juglan, **"Understanding of lactobionic acid in aqueous-glycol mixtures at different temperatures: Ultrasonic investigation and spectroscopic study"** (2024) 125117 published in ***Journal of Molecular Liquids*** with impact factor **5.3** **https://doi.org/10.1016/j.molliq.2024.125117**
5. Manisha Lamba, **Kanika Bhakri**, Nabaparna Chakraborty, Kailash Chandra Juglan, **"Ultrasonic and volumetric investigation of aqueous disodium EDTA with PEG 400 and PEG 4000 at different temperatures"** (2024) 105027 published in **Physica Scripta (IOP publishing)** with impact factor **2.6** **https://doi.org/10.1088/1402-4896/ad73bc**

6. **Kanika Bhakri,** K.C. Juglan, Nabaparna Chakraborty, Harsimran Kaur "**Exploration of the Molecular Interactions between Polyhydroxy acid: Gluconolactone and Glycols: A Thermoacoustic and Spectroscopic Method**" (2025) is published in **International Journal of Thermophysics (Springer) with impact factor 2.5** **https://doi.org/10.1007/s10765-025-03580-y**

List of Communicated papers

1. **Kanika Bhakri**, Nabaparna Chakraborty and Kailash Chandra Juglan, "Exegesis of molecular interactions of mixes comprising Polyethylene glycol-4000 and Polyhydroxy acids (PHAs) with spectroscopic analysis" submitted to *Journal of Indian Chemical Society.*
2. **Kanika Bhakri**, Kailash Chandra Juglan, Nabaparna Chakraborty and *Arun Upmanyu* "An Investigation of the Effects of Glycols on the Thermodynamic and Acoustic Parameters of Polyhydroxy Acid at Different Temperatures" submitted to *AIP Proceeding*.
3. **Kanika Bhakri**, Manisha Lamba, Nabaparna Chakraborty and Kailash Chandra Juglan, "Insights into Water-Based PHA in Glycol Media: A Multi-Technique Molecular Dynamics Approach" submitted to *ChemTexts.*
4. **Kanika Bhakri**, Ashpinder Kaur Gill, K.C. Juglan, Nabaparna Chakraborty, "Volumetric and acoustical studies of glycols with water-soluble lactobionic acid solutions at different temperatures" submitted *Journal of Molecular Liquids*.
5. **Kanika Bhakri**, K.C. Juglan, Nabaparna Chakraborty, "An Investigation to Display Galactose's Physico-Chemical Behaviour with PEGs: A Thermo-Acoustical and Spectroscopic Study" submitted to *International Journal of Thermophysics.*

List of Conferences/ Seminar/ Short term courses attended

Conferences

1. **Recent Advances in Fundamental and Applied Sciences**, Lovely Professional University, Phagwara, Punjab, 25th June 2021 and 26th June 2021, "Physicochemical studies of polyethylene glycols in aqueous biotin solutions at different temperatures and constant pressure". (Poster Presentation)
2. **Fundamental and Applied Sciences**, Sardar Vallabhbhai National Institute of Technology, Surat, Gujarat, 20th October 2021 and 21th October 2021 "Investigation on temperature-dependent volumetric and acoustical properties of PEG 400 and PEG 4000 in aqueous niacin solutions". (Oral Presentation)
3. **Recent Advances in Fundamental and Applied Sciences**, Lovely Professional University, Phagwara, Punjab, 24th March 2023 and 25th March 2023, "An Investigation of the Effects of Glycols on the Thermodynamic and Acoustic Parameters of Polyhydroxy Acid at Different Temperatures". (Oral Presentation)
4. **Recent Advances in Fundamental and Applied Sciences**, Lovely Professional University, Phagwara, Punjab, 19th April 2024 and 20th April 2024, "Thermodynamic investigation of ternary mixtures, involving Galactose and polyethylene glycols using analytical, acoustic and spectroscopic methods." (Oral Presentation- III Position)
5. **9th National Symposium on Advances in Chemical Sciences**, Guru Nanak Dev University, Amritsar, Punjab, 6th and 7th March, 2025, "Exegesis of molecular interactions of mixes comprising Polyethylene glycol-4000 and Polyhydroxy acids (PHAs) with spectroscopic analysis." (Oral Presentation)